Ural Federal University named after the first President of Russia B.N.Yeltsyn

Università degli Studi di Firenze

Manuscript

Ilia Murmanskii

IMPROVEMENT AND DESIGN OF EJECTORS FOR STEAM TURBINES AND CHILLERS

Ph.D thesis

Scientific coordinators:

from UrFU:

Professor Konstantin Aronson

from UniFI:

Professor Adriano Milazzo

Ekaterinburg – 2019

CONTENT

LIST OF TERMS

Definitions

Condensing turbine – an electric steam turbine, only for power generation. All steam consumption flows into the condenser unit.

Cogenerating (heating) turbine – a turbine that generates both electric power and heat by condensing high-potential steam in the heat-exchangers: heat exchangers are connected to the heating extracts.

Condenser unit – a vacuum condenser set downstream from the turbine, with air-removing devices, water pumps and fittings.

Circulating water – the condenser's cooling water. Usually, it is taken from a river or cooling towers.

General ejector – an ejector of a condensing unit in a steam turbine, used for removing incondensable gases from the turbine's vacuum system. Besides general ejectors, there are also auxiliary ejectors, start ejectors and others.

Serial ejector – a widely-used ejector, usually designed by turbine power plants and tested for decades.

Multistage ejector – an ejector unit consisting of 2 or 3 stages. A multistage ejector has intercoolers at each stage, where the primary steam from the upstream stage is condensed in order to decrease the flow rate in the following stages.

Ejector stage – a jet device (an ejector) with an intermediate condenser (intercooler) downstream for condensing steam.

Jet device – the nozzle, suction chamber, mixing chamber and diffuser of the ejector.

Mixing chamber – [according to Prof. Sokolov] part of the diffuser that includes a narrow section and a throat. Primitive ejectors have narrow and cylindrical sections.

Intercooler – a condensing heat-exchanger, where the steam is condensed and the air is removed (either to the next stage or to the atmosphere).

Cooling condensate (water) – water inside the tube bunch of the intercooler: usually, this is the turbine condenser's condensate flowing back to the boiler and the turbine. Thus, the temperature of the cooling water depends on the vacuum value,

which in turn depends on the circulating water temperature and the state of the condenser.

Geometrical characteristics (parameters) – general dimensions and their relations.

Primary (working) stream (fluid) – a medium supplied to the nozzle of the ejector.

Entrained (secondary) stream (fluid) – a medium removed by the ejector.

General geometric parameter – the ratio of the area of the critical sections of the mixing chamber and the nozzle.

Nominal (design) characteristic – a characteristic of the ejector regulated by the manufacturer.

Performance (operating) characteristic – a characteristic of the ejector obtained during experimental tests.

Capacity of the ejector – maximum secondary flow rate, which can be removed by the ejector in on-design mode.

Compression ratio – the degree of pressure increase in the jet device.

Effective area – an annular section for the secondary fluid, where this medium accelerates to the speed of sound.

Critical section – throat of the nozzle and the diffuser.

One-circuit nuclear power station – a type of power plant where the turbine steam is boiled inside the reactor without any intermediate heat carrier. This type of NPP is the most dangerous because all the equipment is radioactive.

Symbols

Δ – difference;

μ - coefficient: describes the position of the “effective cross section” determined as the ratio of the “effective area”, where the secondary stream velocity increases to sonic speed to the cross section of the diffuser’s cylindrical part;

d – diameter;

F – section area;

F* - general geometric parameter;

G, D – flow rate;

l_1 – distance between the nozzle exit plane and diffusers in the cylindrical part of the inlet;

NXP - distance between the nozzle exit plane and the diffusers in the narrow part of the inlet;

P – pressure;

T – temperature;

W – flow velocity.

It should be also noted that many symbols have been used in the design method to designate parts of the ejector's jet device. These symbols are presented with an index of abbreviations in Fig. 1.

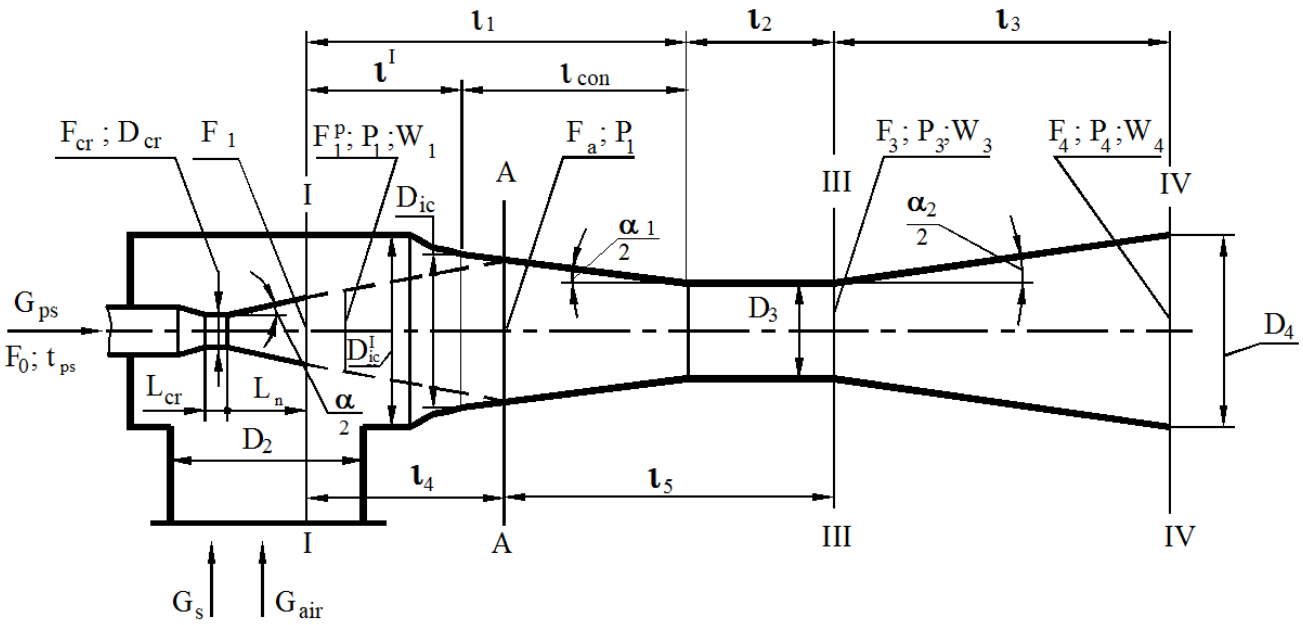

Fig. 1. The schematic of a steam-driven ejector with a description of the basic geometrical parameters and flows: F – cross-section area; D – diameter; P – pressure; t – temperature; W – velocity; G – mass flow rate; L – element length; l – section length; α – angle. Sections: I – nozzle exit section; A-A – "the effective section"; III – the output section of the mixing chamber / the inlet of the diffuser; IV– output section of the diffuser. Indexes: 0 - initial parameters; cr – critical section; ps – primary steam; con – conical part; air – air; s – steam; 1, a, 3.4 – sections of I, A, III and IV, respectively.

Abbreviations

I, II, III – 1^{st} ,2^{nd} and 3^{rd} stage of the ejector, respectively;

0– Initial parameters;

c, cond – condenser;

cr – critical;

in – inlet;

out – outlet;

air – “dry” air;

d – diffuser;

n – nozzle;

ps – primary stream;

i – entrained stream;

cc – cooling condensate;

SAM – air-steam mixture;

lim – limiting;

eff – effective area;

u – entrainment ratio.

Acronyms

TPP – thermal power station;

NPP – nuclear power station;

STU – steam turbine unit;

CU – condenser unit;

LPP – low pressure part;

SAM – steam-air mixture;

UTZ – Ural turbine plant

LMZ – Leningrad metal plant;

HTZ – Harkov turbine plant;

KTZ – Kaluga turbine plant;

MEI – Moscow Power Engineering Institute;

VTI – Russian Heat Engineering Institute;

CRMC – constant rate of momentum change.

INTRODUCTION

Currently, a high overspending of designed running hours in steam turbine units (STU) [1-8] and limited investment in maintaining equipment leads to the appearance of difficult-to-eliminate defects (warping of case flanges, etc.), causing air to enter the vacuum system. In turbine units installed in TPPs, excessive air suction (up to 5-6 times above standard values) occurs practically everywhere. The ejectors that currently operate as part of STUs were developed in the 1950s-80s and cannot ensure the normative functioning of condensing units in the non-design modes of their operation [9-15]. These problems require the development of new high-performance and highly efficient general and auxiliary ejectors that remove air from turbine vacuum systems.

The results of studies on gas-dynamic processes in ejectors are given in the works of G. N. Abramovich, M. D. Millionshchikov, Yu. N. Vasilyev, L. D. Berman, E. Ya. Sokolov, A. V. Robozhev, M. E. Deitch, N. M. Singer, G. G. Shklover, G. I. Efimochkin, M. I. Putilov, A. M. Leshchinsky, O. O. Milman, A. I. Belevich, V. G. Tsegelsky, A. V. Sobolev and others [16-37].

It should also be noted that in recent decades, global interest in studying ejectors and their various applications (refrigeration cycles, solar energy conversion plants, converting chemical energy of fuel into electrical energy, the refining industry, etc.) has increased significantly [38-63]. Studies carried out in Russia in the field of improving ejectors (jet pumps) mainly cover the design aspects of jet devices [34, 35] or the functioning of ejectors [33, 36, 37]. In international publications, gas dynamics is studied in jet devices using up-to-date experimental methods and with the help of numerical calculations in specialized software systems [39-44, etc.].

In this thesis, we propose improving multistage steam ejectors of steam turbines in terms of reducing their damageability, developing more reliable designs, generalizing operating experience, testing, generalizing the geometric

characteristics of ejectors, refining the calculation methods and looking at the mutual influence of jet devices and intercoolers.

The relevance of improving steam turbine ejectors is determined by the need to maintain high vacuum values in turbine condensers at increased air suctions values. Ejectors developed in the 1950s-80s do not meet modern requirements in terms of condensing unit reliability and efficiency. New opportunities for improving ejectors have been brought about by the advent of modern methods in experimental and computational research and accumulated experience in calculating, developing, testing and operating ejectors.

The object of research and development are the multistage steam ejectors of condensing units in steam turbines.

The aim of the study is to improve multistage steam-driven ejectors in order to increase the efficiency and reliability of steam turbine condensing units.

The degree of development of the chosen topic is presented in the flowchart of the research carried out within the framework of this dissertation (Fig. 2).

In the study of ejectors in STU condensation units, reliability analysis, industrial tests under various operating conditions, generalization of geometric characteristics, analysis of the efficiency of existing serial ejectors from various manufacturers and numerical studies of the gas dynamics in ejector jet devices were carried out. On the basis of the obtained results, a method for designing multistage steam ejectors has been refined and the new EPO-3-80 and EPO-3-120 ejectors developed. When testing the new EPO-3-80 ejector, we recorded the gas-dynamic effect of a significant change in pressure in the ejector’s intermediate coolers. To describe the effect obtained, a physico-mathematical model has been developed.

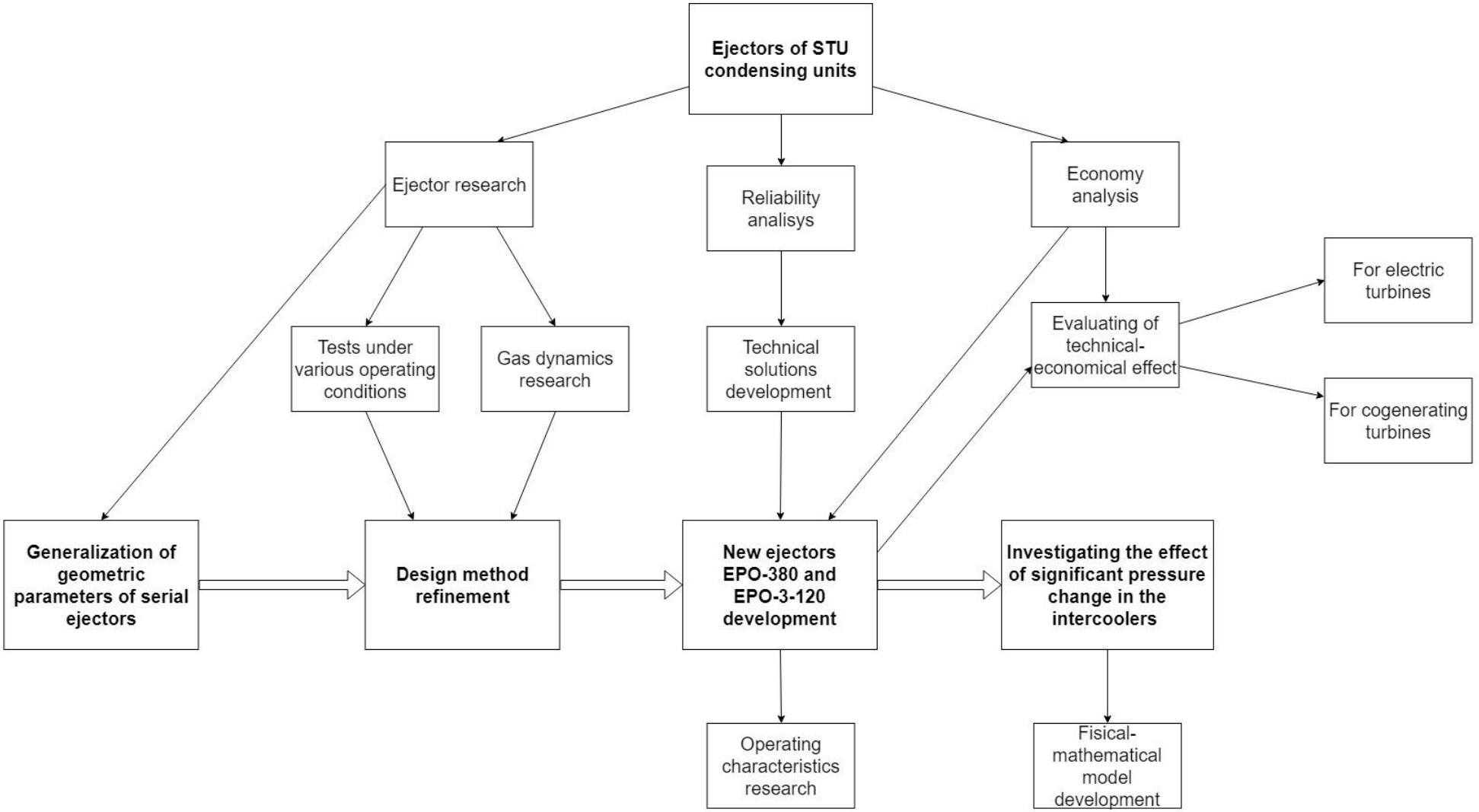

Fig. 2. Flowchart of the research

The research objectives are as follows:

- Analysis and industrial testing of steam-driven ejectors of various sizes and in various operating conditions in TPPs to assess the performance of the ejectors and their reliability as part of condensing units.
- Summarising and analyzing the geometric characteristics of serial steam ejectors.
- Studying gas-dynamic processes in jet devices and the intercoolers of multistage steam-driven ejectors.
- Designing a specific method for designing multistage steam-driven ejectors of steam turbines based on test results, analysis of the geometric characteristics of serial ejectors and numerical studies of gas dynamics in jet devices.
- Designing a new multistage steam-driven ejector with increased capacity for condensing steam turbines and conducting experimental studies on the ejector under the operating conditions in thermal power plants.

The scientific novelty of the work is as follows:

- The correlation between the geometrical parameters, performance characteristics and purpose (for condensation or cogeneration turbines) of multistage steam-driven ejectors has been identified and summarized. The analysis was based on a study of 24 serial ejectors analyzing the position of the "effective cross section" (in which the entrained mixture reaches or passes the speed of sound), the ejector's general geometric parameter (the ratio of the areas of critical sections of the mixing chamber and the nozzle), various values of the axial position of the nozzle, the distribution of compression ratios in multistage ejectors and changes in the critical diameters of nozzles in the ejector's stages.
- A specific methodology for the design and calibration of calculations for multistage steam-driven ejectors was developed based on the analysis and synthesis of the results of industrial tests, a summary of the geometric characteristics of serial ejectors and numerical simulation. The methodology for the design and calculation was refined in order to reduce the consumption of working steam, to determine the

position of the “effective cross section”, to choose the main geometrical parameter of the ejector and to distribute the degrees of compression over the ejector’s stages. The developed methodology for the calibration calculation allows one to determine the characteristics of the ejector stages with the given geometric dimensions of jet devices and the flow shares of the steam condensing in the intermediate coolers.

- A gas-dynamic effect of a significant change in the pressure of the steam-air mixture in the ejector’s intercoolers was detected. Compared with the inlet pressure, the pressure of the steam-air mixture at the outlet from the coolers decreases by $\Delta P = 1.0 ... 4.0$ kPa or increases by $\Delta P = 1.0 ... 8.6$ kPa. A physico-mathematical model has been developed that describes the effect of pressure increase as a pressure leap in a two-phase, two-component medium formed at the inlet to the heat exchanger.

All major scientific results have been confirmed experimentally.

Reliability and validity of the results are ensured by the use of approved measurement methods and metrologically verified tools while conducting experimental studies, a high level of compliance in the test results from the ejectors with the data of other authors and with the results of calculations performed in accordance with the method specified by the author and the successful operation of the developed EPO-3-80 ejector as part of the condensing installation of a K-200-130 LMZ turbine at Surgut GRES-1 for more than one and a half years.

Theoretical and practical significance of the work:

- A refined methodology has been developed for the calculation of multistage steam-driven ejectors in a wide range of operational parameters.
- An extended measurement scheme for multistage ejectors has been developed, which allows for a detailed study of the ejector’s parameters, including the gas-dynamic resistance of the intercoolers.
- The gas-dynamic effect of a significant change in pressure in a multistage ejector’s intercoolers was recorded.
- Developed and justified measures to improve the design of multistage steam-driven ejectors.

- Developed technical solutions to improve the efficiency and reliability of multistage steam-driven ejectors.
- The results of the industrial tests of 34 serial ejectors of various manufacturers are summarized and analyzed.

The implementation of the results. The results have been used to upgrade serial ejectors and to calculate and design new highly efficient ejectors for the condensing units of TPP turbines. More than 50 multistage steam-driven ejectors in turbine condensing units with a capacity from 50 to 500 MW were upgraded and installed in TPPs. The refined method for calculating formulas for multistage steam-driven ejectors has already been used to develop a number of highly efficient ejectors that increase the efficiency of steam turbine condensing units. The developed EPO-3-80 ejector has been tested and is successfully operating as part of a K-200-130 LMZ turbine, in a condenser where pressure is maintained close to the standard level despite an air inflow of about 120-130 kg/h (with a standard value of 21 kg/h) in the Low Pressure Part (LPP). The successful implementation of the new ejector was confirmed by an implementation report from Surgut GRES-1. The improvement of the efficiency and reliability of multistage steam-driven ejectors implemented at Nestandartmash CJSC and Energotech Ejector LLC is confirmed by implementation acts.

A number of the obtained results have been used at Ural Federal University in the training courses “Heat exchangers of turbine plants” and “Thermal and nuclear power plants.” [65-67].

The personal contribution of the author is in the formulation of the research objectives; the collection, processing and analysis of the data on the structural and geometric characteristics of the equipment; performing statistical and computational studies; direct participation in the testing of research results; the development of an improved methodology for calculating the ejector; the development of a measurement scheme; the planning and implementation of experimental studies on

new ejectors; the processing and interpretation of experimental data; developing a model to explain the effect of pressure increasing in an ejector's intercooler; and the preparation of publications.

The study was carried out on the basis of state budget and contractual research, as well as agreements on scientific cooperation with the Ural Turbine Plant JSC. Part of the research was carried out within the framework of RFBR grants for research projects carried out by young scientists under the guidance of candidates and doctors of science in scientific organizations of the Russian Federation.

In the dissertation, in addition to the results obtained by the author himself, data obtained together with the following colleagues are used: Prof. K. E. Aronson, Prof. Yu. M. Brodov, Prof. A. Yu. Ryabchikov, D. V. Bresgin (Ph.D.), N. V. Zhelonkin (Ph.D.), engineer V. K. Kuptsov, M. Stepanov (employee of JSC UTZ), and a scientific group from the University of Florence consisting of Prof. A. Milazzo, Andrea Roccetti (Ph.D.), Federico Mazzelli (Ph.D.), Jafar Mahmoudian, Francesco Giacomelli (Ph.D.) and Furio Barbetti. When implementing the results of the research, the staff of Surgut GRES-1, Energotech-Ejector LLC and Nestandartmash CJSC also provided great assistance.

The author expresses deep appreciation to all the aforementioned colleagues for the attention and participation in discussing the results of the work.

Presentations of the research. The main results of the work were reported at the All-Russian Scientific-Practical Conference of Students, Graduate Students and Young Scientists with International Participation (Ekaterinburg, 2014, 2015 & 2016); the XX and XXI Seminar Schools for Young Scientists and Specialists under the Guidance of RAS Academician A. I. Leontiev "Problems of Gas Dynamics and Heat and Mass Transfer in Power Plants" (Zvenigorod, 2015; St. Petersburg, 2017); the Fifth International Conference "Heat and Mass Transfer and Hydrodynamics in Swirling Flows" (Kazan, 2015); the International Conference "IX Seminar of

Universities in Thermal Physics and Energy" (Kazan, 2015); the Scientific-Practical Conference "Energy. Ecology. Energy Saving. Dedicated to the 25th Anniversary of the Founding of the NSAID Turbokon" (Kaluga, 2016); the First and Second Scientific and Technical Conferences of Young Scientists of the Ural Energy Institute (Ekaterinburg, 2016, 2017); the XV Minsk International Forum on Heat and Mass Transfer (Minsk, Belarus, 2016); the International Conference "Wessex Energy Quest 2016" (Ancona, Italy, 2016); the Jubilee Conference of the National Committee of the Russian Academy of Sciences on Heat and Mass Transfer "Fundamental and Applied Problems of Gas Dynamics and Heat and Mass Transfer"; the International Scientific and Technical Conference "The State and Prospects for the Development of Electrical and Thermal Technology" (XIX Benardos Reading, Ivanovo, 2017); and the International Conference "Modern Problems of Thermal Physics and Energy" (Moscow, 2017).

Publications. The main provisions and conclusions are presented in 49 publications, including 6 articles published in scientific journals in Scopus, 5 in WoS, a certificate of registration for a software package, a patent for a utility model, a patent for an invention, and 4 course books for students. The complete list of the author's published works is presented in Appendix 2.

The main provisions for the defense:

- Results of the statistical analysis of the reliability of the STU condensing unit equipment.
- Results of comparative experimental studies on the serial ejectors of condensing units in various operating conditions.
- Results of the generalization of the geometrical and constructive parameters of ejectors.
- The developed refined methods for the design and calibration calculations of multistage steam-driven turbine ejectors.

- Results from experimental studies of the newly developed EPO-3-80 ejector with a changing nozzle exit position, including the recorded gas-dynamic effect of a significant pressure change in the ejector's intercoolers.
- A physico-mathematical model describing the gas-dynamic effect of a pressure increase in the intercoolers of multistage ejectors.

The structure and scope of the thesis. The thesis consists of an introduction, 5 chapters, a conclusion, a list of references containing 141 titles and an appendix. The material is presented on 176 pages of typewritten text, including appendices, 50 figures and 12 tables.

CHAPTER 1

LITERATURE REVIEW AND STATEMENT OF THE RESEARCH PROBLEMS

Effective air removal is of great importance for the reliable operation of condensers. Air suctions that cause an increase in the absolute pressure in the condenser and worsen its operating parameters can occur via the horizontal flange connection of the low pressure part (LPP), flanged couplings of air lines, the telescope connection between the turbine and the condenser, LPP labyrinth seals, the exhaust atmospheric valve, the low pressure heater and the glands of the valves, fittings and other connections operating in a vacuum (fig. 1.1) [1–8]. Air and steam from the turbine get inside the condenser as well, although the amount of this air is very small.

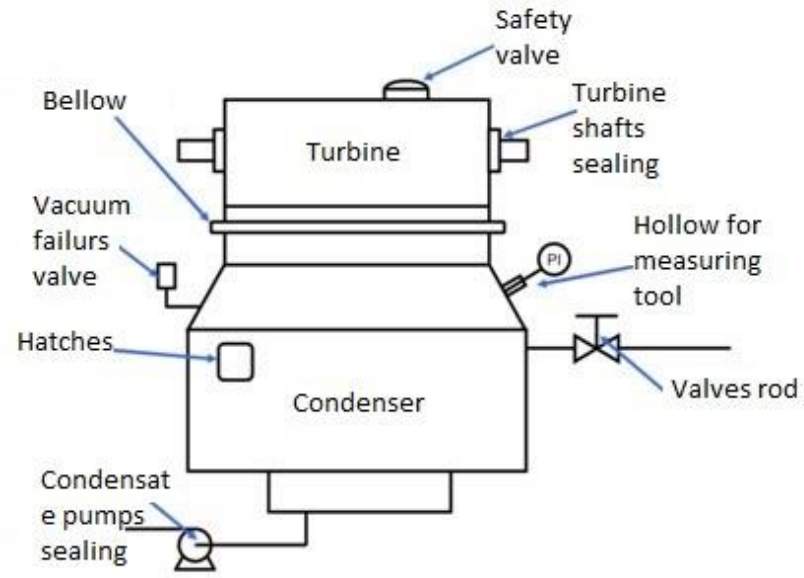

Fig. 1.1. General sources of air entering the condenser

Air inside the vacuum system of a turbine diminishes the functioning of the condenser, causing a number of undesirable phenomena. First of all, air significantly

worsens the heat transfer coefficient in the condenser, causing additional thermal resistance. Accumulating in stagnant zones, the air switches off part of the condenser's heat exchange surface. A further source of thermal loss in a turbine unit caused by air suction in a vacuum part is condensate overcooling: this also leads to an increase in oxygen concentration in the condensate [1, 3].

In Russian turbine plants, multistage steam-driven and water-driven ejectors are used as air deleting devices [4, 9]. Steam-driven ejectors are constructed with built-in or portable intermediate coolers: they are installed by manufacturers on turbines with up to 500 MW. The powerful turbines (from 300 to 1200 MW) of the LMZ turbine plant are equipped with water-driven ejectors. The loss of working steam in ejectors is about 0.1-0.3% of turbine steam consumption. Water-driven ejectors allow for the support of a deeper vacuum in the turbine condenser at small (to standard values) air flow rates; however, these require electric power of their own, an additional cost. Water flow rate in water-driven ejectors is about 5-7% of the consumption of circulating water in the turbine condenser [10].

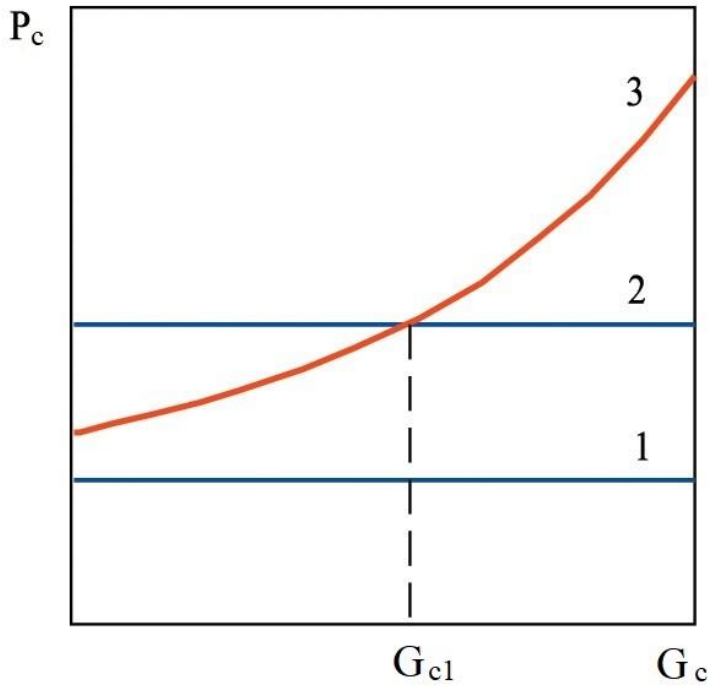

Fig. 1.2. Performance of the system "condenser — ejector":
1,2 – ejector performance curves at various air flow rates D_{air} ($D_{air1} < D_{air2}$), 3 – condenser performance curve

In Fig. 1.2, the qualitative performance of the system “condenser — ejector” in the form of the dependence of condenser pressure P_c from steam consumption to the condenser G_c is shown (the flow rate and temperature of the cooling water are constant).

At D_{air1} (the air suction value), when the ejector suction pressure (line 1, Fig. 1.2) is lower than the pressure in the condenser, the vacuum of the system is defined only by the condenser. At the same time, the ejector reduces the vacuum because of the suction of excess steam. At air suction values $D_{air2} > D_{air1}$ (line 2, Fig. 1.2), lower than the line of steam consumption D_{c1} the vacuum of a system is defined by the ejector, which is not able to support the vacuum determined by the condenser. To deepen the vacuum, it is necessary to reduce the air suction value or to connect an additional ejector (thereby reducing D_{air} through each ejector reduces suction pressure). At air suction values $D_c > D_{c1}$, the vacuum of the system will be defined by the condenser.

Water ring pumps have gained widespread popularity and distribution for modern steam turbines produced by global manufacturers and as part of the CCGT. However, in recent decades powerful steam turbines have been equipped with steam-driven ejectors. Usually, each condenser is equipped with 2 two-staged or three-staged steam-driven ejectors with general intermediate and downstream coolers [11]. In comparison with water ring pumps, steam-driven ejectors have the following advantages: a lack of rotating elements and no losses of warmth in the cooling heat carrier, as all condensates from the coolers are returned to the cycle rather than being lost with circulating water (as occurs when using water ring pumps and water-driven ejectors). Equally, steam-driven ejectors are 40% cheaper than water ring pumps [11].

The water consumption in water ring pumps is several times lower than in water-driven ejectors. The suction ability of vacuum pumps decreases with the increase of the inlet temperature of the circulating water and with reductions in loading [11].

If during the operation of the water ring pump the initial difference of temperatures is small, it can lead to problems like cavitation. This problem is solved with the use of the hybrid vacuum pumps consisting of the first-stage ejector, the intermediate cooler and the water ring vacuum pump. During operation, the steam-air mix from the condenser is ejected by the first-stage ejector, enters the intermediate cooler, and then moves to the vacuum pump [11].

The choice of air-removing system depends on the availability of working steam (water) with the necessary parameters, the cost and the preferences of the designer and the end operator. To ensure the effective functioning of an air-removing system, the value of the capacity of ejectors is recommended by [12].

The production of the air-removing devices is organized by specialized companies like the American company Graham or producers of condensers, such as the SPX Heat Transfer company and its Belgian branch Ecolaire.

The research devoted to the improvement of multistage steam-driven ejectors can be divided into the following trends:

– Development of technical solutions connected with the optimization of the design and geometrical parameters of multistage ejectors with intercoolers [33-37, 71-86];

– Research on gas-dynamic processes and the improvement of ejector device design (Fig. 1.3) using modern experimental and calculation methods [33-63];

– Development and specification of design methods for ejector devices (motive nozzles, mixing chambers and diffusers) [16-19, 22, 30-33] and their intercoolers [16, 68-70].

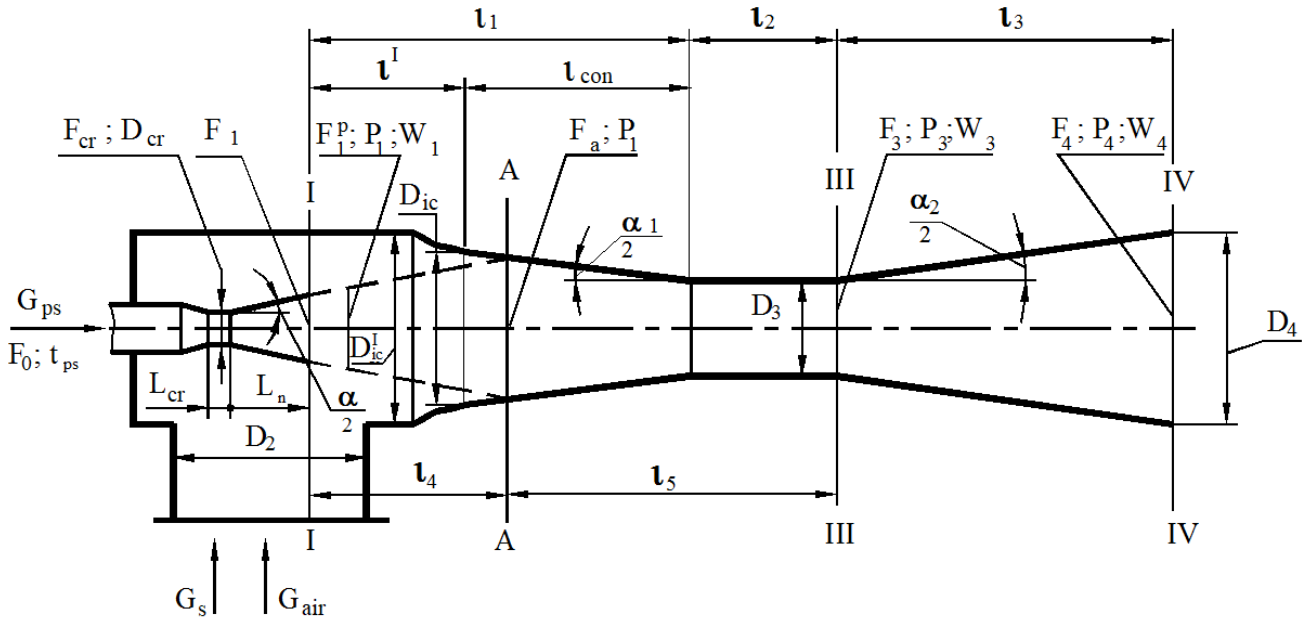

Fig. 1.3. The schematic of a steam-driven ejector with descriptions of the basic geometrical parameters and flows [18]: F – cross-section area; D – diameter; P – pressure; t – temperature; W – velocity; G – mass flow rate; L – element length; l – section length; α – angle. Sections: I –nozzle exit section; A-A – "the effective section"; III – the output section of the mixing chamber / the inlet of the diffuser; IV– output section of the diffuser. Indexes: 0 - initial parameters; cr – critical section; ps – primary steam; con – conical part; air – air; s – steam; 1, a, 3.4 – sections of I,A,III,IV, respectively.

1.1. STANDARD DESIGNS AND CHARACTERISTICS OF MULTISTAGE EJECTORS IN VARIOUS TURBINE PLANTS

The majority of steam-driven ejectors on thermal power plants (TPP) in Russia have the same design. They are three (or two) stage ejector devices set in one case with intermediate coolers. The advantages and disadvantages of these and other designs are considered in this section.

Multistage designs

The operating principles of multistage ejectors are presented in the following schematic (Fig. 1.4).

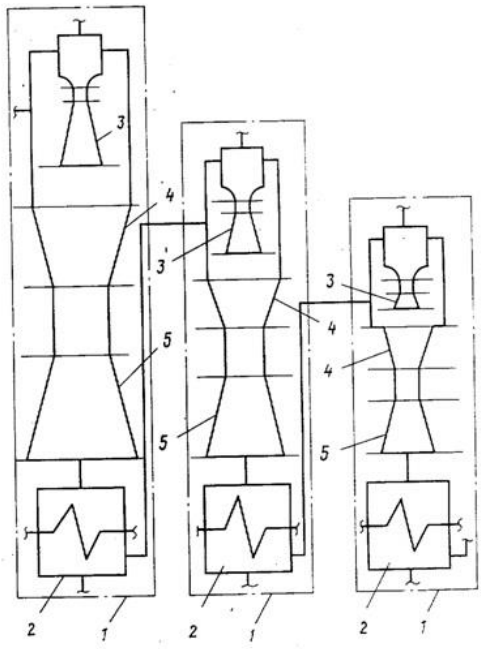

Fig. 1.4. Schematic of the principals of a multistage ejector:
1 – ejector unit (stage); 2 – intercooler; 3 – primary nozzle;
4 – mixing chamber; 5 – diffuser.

As has been shown elsewhere [16–19], multistage ejectors are used in order to achieve a set compression ratio and minimal flow rate for the primary fluid of the ejector. The ejector's compression ratio is defined according to (1.1):

$$\varepsilon = \frac{p_{cp}}{p^{I}_{c\,(lim)}}, \tag{1.1}$$

where $P_{cp\,(lim)}$ –extreme limit of the last stage's counter-pressure;
$p^{I}_{c\,(lim)}$ – ejector suction pressure.

The application of intermediate coolers is necessary to reduce the volume of the mixture in the following stage [16–19]. At the same time, the schematic positions of intermediate coolers may vary. Research [14] on setting the cooler before the first stage (in the supply pipeline of the ejector's steam-air mix) in order to reduce the amount of steam in the injecting mix has been conducted. The proposed solution is interesting with regards to condensing installations with a high air flow rate in the low pressure part of the turbine, where entrained stream can overload the ejector.

According to [32], ejectors in the condensing installations of one-circuit nuclear power plants (NPPs) must have adjustable consumption for the cooling

condensate in the last stage of the cooler: this is in order to reduce the condensed steam and maintain explosive gas levels at the maximum allowed concentration. For example, the EP-3-100/300 ejector has no third-stage cooler at all.

According to the specifications of several ejectors [18, 19, 108], the efficiency assessment of multistage ejectors should be provided by the maximum capacity G_{SAM}, pressure and flow rate of the primary fluid G_{ps} (i.e. entrainment ratio k_ε):

$$k_\varepsilon = \frac{G_{SAM}}{G_{ps}}. \qquad (1.2)$$

Increasing the efficiency of multistage ejectors can be achieved by redistributing compression ratios between the stages. For example, in [79] in order to obtain the highest entrainment ratio it is recommended to reduce the cross-sectional areas of the cylindrical parts of the mixing chambers twice from stage to stage.

Standard designs of intermediate coolers

In terms of the distinctions between the arrangements of intercoolers, it is possible to identify four types of multistage steam-driven ejectors [16, 22, 88-92, 108] (Fig. 1.5).

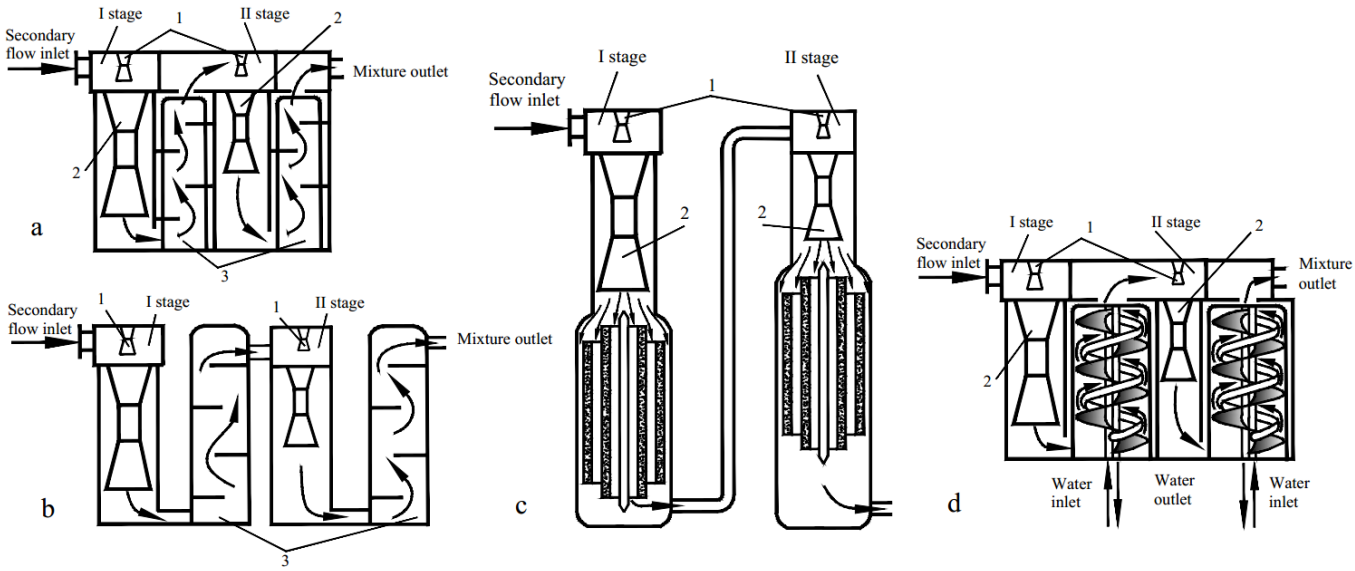

Fig. 1.5. Designs of intermediate coolers of multistage steam-ejecting ejectors: a —built-in tube bundle type; b —external tube bundle type; c — annular pipe type; d — screw type.

"A" type ejectors with a built-in tube bundle are the most common and were installed on turbines manufactured by LMZ, HTZ and UTZ. The ejector coolers are equipped with U-shaped heat exchange surfaces according to [32]. These include the EP-3-2, EP-3-3, EP-3-600, EP-3-700 and EPO-3-25/75 ejectors, and some others. The main advantages of these ejectors are compactness and maintainability in comparison with ejector types "c" [88] and "d" [22]. Ejectors with screw tubes in the intermediate coolers are used by the KTZ plant and are compact, much like type "a". The increased condensation efficiency in such coolers has been subject to research [109,110]. This achieved by high flow velocities along the entire length of the heat-exchanging surface, which is possible because of the lack of stagnant zones. At the same time, such coolers have increased gas-dynamic resistance; however, it is highly complicated to maintain these designs [133].

In the analysis of the considered designs, it is possible to identify presumable design faults. Firstly, because of the common internal space of the casing, it is extremely difficult to conduct a leak check on the intercoolers when the ejector is assembled. As such, it is impossible to verify the absence of overflows in the steam-air mix between stages. Some designs (for example, EP-3-2) are equipped with internal casings to ensure the tightness of the cooler.

For the implementation of intercooler drainage into the condenser's steam space and in order to protect the condenser against additional air, manufacturers have developed various schemes with latches and hydrolocks on the drainage pipelines [105]. At the same time, a number of schematic merge all the ejector drainage in the condenser of the first-stage intercooler and the condensate of the second-stage intercooler; in some schematics, the third-stage intercooler merges with the first by way of a cascade. Such solutions can result in overflow in the first-stage intercooler and thus ejector malfunction.

"B" type designs (with external tube bundles) are used by UTZ in the EPO-3-135 [88] ejector according to various studies [71]. Increased reliability can be provided due to the strict isolation of ejector devices from the intermediate coolers and from each other. However, inclined portable coolers are installed on the EPO-3-135 ejector with straight tubes, which can cause tension in cooler tubes during temperature expansions. A further defect often found in this design is corrosion deterioration of the inclined transitional branch pipes between the ejector device and the intermediate cooler.

"C" type ejectors (with annular pipe bundles) are also developed by the UTZ [88] plant. The design is used in the EPO-3-200 [71] ejector. The main advantage of the EPO-3-200 ejector is high capacity (200 kg/h). It is also necessary to note that all structural elements, including the heat exchange surfaces, are made of ferrous metal, unlike the majority of existing designs where they made from stainless steel or brass. Using ferrous metal can reduce the price of an ejector during production. The main disadvantages of EPO-3-200 ejectors are the bulkiness of the design and the fact that they are nearly impossible to maintain [71].

1.2. TRENDS IN THE IMPROVEMENT OF EJECTORS

The basic designs of ejector devices in multistage steam-driven ejectors are described in [32, 88-91, etc.]. There are several main parameters that determine the optimization of processes in a jet device. These parameters include the geometric parameters, the nozzle axial position (NXP) and the shape of the suction chambers, mixing chambers and diffusers.

It is widely known that studies aimed at improving the efficiency of jet devices by increasing the number of nozzles have taken place and have been the subject of invention patents. According to research [74], there is an ejector that consists of several nozzles directing the flow to separated mixing chambers and diffusers. Correspondingly, these nozzles are connected by a common receiving chamber. This

solution is noteworthy in terms of increasing the area of the ejector's working jet and the suction mixture's flow rate. Therefore, such a solution allows for the reduction of the geometrical dimensions of the nozzle and the diffuser while maintaining the operating parameters. However, it is relatively complex to use.

Solutions are proposed in papers [76,78] whereby an ejector consists of several parallel nozzles and one mixing chamber with a diffuser. According to the stated characteristics, these designs expand the range of the device's operation by regulating the flow of active fluid: they do so by using a rod [76] or a nozzle as a gas-dynamic shutter [78]. At the same time, it is not obvious how the coaxiality of the nozzles and the mixing chamber with the diffuser is attained. It could be possible that the use of such solutions is effective in an ejector whose working conditions are fundamentally different from the ejectors of condensing units. For example, this is the case if the ejector has high performance but a low compression ratio.

Research has been conducted on the shapes of cylindrical and isobaric ejector chambers. The effectiveness of isobaric chambers is shown in the studies of V. Yu. Aleksandrov, V. G. Tsegelsky, Yu. N Vasilyev, et al. [33-37,93-95]. It is assumed that an isobaric chamber is one where the outlet section of the nozzle and the inlet section of the mixing chamber coincide.

Furthermore, this area of development also includes a number of works aimed at intensifying the process of mixing flows and equalizing velocity diagrams. According to G. G. Shklover and O. O. Milman [22], studies have been conducted concerning changing the length of the nozzle while maintaining all other geometric characteristics. The influence of the length of the expanding part of the nozzle on the estimated jet shape was shown experimentally. Accordingly, the recommended range of opening angles that should be maintained when designing the nozzle was established.

Therefore, an ejector was designed with a projection on the inner surface of the chamber [77]: one with a projection on the outer surface of the nozzle was investigated in [75]. The proposed design solutions contribute to the reduction of

aerodynamic losses in the input and middle compartments of the receiving chamber, respectively. Thus, the reduction in aerodynamic losses leads to an increase in the entrainment ratio.

In a number of works, the influence of the shape of the diffuser's mixing chamber on the intensity of the mixing flow and the characteristics of the ejector is considered. In [18, 32, 33, 93], it was shown that the presence of a conical part in the mixing chamber increases the entrainment ratio in comparison with a cylindrical mixing chamber. All manufacturers of steam jet ejectors have applied this development. Moreover, currently existing serial ejectors in condensing units are equipped with cone-cylinder shaped mixing chambers formed by two linear functions. These consist of an input conical (converging) part and a cylindrical section.

Large-scale experimental studies of ejectors with such mixing chambers were carried out by E. Ya. Sokolov, L. D. Berman, G. G. Shklover, O. O. Milman, A. M. Leschinsky and many others [16, 18, 22, 71]. It was found that mixing chambers with a similar shape operate on design characteristics in a wide range of parameters, which is important for condenser ejectors because the flow rates and temperatures of the vapour-air mixture and the temperature of the circulating water may change during operation. This characteristic probably required the use of such geometry when designing the serial ejectors of condensation units (along with the technological simplicity of the manufacturing process).

Some recent papers [96-98,99] suggest describing the form of the adjacent ejector via complex mathematical functions. Thus, in study [96] the profile of the mixing chamber is based on the condition of the jet's constant momentum along the mixing chamber (CRMC). Furthermore, the cross-sectional area of this chamber continuously decreases along the jet while the transition area from the mixing chamber to the diffuser represents a critical section. In study [97], a "curvilinear" mixing chamber is described by second-order Bezier curves. Therefore, these methods for improving the ejectors of condensation units in steam turbine units

(STU) could be considered to have high potential: however, they require further research, as they were tested in an ejector designed to work in one fixed mode.

The geometric characteristics of the mixing chamber are considered in papers [40, 48, 49]. Smoothing the shape of a cone-cylinder type mixing chamber into an CRMC shape was proposed in paper [48]. The results of a numerical simulation confirm that the use of a "curvilinear form" increases the ejector's efficiency (reducing the suction pressure with a constant entrainment ratio) up to 5-10%, depending on the mode in which the ejector is operating.

In paper [99], two types of mixing chamber were experimentally investigated: the "cone-cylinder" and the "curvilinear". The mixing chambers were studied with the ejector possessing two different basic geometrical parameters. It was shown that the transition to the "curvilinear" shape increases the entrainment ratio up to 30 percent while maintaining the diameter of its critical section. However, the change in the entrainment ratio is incommensurately small compared to the decrease in capacity, since the ejector switches to the off-design mode earlier (with lower secondary flow rate).

One of the crucial research directions is the search for the nozzle's optimal position. This requires studying the influence of the distance between the nozzle section and the inlet section of the mixing chamber's cylindrical part. A. Leschinsky [71] conducted such experimental studies to determine the most effective positions of the nozzles in specific UTZ ejectors at the test-bench of UTZ. The data obtained for the UTZ ejectors are qualitatively described by an empirical formula for the limiting operating mode of the ejector (1.3):

$$l_1 + L_n = \frac{55{,}79 * d_{\text{d}}^{\text{cr}}}{12{,}64 - (\frac{d_{\text{d}}^{\text{cr}}}{d_{\text{n}}^{\text{cr}}})}, \tag{1.3}$$

where l_1 – the distance from the outlet section of the nozzle to the inlet section of the mixing chamber's cylindrical part;

L_{n} – length of the expanding part of the nozzle;

d_{n}^{cr} – critical diameter of the nozzle throat;

d_{d}^{cr} – diameter of the critical section of the diffuser.

Experimental studies have been based on testing the designs of jet devices in EPO-3-135 and EPO-3-200 ejectors. It can be assumed that this empirical formula is suitable for a fairly narrow range of ratios of geometric dimensions (for example, the main geometric parameter of the ejector).

According to M. Putilov's experimental studies [25, 26], the entrainment ratio smoothly increases to a critical value with an increase in this distance, after which it sharply decreases. The optimal positions of nozzles were found for narrow ranges of ejector function in these works. It is recommended to set the margin of the entrainment ratio for designing jet devices. The results of these studies can only be used in combination with dependencies to determine the critical point of the nozzle position, i.e. at the maximum entrainment ratio. However, the absence of influence from the temperatures of the primary and secondary streams on the choice of the nozzle position was shown in work [100].

Putilov's empirical formula can be obtained from paper [25]. This formula describes the calculation of the distance from the nozzle exit section to the mixing chamber's cylindrical section:

$$\frac{l_1}{d_3} = \frac{\sqrt{0,072 + 0,104 \cdot u} - 2,268}{0,104 \cdot C} \cdot \frac{F_1}{F_3}, \qquad (1.4)$$

where C = 0,27 — experimental constant for the initial part of the jet.

Formula (1.4) is obtained for a steam-jet device with cylindrical mixing chambers and an inlet conic section with a rounded inlet edge. The primary steam pressure in the experiments was P_{ps} = 0.9 ... 1.3 MPa.

According to paper [87], the flow rate of entrained air at a constant suction pressure increases in the on-design mode, while the backpressure and compression ratio decrease with increasing distance between the nozzle and the diffuser. Consequently, if the distance between the nozzle and the diffuser approaches the minimum possible distance, then a decrease in ejector performance is not

accompanied by an increase in backpressure or compression ratio. On the other hand, if the nozzle is too far from the diffuser, then the operation of the apparatus becomes unstable at pressures close to the unloaded ejector's suction pressure.

Moreover, E. Sokolov provides a formula [18] that represents the dependence on the entrainment ratio and the critical diameter of the nozzle:

$$l_{nxp} = \left(\sqrt{0.083 + 0.76u - 0.29}\right)\frac{d_1}{2a}, when\ u \leq 0.5$$

$$l_{nxp} = \frac{0.37+u}{4.4a}d_1, when\ u \geq 0.5 \qquad (1.5)$$

where l_{nxp} – distance between the nozzle and the mixing chamber;
u — designed entrainment ratio;
d_1 — nozzle exit diameter;
a = 0,07…0,09.

This formula is designed for jet devices with a cylindrical mixing chamber. Moreover, it is based on determining the length and diameter of the free jet leaving the nozzle. It is worth mentioning that experimental validation of the formula has not been found.

There are a large number of modern experimental publications [41-53] devoted to the study of the axial position of the nozzle. The given numerical and experimental studies were performed for various substances used as working and suction flows, but not for water and steam.

Moreover, according to study [40], numerical simulation methods showed the possibility of increasing the entrainment ratio to 25% when setting the axial distance between the nozzle and the diffuser. It is also established that the entrainment ratio smoothly increases, and then drops sharply when the nozzle is removed from the mixing chamber. It should be noted that no more than one optimal position of the nozzle is determined (with the maximum entrainment ratio) in the works presented for the studied ejectors. It is shown that an increase in the diameter of the critical section of the mixing chamber increases the entrainment ratio. The increase in the length of the mixing chamber relative to the minimum calculated value does not

significantly affect the performance of the ejector. The absence of the influence of the length of the mixing chamber on the entrainment ratio was also experimentally confirmed in paper [49].

There are a huge number of invention patents in Russia that register a change to the axial position of the nozzle by moving the nozzle [80-84] or diffuser [85]. The proposed devices are used to adjust the position of the nozzle during operations: they do not require structural changes to the jet device and can be adapted and applied to multistage ejectors in condensing units. At the moment there are no publications on the implementation and testing of such models.

Another modern research trend in the improvement of ejector jet devices is numerical modelling of the gas-dynamic processes in ejectors. Such began to be engaged in theoretical and pilot studies with the help of applied software packages in the early 1950s. The aim of this research was not only to study the essential fundamentals of gas dynamics and heat exchange, but also to look at the operating and service conditions. In paper [38], some of the first results of ejector design research with a one-dimensional model are presented. However, this model with the cylindrical mixing chamber does not allow for the correct reproduction of features of the flow in all areas of the nozzle, mixing chamber and diffuser. As a rule, all the works of this period are concentrated on studying the design of the ejector, its characteristics and phenomena like “flow disruption”, “shock wave”, the interaction of a viscous boundary sublayer and the flow core, the processes of mixing media flows and many others. The tasks were mainly considered in terms of a one-dimensional model; i.e., all processes were investigated exclusively along the axis parallel to flow movement due to the limitations imposed by computer capacities of the time. Nevertheless, a lot of later research on gas dynamics inside ejector devices with two-dimensional and three-dimensional models appeared in connection with the development of computing power.

It should be noted that a fairly large number of works devoted to this topic are published in the periodical literature [34-63]. So, although research on applied CFD packages continue to appear, new approaches and methods are emerging to study gas dynamics and heat exchange inside jet devices via numerical methods.

It is observed that numerical simulation can be used for both qualitative and quantitative assessment of the processes occurring in ejector jet devices. This is shown in study [39], which was dedicated to comparing the results of numerical simulations and experimental studies. In paper [40], the authors emphasized the need for modelling jet devices while taking into account the characteristics of the environment used, since a significant deviation in the results of calculations and experiments can occur if such is not done. Consequently, the entrainment ratio of a theoretical steam ejector relative to an actual one may be underestimated by 20-40% due to the numerical calculations for an ideal gas.

Most research using numerical simulation methods are carried out to optimize the design of jet ejectors for use in refrigeration cycles. According to the first studies on such a use of ejectors [42, 43], the replacement of compressors with ejectors in installations for the conversion of thermal energy into refrigeration increases the reliability of such systems due to the absence of moving parts. The exergy losses of a system with a compressor are equal to the compressor's electric power. By using an ejector instead of a compressor, exergy losses equal to the electric power of a primary pump plus the exergy of a heating source are obtained. The electric power of primary pumps is significantly lower because liquid is compressed instead of vapour: the heating fluid is usually cheap because it is industrially produced for the majority of systems. So, the consumed energy, though quantitatively more, is qualitatively less valuable. Moreover, the use of ejectors opens up many ways to improve the efficiency of refrigeration units by optimizing the characteristics of ejectors.

Papers [44-47] concentrate on the modernization of the nozzles of jet devices. Thus, study [44] recommends clarifying the calculation of the geometric

characteristics of nozzles. In particular, it is recommended taking the Mach number in the output section of the nozzle, which depends on the ratio of the areas of the output and critical sections of the nozzle when designing an ejector. An increase in the ratio of these areas does not affect the entrainment ratio, but may increase the degree of compression in a stage.

It is noteworthy that paper [45] considers critical section forms like an “ellipse”, a “square”, a “cruciform” and others in addition to the established form of the cross section of the nozzle “circle”. As a result of numerical simulation, it was found that a nozzle with a “cruciform” critical section has the highest entrainment ratio due to the intensification of the mixing process in the mixing chamber.

The regulation of the diameter of the nozzle throat depending on the required flow rate of the entrained flow was proposed in paper [46]. The adjustment is carried out via a movable rod placed coaxially with the nozzle and partially overlapping the supply of the working environment.

Furthermore, analysis of the influence of working pressure on the characteristics of the functioning of the ejector is presented in study [47]. It was experimentally shown that the entrainment ratio increases and then decreases with the increasing pressure of the primary fluid. At the same time, the entrainment ratio decreases linearly with a constant suction pressure and increasing pressure of the primary fluid.

Following research [50], numerical studies of jet devices are aimed at studying the geometric characteristics of nozzles. Moreover, it should be noted that there were two series of pressure shocks. The first one was in the entrance section of the mixing chamber, where the velocity of the entrained flow did not reach the speed of sound: in the second one, at the entrance to the diffuser, the entrained flow became subsonic again. Thus, increasing the flow rate of the primary flow shifts the second zone of jumps deep into the diffuser by increasing the velocity of the entrained flow in the mixing chamber. Similar results were obtained in study [51]. It was shown in [52] that a significant decrease in pressure shocks and the almost complete disappearance

of the second group of shocks is due to a change in the shape of the mixing chamber. Therefore, there are two groups of shocks that coincide with parts of the jet device, where the velocities of the entrained flow are subsonic. This statement is based on paper [53], where the results of numerical simulation match with experimental data. It was decided to combine the fixed shocks into two groups, which were dubbed “shock trains”.

1.3. METHODS OF CALCULATING JET DEVICES AND INTERMEDIATE EJECTOR COOLERS

Despite the external simplicity of the device of a steam ejector, the thermo- and gas-dynamic processes occurring in it are complex and have not been fully studied yet. The peculiarities of these processes are the subject of a large number of experimental and theoretical works by both Russian and foreign researchers [16-19, 22, 32, 33, 68-70].

Review of existing approaches to the calculation of ejectors

Currently, there are three trends in the design of steam-driven ejectors. One (theoretical) is based on separate consideration of the processes of expansion, mixing and compression of flows with a detailed quantitative assessment of losses at each stage. Therefore, the usual thermodynamic dependences of the outflow of gases and steam are used to describe the processes taking place. Kaula and Robinson [101] were the first to describe this theory in relation to the ejectors of steam turbine condensation plants. A. Radzig and M. Yanovsky made a number of additions to it. Later, the theory was developed and systematized by A. M. Kazansky and V. P. Blyudov. [15]

Detailed consideration of the processes in the individual elements of the ejector’s flow section (nozzle, mixing chamber, diffuser) is the merit of the methods in the theoretical trend. However, a number of assumptions reduce accuracy, so the

bulkiness of these methods becomes unjustified.

It should be noticed that a distinctive feature of the second research trend (semi-empirical) is the rejection of making a detailed assessment of the processes in separate parts of the ejector's flow section and the use of gas-dynamic functions in the calculation [18, 19, 31, 87]. The authors of these techniques derived calculation equations to determine the relationship between the geometric and gas-dynamic parameters in a number of basic sections of the ejector: in the critical section and at the nozzle exit, at the beginning and end of the mixing chamber and behind the diffuser. In these studies, calculated equations are derived, including through the use of gas dynamics [20]. Subsequently, the nature of physical processes in a steam ejector (limit modes) is modelled on this basis: the variable modes (characteristics) of both a single-stage and multistage ejectors are investigated, while the most economical (limit) mode is also stated. Thus, the ratio of the area of these flow sections is calculated assuming that in two sections of the flow part of the ejector (in the critical section of the nozzle and in the cylindrical part of the diffuser), critical (at the speed of sound) gas flow modes are realized. The determination of the axial dimensions of the jet pumps is carried out using experimental data and by introducing various correction factors. This approach significantly distinguishes it from the first trend and imposes some limitations associated with the possibility of calculating only those modes and structures for which the necessary empirical values are known.

Taking into account the complexity of gas-dynamic processes in a supersonic ejector, the authors of the third trend - the empirical one - reject the conclusions of cumbersome calculation equations. The empirical method of calculation is most fully developed by Wiegand [102]. This research is based on the results of studying a large number of steam ejectors. Wiegand found that the entrainment ratio of the ejector depends on three quantities: the pressure of the primary steam, the vapour pressure at the nozzle outlet and the pressure of the compressed mixture. Moreover, it is more convenient to express the steam consumption depending on the ratios

between these quantities, namely, the degree of expansion $E = P_{ps}/P_1$ of the steam in the nozzle and the compression ratio $\varepsilon = P_4/P_1$ of the steam-air mixture in the ejector from the practical point of view. Consequently, the entrainment ratio, which is equal to the ratio of the flow rate of the entrained vapour-gas mixture to the flow rate of the primary steam, is determined by the functional dependence (1.6):

$$u_\varepsilon = f(E, \varepsilon). \quad (1.6)$$

From this expression it follows that geometrically similar ejectors have the same performance characteristics under the same operating conditions. The functional relationship (1.6) can be used to design ejectors that remove clean steam, steam-air mixture, or air. The determined entrainment ratios are somewhat underestimated relative to the real ones. This leads to an increase in the flow rate of the primary steam per stage. According to V. Ramm [86], the reserve for steam consumption is 20–30%. Nonetheless, a more reliable operation of the calculated ejectors is ensured under production conditions.

Ramm assumes that a critical flow rate is reached in both sections (equal to the local speed of sound) in determining the main geometrical parameter of the ejector $F_{кр}/F_3$ ($F_{кр}$ is the nozzle throat area, F_3 the sectional area of the diffuser's cylindrical section). Therefore, it possible to use simple thermodynamic dependences:

$$F_{cr} = \frac{G_{ps}}{3600 \cdot 203 \cdot \sqrt{\frac{p_{ps}}{\upsilon_{ps}}}}, \quad (1.7)$$

$$F_3 = \frac{G_{ps} + G_{asm}}{3600 \cdot 199 \cdot \sqrt{\frac{p_4}{\upsilon_4}} \cdot \varphi}, \quad (1.8)$$

where, G_{ps}, G_{SAM} – consumption of the primary steam and the ejected mixture respectively, kg / h;

p_{ps}, p_4 – absolute vapor pressure in front of the nozzle and the mixture behind the diffuser, kgf / cm ^{2};

υ_{ps}, υ_4 – the specific volume of working vapor in front of the nozzle and in the mixture at the outlet of the diffuser (accepted for saturated steam at a pressure of p_0, p_4), m^3 / kg;

φ – correction factor, $\varphi = 0{,}95$,

203 and 199 – experimental coefficients of the authors.

Other examples of the empirical approach are design techniques of steam jet

ejectors based on a large number of experimental materials. These are presented in papers [22, 103, 104]. Currently, technique [103] is still used in EU countries by the developers of jet ejectors in various areas of technology. The advantage of empirical methods is the simplicity of calculation and reliability. The disadvantage is the limitations of their application.

It should be noted that a number of methodologies for calculating ejectors related to the semi-empirical and empirical trends became widespread due to the development of multistage air-suction devices for steam turbine installations in thermal power plants.

Technique of the Kaluga Turbine Plant (KTZ)

The considered method is based on a large amount of experimental data for two-stage ejectors. The data was obtained for the specific geometric characteristics of each stage, but they can be widely used in practice. A number of studies, such as VTI [16] and KTZ [22], confirmed that the technique is applicable to a wide range of variations in steam parameters, entrainment ratios and compression ratios for steam-driven ejectors.

As a result of processing a large amount of experimental data [22], a generalized diagram (Fig. 1.6) was constructed for calculating the stages of 2-stage steam jet ejectors. It should be noted that the diagram uses the data obtained when testing ejectors with a jet device made according to the type of schematic shown in Fig. 1.3 at the optimal distance of the nozzle from the mixing chamber. The use of the diagram greatly simplifies the calculation of the ejector stages and ensures the high reliability of the data, which is based on the results of numerous experiments. The most important characteristic of an ejector for given steam parameters is the ratio of the cross section of the cylindrical mixing chamber F_3 to the critical section of the working nozzle F_{cr} (the general geometric parameter of the ejector) (see Fig. 1.3):

$$F^* = \frac{F_3}{F_{cr}} = \left(\frac{d_3}{d_{cr}}\right)^2 . \quad (1.9)$$

The choice of this parameter largely determines the dimensions of the ejector stage.

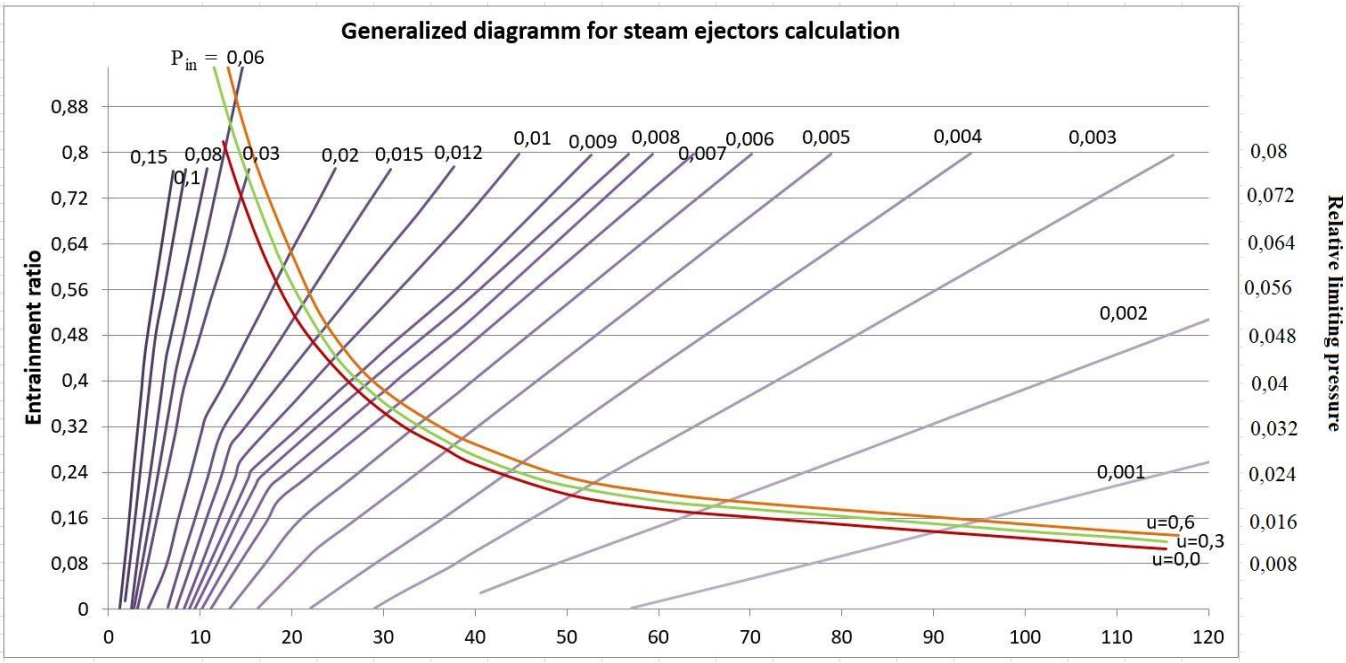

Fig. 1.6. The dependence of the entrainment ratio on the main geometric parameter of the ejector $F^*=F_3/F_{cr}$

This diagram shows the entrainment ratio of the stage. Moreover, the relative value of the counter pressure of the ejector stage $\overline{P_{lim}} = \frac{P_{lim}}{P_{ps}}$ and two types of dependencies are considered: $u = u(F^*)$ for P_{SAM} = const (ascending with F*, increasingly "broken" curves) and $P_{lim} = P(F^*)$ for u = const (descending curves).

Changing the flow rate of the primary steam could change the characteristics of a steam ejector. At the same time, an increase in steam consumption at any fixed position of the nozzle causes an increase in the compression ratio, and also leads to an increase in the suction pressure at low air flow rates. The efficiency of the ejector also decreases in the region of low suction pressures and increases in the region of elevated suction pressures with an increase in the flow rate of the operating steam. Thus, it is possible to obtain large amounts of ejected air for ejectors of any size in the area of elevated suction pressure if the consumption of primary steam is

increased. Consequently, it is possible to reduce capital costs by reducing the size of the ejector, but this, in turn, leads to an increase in operating costs.

The required airflow rate at specified suction and compression pressures can be obtained with various ratios of the nozzle positions and steam flow rates. However, the required performance is ensured with a minimum flow of primary steam only at the optimal ratio of these parameters.

Nevertheless, it should be mentioned that the application of the KTZ calculation method (which is based on the generalization of a large number of tests of two-stage ejectors) is scarcely applicable to the development of three-stage ejectors.

Technique of the Kharkov Turbine Plant (HTZ)

Following the study [106], this technique is based on an approach that uses an estimation of flow parameters in the critical sections of a jet device. The initial data are the parameters of the primary steam, the vapour pressure in the condenser, the temperature of the circulating water at the inlet to the condenser and the amount and temperature of the main condensate entering the ejector coolers.

The calculation involves the cost of the primary steam at each stage and the compression ratio of the mixture, which is taken as the same pre-set values for all stages of the ejector (obtained on the basis of preliminary estimates). Moreover, it should be noted that the value of the heat transfer coefficient in the heat exchanger is taken as specified during the calculation of the ejector coolers. The diameters of the critical section and the outlet of the nozzle, as well as the diameter of the diffuser's cylindrical part, are calculated. The other geometrical characteristics of the jet devices are not presented.

It is found that this method cannot be used for the design of a three-stage ejector. This might be explained by the fact that the input data are the values that should be determined by calculation — the flow rates of the primary steam and the

compression ratio of the steam-air mixture at each stage. In addition, the methodology does not present algorithms for calculating many geometrical parameters of the ejector's jet device.

The VTI method of calculation

This technique is presented in a number of publications, which include the theoretical and experimental results of numerous studies devoted to ejectors [16, 18, 20, 31, 105]. The calculation's task is to determine the main dimensions of the flow parts of the steam jet device, as well as the surface and layout of its heat exchanger. Moreover, it should ensure the required performance when removing non-condensable gases with the given parameters of the vapour-air mixture ejected. This problem is solved with a varying distribution of compression degrees in the ejector's steam jet device and with different heat exchanger surfaces, meaning different degrees of condensation of steam in them.

The calculation of the ejector is accomplished in several stages. In this method, three groups of calculations are carried out for each stage: the parameters of the ejected medium, the primary steam and entrainment ratio; the ejector cooler; and the limit backpressure of each ejector stage.

In the first stage, the optimal costs, parameters and geometrical dimensions of the steam jet device of each ejector stage are determined. They require the suction of a given amount of air.

In the second stage, a calibration calculation of the heat exchanger system of the adopted design is carried out, with the initial data corresponding to the optimum costs and parameters of the vapour-air mixture determined in the first stage. The costs and parameters of the vapour-air mixture along its movement in the annular space of the heat exchanger and the costs and heating of the cooling water in the heat exchanger tubes are determined in the calculations. It is common to choose the design of the heat exchanger when the degree of steam condensation obtained as a

result of the calculation in the second stage is equal to the stage adopted for designing the steam jet device in the first stage of the ejector.

Accordingly, in the third stage, the limiting entrainment ratio is calculated at the normalized airflow, while the limiting back pressure of the first stage is determined. In the same stage, the characteristics of the primary vapour jet in the receiving chamber of the ejector's first stage are determined with reference to the second limiting flow mode (entrainment ratio). Based on these calculations, the results of studies of the flow of the submerged jet are used in accordance with the theory proposed in research [20]. This makes it possible to estimate accurately the flow modes of the medium in the mixing chamber of jet devices.

It is also stated that the minimum total flow rate of the primary steam per ejector is the criterion for optimizing the distribution of a pressure increase in the steam jet device of the ejector. It is appropriate to apply a combination of the degree of increase in the pressure of the vapour-air mixture. This method ensures the minimum consumption of the primary steam per ejector.

A system of 20 equations is widely applied for the further calculation of the geometrical dimensions of the steam ejector unit. To design the heat exchanger (intercooler), a system of 19 equations is used. Consequently, a system of 37 equations should be used to determine the maximum back pressure in stage I with a nominal air flow rate. A detailed description of the equations is given in studies [18, 31, 32]. Thus, more than 75 equations have to be solved when using this method.

Although massive, the VTI method is the most complete and most recent method of designing main turbine ejectors. However, some authors, such as in paper [18], emphasize that the technique is valid only for certain modes and geometrical characteristics of steam-driven ejectors.

The calculation method of MEI

It is crucial to highlight the technique [19] developed at the Department of Moscow Power Engineering Institute under the guidance of Professor Deich. This

method is also based on the definition of gas-dynamic functions in critical sections of a steam jet apparatus [18]: it is similar to the VTI technique. The pressure in the first stage's mixing chamber and the operating pressure behind the last stage's diffuser are found when using this method to design a multistage ejector. Hence, these values determine the total compression ratio of the ejector. In this case, a question arises about the number of stages and the optimal distribution of compression levels in individual stages. Moreover, this issue is not resolved generally. Thus, it is necessary to carry out a number of variant calculations in order to choose the best option in each particular case.

The technique assumes that the axial velocity of the ejected medium is negligible. Moreover, the pressure and velocity fields in sections 1–1 and 3–3 (Fig. 1.3) are uniform and the forces of gas friction against the wall of the flow section are insignificant. Furthermore, a force effect of the wall of the inlet section on the jet is absent. In this case, the impulse equation and the continuity equation for sections 1–1 and 3–3 are written as:

$$\frac{G_1}{g} w_{1_m} + \mathrm{P}_1 F_1 + \mathrm{P}_k (F_2 - F_1) = \frac{G_1 + G_3}{g} w_{3_m} + \mathrm{P}_2 F_2, \tag{1.10}$$

$$G_3 = G_1 + G_2 = F_3 \cdot w_{3_m} \cdot \mathrm{P}_3, \tag{1.11}$$

where the index "m" means that the velocities are theoretical, that is, they correspond to the accepted assumptions; g – gravity acceleration.

According to the substantial distance of the flow mix when turbulence is high, it is assumed that the temperature field in section 3–3 is uniform. Therefore, the critical flow velocities averaged by the energy equations $a^*_э$, amounts of movement $a^*_{кд}$ and continuity $a^*_н$ are equal. The method [19] also uses established gas-dynamic relations [18].

The technique allows one to find the entrainment ratio u for the given conditions of the ejector. Using equation (1.10), the general geometric parameter of the ejector stage $\frac{F_р}{F_з}$ should be determined (Fig. 1.3):

$$\frac{F_2}{F_{*c}} = \frac{q_0}{\left(\frac{k_1+1}{2}\right)^{\frac{1}{k_1-1}} \cdot p_к} \times \left(A(1+u)\sqrt{r\tau}\,\psi\,(\lambda_3) + \zeta - \psi(\lambda_1)\right) + \frac{F_1}{F_{*c}}, \qquad (1.12)$$

where $A = \sqrt{\frac{k_1}{k_3}\frac{k_3+1}{k_1+1}}$ – coefficient depending on the isentropic indices of the primary steam in cross section 1–1 (k_1) and the mixture in cross section 3–3 (k_3);

$r = \frac{R_3}{R_1}$ – ratio of gas constants;

R_1 and R_3 – gas constants of working fluid and mixture;

$\tau = \frac{T_{03}}{T_{01}}$ – stagnation temperature ratio in cross section 1–1 and in cross section 3–3;

$\psi(\lambda_3) = \frac{1}{\lambda_{зн}} + \lambda_{зн}a$ – function (reduced pulse), depending on speed $\lambda_{зн}$ and the non-uniformity of the velocity field in section 3–3;

$\lambda_{зн}$ – dimensionless velocity averaged by the continuity equation in a section of 3–3;

$\omega_{зн}$ – the actual average speed of the mixed flow in section 3-3;

$a_{*зн}$ – critical velocity in section 3–3, averaged by the continuity equation;

$\alpha = \frac{2k_3\nu_1 - (k_3-1)\nu_2^2}{k_2+1}$ – coefficient depending on the non-uniformity of the velocity field in section 3–3 (where $\nu_1 = \frac{\lambda_{зкд}}{\lambda_{зн}}$; $\nu_2 = \frac{\lambda_{зэ}}{\lambda_{зн}}$);

F – cross sectional area; the index at F indicates the location of the section.

The main difficulties arise with a preliminary assessment of the individual quantities included in the calculated equations when using the technique. These values include the ratio of stagnation temperatures and the magnitude of the function ψ (λ_3), depending on the non-uniformity of the velocity field in section 3–3.

Technique [19] is based on determining the limiting entrainment ratio at each step according to the equation of the third limiting mode. Moreover, the costs of steam per ejector are slightly overestimated.

1.4. THE INFLUENCE OF OPERATING CONDITIONS ON THE EFFICIENCY OF EJECTORS IN STEAM CONDENSERS

The general ejector of a condensing unit is a complex system; thus, there are some factors that determine the interaction with the condenser of a steam turbine unit [3, 6, 17, 108], such as the parameters of the primary steam, the suction of the steam-air mixture and the cooling condensate.

When discussing the operation of the ejector, it is important to look at its characteristic curve. The nominal characteristic of a multistage ejector is a relation of its secondary flow rate to the suction pressure at this flow rate in the first stage of the ejector. An example of a classical characteristic is presented in Fig. 1.7.

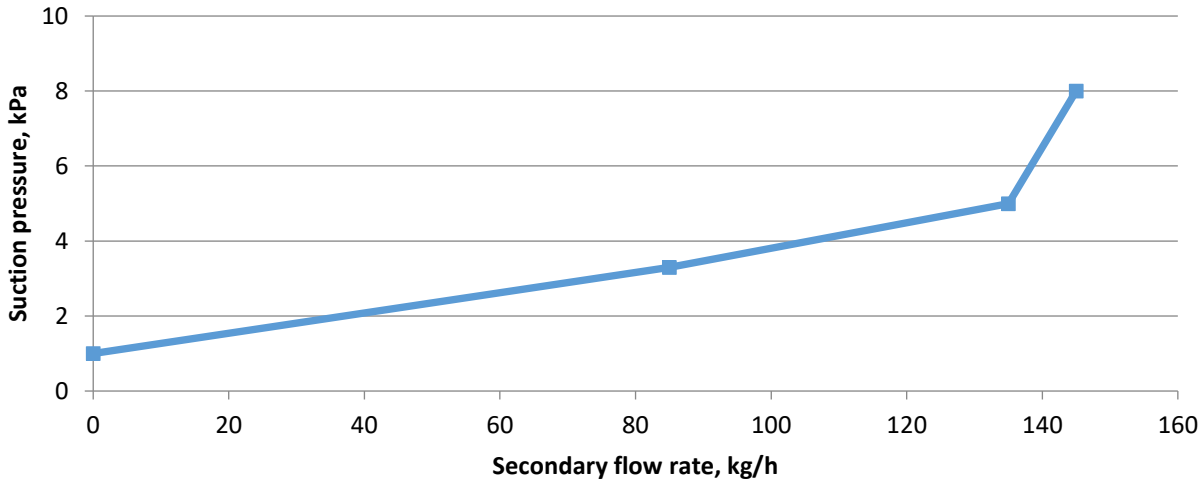

Fig. 1.7. The characteristic of an ejector.

As can be seen from the figure, the characteristic consists of 2 or 3 parts. The right part with a big incline angle corresponds to the off-design mode of the ejector, when a small addition of the flow rate increases the suction pressure to an extreme extent. The left part can be linear or consist of two parts with a very small angle between them. This cross point, according to [18], means moving the “effective area” from the narrow part to the cylindrical or back parts. The cross point of the two parts of the graph determines the capacity (efficiency) of the ejector – the maximum flow rate which can be removed by the ejector. Most existing design methods are aimed at calculating precisely this point.

Primary steam parameters

The influence of primary steam parameters on ejector performance is considered in studies [22, 32, 68, 100, 108, 111-115]. It should be noted that the main parameter of the primary steam is the pressure when choosing a source [18, 20]. According to research [113, 114], the amount of superheating of the steam relative to the saturation temperature at its pressure does not significantly affect the operating parameters of the ejector. Moreover, an increase of the magnitude of

overheating leads to a decrease in the flow rate of the primary steam through the nozzle due to the increase in specific volume. At the same time, the primary steam at a higher temperature has more energy and increases the entrainment ratio. It is observed that a reduction in steam consumption and an increase in the entrainment ratio balance each other out (provide an equal reverse effect). However, the influence of steam temperature on the intercooler is not observed.

According to [115], the first multistage steam jet ejectors at the LMZ plant (EP-3-600, EP-2-400) were replaced with ejectors with lower vapour pressure. Firstly, these ejectors were designed according to the pressure of the primary steam P_{ps} = 1,3 MPa [16,18]. When replacing these ejectors, the primary steam pressure was decreased to P_{ps} = 0,49 MPa. Ejectors with such a characteristic are most often installed on modern turbines. This can be explained by the fact that steam taken from the top of deaerators (popular source) can used at a pressure of about P_{ps} = 0,6-0,7 MPa [32, 88] as a primary fluid.

UTZ and HTZ developed three-stage steam jet ejectors for the pressure of the primary steam P_{ps} = 0,49-0,51. KTZ's ejectors for NPP turbines are an exception. The working vapour pressure of these ejectors is up to P_{ps} = 0,82 MPa [32,88-90].

It is interesting to note that some ejectors were designed for specific operating conditions and sources of primary steam. The examples are a number of KTZ ejectors, which were designed for a working vapour pressure of P_{ps} = 1,6 MPa [22, 32, 91].

There are a number of works related to the transfer of ejectors to low pressures of primary steam.

According to [116], the authors performed calculations for a jet device with a pressure of primary steam P_{ps} = 0,5 MPa, as well as proposed solutions for the implementation of new jet apparatus for the EP-3-600 ejector (the design pressure of which is P_{ps} = 1,3 MPa). At the same time, the replacement of jet devices with new ones designed for a pressure of P_{ps} = 0,5 MPa is carried out without any structural changes to the ejector case. This is explained by the fact that although the

output diameter of the first stage nozzle is significantly increased, the nozzle was designed in two parts, which are assembled together. The outlet part with the high outlet diameter is connected to the inlet part from the suction chamber instead of inserting it from the top.

It is interesting to note that, according to [117], the calculated pressure values of the primary steam supplied to the ejectors during the operation are underestimated with respect to the actual values. Based on data provided in the study [18], this can lead to a deterioration in the efficiency of the ejector (an increase in the suction pressure and the lowering of the pressure below the calculated one).

Coolant Condensate Parameters

An important feature of multistage ejectors is the temperature of the main condensate of the turbine, which is used as cooling water for the general ejectors (Fig. 1.8) [31, 32]. The temperature change is related to the fact that the ejector coolers are the first stage in the system of regenerative turbine heating [17, 88, 105].

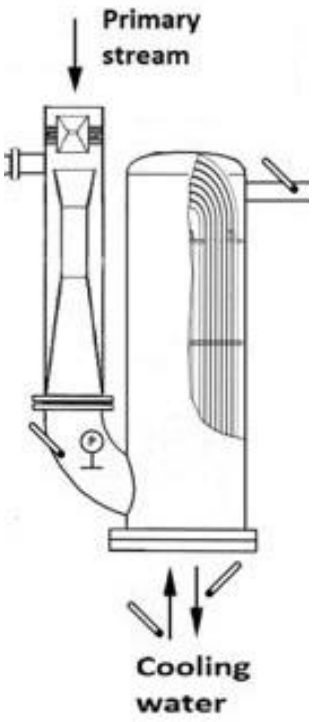

Fig. 1.8. Scheme of ejector steam and cooling water supply.

There are a number of papers [69,70], including the study [119], that propose designs for condensing heat exchangers, but they are not applicable to the design of intermediate coolers due to the incomplete condensation of steam.

According to the known methods for designing multistage ejectors [18, 19], the fixed value of the fraction of steam condensing in the previous intercooler is 95% during calculation of the second and subsequent stages of an ejector. Thus, it is assumed [88] that the temperature of the cooling condensate does not affect the condensation process up to the limit values specified in [105].

According to [68], there is a model for calculating the dependence of the suction pressure of the following chilling stages in terms of the cooling area. Based on this model, the temperature of the cooling condensate at the inlet is taken into account only to determine the temperature and pressure in the cooler. Moreover, it is not considered that the intercooler is a heat exchanger with an incomplete condensation of steam.

It is stated in [1, 3, 6] that the pressure in the condenser is sufficiently high (more than P_c = 5 kPa) for a number of cogeneration turbines in design operation modes (cogeneration modes). It is worth mentioning that in such models the temperature of the main condensate is increased at the inlet to the ejector coolers. Consequently, this may lead to a deterioration of the condensation process. Based on [32], the most significant effect is in those modes where the temperature of the cooling condensate is close to or exceeds the saturation temperature, corresponding to the pressure created in the first stage in the intercooler. In this case, the proportion of condensing steam tends to zero: all steam enters the next stage, thereby overloading it.

Another interesting feature of ejectors in cogenerating turbines is the much smaller effect of pressure in the condenser on the efficiency of the turbine, as well as the elevated temperature of the cooling condensate [88, 120].

According to [105], it is necessary to ensure the adequate flow of cooling condensate for the normal operation of the ejector. Thus, based on recommendations

from research [88,108], the heating in the coolers should not exceed $\Delta t = 5\ ^\circ C$ while ensuring the nominal flow rate of the main condensate to the ejector.

Proposals to replace cooling water ejectors with a collector of chemically treated water or circulating water as a colder source are observed in engineering practice. The use of circulating water should lead to contamination of the inner surface of the tubes, especially in the U-shaped bends that are the basis of most existing structures. The use of chemically treated water is also not rational because its temperature exceeds 35-40°C, i.e. higher than the temperature of the main condensate in the design modes of the turbine. At the same time, the required flow rate of cooling water for ejectors exceeds the flow rate of chemically treated water at most thermal power plants.

Parameters of the steam-air mixture

Another parameter that can affect the functioning of the ejector is the temperature of the vapour-air mixture drawn from the condenser [100, 120]. An increase in the temperature of the aspirated medium determines the increase in the vapour content of the mixture aspirated from the steam turbine condenser. It is known that an optimal location for the steam-air mixture suction nozzle from the condenser (from the air-cooler zone) is necessary to ensure the minimum temperature of the aspirated medium [22, 88, 108].

The results of an experimental study of the effect of secondary stream temperature on the suction pressure of an ejector are presented in [100]. In this paper, experimental studies of an ejector on the test-bench were performed. It was possible to use air, steam or vapour-air mixture as entrained gases. Thus, a conclusion about that the position of the “effective area”, which is the critical section of the entrained flow (where it reaches the speed of sound due to interaction with the primary flow), was formulated. This position is changed when the parameters of the aspirated fluid

in the ejector are changed. Thus, a revision of the existing methods for calculating the “effective area” position is required.

1.5. RESULTS

1. The existing designs of serial ejectors installed in UTZ, HTZ, LMZ and KTZ have various design features. These features affect the efficiency and reliability of ejector operation. It is necessary to conduct research aimed at improving the reliability of multistage ejectors by developing new technical solutions. It is advisable to create a new, more modern design for a multistage ejector, taking into account the existing shortcomings of serial designs.

2. It is observed that a significant amount of studies aimed at optimizing the functioning of jet devices propose various technical design solutions, i.e. changing the geometric parameters and the axial position of the nozzle, upgrading the shape of suction chambers and mixing chambers, and others. It is necessary to conduct studies of gas-dynamic processes via numerical methods in order to assess the effectiveness of the change in traditionally accepted forms of jet device.

3. An analysis of the most well-known methods for designing gas-driven ejectors is conducted. Manufacturers of steam turbines use these methods. Accordingly, a number of techniques cannot be adapted for designing multistage ejectors due to accepted assumptions and inaccuracies. It is crucial to develop a refined method of design that fully takes into account all the parameters of the gas-dynamic and thermo physical processes in a multistage steam ejector.

Based on this review, the following research objectives were formulated:

- Surveying and industrial testing of the many types of steam-driven ejectors in various operating conditions of TPPs should be conducted to assess their performance and reliability as part of condensing units.

- Analysis and generalization of the geometric characteristics of serially manufactured steam ejectors.
- Studies of gas dynamics in the jet devices and intercoolers of multistage steam jet ejectors.
- Development of a refined method for designing multistage steam jet ejectors in steam turbines based on a compilation of test results and analysis of the geometric characteristics of serial ejectors and numerical studies of gas dynamics in jet ejectors.
- Development of a new multistage steam-driven ejector with increased capacity for steam turbine condensers and experimental studies on the ejector under operating conditions at thermal power plants.

Chapter 2.

DEVELOPMENT OF A REFINED DESIGN METHOD FOR MULTISTAGED STEAM-DRIVEN EJECTORS IN STEAM TURBINE CONDENSATION INSTALLATIONS

2.1. ANALYSIS AND GENERALIZATION OF EXPERIMENTAL RESEARCH ON SERIAL EJECTORS OF STEAM CONDENSATION UNITS

As part of the dissertation research, more than 100 serial ejectors were surveyed: extended industrial tests of 36 STU ejectors under various operating conditions at TPPs were also conducted.

The survey included disassembling and inspecting jet devices, pipe systems and the cases and water chambers of ejectors from various manufacturers: UTZ (EP-3-2, EP-3-3), LMZ (EP-3-600, EP- 3-700, EP-3-750), HTZ (EPO-3-25/75, EPO-3-50/150) and KTZ (EO-50). In the examined ejectors, jet devices are built into a single case with intercoolers. According to the results of the analysis and generalization of the identified defects, the reliability of the operation of serial ejector designs was evaluated.

Industrial tests of ejectors included the refinement of the experiment procedure, the refinement of the measurement scheme, the estimation of instrument errors, and obtaining performance characteristics and other parameters of the operation of multistage steam ejectors. In the process of testing in various operating conditions, the following parameters of ejector operation were measured: primary steam pressure, flow rates and temperatures of the cooling condensate and temperature of the drainage removed from the intermediate coolers.

2.1.1. ANALYSIS OF THE RELIABILITY OF SERIAL EJECTORS

For the development of technical solutions for improving ejector designs, analysis of the damage to and main disadvantages of serial multistage steam ejectors

was conducted. The analysis and synthesis of statistical information for the 25-year period of operation of more than 500 turbines with a capacity ranging from 100 to 500 MW was carried out according to the data of [122,123] and the data obtained by the author. Analysis of the typical damage sustained by serial ejectors was carried out directly at CJSC Nestandartmash during the ejector repair.

Fig. 2.1 shows the distribution of damage (failures) among the various technological subsystems of STU [122,123]. The largest percentage of failures (37%) is accounted for by the turbine itself, while up to 23% of failures are caused by damage to the feed pump and 13% and 15% by the condensing unit and the turbine regeneration system, respectively. 9% of failures are caused by pipelines and fittings and 3% by the oil system.

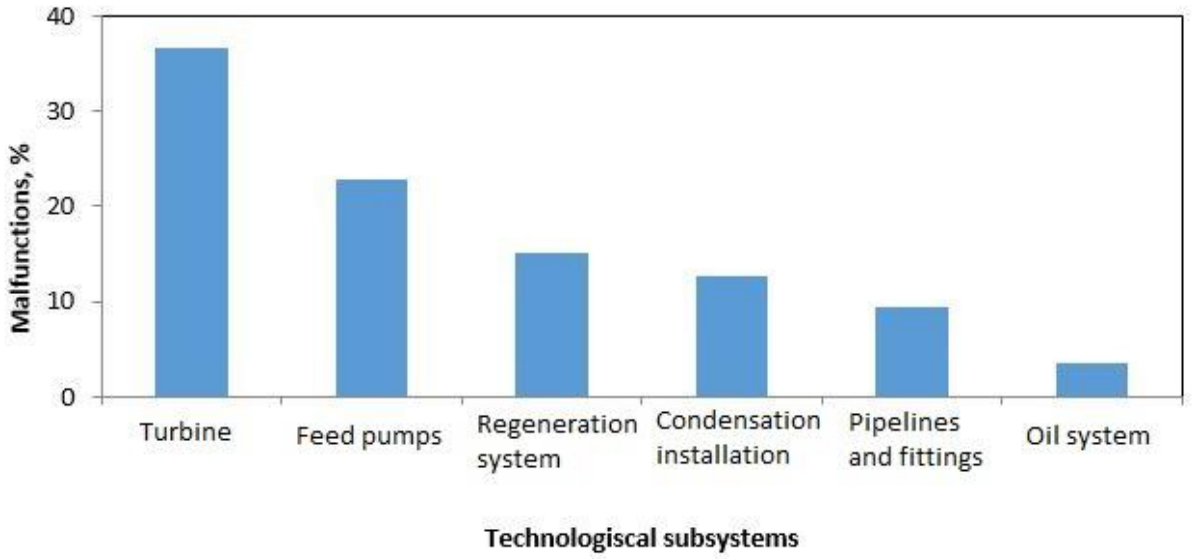

Fig. 2.1. Damage distribution (O, %) by technological subsystems of a steam turbine plant

Analysis of damage (failures) in the elements of the condensing unit shows that the largest share of failures (46%) belongs to condensers, then circulation pumps (24%), ejectors (19%) and condensate pumps (11%). Concerning the ejectors, we estimate that 19% of 13% is about 2.5%. Although this figure does not seem very high, we should consider that almost every ejector failure causes the turbine plant to stop, which is a huge loss.

This analysis of failures of the condensing unit's equipment is provides for damage which stops the STU from functioning (Fig. 2.2). A somewhat different picture arises in such an analysis. Up to 56% of such failures are caused by condensers, while 23% of shutdowns are connected with ejector failures; the share of circulating and condensate pumps accounts for 10–11% of cases.

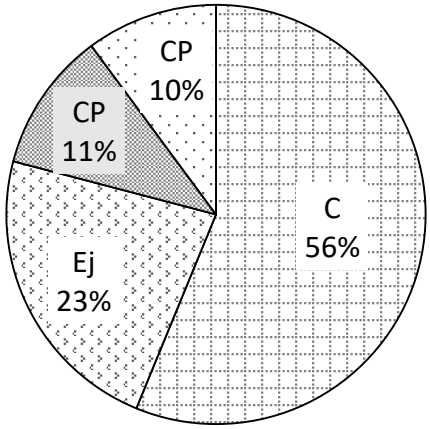

Fig. 2.2. Distribution of failures in the elements of a condensing unit, causing a shutdown of the STU: C - condensers, CP - condensate pumps CP - circulation pumps, Ej - ejectors

It should be noted that almost every ejector failure (up to 96%) causes the turbine to stop. This can be explained by several facts. Firstly, according to rules of the technical operation of TPPs [64], it is recommended to operate them with one general ejector switched on. The second ejector (usually there are two) should be switched off for overall efficiency and kept as a reserve. However, as the failure of the ejector leads to the turbine to stop in a minute or less, the operational staff has no time to switch the reserve ejector on. Secondly, as was mentioned before, the technical state of the turbines is very low due to elaboration of existing resource. This leads to large amounts of air into the LPP which cannot be removed by existing ejectors – these ejectors thus suffer from much reduced capacity. In such cases, the operational staff usually uses both ejectors, with none in reserve. When one of the

ejectors is damaged, the turbine stops. These are the most popular reasons behind the shown statistics.

The generalization of the data [122,123] and the author's data showed that the specific number of ejector failures per turbine per year is, depending on the type of turbines, from 0.036 to 0.098.

As can be seen from the above analysis, ejector reliability is of great importance for the reliable operation of a STU condensing installation; the effect of ejectors is more significant than that of circulating or condensate pumps.

As shown in Chapter 1, in most general steam ejectors installed on Russian turbines from various manufacturers, the jet devices are installed into the same case as the intercoolers. As a result of a survey of more than 100 ejectors, the main deficiencies in ejector designs were revealed. These lead to the appearance of defects during operation and repairs and, as a result, the following equipment failures:

- destruction of the internal enclosures of the coolers, which leads to abrasion of the tubes (heat exchange surfaces) when interacting with elements of the enclosures (for EP-3-2 and EP-3-3 UTZ ejectors);
- erosion of the mixing chambers and diffusers (material - black steel), which causes a decrease in the degree of compression in the diffuser;
- loss of tightness in the joint between the tube plate and the body partition between the coolers (washing of the gasket), which leads to the flow of a steam-air mixture between the coolers;
- formation of fistulas in the welds of the ejector body.
- corrosion-erosion and vibration destruction of the cooler surface tubes;
- depressurization of the rolled connection of tubes in the cooler tube plates;
- interruption of tightness between the nozzle chamber and the case;
- misalignment of elements of the jet apparatus due to design flaws in the diffuser mount;

- overflow of the ejector body with condensate due to insufficient flow area or an improperly organized drainage scheme for draining condensate from the ejector stages, as well as due to depressurization of the rolled connection of tubes in the cooler tube plates;
- nonobservance in the operation of the jet apparatus due to the removal of scale and hail on the ejector nozzles;
- erroneous assembly of the jet device after the repair of the ejector due to the mismatch of the nozzle with the number of the stage, unreliable fixation of the mixing chamber, etc.;
- corrosive deterioration of the branch pipes of ejectors with portable coolers (EPO-3-135) in areas with stagnant condensate.

Taking into account the identified design flaws encountered in various serial ejectors, a number of new design solutions have been developed for multistage ejectors, especially in the design of intercoolers. It is proposed to use a design with external intercoolers, since this is one of the most reliable and maintainable.

2.1.2. RESULTS OF INDUSTRIAL TESTS OF EJECTORS

The results of industrial tests of 36 serial ejectors under the operating conditions of 17 various thermal power plants with turbines with power ranging from 50 to 500 MW are summarized here. The tested ejectors are presented in Table 2.1.

The tests were carried out with cooling condensate temperatures varying from 24°C to 54°C. In most TPPs, the temperature of the cooling condensate is 40°C or more.

It should be noted that the tested EP-3-600M ejector is a modernized EP-3-600. Thanks to modernization, the ejector now works at the reduced working steam pressure of P_{ps} = 0.49 MPa: the jet devices were replaced with new ones according to recommendations [116] and the author's design.

Table 2.1

Manufacturer	Ejector type	Primary steam pressure, MPa	Primary steam consumption, kg/h	TPP	Turbine	CC temperature, °C	Number of ejectors	№ Turbine unit
UTZ	EP-3-2	0.49	850	Kazan TPP-2	T-50-130 UTZ	40	2	7,9
				Krasnoyarsk TPP-2	T-100-130 UTZ	44-46	2	1
				Nizhnekamsk TPP-1	T-100-130 UTZ	40	1	5
				Chelyabinsk TPP-2	T-100-130 UTZ	52	1	3
				Petrozavodsk TPP	T-110/120-130 UTZ	41-42	2	2,9
				Tobolsk TPP	PT-135/165-130 UTZ	45	1	1
				Nizhnekamsk TPP-2	PT-135/165-130 UTZ	54	2	1
	EP-3-3	0.49	850	Moscow TPP-23	T-250/300-240 UTZ	37	2	5,6
				South TPP-22 (SPb)	T-250/300-240 UTZ	42-45	3	1
LMZ	EP-3-600	1.27	600	Krasnoyarsk TPP-1	PT-60-90 LMZ	35	2	9
	EP-3-600M[1]	0.49	700	Kazan TPP-2	T-50-130 UTZ	40	1	9
				Urussu SDPS	PT-25-90 LMZ	45	1	4
				Verhnii Tagil SDPS	K-100-90 LMZ	43-46	3	1,3,4
				Verhnii Tagil SDPS	K-200-130 LMZ	24-27	2	8,9
				Krasnoyarsk TPP-1	IIT-65/75-90/13	33	1	9
				MMK TPP	T-50/90/13 LMZ	27-43	1	3
	EP-3-700	0.49	700	Kazan TPP-1	PT-60/75-130/13 LMZ	46	2	5,6
				Verhnii Tagil SDPS	K-200-130 LMZ	24-27	2	8,9
				Shatura SDPS	K-200-130 LMZ	24	1	1
HTZ	EP-3-25/75	0.51	800	Tobolsk TPP	Dearator	39	2	4
	EP-3-50/150	0.51	2100	Troitsk SDPS	K-500-240 HTZ	35	2	8

[1] The upgraded EP-3-600 ejector is operating at the reduced working steam pressure of R_{ps} = 0.5 MPa due to the replacement of jet devices.

Within the framework of the tests carried out, the performance characteristics of the ejectors were obtained - the change in the suction pressure in each ejector stage depending on the consumption of “dry” (atmospheric) air admitted into the ejector.

Industrial tests were carried out in accordance with recommendations from [105]. At the same time, the suction pressure of each stage was measured using absolute pressure sensors, along with working steam temperature, cooling condensate and intercooler drainage using an infrared pyrometer and resistance thermometers. A detailed description of the instruments used in the measurements, as well as an estimate of the measurement errors are presented below in the description of the measurement scheme of the new EPO-3-80 ejector (chapter 3.4).

For industrial testing, the ejectors are disconnected from the condenser in the steam-air mixture suction line. The supply of “dry” atmospheric air to the ejector was realized from the machine hall through calibrated flow washers with critical outflow. The change in the flow rate of air drawn in was carried out in increments of about 10 kg / h. During stable operation, with each value of the “dry” air flow rate, the pressure in the receiving chambers of each stage were fixed, as well as the temperature of the cooler drains and the temperature of the cooling condensate at the inlet and outlet.

For comparison and analysis of test results, the studied ejectors were grouped by type and manufacturer. Thus, the EP-3-2 and EP-3-3 ejectors have identical jet apparatuses, although they differ slightly from each other in certain areas (the designs of the water chambers and the steam-air mixture supply pipe in stage I); nonetheless, they remain comparable. In Fig. 2.3, as an example, a comparison of the nominal characteristics of the EP-3-2/EP-3-3 ejectors with the performance characteristics of the EP-3-3 (Southern TPP-22) and EP-3-2 (Tobolsk TPP) ejectors is presented. The performance characteristics are fixed at a nominal working steam pressure of P_{ps}=0,49 MPa and an increased pressure of P_{ps}=0,77 MPa. The tests were carried out at cooling condensate temperatures of T_{cc} = 40-45°C.

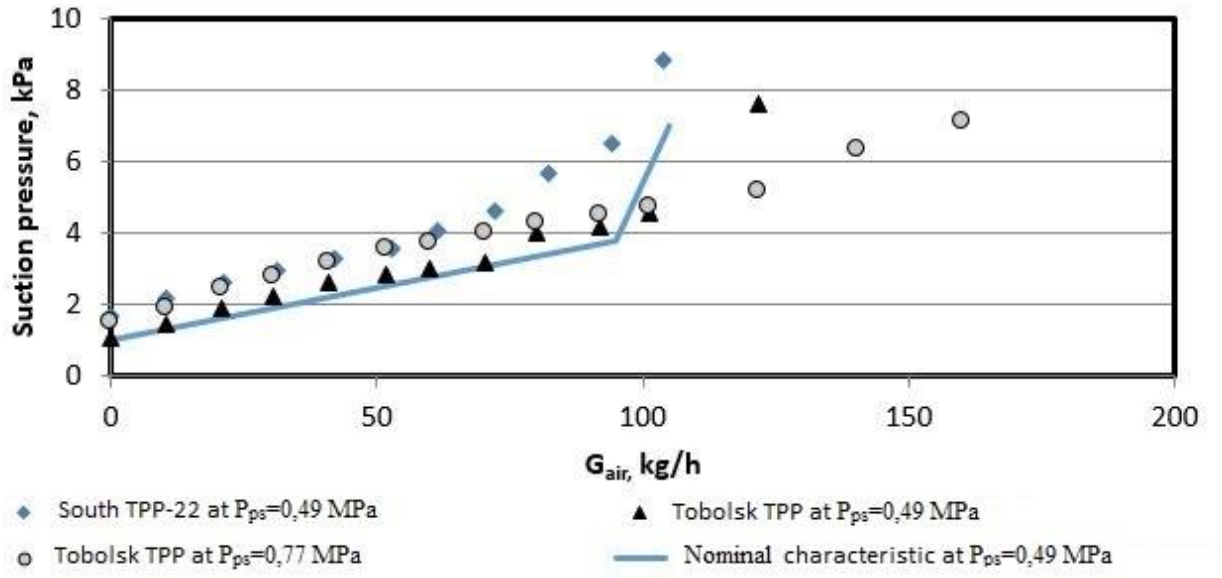

Fig. 2.3. Comparison of the nominal and performance characteristics of EP-3-2 and EP-3-3 ejectors

According to the comparison of the characteristics with working steam pressure of P_{ps}=0,49 MPa, it can be seen that the experimental data is higher than the nominal characteristics for ΔP = 0,5 kPa with an air flow rate of G_{air} = 60 kg/h in the EP-3-3 South TPP-22 ejector and up to G_{air} = 100 kg/h for the EP-3-2 ejector of the Tobolsk TPP. The ejectors' performance coincides with the nominal capacity G_{air} = 95 kg/h. With an increase of working steam pressure from P_{ps}=0,49 MPa to P_{ps}=0,77 MPa, the capacity of the ejector increases to G_{air} = 120 kg/h.

The geometrical characteristics of the jet apparatus of the EP-3-2, EPO-3-135 and EPO-3-200 ejectors are similar. In Fig. 2.4, a comparison of the nominal characteristics of these ejectors is presented. The nominal characteristics were obtained experimentally at the plant at a working steam pressure of P_{ps}=0,49 MPa.

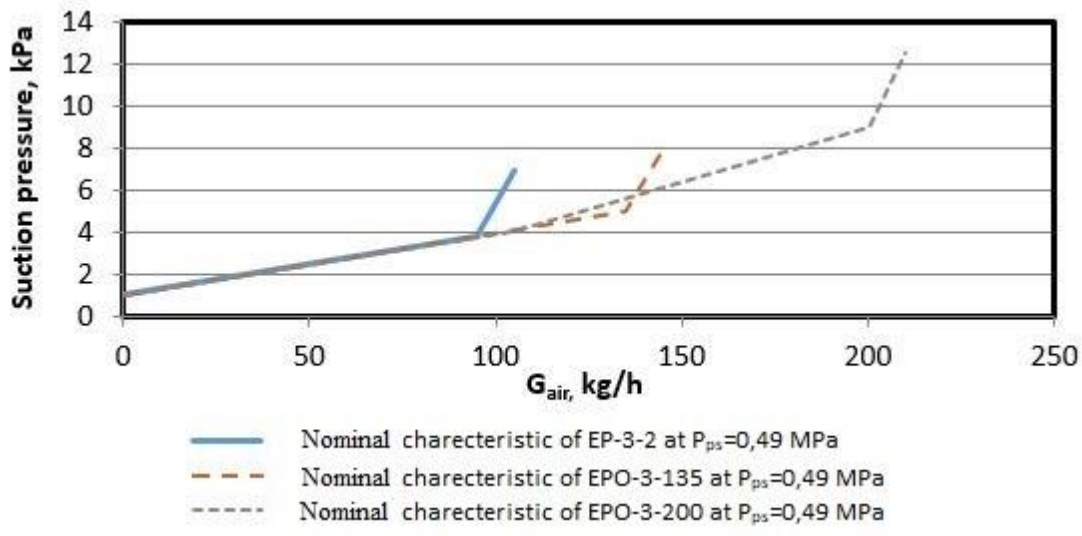

Fig. 2.4. Comparison of the nominal characteristics of UTZ ejectors

The capacity of the EP-3-2 ejector, G_{air} = 95 kg/h, is significantly less compared to the EPO-3-135 and EPO-3-200 ejectors (G_{air} = 135 kg/h and G_{air} = 200 kg/h, respectively). At the same time, an increase in the performance of the EPO-3-135 and EPO-3-200 ejectors is achieved with increasing of the suction pressure. This means that when working with an increased flow rate of sucked air, the EPO-3-135 and EPO-3-200 ejectors do not provide greater under-pressure and their use makes sense only when the air flow rate is higher than the capacity of the EPO-3-2 and EPO-3-3 ejectors. It is reasonable to suppose that the increased capacity of the EPO-3-135 and EPO-3-200 ejectors is achieved due to the fundamentally different design of the intercoolers [88]. The advantage of the EPO-3-135 ejector over the EPO-3-200 ejector is that about G_{ps}= 50 kg/h of working steam pressure is saved (according to the nominal documentation).

In the nominal characteristics of the EPO-3-200 ejector there is a fracture point at G_{air} = 105 kg/h. Such break points are found in a number of performance characteristics and may be associated with the transition of the ejector from one limiting mode to another (moving the critical section from the tapering part to the cylindrical part or back).

In Fig. 2.5, the performance characteristics of the EP-3-700 LMZ ejector at the Kazan TPP-1 and Kazan TPP-2 at a working steam pressure of P_{ps} = 0.49 MPa are presented. The temperature of the cooling condensate is t_{cc} = 39-46°C.

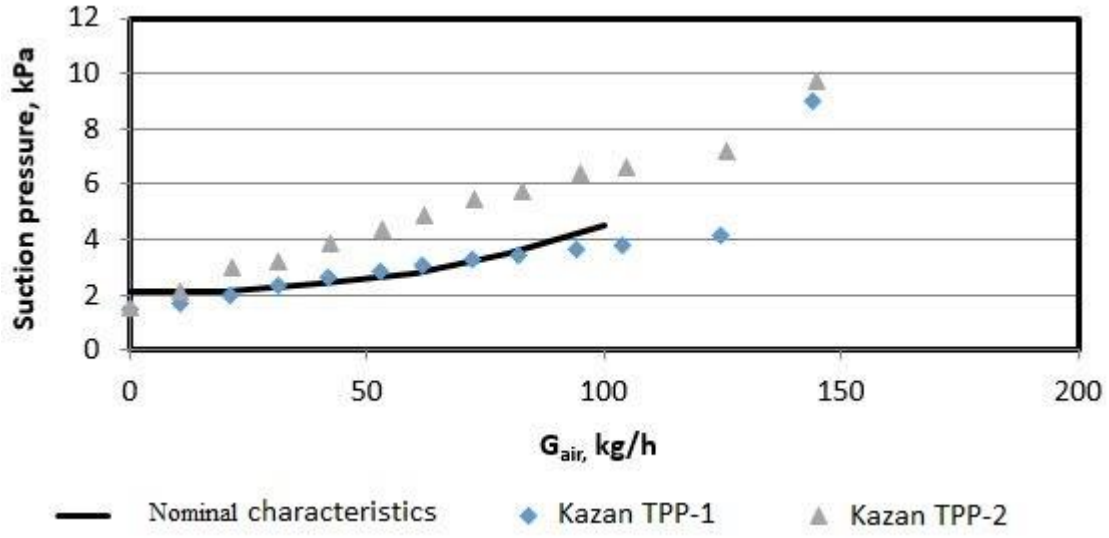

Fig. 2.5. Comparison of the nominal and performance characteristics of the EP-3-700 ejector

From the graph it is clear that the actual characteristics of the EP-3-700 ejector at Kazan TPP-1 coincides with the nominal ones. At the same time, the actual capacity of the ejector, G_{air} = 125 kg / h, is significantly higher than the nominal capacity, G_{air} = 80 kg / h. The characteristics of the ejector at Kazan TPP-2 have the same starting point and capacity, but the suction pressure is much higher.

Fig. 2.6 presents the performance characteristics of the EP-3-600M LMZ ejector at a primary steam pressure P_{ps} = 0.49 MPa and at different temperatures – t_{ps} = 180°C (superheating of the steam relative to the saturation temperature is Δt_{ps} = 20°C), t_{ps} = 370°C (Δt_{ps} = 210°C) and t_{ps} = 500°C (Δt_{ps} = 340°C). The tests were carried out at the TPP MMK and Krasnoyarsk TPP-1 stations, where the opportunity to change the source of the primary steam to obtain various steam temperatures under the same boundary conditions was realized. The tests were carried out at cooling condensate temperatures of t_{cc} = 27-43°C.

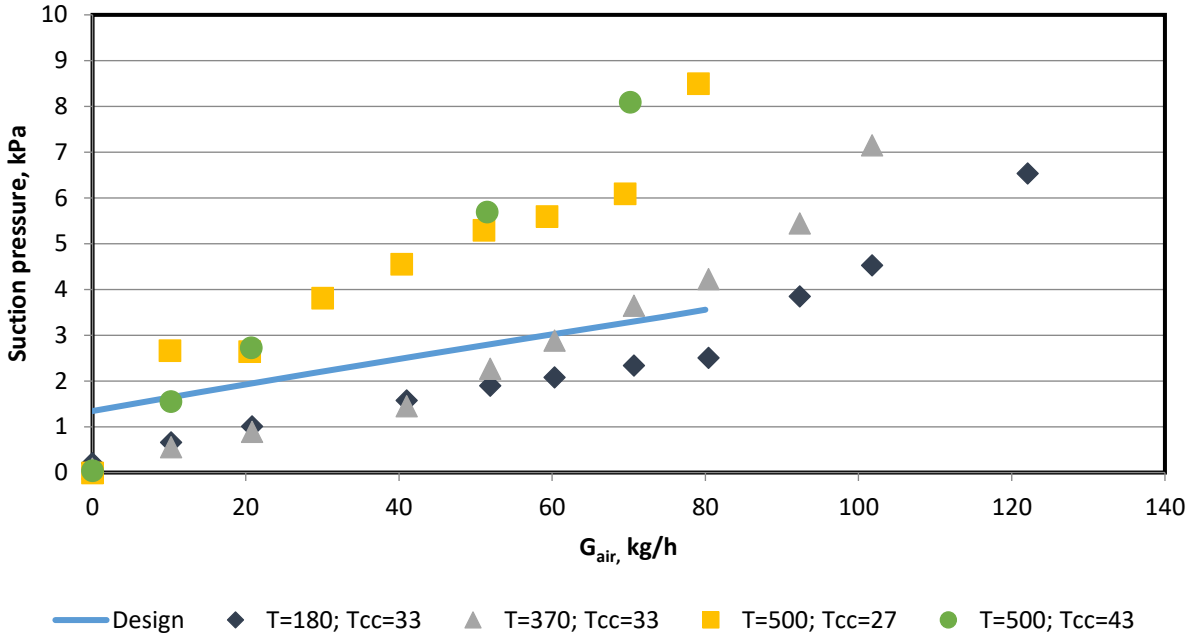

Fig. 2.6. Comparison of the nominal and performance characteristics of the EP-3-600 ejector

From the graph it is clear that when the ejector is operating with saturated primary steam, the actual characteristics lie below the calculated ones but coincide with them in terms of capacity. The increase of steam overheating with respect to saturation temperature from Δt_{ps} = 20°C to Δt_{ps} = 210°C reduces the capacity of the ejector 2 times - from G_{air} = 80 kg / h to G_{air} = 40 kg / h. It can be assumed that a further increase in steam overheating to Δt_{ps} = 340 ° C would also reduce the capacity of the ejector. It is necessary to pay attention to the angle of the characteristics. The overload sections (to the right of the kink point) of an ejector operating on saturated steam run equidistantly to each other. The characteristics of the ejector at t_{ps} = 500°C throughout the investigated range lie at the same angle. This indirectly indicates that at t_{ps} = 500°C, ejectors function in the overload mode along the entire length, which is unacceptable according to [68].

In Fig. 2.7, the performance characteristics of the EP-3-25/75 HTZ ejector at the Tobolsk TPP with a primary steam pressure of P_{ps} = 0.51 MPa and a cooling condensate temperature of T_{cc} = 39°C is presented.

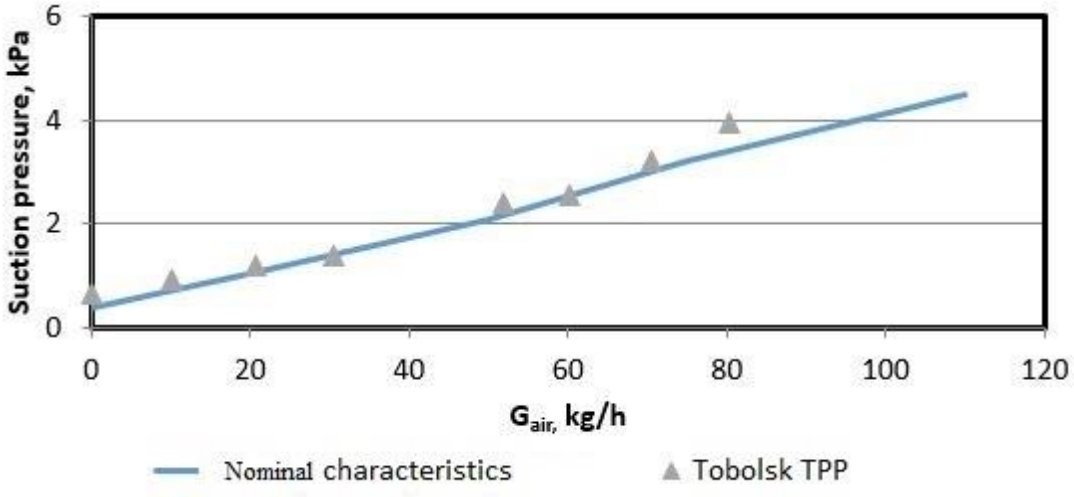

Fig. 2.7. Comparison of the nominal and performance characteristics of the EP-3-25/75 ejector

The experimental points obtained during testing are in strong agreement with the nominal characteristics of the EP-3-25/75 ejector. It can be assumed that the overload area of the ejector was not reached in the tests, while a slight change in the angle of inclination is the effect noted earlier in testing the UTZ and LMZ ejectors – this is the transition of the "effective section" from the conical part of the mixing chamber to the cylindrical one. The performance of the ejector, G_{air} = 80 kg/h, is close to the nominal one, G_{air} = 75 kg/h.

In Fig. 2.8, the performance characteristic of the EP-3-50/150 HTZ ejector at the Troitsk SDPS with a primary steam pressure of P_{ps} = 0.51 MPa and a cooling condensate temperature of t_{cc} = 35°C is presented.

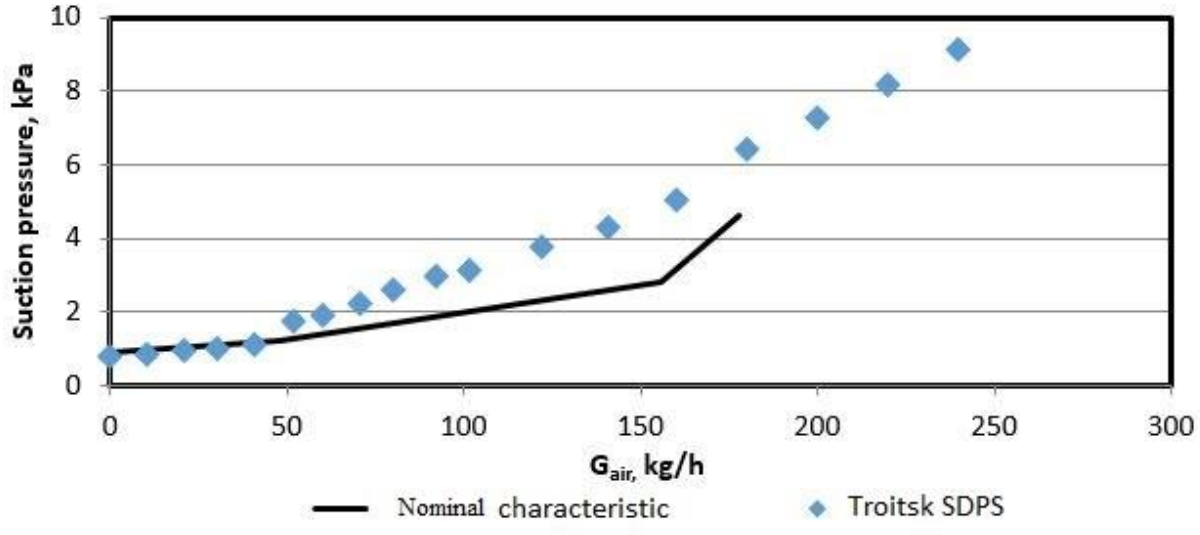

Fig. 2.8. Comparison of the nominal and performance characteristics of the EP-3-50/150 ejector

The experimental characteristics of the EP-3-50/150 ejector also have a perceptible break point in the operating area at G_{air} = 50 kg/h. The first section of the performance characteristics is fully consistent with the calculated values. The second section is much higher. In this case, it can be assumed that the experimentally obtained characteristics show a significantly higher capacity than the nominal values of G_{air} = 150 kg/h, since the transition to the overloading section is not observed throughout the entire investigated range.

To compare the performance characteristics of ejectors with similar performance values, the nominal and performance characteristics of ejectors from various manufacturers (EP-3-2 UTZ, EP-3-700 LMZ, EP-3-25/75 HTZ) are presented in Fig. 2.9. Tests were carried out at the recommended working steam pressure of P_{ps} = 0.49-0.51 MPa and a cooling condensate temperature of about t_{cc} = 39-46°C.

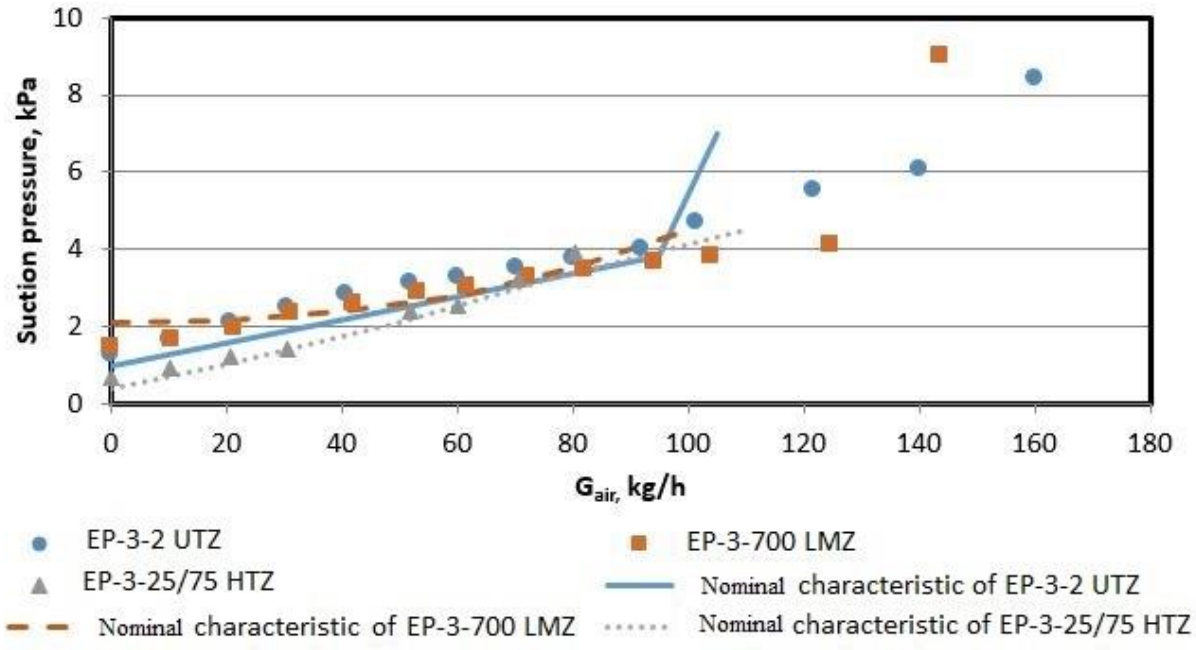

Fig. 2.9. Performance and nominal characteristics of the serial ejectors UTZ, LMZ, HTZ

From the graphs it can be seen that the EP-3-25/75 HTZ ejector, compared with other serial ejectors, has a lower suction pressure of about ΔP = 0.5-1.5 kPa almost along the entire length. This feature is an advantage when using an ejector as part of

condensing turbines. For condensation-type turbines, the values of the vacuum in the condenser have a more significant effect on the efficiency of the turbine than in cogenerating heat turbines. At the same time, the capacity of the ejector is also the lowest, amounting to G_{air} = 80 kg/h.

The nominal characteristics of the EP-3-700 LMZ ejector in Fig. 2.9 are slightly higher than those of the EP-3-2 UTZ ejector. The performance characteristics of the UTZ and LMZ ejectors coincide practically along the entire length of the operating sections. The capacity of the EP-3-2 ejector can be considered equal to 140 kg/h, while the performance of the ejector EP-3-700 is 125 kg/h.

The results of the generalization of industrial tests for ejectors in condensation units under the conditions of TPPs show that most of the performance characteristics of serial ejectors do not satisfactorily agree with the characteristics obtained under the conditions of the manufacturer. This may be due to the influence of various operating conditions, the deterioration of ejector jet devices and defects that have appeared during operation.

2.2. ANALYSIS AND GENERALIZATION OF THE GEOMETRIC CHARACTERISTICS OF SERIAL EJECTORS

To estimate the influence of the geometric parameters of ejectors on their characteristics, analysis and synthesis of data from the jet devices of 24 standard-size serial ejectors were carried out. The collected data is presented in Appendix 3.

The following geometric parameters were analyzed: the position of the critical section of the entrained flow, where its velocity reaches the speed of sound (parameter μ); the main geometrical parameter of the ejector (the ratio of the cross-sectional areas of the mixing chamber's cylindrical part and the critical section of the nozzle); the axial distance between the critical section of the nozzle and the cylindrical part of the mixing chamber (axial position of the nozzle - NXP); and the ratio of the diameters of the critical sections of nozzles in different stages.

The position of the “effective cross section” of the entrained flow

When calculating jet pumps, the position of the “effective cross section” of the entrained flow, which actually determines the entrainment ratio, is estimated. The “effective area” is the area of the “effective section” - an annular section of a suction fluid, where this medium accelerates to the speed of sound. After this section, the mixing of the working and entrained media begins, and the flow parameters are equalized. Determining the position of the cross section is an important task in the calculation method. The displacement of this “ring” towards the diffuser leads to a decrease in the flow area for the suction mixture, therefore reducing the flow rate of the ejected medium and, consequently, the entrainment ratio. The displacement of the cross section of the “effective area” closer to the working nozzle leads to an increase in energy losses from the working steam, up to the disruption of the working flow in the expanding part of the nozzle [18, 31].

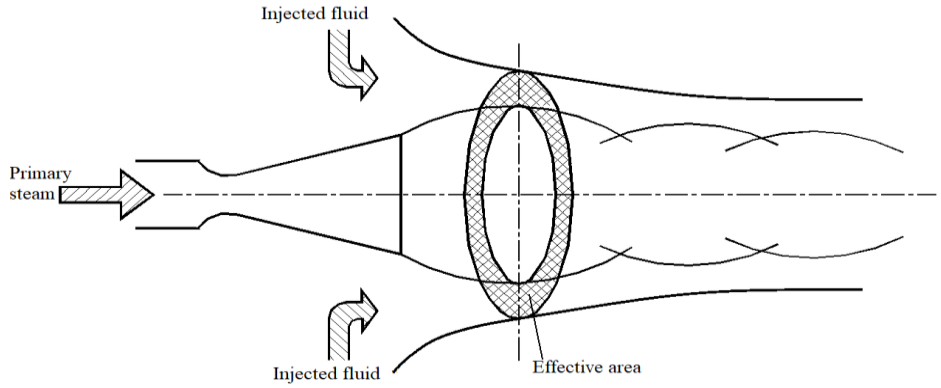

Fig. 2.10. Effective area of the jet device.

The position of the “effective cross section” is determined by the parameter μ - the ratio of the area of the section where the secondary stream is accelerated to the speed of sound (F_{eff}) to the cross section area of the mixing chamber’s cylindrical part (F_{cyl}):

$$\mu = \frac{F_{eff}}{F_{cyl}}. \quad (2.1)$$

It is important to note that F_{eff} refers not to the shaded area in Fig. 2.10, but to the area of the entire mixing chamber section. This section should be formed in the narrow conical or cylindrical part of the mixing chamber. Therefore, the value of μ

must be at least 1. The position of the cross section determines the type of limit mode implemented in the jet apparatus of the ejector [18].

According to recommendations from [18], parameter μ is taken in the range of 1.0 to 1.5. To determine the actual value of μ, the author analyzed the test results of 17 serial ejectors from various manufacturers. When summarizing the results of industrial tests for the studied ejectors, a calibration calculation was performed according to the method specified by the author. The coefficient μ, which ensure the coincidence of the performance characteristics of the ejector with the characteristics obtained as a result of calibration calculations, is determined. According to the results of the analysis, the serial ejectors of each manufacturer are characterized by specific values of parameter μ (Table 2.2).

Table 2.2

Manufacture	UTZ	LMZ	HTZ
μ	1.35…1.5	1.30…1.35	1.0…1.1

For example, in the EP-3-2 and EP-3-3 ejectors of the Ural Turbine Plant μ = 1.35, and in the EPO-3-135 and EPO-3-200 ejectors developed later by UTZ - μ = 1.5.

When analyzing the geometric characteristics of serial ejectors, a connection was found between the value of the coefficient μ and the general geometric parameter (F*) of the ejector, which is the ratio of the critical section area of the mixing chamber's cylindrical to the nozzle ($F^* = F_3/F_{cr}$).

In Table 2.3, as an example, the parameters F* and μ are presented for the first stages of ejectors from various manufacturers.

Table 2.3

Manufacture	UTZ		LMZ	HTZ	
Ejector model	EP-3-2	EPO-3-135	EP-3-700M	EP-3-25/75	EP-3-50/150

General geometrical, *F**	31	31	23	66	71
Coefficient μ	1.35	1.50	1.35	1.00	1.10

The table shows that with a high value of F*, the value of μ is 1.0 ... 1.1. This can be explained by the fact that at high values of F* (respectively, the area of the cylindrical part of the mixing chamber), a decrease in μ to a value of 1.0 determines the shift of the "effective area" section into the cylindrical part of the mixing chamber.

The results of the presented analysis show that the following correspondences between the geometrical parameters of the ejector were chosen by the manufacturers when designing ejectors: at F * = 25...35 μ = 1.35...1.50; at F * = 60...70 μ = 1.1...1.0.

Nozzle exit position

As part of the study, data on the value of one of the design parameters of jet devices (the distance between the nozzle exit section and the inlet cross section of the mixing chamber (axial position of the nozzle)) were collected. For existing serial ejectors installed in TPPs, the axial position of the nozzle is determined experimentally by each manufacturer.

This parameter was calculated using known empirical dependencies (Section 1.2). It is established that the existing formulas are not valid for most serial designs.

It seems that the formulas are not universal and are not suitable for determining the axial position of the nozzle. Taking into account the analysis performed, it can be concluded that the most reliable way to ensure the optimal position of the nozzle is experimental tuning each jet device. The nozzle fixing unit, which allows one to adjust the axial position, was developed and implemented in the new EPO-3-80 and EPO-3-120 ejectors.

Change of the critical diameters of multistage ejector nozzles in stages

Of interest in the results of the generalization of the geometric characteristics of ejectors is the analysis of changes in the diameters of the critical sections of nozzles from one stage to the next. According to the results of the generalization of the geometric characteristics of 24 standard-size serial multistage ejectors, it was revealed that each manufacturer has a specific strategy for increasing or decreasing the diameters of the critical sections of nozzles from the first stage of the ejector to the last.

For example, Table 2.4 shows the nozzle diameters of several multistage ejectors from various manufacturers. The main geometrical parameters of each stage are also given. Full tables with the values of all the geometric characteristics of the studied ejectors are given in Appendix 3.

Table 2.4

Manufacturer	UTZ			LMZ		
Ejector	EP-3-2 (EP-3-3; EPO-3-135)			EP-3-700 (EP-3-750)		
Stage №	I	II	III	I	II	III
Nozzle critical diameter, mm	12	12	10.4	13.5	11.2	10
General geometrical parameter of a stage F*	31	13	7	23	9	7

Manufacturer	HTZ						KTZ	
Ejector	EP-3-25/75			EPO-3-150			EO-50	
Stage №	I	II	III	I	II	III	I	II
Nozzle critical diameter, mm	9	12.4	15.6	13.5	19.5	22	8	9.45
General geometrical parameter of a stage F*	66	20	5	71	19	5	4.9	2.5

According to the given data in all ejectors of the UTZ plant, as well as ejectors of LMZ operating at low working steam parameters (P_{ps} = 0.5 MPa), the diameters of the critical sections of nozzles increase from the first stage to the last. At the same time, for the HTZ ejectors and most of the KTZ ejectors, the diameters of the critical sections of nozzles decrease from the first stage to the last.

The compression ratios, in contrast, reduce from the first stage to the last for the UTZ and LMZ ejectors. These ejectors are characterized by a small value of the

general geometric parameter F* at the first stage, which corresponds to the recommendations from [18, 31]. For HTZ ejectors with a large F* value of the first stage, the compression ratio from the first stage to the last, in contrast, increases.

Ejectors with a high F* value for the first stage allow for the achievement of a high entrainment ratio at low suction pressure. Such a strategy for ejector design may turn out to be more efficient for condensing turbines, where the value of the vacuum in a condenser has a more significant effect on the efficiency of a turbine than in cogenerating heat turbines. It should be noted that the strategy of increasing the compression ratio from the first stage to the last can lead to an increase in steam consumption per ejector, and the choice of a particular strategy in the design of the ejector should be determined not only by the initial data on the generated vacuum and capacity, but also on the type of turbine on which this ejector is installed. It is interesting to note that HTZ - the manufacturer of condensing turbines - selected the distribution of compression levels, which corresponds to the minimum pressure in the condenser, while UTZ - mainly the manufacturer of cogenerating turbines, where the vacuum value in the condenser is less important – the inverse distribution of compression levels. In section 2.1 of Fig. 2.9, a lower suction pressure of an ejector produced by HTZ when comparing both nominal and performance data is confirmed.

The analysis showed various strategies for the selection of various geometrical parameters of three-stage ejector jet devices for condensing and cogeneration heat turbines.

2.3. NUMERICAL SIMULATION OF GAS DYNAMICS IN AN EJECTOR

To analyze the gas-dynamic processes occurring in the jet device, namely the distribution of pressures and velocities of the primary and entrained streams along the length and cross section of the jet device, a number of numerical experiments

were carried out, which also made it possible to formulate recommendations to clarify the design methodology of the ejector.[2]

Formulation of the problem

A series of numerical experiments were carried out, which allowed us to interpret the influence of various geometric and regime parameters on the processes occurring in the jet device of the ejector (Fig. 2.11).

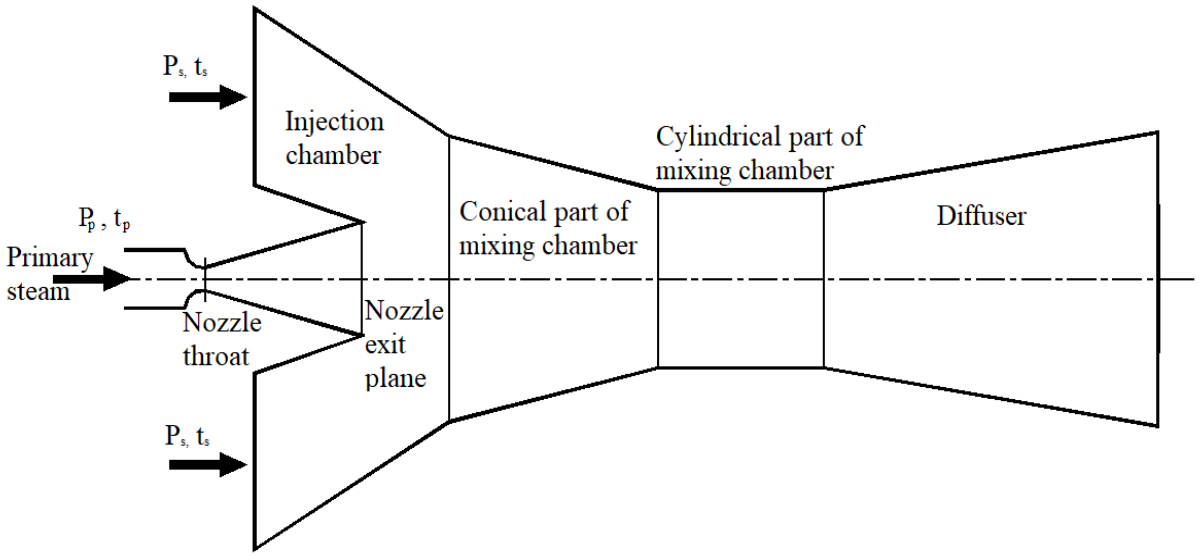

Fig. 2.11. Ejector jet device

The key parameters selected in the process of solving the problem and affecting the result of modeling the processes of gas dynamics and heat transfer are:

- Finite-volume grid model (type of selected elements, density of nodes for modeling a viscous boundary layer, structured or non-structured mesh, etc.);
- Solver (joint or separate solver of equations of energy, moments and masses);
- Turbulence model;
- Initial conditions (characteristics of the working fluid, initial pressure, temperature and velocity distributions);
- Boundary conditions (correct thermophysical parameters of input and output sections);

[2] *Numerical simulation of gas dynamic processes was performed together with the lead researcher of the turbines and engines department at UrFU, D. Brezgin, Ph.D.*

- Model of solutions for viscous parietal layer.

The choice of the grid model is based on [39, 55-57]. In the framework of this research, several variants of the finite element mesh are used, in particular, meshes “trimmed with prismatic layers near the walls”, structured meshes and mesh models of polyhedrals with prismatic elements. The solver used is the joint solver of the equations of energy, moments and masses (*Coupled Implicit Solver*) in connection with supersonic flows arising in ejectors.

Initial and boundary conditions

To construct a finite-volume three-dimensional grid, taking into account the axisymmetry of the problem, a ¼ part of the entire model was chosen. It should be noted that the 3D grid was not used directly for modeling, but a 2D model was generated in the XY plane on its basis: the entirety of the further research process was conducted in a two-dimensional formulation.

The number of elements in the 2D grid ranged from 20,000 to 1,500,000.

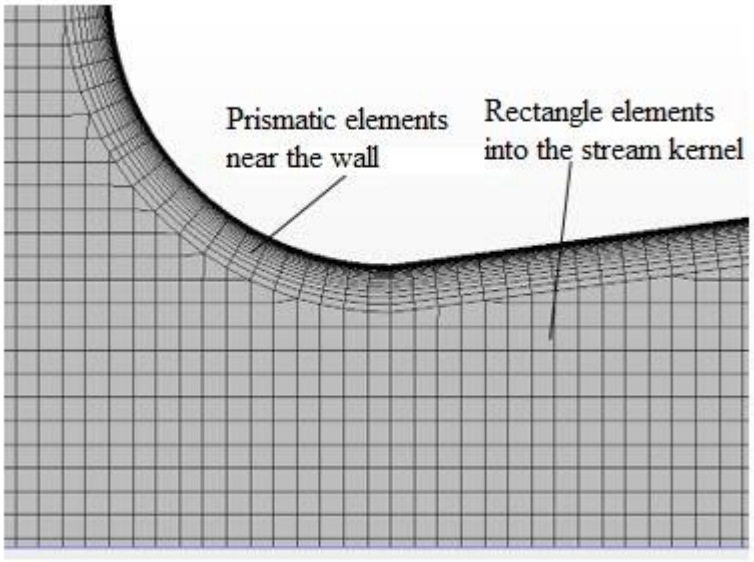

Fig. 2.12. Fragment of the nozzle throat section with 2D mesh

In the initial stage of modelling, the following initial and boundary conditions of the physical model were initialized:

- Fluid 1 – air (P_s = 5 kPa, t_s = 25 °C).

• Fluid 2 – superheated water vapour (P_p = 300 kPa; t_p = 155 °C; μ = 1,6E-5 Pa-s; C_p = 2121 J/kg-K; λ = 0,036 Wt/m·K).

• Ideal gas model.

• The combined solver of the equations of energy, moments and masses (Coupled Implicit Solver).

• Realizable k-ε turbulence model.

• Courant number = 50.

• Expert initialization options switched on.

• Target functions - static pressure at the working nozzle cut and static pressure distribution in the center of the stream along the jet apparatus.

• The task is considered to be solved when reaching the residuals of energy, T_{ke}, T_d level 1E-04 and target functions less than 1 Pa.

Calculation results

It should be noted that, on average, 5,000 to 7,000 iterations were required to solve one task. To analyze and compare the calculation results, we consider the pressure distribution in the flow part of the steam jet device according to [18], presented in Fig. 2.13.

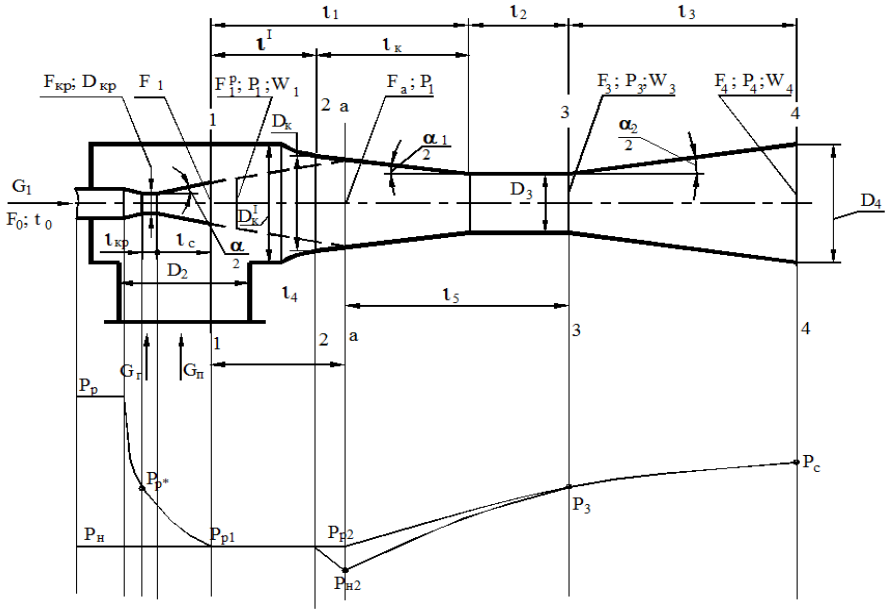

Fig. 2.13. Distribution of pressures in the flow part of a steam ejector

According to [18], the pressure of working steam monotonically decreases in the nozzle from the value of P_p at the inlet to P_{p1} at the outlet. The pressure of the working steam in the receiving chamber of the ejector is equal to the pressure of the entrained flow $P_н$. A jet of working steam flowing from the nozzle into the receiving chamber captures the steam-air mixture entrained from the condenser and enters with it into the conical part of the mixing chamber. The velocity of the entrained mixture increases; in section (a-a) of the conical part (or the cylindrical part of the mixing chamber), this velocity reaches the speed of sound. In this case, the pressure of the entrained mixture reaches the minimum – $P_{н2}$. The flow rate of the entrained mixture and, consequently, the attainable entrainment ratio is determined by the difference between the area of a given section and the section of the working jet. After the cross section (a-a), the pressure of the ejected mixture and the working jet begins to increase smoothly. Both flows are mixed; velocities are reduced. In the diffuser, the mixed flow is slowed down with increasing pressure to the value of p_c.

Fig. 2.14 presents the results of calculations of the distribution of static pressures and Mach numbers along the length of the jet device.

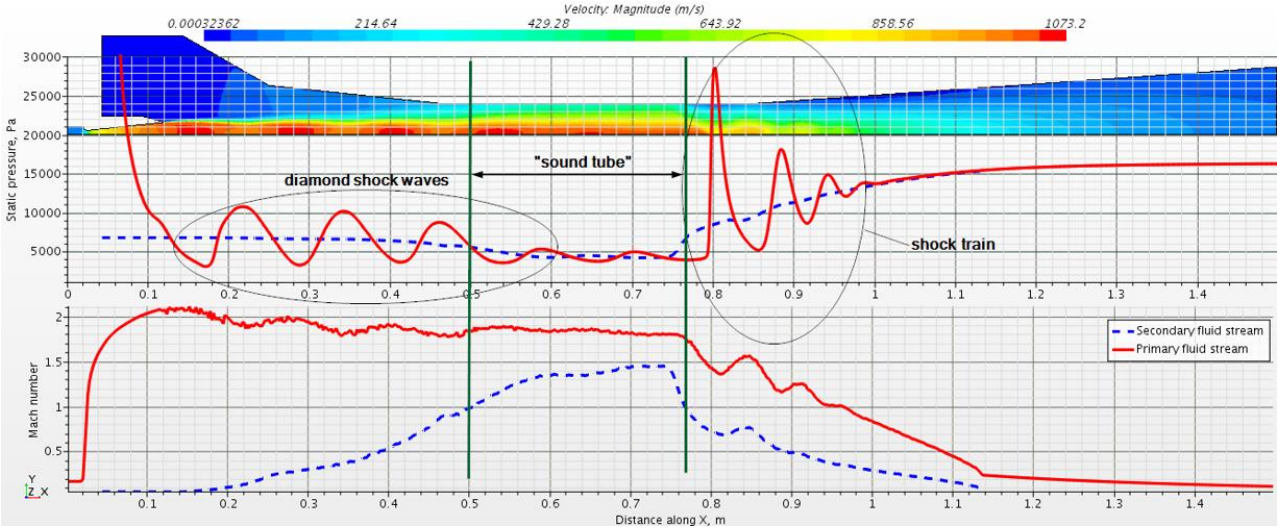

Fig. 2.14. The distribution of reduced total velocities and static pressures along the length of the jet device: a – the jet profile, b – the distribution of static pressures, c – the distribution of flow rates, — — — steam-air mixture, —— working steam; I – the acceleration section for the entrained stream, II – the section of the supersonic flow of the entrained stream, III – the inhibition section of the entrained flow.

In the suction chamber immediately behind the nozzle, characteristic direct and/or oblique shock waves occur in the flow kernel. These pressure drops correspond to “barrel-shaped” velocity profiles and are the result of the complex interactions between the pulses of two media, manifested in a series of oscillations of the values of the reduced velocity and static pressures along the axis of symmetry of the mixing chamber. Such shocks are most likely a consequence of the unplanned mode of operation of the nozzle with under-expansion (i.e., the vapor pressure at the nozzle exit is higher than the pressure of the medium in the mixing chamber). The results presented in Fig. 2.14 qualitatively agree with the results of [57,58] and a number of others.

Fig. 2.14 also shows that in the section along the abscissa axis x = 0.5 m, in which the value of the reduced velocity of the entrained flow exceeds 1, the pressure drops in the working jet attenuate. This zone (II) extends to x = 0.78 m. The decrease in the amplitudes of the pressure surges is connected, in the authors’ opinion, with the fact that the supersonic flow of the working steam is surrounded by the “sound” (sonic) flow of the entrained medium. We assume that in this zone pressure fluctuations in the working flow lead to a change in the interface between the working and entrained gas. Since the cross section of the secondary sonic flow is limited by the walls of the mixing chamber, opposite direction pressure impulses (to the working flow) arise in it upon deformation of the boundaries, returning the boundary of the entrained gas flow to the initial position. It is suggested to call this effect a “sound tube”. The influence of the “sound tube” on the primary flow can, in the author’s opinion, be explained according to the data of [20].

As a result of the ongoing interaction of the flows, the reduced velocity of the entrained flow becomes less than 1. In this section, corresponding to the section x ≈ 0.78 m, the action of the sound tube stops, and a second group of pressure surges occurs in the working stream (in amplitude, these pressure drops can exceed the first zones). A similar picture was described in [59], where it is noted that a strong oblique

shock wave occurs in the cylindrical part of the ejector's mixing chamber, causing destruction of the boundary layer near the wall. This drop is so strong that it causes not only the destruction (separation) of the boundary layer, but also gives rise to a series, in this case of three, pressure drops of lesser amplitude in the diffuser. We assume that strong pressure surges after the "sound tube" section (in the cylindrical part of the mixing chamber and especially in the diffuser) lead to an increase in wave resistance and a decrease in the compression ratio in the ejector stage. We also note the following fact. In the Russian and foreign literature [18, 53, 59], zone II, defined here as the "sound tube" zone, is characterized by the active mixing of flows. However, in zone II, as noted above, pressure fluctuations in the workflow are reduced. It is logical to assume that in this zone the intensity of transverse mass flows decreases and, accordingly, the mixing of flows may begin only in zone III.

The presented picture of gas dynamics in the jet apparatus of the ejector shows a convention of the coefficient μ estimation (see Section 2.2), which characterizes the position of the critical section of the entrained flow, where it reaches the speed of sound due to interaction with the working flow. However, the quality of the ejector design using the specified coefficient in the method of calculation is sufficient for the ejector to satisfactorily perform its functions as part of the condensing unit of a STU.

Figure 2.15 shows a graph of the change in the length of the "sound tube" depending on the distance from the nozzle throat to the cylindrical part of the mixing chamber (l_1). The figure shows that the length of the "sound tube" increases with increasing l_1. However, with the optimal value of l_1, the length of the "sound tube" is slightly reduced.

Fig. 2.16 presents the dependence of the entrainment ratio on l_1. The entrainment ratio varies from 0.8 at l_1 = 52 mm to 0.86 at l_1 = 132 mm.

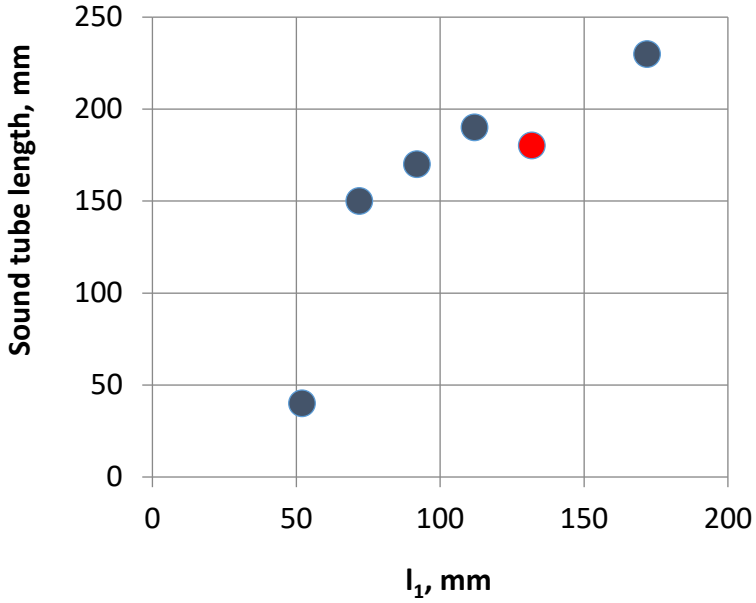

Fig. 2.15. The dependence of the "sound tube" length from the distance between the output section of the nozzle and the input section of the diffuser

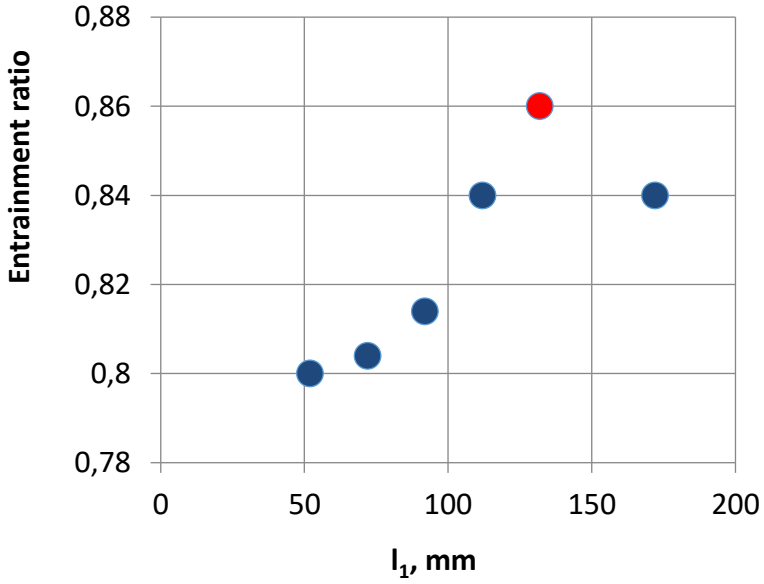

Fig. 2.16. The dependence of the entrainment ratio from the distance between the exit section of the nozzle and the inlet section of the diffuser

One of the most important hypotheses formulated in the design of ejectors using semi-empirical methods is one about the shape of the jet of working vapor (gas) flowing from the nozzle. In [18], it is recommended to set the profile of the initial section of the working jet either with a constant diameter or in the form of a "barrel", determined on the basis of the theory of a free turbulent jet flowing out of the hole [125]. In [18, 31], it is noted that, in the latter case, the results of calculations

of the ultimate entrainment ratio are more accurate. However, as can be seen from the numerical calculations of the sequence of "barrel-shaped" profiles of the speed of the primary stream, a jet model with a constant diameter from the nozzle to the cylindrical part of the mixing chamber is absolutely applicable. To be more detailed, according to CFD the difference in the entrainment ratio with various jet shapes is no more than 5%. At the same time, when applying the "constant diameter" shape, the method is much simpler in terms of the calculation of velocities.

We also note the following feature of the method for calculating the characteristics of an ejector with a conical mixing chamber part. According to [18], the ultimate entrainment ratio in the second limiting mode is calculated by the formula:

$$u_{lim} = \left(\mu \frac{F_{cyl}}{F_{cr}} - \frac{1}{q_{pv}}\right) \cdot \frac{k_i}{k_{ps}} \cdot \frac{N_{ps^*}}{N_{i^*}} \cdot \frac{a_{ps^*}}{a_{i^*}} \cdot \frac{P_i}{P_{ps}}, \qquad (2.2)$$

where F_{cyl}, F_{cr} — the bore area of the cylindrical part of the mixing chamber and the nozzle throat;

μ — the ratio of the cross-sectional area where the entrained flow reaches the speed of sound (F_{eff}) to the cross-sectional area of the cylindrical section of the mixing chamber (F_{cyl}) (it is assumed that the cross section F_{eff} is located in the conical part of the mixing chamber);

k_i, k_{ps} — adiabatic indices of entrained and working flows;

N_{i*}, N_{ps*} — relative pressure of isotropic moving sonic entrained (i) and working (ps) flow to deceleration pressure;

a_{i*}, a_{ps*} — limit speed of the entrained and working streams;

P_i, P_{ps} — total pressure of the entrained and working streams;

q_{pv} — gas-dynamic function, which is the reduced mass velocity of the working stream equal to the ratio of the critical section area of the working nozzle to the section area of the working stream at pressure p_I.

In this expression, the function q_{pv} is determined by the known pressure difference of the workflow $N_{dp} = \frac{P_i}{P_{ps}}$. This expression was obtained with the conventional scheme of the process, which does not take into account the mutual mixing of the flows in the initial part of the mixing chamber, as well as under the condition of the

inequality of the static pressure of steam in the working jet and in the entrained flow. Under this assumption, the calculation is in strong agreement with the working characteristic of the ejector at P_{ps} = 1.3 – 1.6 MPa and the degree of expansion of the working flow $\beta = 1/ N_{dp} = P_{ps}/ P_i \approx 230 – 530$ [18].

The testing of various types of ejectors carried out by the authors at a working vapor pressure of P_{ps} = 0.5 MPa ($\beta \approx 70 – 160$) showed that when calculating the ultimate entrainment ratio from the expression (2.2) in the section where the velocity of the entrained flow reaches the speed of sound, the reduced mass velocity of the working flow (q_{pv}) must be determined from the condition of equality of static pressures in the working and entrained flow. In this case, q_{pv} is determined by the gas-dynamic function:

$$N_{dp} = N_i \cdot P_i/P_{pv}, \quad (2.3)$$

where N_i – relative pressure of the entrained flow equal to the ratio of the pressure of the isotropically moving entrained stream to the pressure of its deceleration.

This condition is in strong agreement with the results of numerical calculations performed in the framework of this study. It has been established that the static pressure in the critical section of a steam jet device is almost the same in both the working medium and the entrained flow (the pressure difference between the axis of the apparatus and the wall is 1–3%). It should be noted that the condition of equality of static pressures in the working and entrained flows is also recommended in the work of M. D. Millionshchikov [27].

According to the numerical simulation, it is accepted to refine the calculation method to take the form of a jet with a constant cross section from the exit section of the nozzle to the entrance section of the mixing chamber’s cylindrical part.

2.4. SPECIFICATION OF THE DESIGN AND CALIBRATION METHODS

2.4.1. DESIGN METHOD

The refinement of the methodology is based on the results of the previous analysis of the geometric characteristics of the ejectors and the generalization of industrial test data and numerical calculations. The selection and justification of the basic ejector design method was carried out on the basis of the analysis of the methods presented in Chapter 1. The analysis carried out is based on the following requirements: the method must be solved by the proposed algorithm, applicable to the calculation of a wide range of gas-jet devices and contain a small number of empirical constants.

The KTZ method [22] cannot be used for refinement, since this technique is based on experimental data from the testing of two-stage ejectors: transferring the results to the design of three-stage ejectors is difficult.

The HTZ method [106] also cannot be used to accomplish the task, since this method uses the values that must be determined by calculation – the primary steam consumption and compression ratios is stages – as the initial data. In addition, the methodology does not present algorithms for calculating some geometrical parameters of the ejector's jet device.

The application of the VTI method [18, 30, 31] is complicated by the necessity of jointly solving more than 75 equations; however, an algorithm and a calculation program have been developed to test the applicability of the technique. A large number of errors were found and fixed. Analysis of the results of calculations according to the VTI method showed that it is impossible to carry out calculations for a large number of modes and combinations of regime factors and the geometrical parameters of a steam jet device. As noted in Chapter 1, this is also confirmed by various authors of the design methods, in particular [18].

The author uses the algorithm described in the MEI method [18] as the basis for the basic methodology for the design of an ejector. A feature of the technique is the calculation of the limiting pressure by equations for the second limiting mode (which comes before the first and third modes and is characterized by the entrained flow reaching sonic speed in the conical section of the mixing chamber) in order to reduce the consumption of primary steam per ejector. Despite the absence of a complete methodology in [18], the formulation of the calculation problems allowed us to develop and supplement the methodology with all the equations necessary for a complete calculation.

The calculation was carried out while taking into account the following accepted specifications:

1. As a result of numerical simulation, the shape of the primary stream jet flowing out of the nozzle was adopted. It is assumed that the pressure in the outlet section of the nozzle is equal to the pressure in the suction chamber (the estimated operating mode of the ejector). In this case, the jet section should have a constant diameter before entering the cylindrical part of the mixing chamber.

2. As a result of numerical simulation, it was also confirmed that the calculation of the ejector should be based on the second limit mode, which comes before the third one. In this mode, the entrained stream accelerates to the speed of sound in the conical part of the mixing chamber.

3. On the basis of a generalization of the results of industrial tests and comparison with the collected geometric characteristics, the recommended values of the coefficient μ were taken. In particular, to design the ejector for operation as part of a condensing turbine, μ is assumed to be equal to 1. The choice of coefficient μ is related to the revealed relationship between the coefficient μ and the general geometric parameters of the ejector.

4. Based on the generalization of data on compression ratios from the first stage of the ejector to the last one, a strategy for changing the diameters of the critical nozzles was determined for a multistage ejector. In particular, for an ejector of a

condensation turbine, it is assumed that the diameters of the critical sections of nozzles should be increased from the first stage to the last one.

2.4.2. SPECIFICATION OF THE CALIBRATION METHOD

The method for the calibration calculation of an ejector (calculating the characteristics of an ejector with dry air or air-steam mixture) has almost never been presented except for a brief description of the calculation sequence given in [18]. To determine the characteristics of the ejector, a new algorithm was developed.

The initial data for creating the characteristics of the ejector are the pressure (P_{ps}, kPa), temperature (t_{ps}, °C) and flow rate (G_{ps}, kg / h) of the primary steam, the diameter of the nozzle throat (d_{cr}, m), the mixing chamber inlet diameter (d_c, m), the diameter of the cylindrical part of the mixing chamber (d_{cyl}, m) and the temperature of entrained air (t_{mix}, °C).

First of all, the speed of sound in the primary steam a_{ps} and in the entrained air $a_{air} = a_{inj}$ was calculated, where a_{inj} – is the speed of sound in the entrained gas.

Then the following areas were determined through the corresponding diameters: the critical section of the nozzle F_{cr}, the output section of the nozzle F_1, the input section of the mixing chamber F_2 and the cylindrical part of the mixing chamber (diffuser) F_{cyl}. The cross-sectional area of the entrained air at the entrance to the mixing chamber is calculated:

$$F_{i2} = F_2 - F_1. \quad (2.4)$$

The relative mass velocity in the conical part of the mixing chamber is determined:

$$\lambda_{pv} = F_{cr} / F_{cyl} \cdot \mu, \quad (2.5)$$

with the use of the gas-dynamic functions:

— relative velocity $\lambda_{pv} = f(q_{pv}, K_i)$;

— relative pressure $P_{pv} = f(q_{pv}, \lambda_{pv})$

defined for the suction chamber.

where $K_i = K_{air} = 1,4$ — adiabatic index for injecting gas.

The pressure in the ejector's suction chamber with a zero amount of entrained steam is calculated:

$$P_{i0} = P_{pv}/P_{ps}. \quad (2.6)$$

Next, calculation of the pressure in the suction chamber is organized in the following way – for the next step, the pressure value is set higher (for 0.5 kPa) than for the previous one.

Relative pressure $P_{pv} = P_i/P_{ps}$ and velocities $q_{pv} = f(K_i, P_{pv})$ are calculated. The critical entrainment ratio is defined:

$$u_{lim} = \left(\mu\frac{F_{cyl}}{F_{cr}} - \frac{1}{q_{pv}}\right) \cdot \frac{k_i}{k_{ps}} \cdot \frac{N_{ps^*}}{N_{i^*}} \cdot \frac{a_{ps^*}}{a_{i^*}} \cdot \frac{P_i}{P_{ps}}, \quad (2.7)$$

where Ni*, Nps* — the relative critical pressure of the entrained gas and the working steam are determined by the value of the adiabatic index of the corresponding medium.

Then the gas constant of the mixture at the outlet of the diffuser is determined, J/kg·K.

$$R_{SAM} = \frac{R_{ps}+u_{lim}R_i}{1+u_{lim}}, \quad (2.8)$$

where $R_i = R_{air}$ — gas constant of entrained gas, J/kg·K.

The adiabatic index of the mixture is calculated as:

$$K_{SAM} = \frac{\frac{K_{ps}}{K_{ps}-1}+u\cdot\frac{K_S}{K_S-1}\cdot\frac{R_S}{R_{ps}}}{\frac{1}{K_S-1}+u\cdot\frac{K_{air}}{K_S-1}\cdot\frac{R_S}{R_{ps}}}, \quad (2.9)$$

where R_s — gas constant of the steam.

The mixture pressure at the diffuser outlet (P_{mix}, kPa) is set and specified. The partial pressure of the steam in a mixture is calculated:

$$P_{sm} = \frac{P_{SAM}}{1+U_{lim}\cdot 0.622}. \quad (2.10)$$

The temperature of the air-steam mixture satisfying the heat balance equation at the inlet and outlet of the mixing chamber is calculated:

$$t_{SAM} = t_{mix} + \frac{h_{ps} - h_{sm}}{u_{lim} \cdot C_{air}}, \quad (2.11)$$

where $h_{ps} = f(P_{ps}, t_{ps})$ — enthalpy of primary steam, kJ/kg;

h_{sm} — enthalpy of steam in the mix at the outlet of the diffuser, determined by the mix temperature t_{mix} and partial pressure in the compressed mixture, kJ/kg.

C_{air} — air heat capacity, kJ/kg.

The speed of sound of the compressed mixture at the diffuser outlet is calculated [18], m/s:

$$a_{SAM} = \left(\frac{2 \cdot K_{SAM}}{K_{SAM}+1} R_{SAM} \cdot T_{SAM}\right)^{0.5}. \quad (2.12)$$

The relative mass flow rate in section 3-3 at the diffuser inlet is determined:

$$q_{SAM3} = \frac{K_{ps}}{K_{SAM}} \cdot \frac{N_{ps^*}}{N_{SAM^*}} \cdot \frac{P_{ps}}{P_{SAM}} \cdot \frac{a_{SAM}}{a_{ps}} \cdot \frac{F_{cr}}{F_{cyl}} + u, \quad (2.13)$$

where $N_{SAM^*} = \left(\frac{2}{K_{SAM}+1}\right)^{\frac{K_{asm}}{K_{SAM}+1}}$ — relative critical pressure in the mixture.

The gas-dynamic functions in section 3-3 are defined:

— relative velocity $\lambda_{SAM3} = f(q_{SAM3}, K_{SAM})$;

— relative pressure $N_{SAM3} = f(\lambda_{SAM3}, q_{SAM3})$.

The relative flow rate of the entrained mixture in section 2-2 is calculated (Fig. 2.13):

$$q_{i2} = \frac{K_{ps}}{K_i} \cdot \frac{N_{ps^*}}{N_i} \cdot \frac{P_{ps}}{P_i} \cdot \frac{a_i}{a_{ps}} \cdot \frac{F_{cr}}{F_{i2}} \cdot u. \quad (2.14)$$

The gas dynamic functions for the secondary stream $\lambda_{i2} = f(q_{i2}, K_i)$; $N_{i2} = f(\lambda_{i2}, K_i)$ and the primary stream $q_{ps2} = F_{cr}/F_1$, $\lambda_{ps2} = f(q_{ps2}, K_{ps})$, $N_{ps2} = f(\lambda_{ps2}, K_{ps})$ in section 2-2 (at the mixing chamber inlet) are defined.

The compressed mixture pressure is calculated and compared to the value set at the beginning of the iteration cycle:

$$P_{SAM} = \frac{P_i}{N_{SAM3}\left(1+0.5(\beta-1)\left(\frac{P_i}{P_{SAM}}\right)^{0.5}\left(\frac{N_{i2}}{N_{SAM3}}\right)^{0.5}\right)} \cdot \left\{N_{ps2}\frac{P_{ps}}{P_i}\frac{F_{ps2}}{F_{cyl}} + N_{i2}\frac{F_{i2}}{F_{cyl}}\left(1-0.5(\beta-1)\frac{F_{cyl}}{F_{i2}}\right) + \frac{K_{ps}\cdot N_{ps^*}}{0.9}\frac{F_{cr}}{F_{cyl}}\frac{P_{ps}}{P_i}\cdot\left[0.834\cdot\lambda_{ps2} + 0.812\cdot u\frac{a_i}{a_{ps}}\lambda_{i2} - (1+u)\frac{a_{SAM}}{a_{ps}}\lambda_{SAM2}\right]\right\} \quad (2.15)$$

Calculations are repeated for a series of values of secondary stream pressure P_i.

On the basis of the methodology described, the characteristics of stage I of the ejector can be calculated. The characteristics of stages II and III can only be calculated after determining the amount of steam condensed in the intermediate heat exchangers. The amount of steam condensing in the coolers of stages II and III must be additionally determined, for which additional data are required when testing ejectors.

Based on this refined methodology, a certificate for the registration of a software package was obtained [126].

2.5. RESULTS

1. Based on a compilation of statistical information on the failures of more than 500 turbine units with a capacity of 100 to 500 MW over a 25-year operating period, analysis of the damage to turbines and equipment in STU technological subsystems was carried out. It has been established that the percentage of STU failures caused by condensation units is 13%. The percentage of ejectors responsible for the failure of condensing units is 23%. Practically every ejector failure leads to a shutdown of the turbine.

2. As a result of a survey of more than 100 ejectors, characteristic defects were revealed, which are determined by design flaws, operating conditions or ejector repair conditions. Recommendations for improving the design of ejectors were formulated.

3. The analysis of tests of 36 serial ejectors in TPP conditions is presented. The discrepancy of the majority of nominal and performance characteristics of ejectors is shown. This is due both to the technical condition of the ejectors and to the specific conditions required for obtaining these characteristics at the equipment manufacturer and in TPPs.

4. The collection, analysis and generalization of data for the geometrical dimensions of jet devices and the operating parameters of ejectors that are part of various steam-turbine units was carried out. An estimation of the parameter μ characterizing the position of the "effective cross section", where the injecting mixture reaches the speed of sound, has been carried out. The assessment was provided basing on a generalization of the performance characteristics of a number of ejectors from various manufacturers. For UTZ and LMZ ejectors, μ = 1.35 ... 1.5, while for HTZ ejectors – μ = 1.0 ... 1.1. The connection between the parameter μ and the general geometric parameter of the ejector F^* is shown. The manufacturers have chosen the following ratios of the indicated parameters: with F^* = 25 ... 30 – μ = 1.35 ... 1.5, while with F^* = 60 ... 70 – μ = 1.0 ... 1.1.

5. The data on the distribution of compression ratios in multistage ejectors are summarized by various manufacturers. The analysis showed that the critical diameters of the nozzles and the compression ratio of ejector stages decrease from the first stage to the last for the UTZ and LMZ ejectors. For HTZ ejectors, the critical diameters of the nozzles and the compression ratio from the first stage to the last, in contrast, increase. The analysis allows one to recommend ejectors with a low value of the general geometric parameter of the first stage in order to reduce the compression ratio from the first stage to the last one, and for ejectors with a high value of the general geometric parameter of the first stage to increase the

compression ratio. A different approach to the development of ejectors for condensing and cogenerating turbines has been substantiated. The choice of ratios of the geometrical parameters of ejectors for condensing turbines should be based on the approach taken at the HTZ plant, while the UTZ approach should be the basis for cogenerating ones.

6. Numerical simulation of gas dynamics in the jet device of an ejector was performed. A definition of the “sound tube” section located between two groups (zones) of pressure surges is proposed. A connection has been established between the length of the “sound tube” and the axial position of the nozzle. It was found that to design an ejector with working steam pressure of P_{ps} = 0.5 MPa, it is necessary to take a working steam jet with a constant diameter from the nozzle exit section to the cylindrical part of the mixing chamber: this determines the method of calculating the gas-dynamic functions for estimating the limiting entrainment ratio.

7. The choice of the basic design method is justified and the design and calibration methods for a steam ejector are refined. A technique is developed, taking into account the data obtained in the chapter. The recommendation to calculate the limiting regimes of an ejector via the dependencies of the second limiting mode was adopted.

Chapter 3.

DESIGN, EXPERIMENTAL RESEARCH AND INDUSTRIAL APPLICATION OF UP-TO-DATE HIGH-PERFORMANCE EJECTORS FOR STU CONDENSING UNITS

Based on the developed refined methodology, new high-performance EPO-3-80 (1 pc.) and EPO-3-120 (5 pcs.) ejectors with external intercoolers were calculated, designed, manufactured and installed in TPPs. Experimental studies of the developed ejectors are provided. Industrial testing for 1.5 years was conducted. Currently, the EPO-3-80 ejector successfully operates as part of the K-200-130 LMZ turbine, while the EPO-3-120 ejector works as part of the K-210-130 LMZ, T-180-130 LMZ, PT-60-90 LMZ, KT-80/100-90 LMZ and T-87/90-130 LMZ turbines.

3.1. JUSTIFICATION OF THE VIABILITY OF DEVELOPING A NEW EJECTOR

The steam ejectors installed on most turbines were developed in the 1950s-1980s. As shown in section 1.1, the designs of these ejectors (in particular, the placement of the steam jet device and the intercooler in one case [105]) are obsolete and do not correspond to modern requirements for the reliability of power equipment. In addition, over a long operation period some unremovable defects have accumulated in the turbines, which significantly affect the efficiency of TPPs. Such defects include, for example, the leakage of the turbine vacuum system due to deformation of the flange connector of the low-pressure cylinder, etc. The existence of turbines with such defects determines the feasibility of developing new ejectors with increased reliability and capacity, as well as ones that create a deeper vacuum in the suction chamber capable of maintaining a deeper vacuum in the turbine condenser. The expediency of replacing an ejector was determined individually in

each case; as an example, the installation of a EPO-3-80 ejector for in a K-200-130 LMZ turbine is considered.

The K-200-130 LMZ turbine, for which a new ejector EPO-3-80 has been developed, has been functioning for 40 years. After a large number of start-ups (heating-cooling), due to warping of the flanges of the low-pressure cylinder housing, the turbine had a defect – leakage of the flange connector in the low-pressure cylinder seals [127]. To eliminate this defect is extremely difficult. The leakage of the flange connector led to a significant increase in air suction in the low pressure part (LPP) of the turbine and a corresponding decrease in the value of vacuum in the condenser. In Fig. 3.1, a retrospective of the amount of air suction into the vacuum system of the turbine is presented. It is seen that air suction into the condenser is very high, varying from 60 to 130 kg / h. From September 2016, air intakes have amounted to about 100 kg / h, with a standard value of G_{air} = 21.5 kg / h [64].

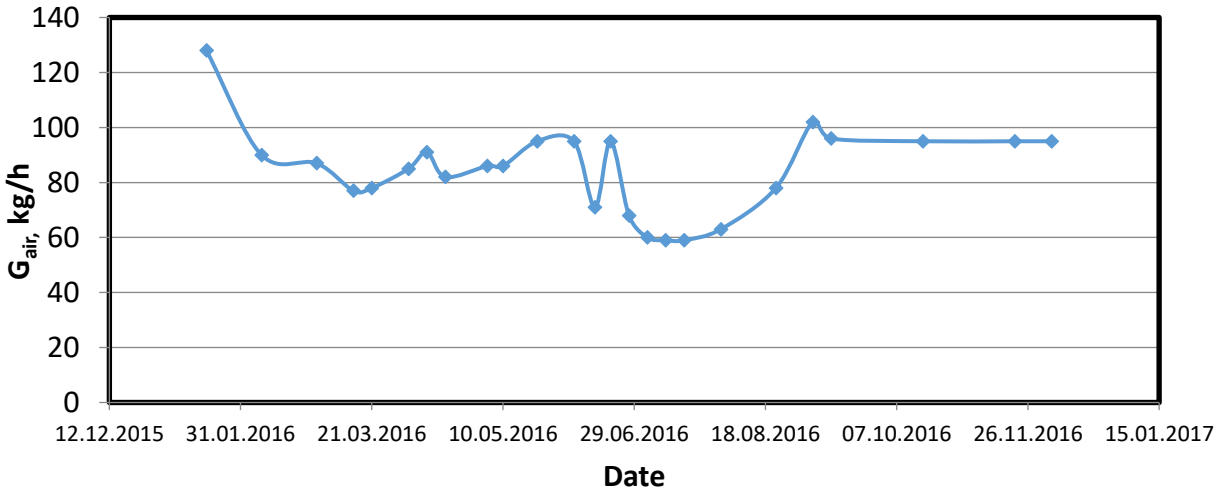

Fig 3.1. Retrospective of air suction into the condenser of the K-200-130 LMZ turbine

The capacity of the standard ejectors installed on the turbine is not enough to maintain a vacuum at the normative values with such a value of air suction. Due to the increased pressure, the efficiency of the condensing unit is reduced due to over burning the fuel. In Fig. 3.2, the burnout of fuel for the STU due to the increase in

vapor pressure in the condenser of the K-200-130 LMZ turbine is presented. Data is given for 10 months of 2016.

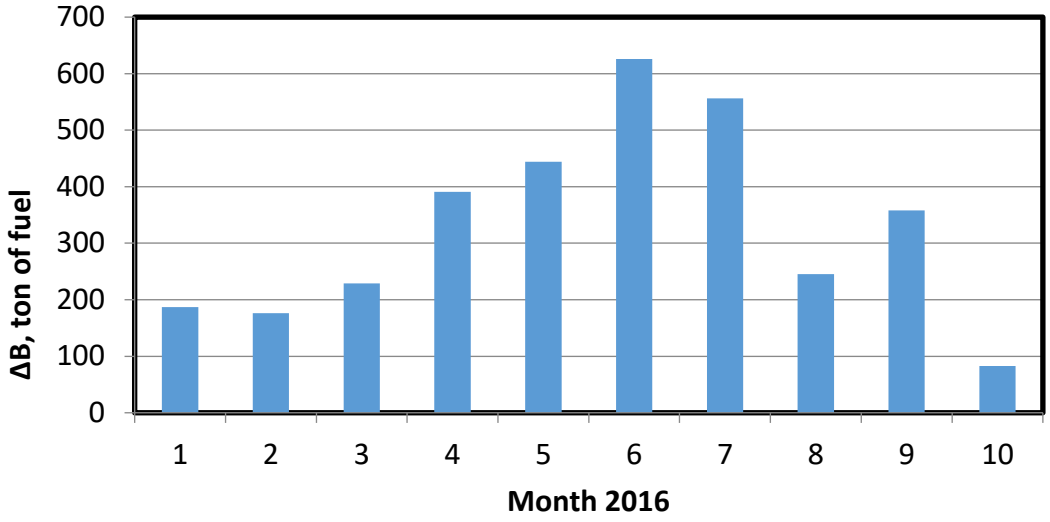

Fig. 3.2. Fuel burnout due to increased condenser steam pressure

The total fuel burnout for 10 months of 2016 from increased vapor pressure in the condenser of the K-200-130 turbine of LMZ was ΔB = 3295 tons of fuel equivalent. When the cost of fuel is S ≈ 3000 rubles / ton of fuel equivalent, the direct losses reach about 10 million rubles (135,000 euro).

To reduce fuel burnout and bring the performance of the condensing unit to standard values, it is necessary to develop a new ejector with an increased capacity of at least G_{air} = 100 kg / h with a fairly low suction pressure.

3.2. EJECTOR CALCULATION VIA THE SPECIFIED METHOD

3.2.1. DESIGN CALCULATION OF AN EJECTOR

To design the ejector's jet device, calculations were made according to the method refined via research in the present work (see Chapter 2). As the initial data for the calculation, the values of the parameters listed in Tables 3.1.1 (for EPO-3-80) and 3.1.2 (for EPO-3-120) are taken.

Table 3.1.1

№	Parameter	Designation	Stage I	Stage II	Stage III
1	Primary steam pressure, MPa	P_{ps}	0.49	0.49	0.49
2	Primary steam temperature, °C	T_{ps}	155	155	155
3	Entrained air flow rate, kg/h	G_{air}	100	100	100
4	Air-steam mixture temperature, °C	t_{mix}	35.0	40.0	40.0
5	STU condenser pressure, kPa	P_k	5.5		
8	Temperature of STU condenser cooling water, °C	t_{1w}	12.0	12.0	12.0
9	Compression ratio	P_{i2}/P_{i1}	2.1	2.3	3.2
11	Quota of steam condensing in the intercooler	ε	0.9	0.90	0.95

Table 3.1.2

№	Parameter	Designation	Stage I	Stage II	Stage III
1	Primary steam pressure, MPa	P_{ps}	0.5	0.5	0.5
2	Primary steam temperature, °C	T_{ps}	160	160	160
3	Entrained air flow rate, kg/h	G_{air}	130	130	130
4	Air-steam mixture temperature, °C	t_{mix}	35.0	40.0	40.0
5	STU condenser pressure, kPa	P_k	4.4		
8	Temperature of STU condenser cooling water, °C	t_{1w}	12.0	12.0	12.0
9	Compression ratio	P_{i2}/P_{i1}	2.3	3.4	3.4
11	Quota of steam condensing in the intercooler	ε	0.9	0.90	0.95

According to the results of the calculation using the refined method, the geometrical dimensions of the flow part are obtained: the diameters of the critical and output nozzle sections, the diameters and lengths of the conical and cylindrical parts of the mixing chamber and the diffuser and the distance from the output section of the nozzle to the input section of the mixing chamber.

It is important to note that when designing an ejector, the distribution of compression ratios between the steps was selected corresponding to the minimum consumption of primary steam.

The primary steam pressure was selected in accordance with existing steam extraction in the ejectors on the K-200-130 LMZ turbine.

The general geometrical characteristics of the developed ejectors, obtained as a result of calculation by the refined method, are presented in Tables 3.2.1 (for EPO-3-80) and 3.2.2 (for EPO-3-120).

Table 3.2.1

Parameter	Desig-nation	Unit	St. I	St. II	St. III
Nozzle critical section diameter	d_{cr}	mm	14.1	15.3	14.1
Nozzle exit section diameter	d_{ex}	mm	47.4	38.4	23.5
Inlet of conic part of mixing chamber diameter	d_c	mm	192.2	113.7	60.7
Cylindrical part of mixing chamber diameter	d_{cyl}	mm	135.9	80.4	42.9
Diffuser outlet diameter	d_d	mm	231.8	124.7	53.5
Nozzle conical part length	L_n	mm	158.5	110.1	44.8
Distance between the nozzle exit plane and the mixing chamber inlet	l_1	mm	160	94	43
Conical part of mixing chamber length	L_c	mm	229	136	85
Cylindrical part of mixing chamber length	L_{cyl}	mm	816	402	215
Diffuser length	L_d	mm	390	180	50

Table 3.2.2

Parameter	Desig-nation	Unit	St. I x2	St. II	St. III
Nozzle critical section diameter	d_{cr}	mm	13.9	16.2	15.5
Nozzle exit section diameter	d_{ex}	mm	46.5	40.6	25.9
Inlet of conic part of mixing chamber diameter	d_c	mm	150.2	127.1	67.6
Cylindrical part of mixing chamber diameter	d_{cyl}	mm	106.2	89.9	47.8
Diffuser outlet diameter	d_d	mm	195.2	132.5	76.9
Nozzle conical part length	L_n	mm	155.2	116.2	49.3
Distance between the nozzle exit plane and the mixing chamber inlet	l_1	mm	47.3	56	38
Conical part of mixing chamber length	L_c	mm	179.2	152	81
Cylindrical part of mixing chamber length	L_{cyl}	mm	531.2	449	239
Diffuser length	L_d	mm	362.3	174	119

When designing the EPO-3-120 ejector, it was decided to split the first stage of the ejector into two parallel jet devices in order to increase the reliability of operation, reduce the weight and size characteristics and increase the convenience

(cost) of production. In this case, the area of the critical section of each first stage nozzle is taken as half the area of the calculated nozzle critical section.

According to the results of the jet device design, design documentation (working drawings) for nozzles and diffusers of the EPO-3-80 and EPO-3-120 ejectors was developed.

3.2.2. CALIBRATION CALCULATION OF EJECTORS

To determine the capacity and performance characteristics of the developed ejectors, the calibration calculations of multistage ejectors were carried out according to the procedure given in Chapter 2. The calculation was performed for the ejector operating with a “dry” air and air-steam mixture. In the calculation, the following are taken into account:

- geometrical dimensions of the flow part of the jet devices;
- pressure and temperature of the primary steam and secondary flow;
- temperature of the cooling condensate at the inlet to the intercoolers;
- the estimated portion of non-condensed vapor in the coolers (to determine the flow rate of the secondary stream for stages II and III).

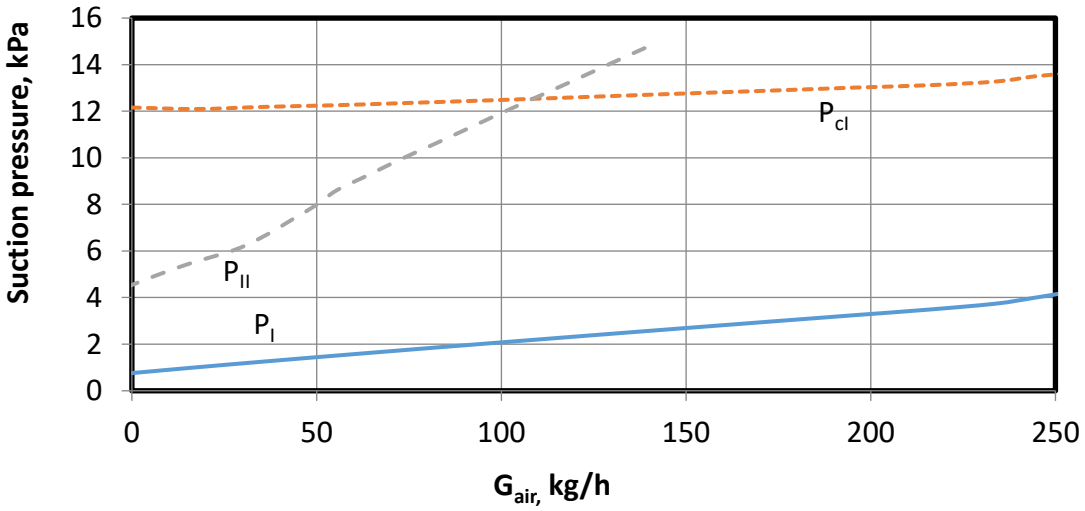

Fig. 3.3.1. Calculated performance of the EPO-3-80 ejector: P_I – stage I suction pressure, P_{II} – stage II suction pressure, P_{cI} – stage I back pressure

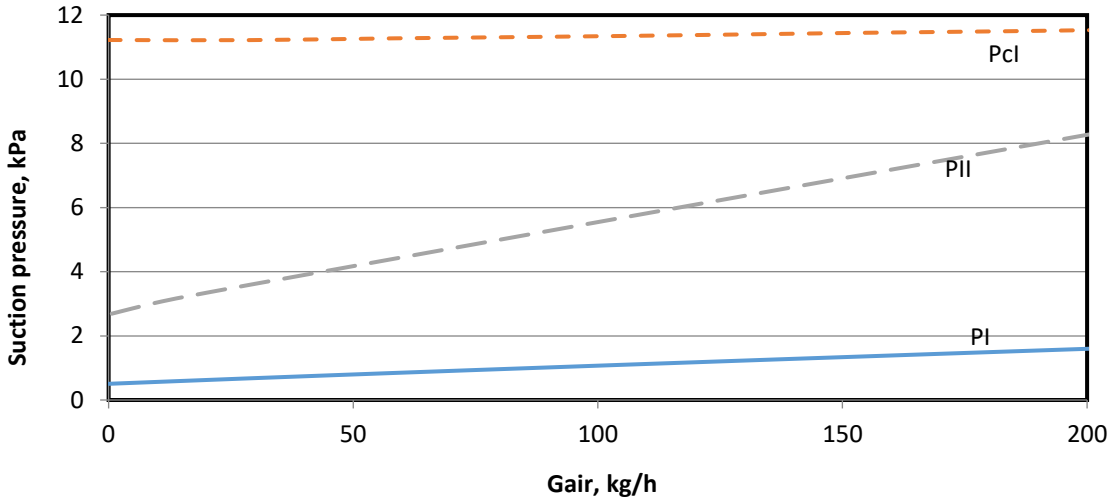

Fig. 3.3.2. Calculated performance of the EPO-3-120 ejector: P_I – stage I suction pressure, P_{II} – stage II suction pressure, P_{cI} – stage I back pressure

Figs. 3.3.1 and 3.3.2 show the dependence of the pressure in the suction chamber of stage I, stage II and the back pressure of stage I from the flow rate of dry air. The figures show that the capacity of the EPO-3-80 ejector for “dry” air (the point of the intersection of stage I backpressure and stage II suction pressure) is G_{air} = 110 kg / h. At the same time, the EPO-3-120 ejector does not have significant capacity – the backpressure of stage I does not cross the stage II characteristic. This can be explained by an incorrect cooler resistance calculation. The design of a not-full-condensation condensing heat exchanger could be the subject of relevant research.

3.3. NEW TECHNICAL SOLUTIONS IMPLEMENTED IN THE EJECTOR DESIGN

When developing the EPO-3-80 ejector, a number of the following new technical solutions, protected by patents rights [128,129], were implemented in the design:

1. Coolers are external and vertical; the cooler case diameters are standardized, while the transition pipes (supplies) between the nozzle and the diffuser are also located vertically.

2. The cooler tubes are U-shaped.

3. The layout of the jet devices and coolers is triangular.

4. The nozzle fixing unit allows for changing the axial position of the nozzle (the distance between the nozzle and the diffuser) with a step of 5 mm.

In Fig. 3.4, a 3D model of the developed EPO-3-80 ejector is presented.

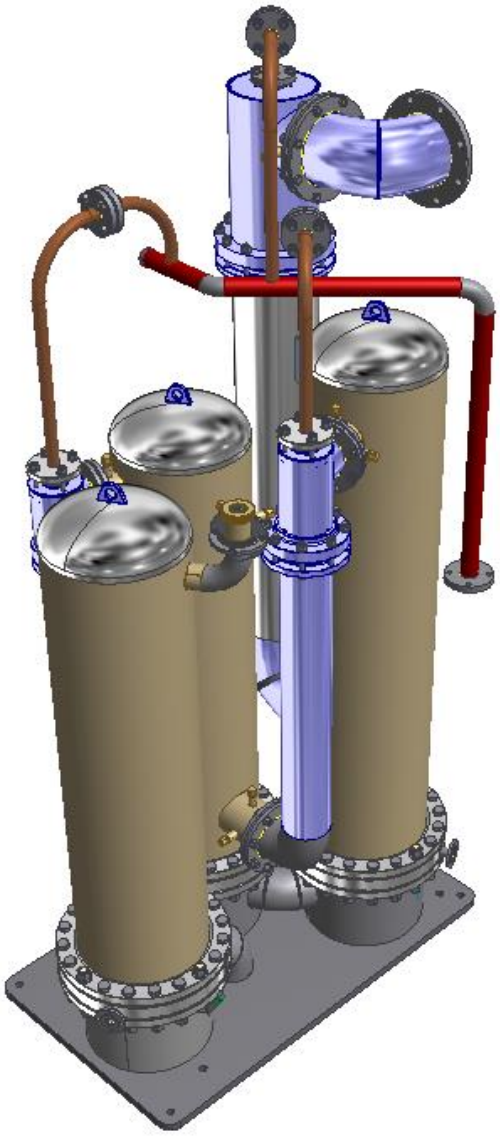

Fig. 3.4. 3D-model of the EPO-3-80 ejector

External vertical intercoolers and supplies

Placing the coolers in separate cases ensures the tightness of each stage, eliminating the possibility of the air-steam mixture flowing into areas with pressure, which is often found in ejectors with coolers in a single case. The implementation of vertical coolers in the designed ejector, as well as new designs for the supply of the intercooler, reduce or completely eliminate the possibility of corrosion-erosion deterioration of the pipes (assuming a smooth rotation of the flow at the entrance to the cooler). The diameters of the cooler cases are the same for the purposes of component unification, which simplifies the manufacturing process and improves the ejector's maintainability under operating conditions.

Heat-exchanging surfaces of intercoolers

U-tubes (material 08Kh14MF; Ø16x1.2) are installed on the intercoolers of the developed EPO-3-80 ejector. Such material allows for avoiding both corrosion-erosion damage of the tubes and thermal stresses due to thermal expansion. Since the cooling condensate of intercoolers is taken from the STU condenser drain, the pollution of the tubes, in particular the U-shaped bends, is practically impossible.

The feeding of cooling condensate into the intercoolers is designed consecutively (one after another), which allows for measuring the water temperature at the inlet and outlet of each cooler.

Ejector layout

Each cooler has a separate water chamber installed on the water chamber bloc. The ejector is designed in such a way that the steam-air mixture suction pipeline, drainage pipes, cooling water inlet and outlet relative to each other are located similarly to the corresponding EP-3-700 ejector pipes – the standard ejector of K-200-130 LMZ turbine. Such a design solution simplifies the replacement of serial ejectors with the newly designed ejectors.

To reduce the overall dimensions of the ejector, the intercoolers and jet devices attached to them are arranged in the shape of a triangle. The triangular arrangement of the coolers (Fig. 3.5 - top view) minimizes the space required for the ejector in the production area.

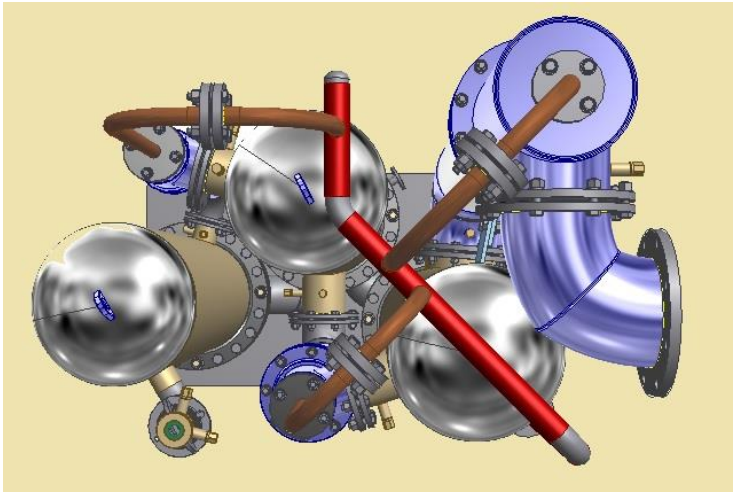

Fig. 3.5. Layout of the EPO-3-80 ejector elements (top view)

A pipeline for the primary steam supply has been designed and manufactured especially for the designed ejector and for the jet devices, which are located at different heights. For determining the pressure of the primary steam in front of the nozzles with more accuracy, the gas-dynamic resistance of the collector in the areas where the primary steam is supplied to each of the stages is determined. The calculation of the gas-dynamic resistance of the pipeline was carried out according to the method proposed by [130].

A diagram used for the calculation of the sections of the primary steam collectors is presented in Fig. 3.6.

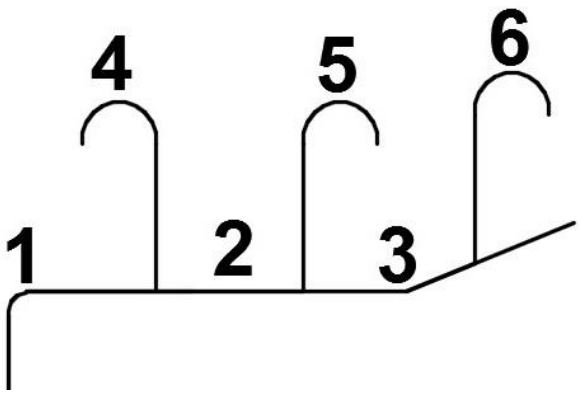

Fig. 3.6. A schematic for the design of the primary steam collectors

The gas-dynamic resistance of the steam supply collector for each stage ranges from 21.5 to 46.2 kPa, depending on the pressure of the primary steam. These values are quite high, which should be taken into account during experimental data processing and in the future design of a new supply.

Nozzle fixing unit for changing the distance between the nozzle and the diffuser

The use of a design that allows for the nozzle's axial movement in jet devices is justified in Section 2.2 and is necessary for adjusting the ejector under various operating conditions in a specific STU. When setting up the ejector, the nozzles are installed in various positions determined by the parameters of its operation. Installing a specific axial distance can improve the performance of the ejector. In the designed fixing unit, the possibility of changing the axial position was 110 mm for stage I, 25 mm – for II and 65 mm – for III. The nozzle attachment unit is described in the description of the "patent right for a utility model" [128]. The design of the unit for nozzle axial movement is shown in Fig. 3.7.

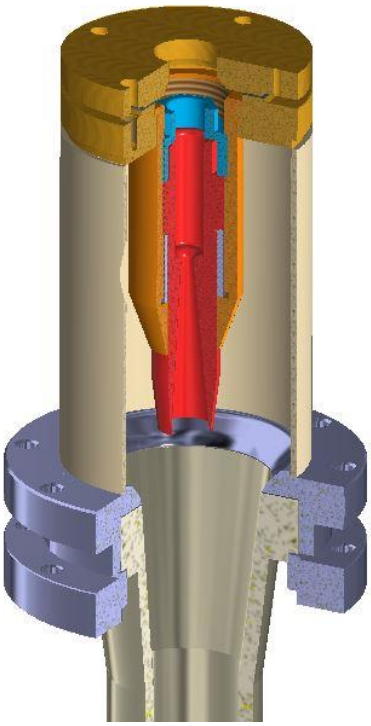

Fig. 3.7. Nozzle fixing unit

A nozzle is fixed in the body with a recess: the flange is clamped between the spacer rings and paronite gaskets. The spacer rings are 5 mm thick and the gaskets are 2 and 3 mm thick. The upper spacer rings and gaskets protrude 3-7 mm upwards from the body to ensure the tightness of the composite construction. The tightness of the unit is provided by the flange of the supply of primary steam to the ejector.

The application of the nozzle fixing unit demonstrated the increased complexity of changing the position of the nozzle. To change the axial distance between the nozzle and the diffuser during the operation of the ejector without disassembling its components, a new design has been developed and is protected by an “invention patent” [129]. In the patented jet device, the distance between the nozzle and the mixing chamber is supposed to be changed by moving the mixing chamber and the diffuser relative to the receiving chamber and the nozzle (Fig. 3.8.).

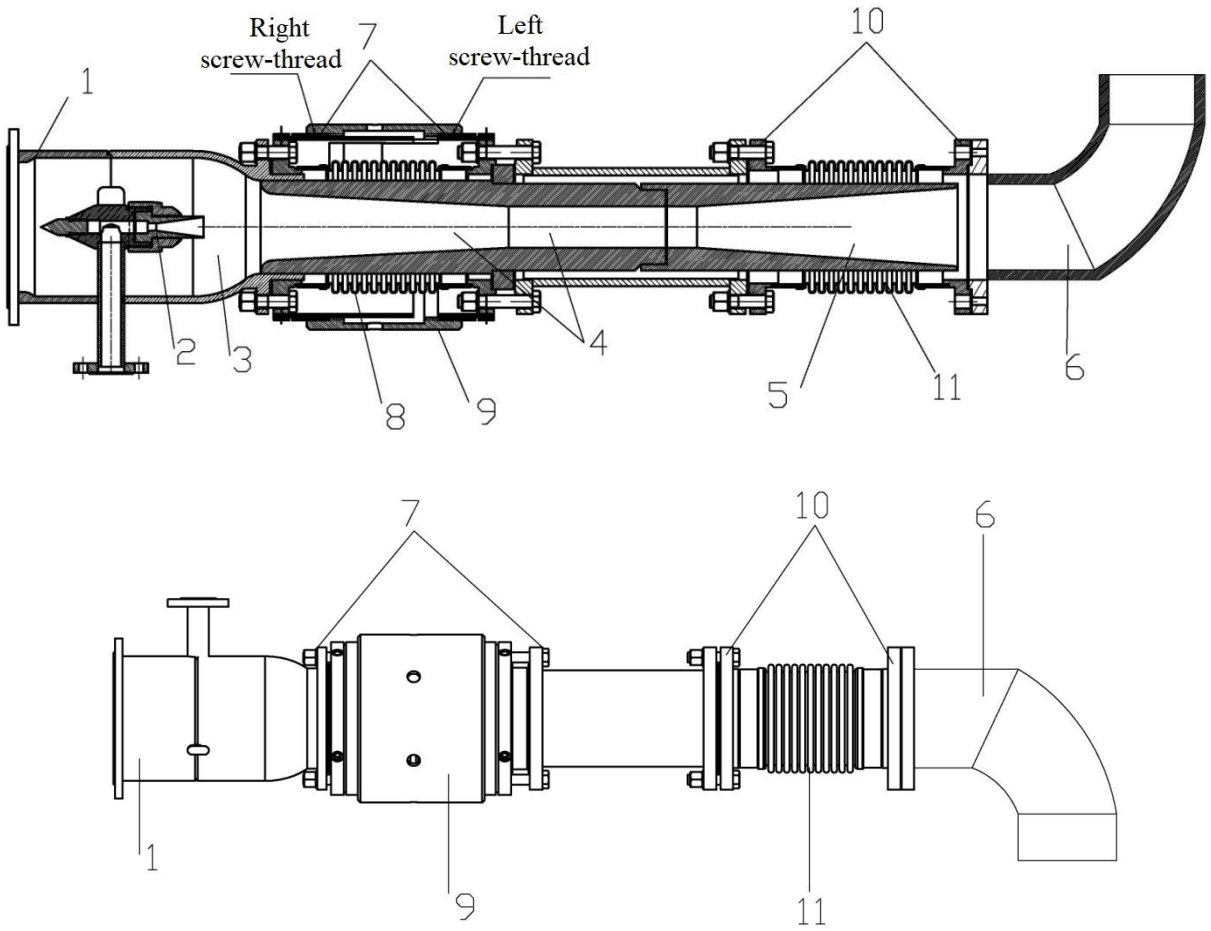

Fig. 3.8. Jet device with a changing NXP: 1 – air-steam mixture supply; 2 – nozzle; 3 – suction chamber; 4 – mixing chamber; 5 – diffuser; 6 – cooler supply; 7,10 – dissected holder; 8,11 – bellows; 9 – swivel nut

In such a design, a coaxial supply of the primary steam and the secondary mixture is provided. The proposed solutions offer a velocity increase in the secondary medium supply and a reduction in irreversible losses from flow mixing.

When developing the EPO-3-120 ejector, the following additions to the design have been made:

1. Stage I is divided into two parallel jet devices.
2. The flanges of the connection between the jet device and the cooler bodies are horizontal, not vertical.
3. The nozzle fixing unit has been modified and made with the threaded installation of the nozzle in the receiving chamber.

4. The ejector coolers are set in one line.

A model of the EPO-3-120 ejector is presented in Fig. 3.9.

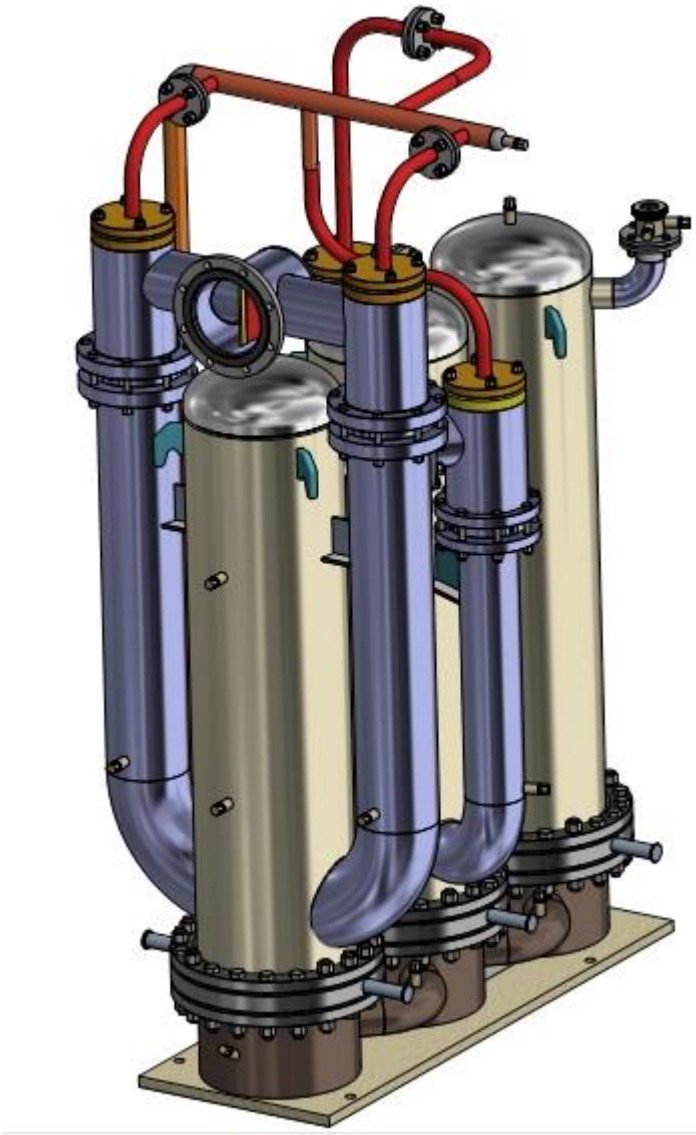

Fig. 3.9. 3D-model of the EPO-3-120 ejector.

The splitting of stage I has been done due to a proportional reduction of the nozzle throat area. This technical solution allowed us:

- To increase the reliability of the ejector: a widespread defect affecting the performance of the ejector is the locking or destruction of the nozzle due to the brick hitting the throat, etc.

- To significantly reduce the weight and dimensions of the ejector, in particular the height and diameter of the first stage. This is connected with the fact that when designing an ejector for high capacity, we are forced to set large values for the diffuser throat diameter (and, accordingly, its length): thus, the diffuser of the first stage of the EPO-3-80 ejector is disproportionately large compared to the other stages. In this case, difficulties arise with the maintenance of the ejector in terms of supplying the vapor-air mixture (the supply is located higher than a man's height), etc.
- When making a diffuser larger, it is difficult to manufacture, assemble, install and maintain it.

Making the flanges of the connection between the jet devices and the cooler housings **horizontal**, rather than vertical, allows one to ensure the tightness of the connection: in the implementation of the vertical design, the diffuser pushes the flange connection out into the upper part.

The modernization of the nozzle fixing unit with a threaded nozzle installation in the suction chamber allowed for the simplification of the assembly and disassembly of the ejector when setting up specific operating conditions. The model of the suction chamber with the threaded fastening of the nozzle is shown in Fig. 3.10.

Placing the ejector coolers in one line can be done without changing the length of the ejector base due to the side arrangement of the jet devices. The location of the coolers is shown from the top (Fig. 3.11).

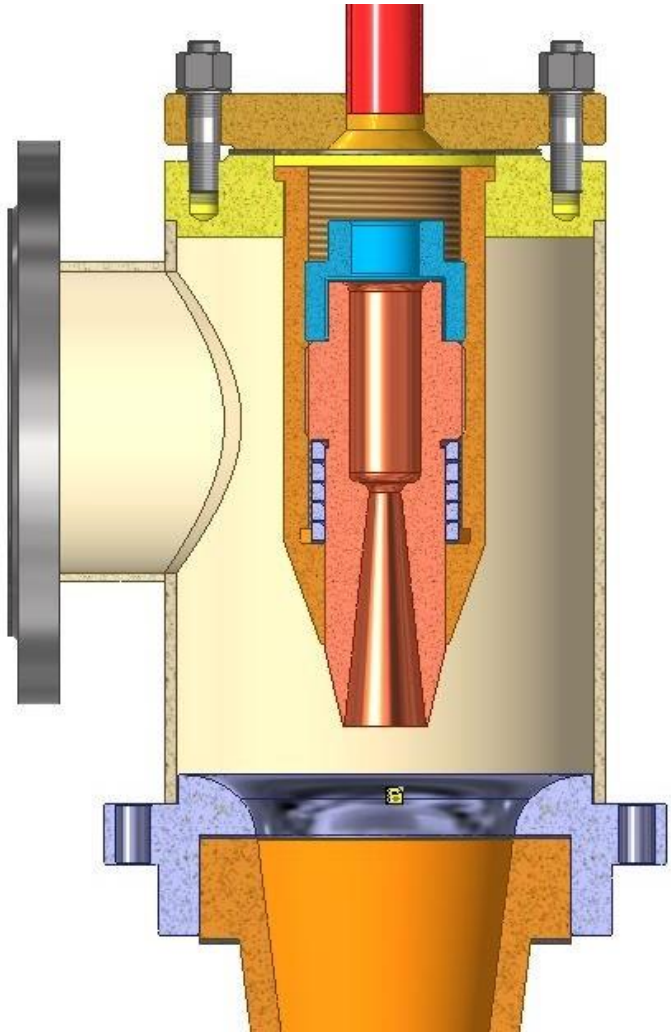

Fig. 3.10. The design of the threaded fixing unit of a nozzle

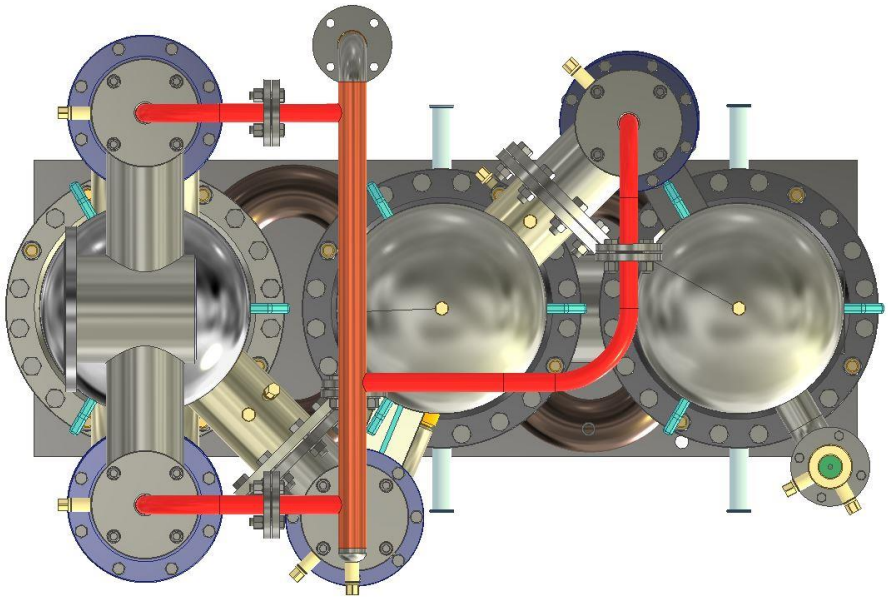

Fig. 3.11. The location of the elements of the EPO-3-120 ejector (top view)

3.4. TEST RESULTS OF DEVELOPED EJECTORS IN OPERATING CONDITIONS DURING JOINT FUNCTIONING OF THE EJECTOR AND CONDENSER

The developed EPO-3-80 ejector was installed as general ejector “A” on the K-200-130 LMZ turbine. The EPO-3-120 ejector was also installed on the K-210-130 LMZ, T-180-130 LMZ, PT-60-90 LMZ, KT-80/100-90 LMZ and T-87/90-130 LMZ turbines. Tests were carried out under the operating conditions in TPPs at various working steam pressures, cooling condensate temperatures at the inlet to the intercoolers and axial positions of nozzles.

The ejectors are put on TPP assembled. Production, assembly, pressure testing of vapor-air space, pipe systems, a primary vapor collector and setting the dimensions of the nozzle devices were carried out as per the manufacturer’s conditions.

Obtaining the performance characteristics of the new EPO-3-80 ejector during testing when the turbine was switched. To organize the drainage of the ejector coolers before the start of testing of the seal steam supply is switched on, the vacuum in the condenser was accumulated and maintained by the second general and starting ejectors. The value of vapor pressure in the condenser was about P_c = 0.047-0.061 MPa (350-450 mm Hg), which is enough to maintain drainage from intercoolers. Testing on a working turbine was not possible due to the increased air suction of the K-200-130 LMZ turbine - about 120-130 kg / h, at a nominal rate of 21.5 kg/h [64]. With such an air suction rate, a single general ejector “B” (type EP-3-700) is not capable of maintaining the necessary vacuum in the turbine condenser. The new ejector at the time of testing was disconnected from the condenser by the valve.

Tests of the EPO-3-120 ejectors were carried out on operating turbines, while the vacuum in the turbine condensers was maintained by the second general ejector.

Tests of the joint operation of ejectors and condensers during turbine operation were also conducted. When conducting joint tests in the EPO-3-120

ejector, a "dry" atmospheric air was added through special sound washers, in addition to the air removed from the condenser.

3.4.1. TECHNIQUE AND ERROR EVALUATION

To conduct experimental studies of a new ejector, a test procedure was refined basing on recommendations from [105]. A new expanded scheme for measuring the performance of an ejector was developed, including a number of new parameters (along with the pressure of the SAM in the suction chambers of the jet devices). It is possible to determine the pressures and temperatures behind the diffusers of each stage, the temperatures in the suction chambers, the temperatures of the drains and cooling condensate at the inlet and outlet of each intercooler and the consumption of cooling condensate. The developed measurement scheme made it possible to fix the gas-dynamic resistance of the intermediate coolers.

Table 3.3 presents the characteristics of the instruments used in the testing process.

Table 3.3

Measurement	**Instrument**	**Unit**	**Range**	**Nominal error**
Suction pressure of stage I (abs.), P_{111} , P_{112}	Diaphragm pressure transducer	kPa	0…10	±0.05
Exhaust pressure of stage I (abs.), P_{12}, and suction pressure of stage II (abs.) P_{21}	Diaphragm pressure transducer	kPa	0…40	±0.1
Exhaust pressure of the stage II (abs.), P_{22}, and suction pressure of stage III (abs.), P_{31}	Diaphragm pressure transducer	kPa	0…63	±0.32
Exhaust pressure of stage III (abs.), P_{32}, and atmospheric pressure P_4	Diaphragm pressure transducer	kPa	0…160	±0.5
Drainage temperature of stages I, II, and III	Infrared pyrometer	°C	-20…300	±2
SAM temperature at the exhaust	Resistance thermometer DTS065-50.A3.100	°C	-50…180	±0.1
Temperature of a cooling condensate upstream and downstream of each intercooler	Resistance thermometer DTS065-50.A3.100	°C	-50…180	±0.1

SAM temperatures in suction chambers and behind the diffusers	Resistance thermometer DTS065-50.A3.100	°C	-50…180	±0.1
Primary steam pressure	Manometer	kg/sm^2	0…16	±0.1
Cooling condensate flow rate	Ultrasound device 'Portaflow 330'	m^3/h	No limit	±0.01
Pressure drop at the air flow meter on the exhaust of ejector	Diaphragm pressure transducer	kPa	0…2.5	±0.013

Resistance thermometers, used to determine the temperature of the vapor-air mixture and cooling condensate, were calibrated in a thermostat using control mercury thermometers with a division value of 0.1 °C. When determining the pressure of the primary steam before the nozzles, the gas-dynamic resistance of the steam collector from the measuring point to each nozzle was taken into account.

During the tests, the air rate was changed by air supply to the ejector through calibrated sonic washers with various nozzle diameters (orifices): from 0 to 16.8 mm. The amount of air was monitored using a special device ("UrFU air flow meter"), which was designed and manufactured for TPP monitoring systems to measure air flow rate at the ejector exhaust. There are several calibrated nozzles at the outlet of the "UrFU flow meter" and a pressure difference measurement upstream and downstream from the nozzle. From 0 to 180 kg / h of "dry" atmospheric air with a step of about 10–12 kg / h was put into the ejector. The remaining measurements were carried out using standard instruments installed on the turbine control panel.

The instrument setup diagram is presented in Fig. 3.12.

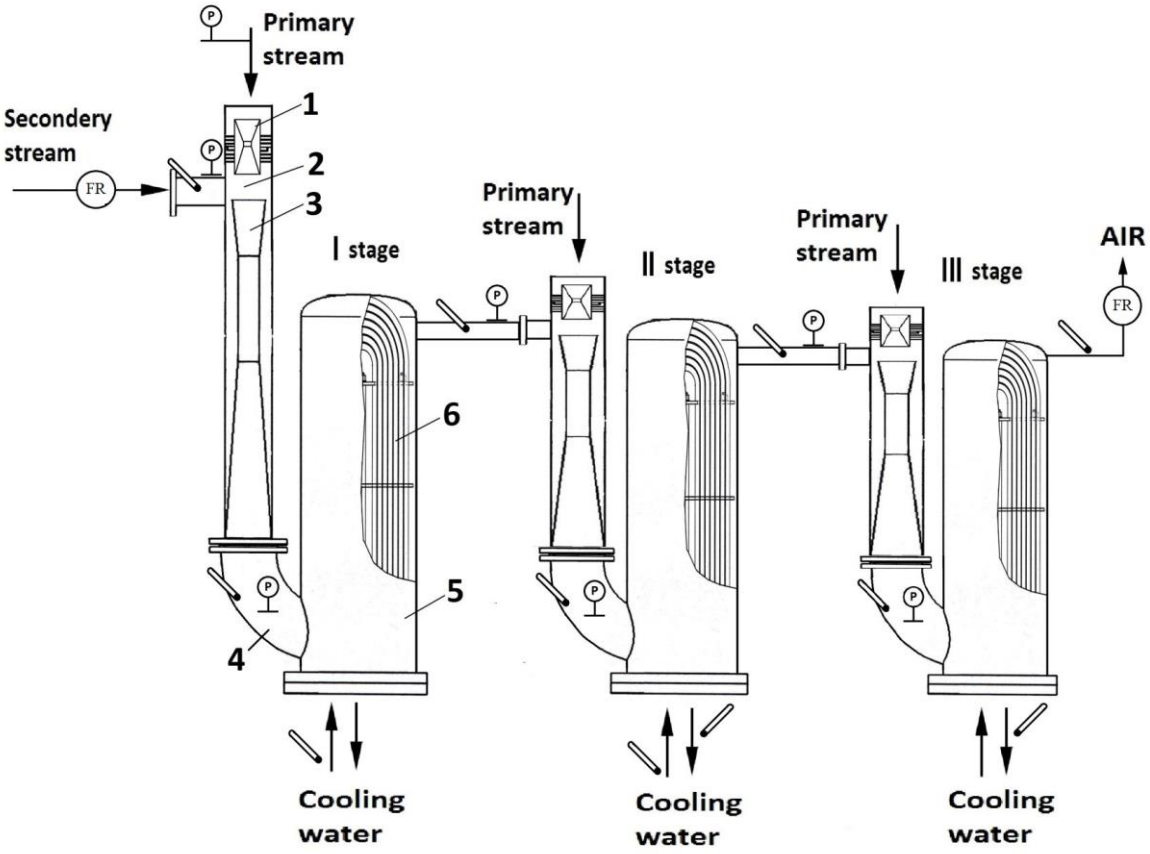

Fig. 3.12. Ejector measurement schematic:
1 – nozzle; 2 – suction chamber; 3 – mixing chamber; 4 – transition pipes (supplies); 5 – intermediate cooler; 6 – heat-exchanging surfaces;

– pressure measurement; – temperature measurement; FR - flow rate measurement

The estimation of measurement errors was carried out on the basis of [124]. The error is calculated for a number of indicators: water heating in coolers, temperature of cooling condensate and the SAM, pressure difference in coolers and steam and SAM pressure.

The number of measurements in each experiment (5-6 times) was chosen in such a way as to exclude random error. In this case, the measurement error is determined by the instrument error.

The relative error of temperature measurement is calculated by the formula (3.1):

$$\delta_{\text{t}} = \frac{\delta t}{t} * 100\,\%, \tag{3.1}$$

where δ t – the absolute error of temperature measurement equal to the instrumental error of the resistance thermometer; t – the absolute value of the measured temperature.

The values of the maximum relative error of temperature measurement are presented in Table 3.4.

Table 3.4

Measurement point	Maximum relative error, %
Cooling condensate temperature	0.5
Temperature of SAM in suction chambers	0.2
Temperature of SAM behind diffusers	0.1

The maximum RMS relative error of heating in coolers was determined by formula (3.2):

$$\delta_{\Delta t} = \frac{\sqrt{\delta t_1^2 + \delta t_2^2}}{\Delta t} \cdot 100\% = 9{,}5\%. \tag{3.2}$$

The relative error of pressure measurement was calculated by formula (3.3):

$$\delta_{\text{P}} = \frac{\delta P}{P} * 100\%, \tag{3.3}$$

where δ P – absolute error of pressure measurement equal to the instrumental error of the sensor; P – the absolute value of the measured pressure.

The values of the maximum relative error of pressure measurement are presented in Table 3.5.

Table 3.5

Measurement point	Maximum relative error, %
Primary steam pressure	1.7
Pressure in suction chambers (I; II; III)	1.7; 1.3; 1.1
Pressure behind diffusers (I; II; III)	1.3; 1.1; 0.5

The maximum RMS relative error of the pressure difference in the coolers was determined by formula (3.4):

$$\delta_P = \frac{\sqrt{\delta P_1^2 + \delta P_2^2}}{\Delta P} \cdot 100\% . \qquad (3.4)$$

The values of the maximum RMS relative error of measuring the pressure difference are presented in Table 3.6.

Table 3.6

Measurement point	RMS error, %
Intercooler I	9.5
Intercooler II	11.3
Intercooler III	7.1

The maximum RMS relative error in determining the heating of cooling condensate in the intercoolers does not exceed ±9.5%. The maximum RMS error of determining the pressure difference in coolers does not exceed ±11.3%. The chosen measurement schematic ensured good repeatability and reliability of the results obtained throughout the planned range of research.

3.4.2. RESULTS OF EXPERIMENTAL RESEARCH ON EJECTOR CHARACTERISTICS

The tests of the EPO-3-80 ejector consisted of four main phases.

1. Obtaining the performance characteristics of the ejector at various pressures of the working steam at the calculated positions of the nozzles in the jet devices of the ejector.

2. Changing the positions of nozzles in the jet devices of the ejector according to the results of the first phase of testing. Obtaining the new performance of the ejector at various pressures of the working steam at the adjusted positions of the nozzles.

3. Obtaining the performance of the ejector at various temperatures of the circulating water at the inlet to the condenser (in the winter and summer seasons). Comparison of the results.

4. Obtaining the control values of the parameters of the ejector functioning in a running turbine when the ejector is connected to a condenser.

The absolute pressure of the working steam on the ejectors during the experimental studies varied from 0.6 to 0.86 MPa.

The testing of the ejector when working with a condenser was carried out without additional air supply to the ejector. The amount of air drawn into the condenser was determined at the exhaust of the third stage of the ejector using a specially installed air-measuring device.

Nozzle exit position

To adjust the axial positions of the nozzles of each stage, the performance characteristics were obtained with the calculated position of the nozzles and a working steam pressure of P_{ps} = 0.6-0.7 MPa. The tests were carried out at a cooling condensate temperature of T_{cc} = 10-12 °C. The characteristics of the ejector with a working steam pressure of P_{ps} = 0.6 MPa are presented in Fig. 3.13. The data obtained from the tests is presented in Appendix 4.

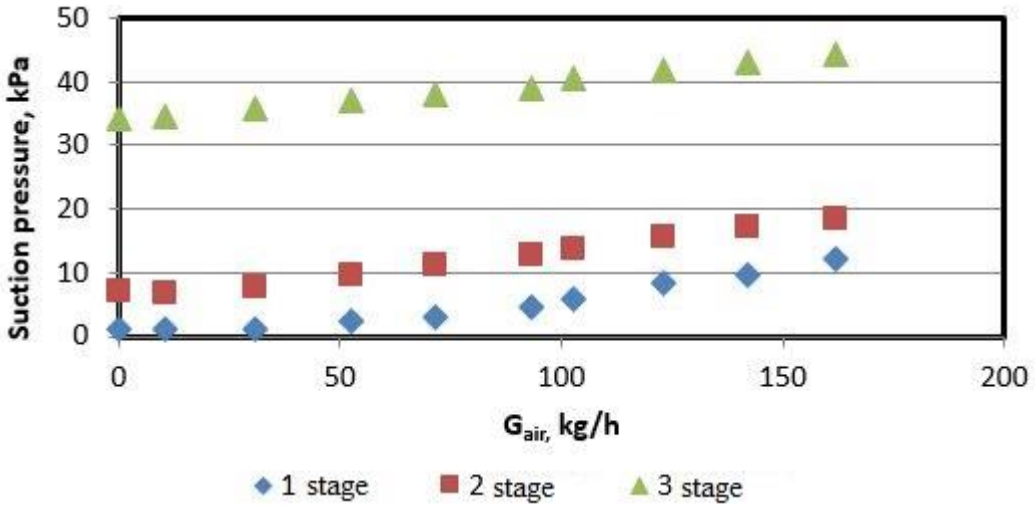

Fig. 3.13. Performance characteristics of the EPO-3-80 ejector with a working steam pressure of R_{ps} = 0.6 MPa and the calculated installation position of the nozzles

From the graph it can be seen that the pressure created by the first stage at zero air flow through the ejector is P_I <1 kPa. With air flow up to 90 kg / h, the first stage of the ejector operates in the “working” section (with air flow rate G_{air} = 90 kg / h, the

pressure in the first stage is P_I = 4.5 kPa). Further, the ejector moves to the "overload" section. The capacity of the ejector corresponds to the stated characteristics; however, the suction pressure is P_I = 4.6 kPa when a calculated value is P_I = 2.2 kPa.

With an increase of the working steam pressure to the ejector up to P_{ps} = 0.7 MPa and the consumption of "dry air" G_{air} = 90 kg / h, the pressure in the first stage changes to P_I = 2.6 kPa.

When adjusting the axial positions of the nozzles, the distance between the nozzles of stages I and II and the corresponding mixing chambers are reduced. When choosing the adjusted position of the nozzles, it was taken into account that the existing air suction (at the time of the test) to the vacuum system of the turbine was G_{air} = 120-130 kg / h, i.e. significantly higher than the estimated maximum performance of the ejector. Table 3.7 presents the calculated and adjusted values of the distance from the nozzle exit to the entrance to the mixing chamber of each stage.

Table 3.7

	Calculated position, mm	Adjusted position, mm
I	160	83
II	94	80
III	43	43

The results of the ejector tests with the adjusted nozzles positions at a working steam pressure of R_{ps} = 0.7 MPa are presented in Fig. 3.14. The data obtained from the tests is presented in Appendix 4.

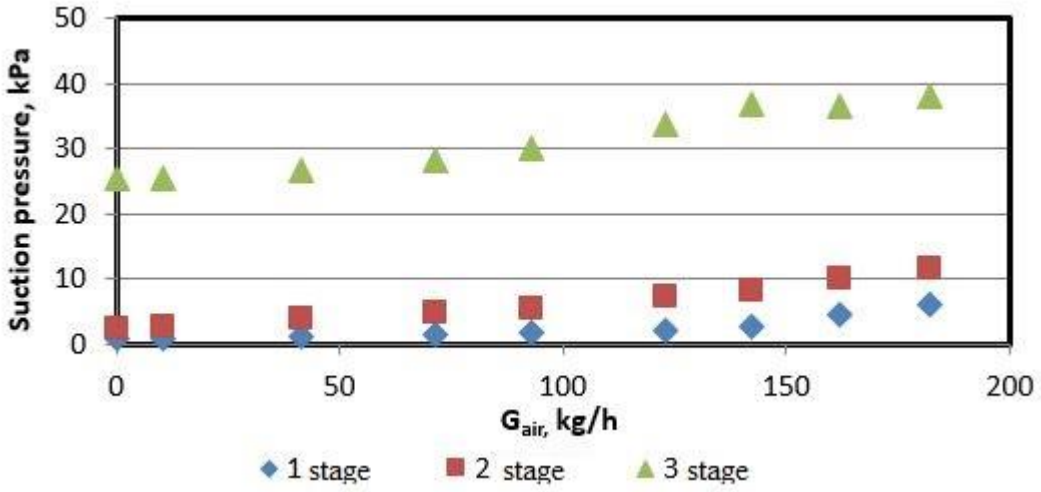

Fig. 3.14. Performance characteristic of the EPO-3-80 ejector with a working steam pressure of R_{ps}=0.7 MPa and the adjusted installation position of the nozzles

From the graph it is clear that the length of the performance characteristics of stage I (maximum ejector capacity) increased to 140 kg / h. At the same time, the suction pressure of the ejector did not exceed 3 kPa.

For comparison, the characteristics of stage I at various positions of the nozzles are shown in Fig. 3.15. The comparison is made according to the performance characteristics of the first stages as determining the functioning of the entire multistage ejector.

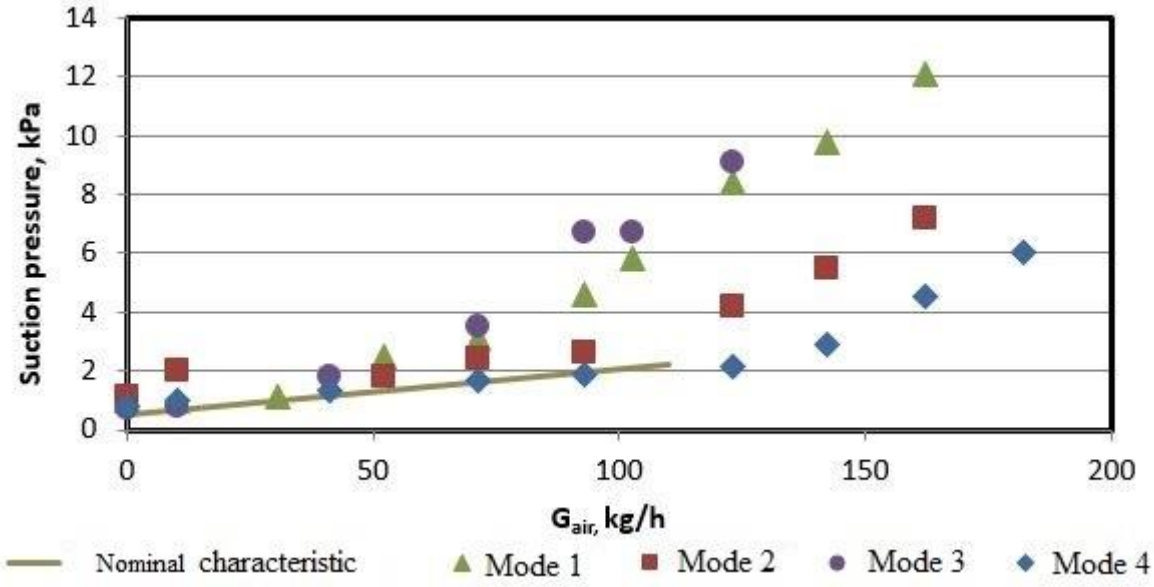

Puc.3.15. Characteristics of stage I of the EPO-3-80 ejector:
Mode 1 – P_{ps} = 0,6 MPa, NXP - calculated;

Mode 2 – P_{ps} = 0,7 MPa, NXP - calculated;
Mode 3 – P_{ps} = 0,6 MPa, NXP - adjusted;
Mode 4 – P_{ps} = 0,7 MPa, NXP – adjusted.

As can be seen from the graph, the change in the distance between the nozzle and the diffuser of stage I led to a decrease of the suction pressure to P_I = 0.8 kPa at zero air suction point. At the same time, the length of the "working" section of the characteristics of the ejector has increased to G_{air} = 140 kg / h. At this flow rate, the pressure in stage I was P_I = 2.4 kPa.

The performance characteristic at the adjusted position of the nozzles and the pressure of the working steam P_{ps} = 0.7 MPa completely coincides with the calculated one and at the same time corresponds to higher capacity.

We can suggest that these data make it possible to conclude that the recommended pressure of the working steam is P_{ps} = 0.7 MPa when operating the EPO-3-80 ejector under the conditions of high air suction into the vacuum system.

The tests of the EPO-3-120 ejector consisted of three main phases.

1. Obtaining the performance characteristics of the ejector at various pressures of the working steam.
2. Obtaining the performance of the ejector at various temperatures and flow rates of the cooling condensate at the inlet to the coolers. Comparison of the results.
3. Obtaining control values of the parameters of the ejector functioning in a running turbine when the ejector is connected to a condenser. Supplying additional air to the ejector and obtaining performance characteristics with the SAM as a secondary fluid.

The absolute pressure of the working steam on the ejectors during the experimental studies varied from 0.6 to 0.7 MPa.

The testing of the ejector when working with a condenser was carried out with additional air supply to the ejector.

According to the test results, the performance characteristic of the ejector at an absolute working steam pressure of R_{ps} = 0.6-0.7 MPa was obtained (Fig. 3.16.).

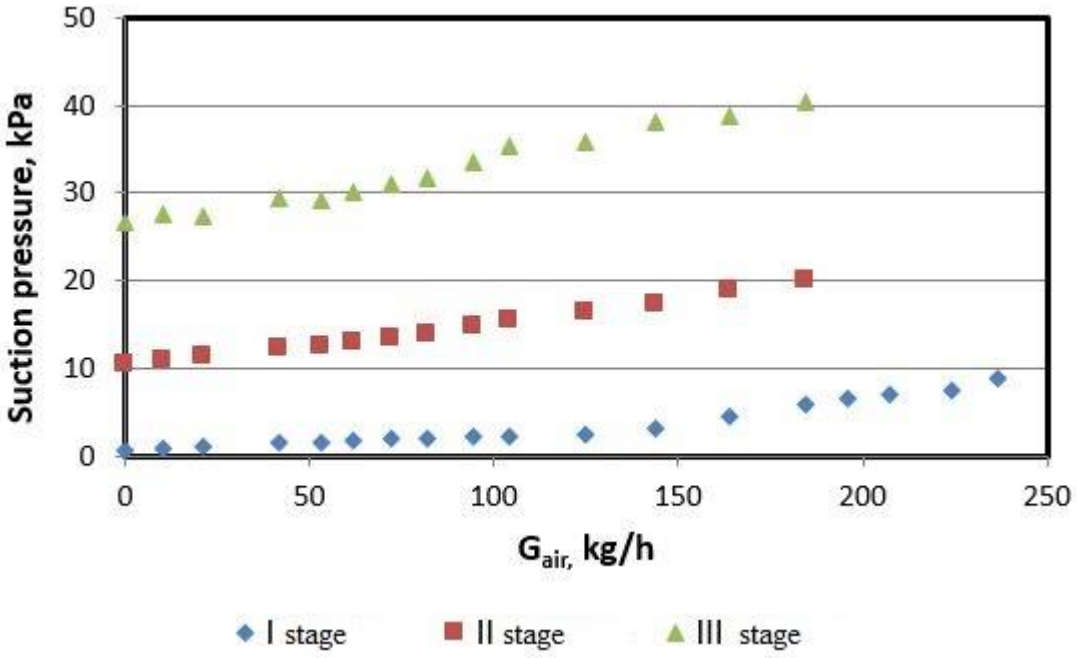

Fig. 3.16. Performance characteristics of the EPO-3-120 ejector with a working steam pressure of R_{ps} = 0.7 MPa.

From Fig. 3.16 it can be seen that the pressure created by stage I at zero air flow through the ejector is P_I <1 kPa. With air flow up to 145 kg / h, the first stage of the ejector operates on the "working" section. With air flow G_{air} = 145 kg / h, the pressure in stage I is P_I = 3.1 kPa. Further, the ejector moves to the "overload" section.

In Fig. 3.17, the test results for stage I of the ejector under a reduced working steam pressure of R_{ps} = 0.6 MPa are presented. The black lines determine the area of the nominal characteristic (min-max).

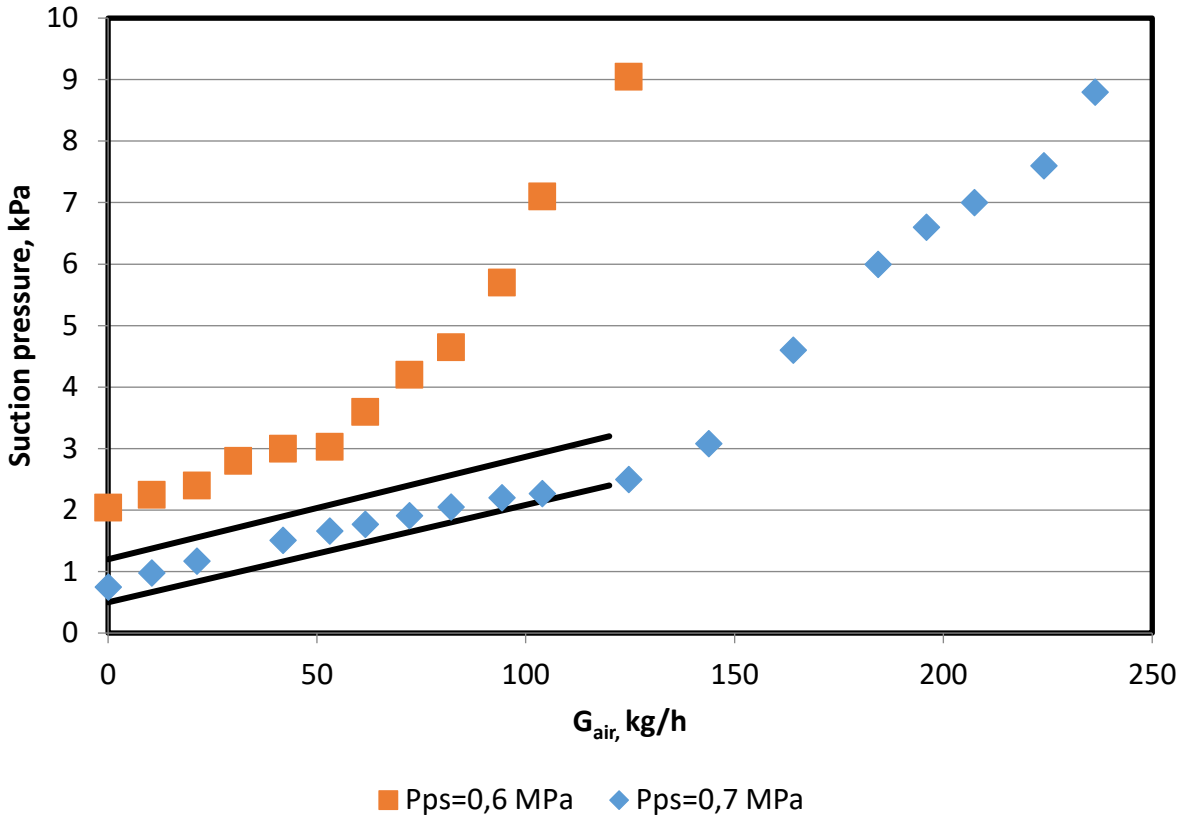

Fig. 3.17. Performance characteristics of stage I of the EPO-3-120 ejector at various primary steam pressures

As can be seen from the graph, the suction pressure is significantly lower at a working steam pressure of R_{ps} = 0.7 MPa. The capacity of the ejector at R_{ps} = 0.6 MPa was 55 kg/h. For reliable and efficient operation of the ejector, it is recommended to maintain the pressure P_{ps} = 0.7 MPa.

Cooling condensate temperature

To study the effect of cooling condensate temperature on the functioning of the ejector, tests were performed at higher temperatures of the circulating water at the inlet to the condenser and, accordingly, the main condensate at the entrance to the intermediate coolers.

The temperature of the cooling condensate varied from t_{cc} = 10-12 °C to t_{cc} = 32-35 °C. The tests were carried out at a higher working steam pressure of P_{ps} = 0.81

and P_{ps} = 0.86 MPa: the position of the nozzles is “adjusted” (see data in Appendix 4).

In Fig. 3.18, a comparison of the characteristics of stage I obtained at various t_{cc} is presented.

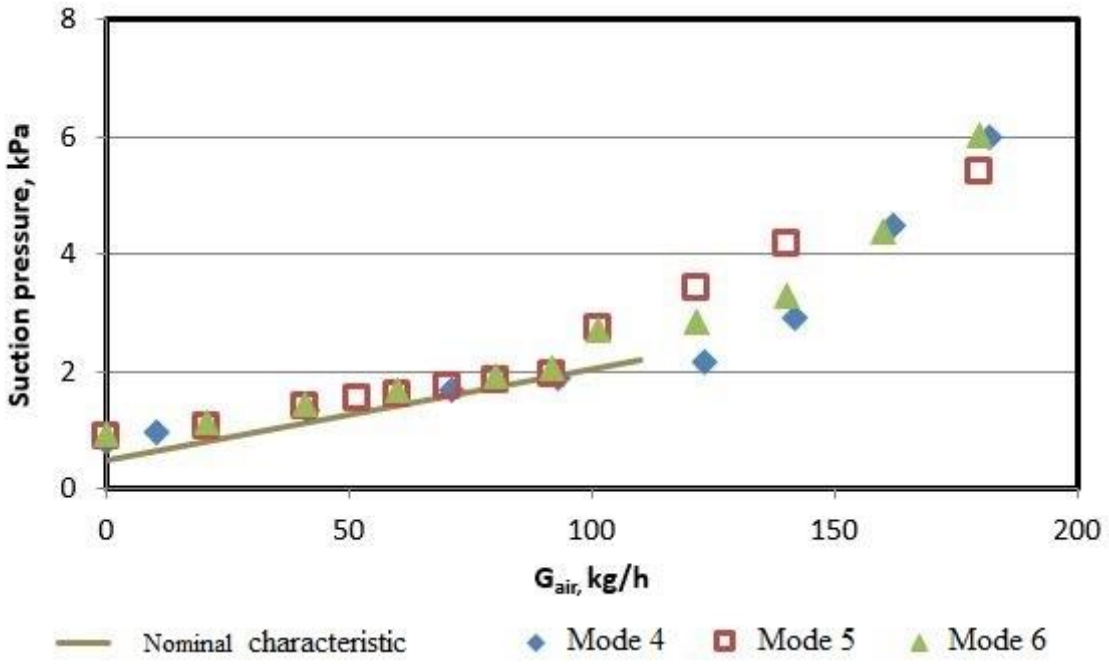

Fig. 3.18. Characteristics of stage I of the EPO-3-80 ejector:
Mode 4 – P_{ps} = 0,7 MPa, *NXP – adjusted, t_{cc}=10-12°C;*
Mode 5 - P_{ps} = 0,81 MPa, *NXP – adjusted, t_{cc}=32-35°C;*
Mode 6 - P_{ps} = 0,86 MPa, *NXP – adjusted, t_{cc}=32-35°C.*

In all investigated modes, the capacity of the ejector is about 140 kg/h. This is a controversial statement, but the change of the angle characteristic is very low, and the right part of the high t_{cc} characteristic is not parallel with the off-design characteristic for low t_{cc}. This leads us to the idea that the capacity may be equal. With a higher t_{cc}, the suction pressure of stage I in the range of air flow from 90 kg/h to 140 kg/h is slightly increased in comparison with the mode at t_{cc} = 10 ... 12 °C. Throughout the rest of the tier characteristic, there is no t_{cc} effect.

In Figs. 3.19-3.20, the characteristics of stages II and III are presented.

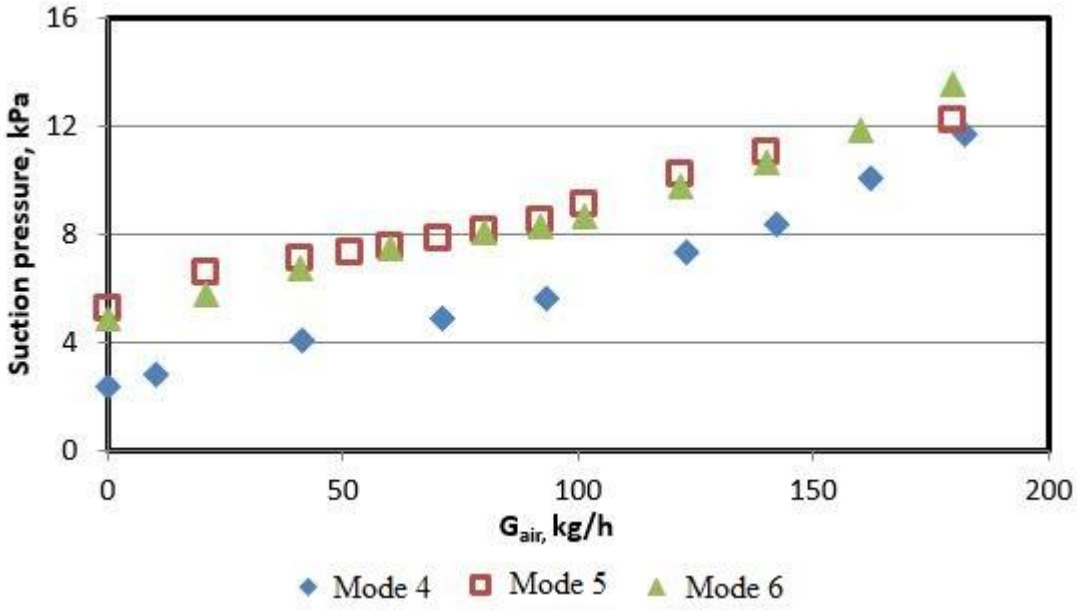

Fig.3.19. Characteristics of stage II of the EPO-3-80 ejector:
Mode 4 – P_{ps} = 0,7 MPa, *NXP – adjusted, t_{cc}=10-12°C;*
Mode 5 - P_{ps} = 0,81 MPa, *NXP – adjusted, t_{cc}=32-35°C;*
Mode 6 - P_{ps} = 0,86 MPa, *NXP – adjusted, t_{cc}=32-35°C.*

It is important to note that the characteristic of stage II is much higher at a higher t_{cc}. This can be explained by the fact that at a higher cooling condensate temperature, the pressure in the intermediate cooler of stage I is also higher - this can be seen from measurements of the absolute pressure at the outlet of the stage I diffuser. The increase in the suction pressure is also partly due to a higher flow rate of the working steam. Not all the steam condenses in the intercooler — the flow rate of the suction mixture in stage II increases. To confirm this assumption, the calculation of the heat balances of the coolers on all measured modes was carried out. According to the results of the calculation, it was shown that in experiment №4 (t_{cc} = 10-12 °C) the steam in cooler I condenses completely, while in experiments №5-6 (t_{cc} = 32 ... 35 °C) about 85-90% of steam is condensed.

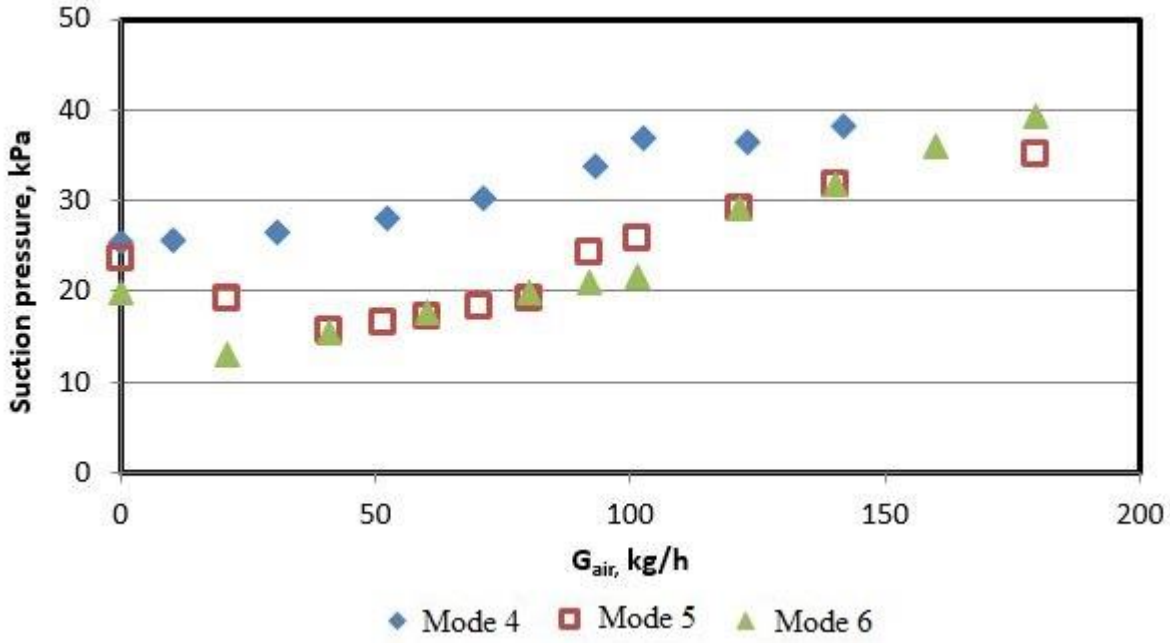

Fig.3.20. Characteristics of stage II of the EPO-3-80 ejector:
Mode 4 – P_{ps} = 0,7 MPa, *NXP – adjusted, t_{cc}=10-12°C;*
Mode 5 - P_{ps} = 0,81 MPa, *NXP – adjusted, t_{cc}=32-35°C;*
Mode 6 - P_{ps} = 0,86 MPa, *NXP – adjusted, t_{cc}=32-35°C.*

The suction pressure of stage III decreases as t_{cc} increases (Fig. 3.20). With an increase in the flow rate of the mixture to stage II, the compression ratio of stage II decreases (as does the pressure at the exit of stage II – at the entrance to stage III). The effect of increasing of the suction pressure at stage III can also be explained by the higher primary pressure. However, it should be much more dependent on the stage II pressure.

In the course of testing the ejector, the effect of a significant change in pressure in the intermediate coolers was discovered. The pressure drop in the cooler changed in the range of $\Delta P = P_1 – P_2 = –3…+11$ kPa. An analysis of this effect is presented in Chapter 4.

When analyzing the results of the experiment, according to the results of measuring temperatures and pressures behind the ejector diffusers, it is noted that in most of the operating modes the coolers receive steam, which is overheated relative to the saturation temperature. In our opinion, steam overheating has a significant effect on the function of the intercooler. With an increase in the degree of

overheating, the proportion of condensable steam from the air-steam mixture decreases.

3.4.3. COMPARATIVE ANALYSIS OF THE CHARACTERISTICS OF SERIAL EJECTORS AND NEW EJECTORS

In Fig. 3.21, the performance characteristics of stage I of the EPO-3-80 and serial EP-3-700 (installed as the second general ejector) ejectors are presented. The characteristics are obtained at the recommended working steam pressure for each ejector – ΔP_{ps} = 0.7 MPa for the EPO-3-80 and ΔP_{ps} = 0.5 MPa for the EP-3-700. The characteristics of the EP-3-700 ejector were obtained by the staff of the SDPS in 2006 and 2014 [131,132].

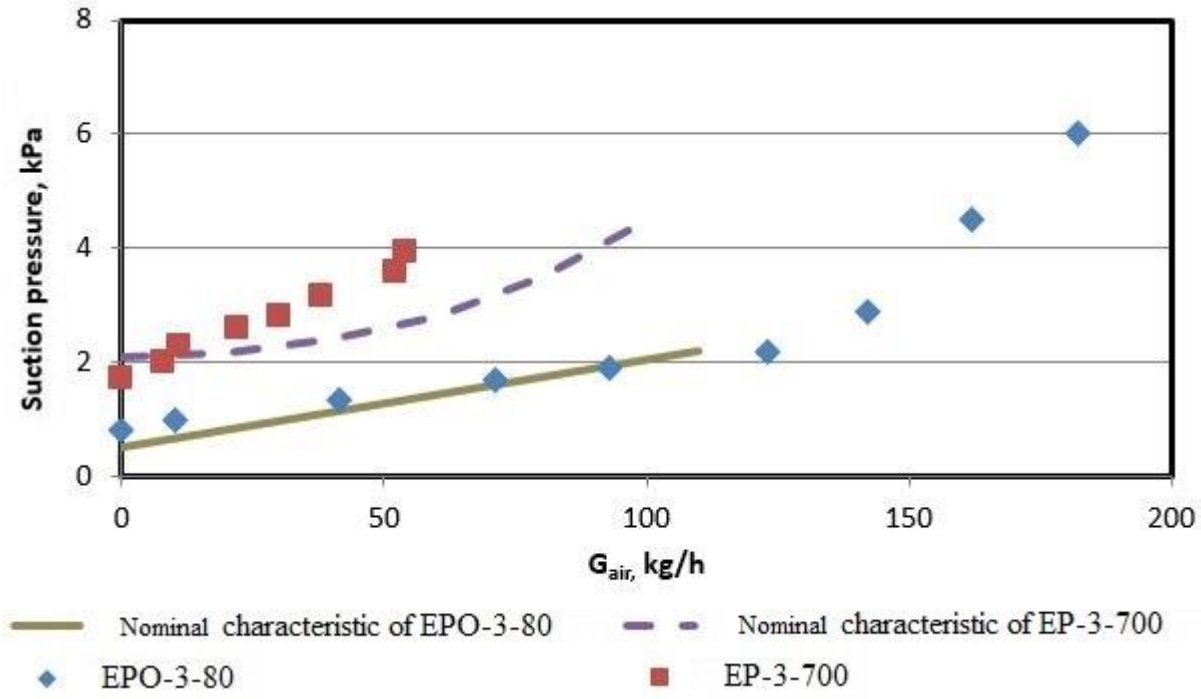

Fig. 3.21. Comparison of the characteristics of EPO-3-80 and EP-3-700 ejectors.

From the presented graph it is clear that the performance and calculated characteristics of stage I of the EP-3-700 ejector are higher than the corresponding characteristics of the EPO-3-80. The initial points of the characteristics of the EP-3-700 are higher than the initial points of the characteristics of the EPO-3-80 for 0.9 kPa. The tilt angle of the characteristics of the ejector EPO-3-80 is much smaller,

which allows for the maintenance of a deep vacuum in the turbine condenser with high air suction in the vacuum system. The capacity of the EP-3-700 ejector is 54 kg/h, while the performance of EPO-3-80 –140 kg/h.

A comparison of the new EPO-3-80 and EPO-3-120 ejectors with serial ejectors from various turbine plants is shown in Fig. 3.22.

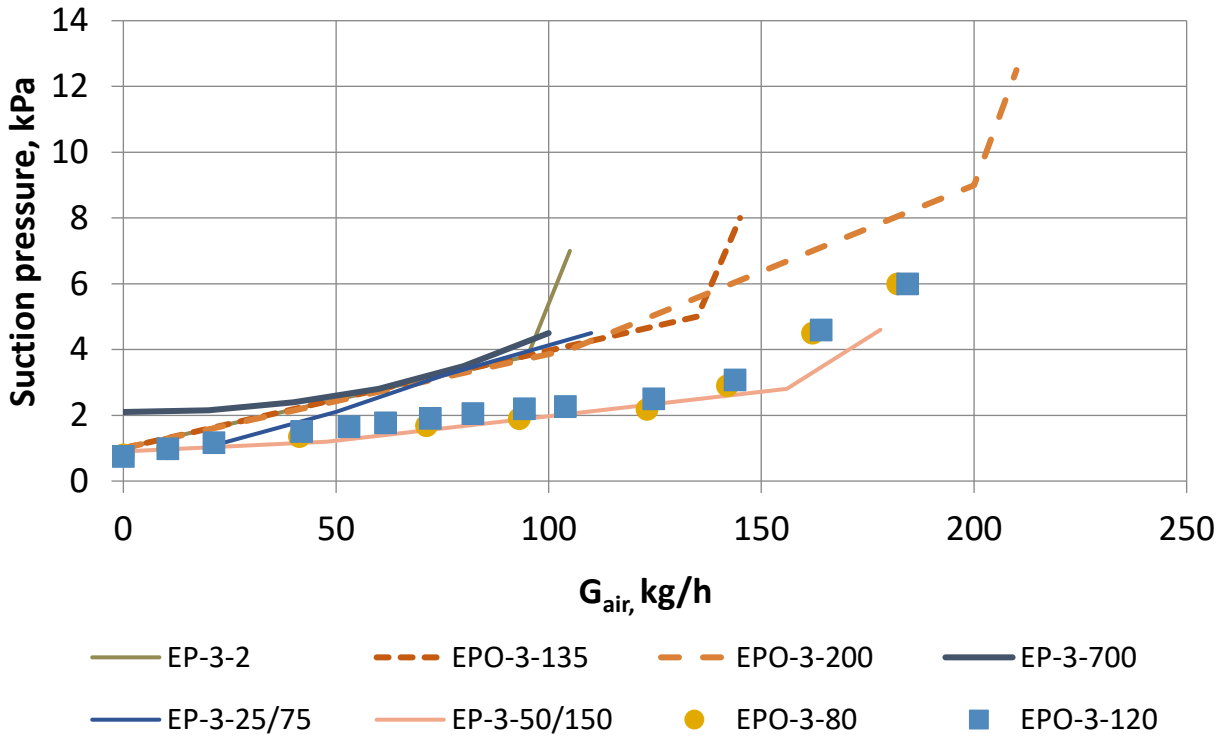

Fig. 3.22. Characteristics of stage I of the EPO-3-120 ejector and serial ejectors at their nominal primary steam pressures.

As can be seen, the two new ejectors have very similar characteristics. Compared to the serial ejectors, the only ejector with a characteristic similar to the new ones is the EPO-3-50/150 HTZ. It is important to mention that the primary steam consumption in this ejector is much higher (about 250 kg/h compared to the EPO-3-120) and the minimum flow rate of cooling condensate is 300 t/h (compared to 140 t/h for the EPO-3-80 or EPO-3-120). The minimum of the flow rate of the cooling condensate determines the nomenclature of the turbines where EP-3-50/150 can be installed. It can be used with turbines with a 500MW capacity or higher. It is also

quite important that the design is old, including internal coolers with all the problems previously mentioned before: huge case (0.5 m higher than the EPO-3-120), etc.

The other ejectors can be used at turbines with a 50 MW-300 MW capacity. Compared to them, the new ejectors have much higher capacity at lower suction pressure.

3.4.4. JOINT FUNCTIONING OF THE NEW EJECTORS WITH CONDENSERS

EPO-3-80 tests

In the framework of experimental studies of the EPO-3-80 ejector, tests were performed on a working turbine with the second ejector connected and disconnected. During the tests, air suctions to the vacuum system amounted to G_{air} = 120-130 kg/h (with a standard value of G_{air} = 21 kg/h). With the operation of both ejectors, the pressure in the suction chamber of stage I of the new ejector (ejector "A") was P_I = 2.2 kPa. The pressure in the condenser was equal to P_c = 3.5 kPa, which corresponds to the standard pressure values.

When the second ejector was disconnected (ejector "B") from the condenser, the pressure in the condenser did not change. The pressure in the suction chamber of the EPO-3-80 ejector was P_I = 2.4 kPa.

According to the results of the tests, it was established that the general ejector "A" allows for the maintenance of standard pressure in the turbine condenser even in the case of very large (significantly higher than standard) air chokes (G_{air} = 120-130 kg/h) and with ejector "B" switched off (the EP-3-700).

EPO-3-120 tests

When testing EPO-3-120 ejector, a performance characteristic with the SAM as a secondary stream was obtained while operating with a condenser. While the EPO-3-120 ("A") ejector was in operation, ejector "B" was disconnected from the capacitor. Monitoring of the condition of the condensation unit was carried out by the suction pressure of the ejector P_I and the pressure in the condenser P_c. In addition

to the air removed by the ejector from the condenser, an additional fixed air flow was supplied directly to the ejector through the SAM supply pipe. Tests were considered finished after the appearance of the influence of ejector parameters on the characteristics of the condenser (after changing the pressure in the condenser).

In Fig. 3.23, the performance characteristics of the EPO-3-120 ejector with "dry air" and the SAM are shown. The characteristics were obtained by operating a turbine with an electric power of N_{el} = 200 MW, steam consumption to the condenser of G_s = 413 t/h and a circulating water temperature of t_{cv}^1 = 19 °C at the inlet and t_{cv}^2 = 28-29 °C at the outlet.

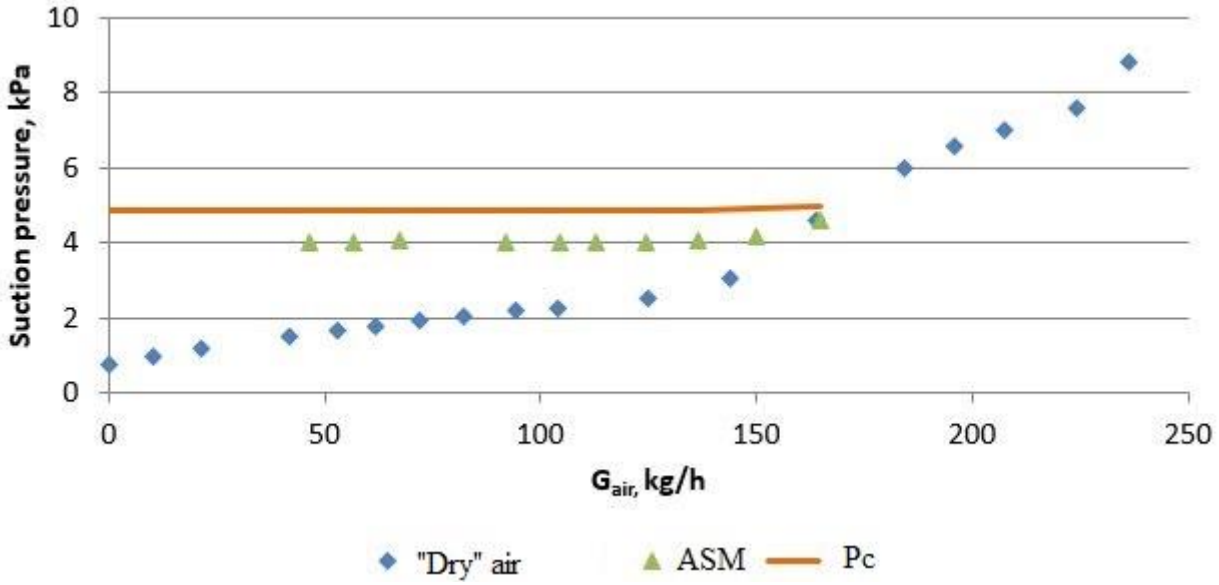

Fig. 3.23. Performance characteristics of the EPO-3-120 ejector with "dry air" and joint with condensing unit at a working steam pressure of R_{ps} = 0.7 MPa

As can be seen from Fig. 3.23, the suction pressure of the ejector when the SAM consumption is lower than the capacity of the ejector (G_{air} = 145 kg/h) does not change and is close to the pressure in the condenser: the gas-dynamic resistance is ΔP_c = 0.7 kPa. With a further increase in the amount of choked air, the ejector moves to the "overload" section and the suction pressure begins to rise.

As is well known, when the air flow to the ejector is lower than the maximum allowable (lower than the ejector capacity G_{air} = 145 kg/h), the ejector, together with

the drawn air, removes steam from the condenser. With an increase in the amount of air, the amount of steam suction in the SAM is significantly reduced. This phenomenon is illustrated in Fig. 3.24.

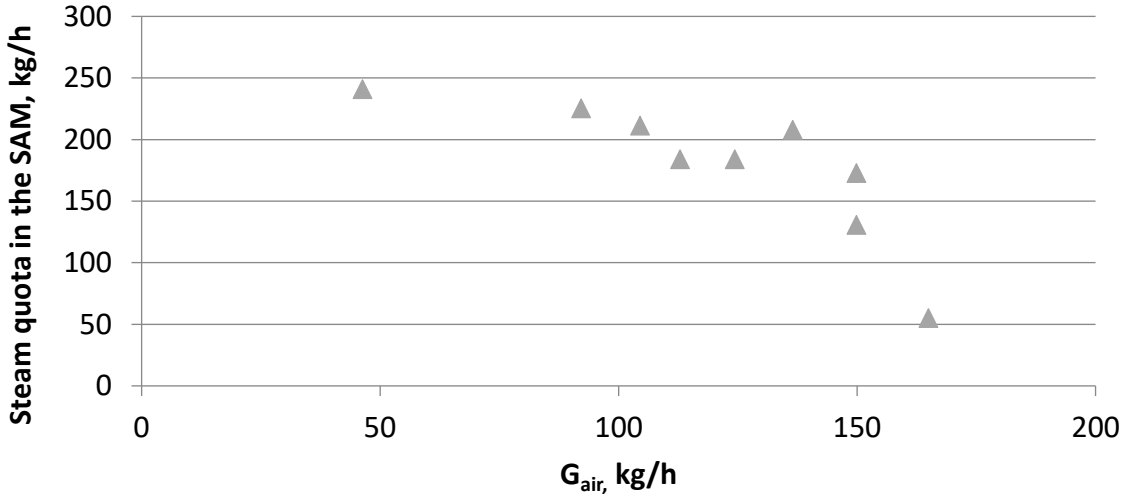

Fig. 3.24. The amount of steam in the SAM removed from the condenser by the EPO-3-120 ejector.

According to Fig. 3.24, the amount of steam in the SAM at the transition of the ejector to the "overload" section decreases from G_{air} = 250 kg/h to G_{air} = 50 kg/h.

In Fig. 3.25, the characteristics of the EPO-3-120 and EP-3-700 ejectors with the SAM as a secondary fluid are presented. The temperature of the SAM was t_{SAM}

= 27 °C.

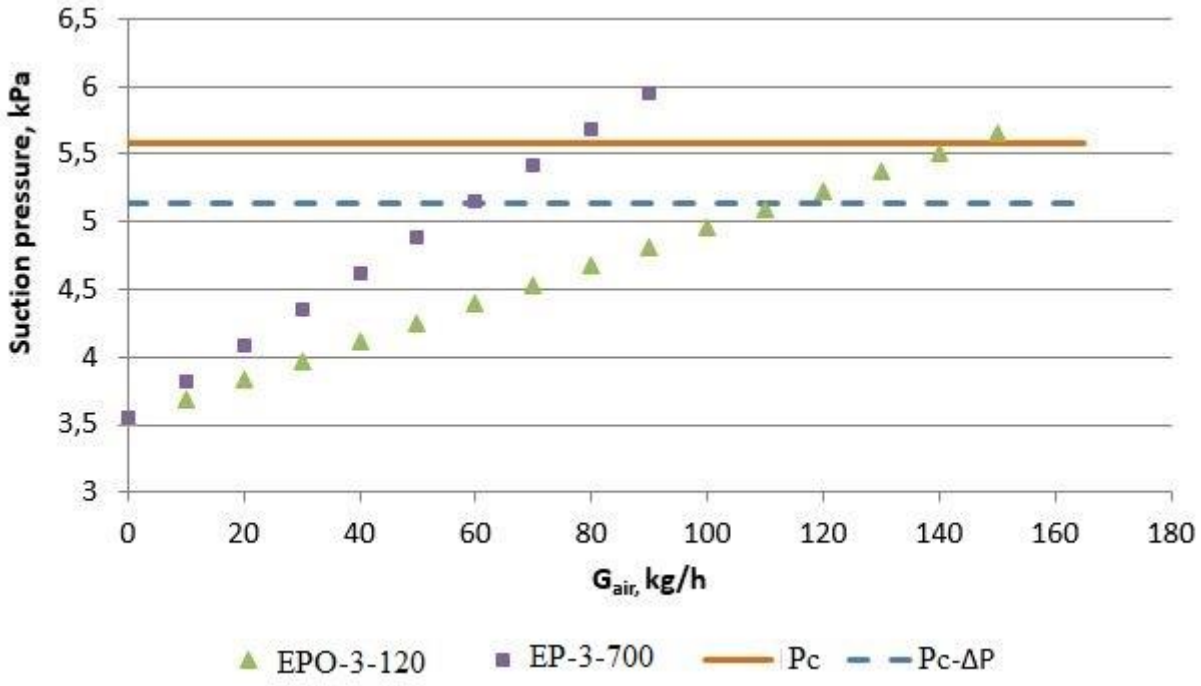

Fig. 3.25. Joint characteristics of the condenser and the EPO-3-120 and EP-3-700 ejectors.

The solid line indicates the rated pressure in the condenser at a significant SAM temperature. The dash-dotted line indicates the pressure in the condenser, taking into account the gas-dynamic resistance.

As can be seen from the graph, the EP-3-700 ejector is able to maintain the standard pressure in the condenser with an air suction no higher than G_{air} = 55 kg/h. The EPO-3-120 ejector is able to maintain the nominal pressure in the condenser with air chokes up to G_{air} = 120 kg/h.

3.5. RESULTS

1. The need to develop a highly efficient ejector for a condensation installation on a K-200-130 LMZ steam turbine with increased air chokes G_{air} = 120-130 kg/h is substantiated. The need to develop a new ejector is determined by the high value of air suction in the LPP of the turbine, which causes the actual vacuum in the condenser to deviate from the standard vacuum and, as a result, burn about

300 tons of fuel equivalent per month. The developed ejector must have the ability to maintain a deep vacuum in the condenser with increased capacity.

2. The optimal values of the parameters for the calculation of the jet devices for the new ejector were determined. The design and calibration calculations of the new EPO-3-80 and EPO-3-120 ejectors were carried out using the developed and refined calculation method. Design documentation for the new ejectors has been developed.

3. A number of technical solutions have been developed and implemented that improve the design of the new EPO-3-80 and EPO-3-120 ejectors. The design of the ejector, built into the connecting dimensions of the EP-3-700 ejector with vertical external coolers located triangularly and including the U-shaped tubes on the heat exchange surface, was developed. A nozzle attachment unit has been developed, which allows for the axial position of the nozzle to be changed in order to set the ejector jet devices for specific operating conditions.

4. An extended measurement scheme has been developed for experimental studies of a new ejector. The scheme includes the measurement of pressures and temperatures upstream and behind the intercoolers to determine the gas-dynamic resistance of heat exchangers, as well as the measurement of temperatures and the flow rate of cooling condensate.

5. Experimental studies of various operating modes of a high-performance ejector as part of a condensing unit have been carried out. Adjustment of the nozzle axial position has been made. Experimental values of parameters were obtained at various positions of the nozzles. The performance of a high-performance ejector with adjusted nozzles was G_{air} = 140 kg / h, while the suction pressure is P_I = 2.4 kPa. An increase in the inlet temperature of the cooling condensate in the range t_{cc} = 10-32 °C does not affect the performance of the ejector, while the suction pressure at the maximum capacity increases by 0.5 kPa. The temperature of the cooling condensate has a more significant effect on the operating parameters of the intercoolers, as well as on stages II and III of the ejector.

6. A comparative analysis of the performance of the new EPO-3-80 and EPO-3-120 ejectors, their design characteristics and the characteristics of serial ejectors from various manufacturers was carried out. Compared with the serial EP-3-700 ejector, the EPO-3-80 ejector has thrice the capacity and ΔP = 1-2 kPa lower suction pressure across all modes. Compared with the nominal characteristics of other serial ejectors, the EPO-3-80 and EPO-3-120 ejectors also had an advantage in capacity and the value of the suction pressure.

7. Ejectors were tested when operating with a condenser. The suction pressure of the ejector was P_I = 2.4 kPa, while the supported pressure in the condenser at the same time was P_c = 3.6 kPa. The characteristics of the ejector with the SAM were obtained.

Chapter 4.

INTERCOOLER RESEARCH

4.1. Experimental results of intercooler research

The existence of an additional factor (the parameter of the technological process) influencing the vapor pressure in the intermediate coolers of multistage steam-ejecting ejectors defines their functioning in comparison with other heat exchangers in steam-turbine installations (the condenser, regenerative heaters, the boiler of heating water). One such a factor, along with steam water mass flow rates and the water temperature and vapor pressure in the input of the device, is vapor pressure at the exit of the cooler. This is connected with the fact that the intermediate cooler is located between jet devices (stages), and the cross-sectional areas for an input of steam-air mixture (SAM) in the cooler and its output are comparable with each other. For the intermediate cooler of a multistage ejector, steam pressure at the input is similar to the pressure behind the diffuser of the corresponding stage, vapor pressure at the exit and inlet pressure in the suction chamber of the following stage (for stage III, the last one, this pressure is a little bit higher than the barometric pressure).

Results of the experimental tests of the EPO-3-80 ejector offered and developed in this dissertation showed that SAM pressure at the entrance and exit of the intermediate cooler can significantly differ from each other. Depending on process parameters, the difference in SAM pressure at the entrance and exit of i-cooler $\Delta P_i = R_{i1} - R_{i2}$ can be significantly different from zero. If a positive value of pressure difference in the heat exchanger can be partially explained by the gas-dynamic resistance of a pipe bunch of the cooler, then a negative difference (an increase of pressure at an exit) demands a special analysis.

In Fig. 4.1, data for the difference in SAM pressure is provided in coolers depending on the consumption of ejected air. Data is provided for two main condensate temperatures, $t_{1в}$ = 11°C and 32°C. From Fig. 4.1 it is clear that for stage

I of the ejector ΔP_1 changes from 1.4 to 2.8 kPa. At low water temperatures at the entrance of the cooler, SAM pressure at the entrance of the cooler in the majority of the modes is lower than at the exit. At $t_{1в}$ = 32°C, SAM pressure at the entrance is higher by 2…3 kPa compared to the exit pressure. A similar situation is recorded in stage II (fig. 4.1, b). At low water temperatures of $t_{1в}$ = 11°C, the change in SAM pressure from the entrance to the exit (in the majority of the modes) reaches ΔP_2 = - 6 kPa, at $t_{1в}$ = 32°C – ΔP_2 – up to 4 kPa. For stage III, SAM pressure, as a rule, increases in the cooler from the entrance to the exit at any $t_{1в}$, while pressure difference reaches ΔP_3 = - 8.6 kPa.

The essential differences for the SAM pressure in the intermediate coolers are defined, according to the author, by the interaction of the previous (upstream) and following (subsequent) jet devices (stages) and the distinction of gas-dynamic and heat-exchanging processes at low and high cooling water temperatures at the entrance of heat exchangers. At a low water temperature at the entrance of the cooler, there is full vapor condensation from the SAM. The following stage is defined only by air consumption (all steam from the SAM was condensed). At a high water temperature at the entrance of the second (following) stage, the steam-air mix is ejected in all modes – the steam in the first-stage cooler is incompletely condensed. As is shown in [133], the quota of t condensed steam in the cooler at $t_{1в} \approx$ 40°C reaches 0.6 … 0.8 from the total amount of steam in the SAM.

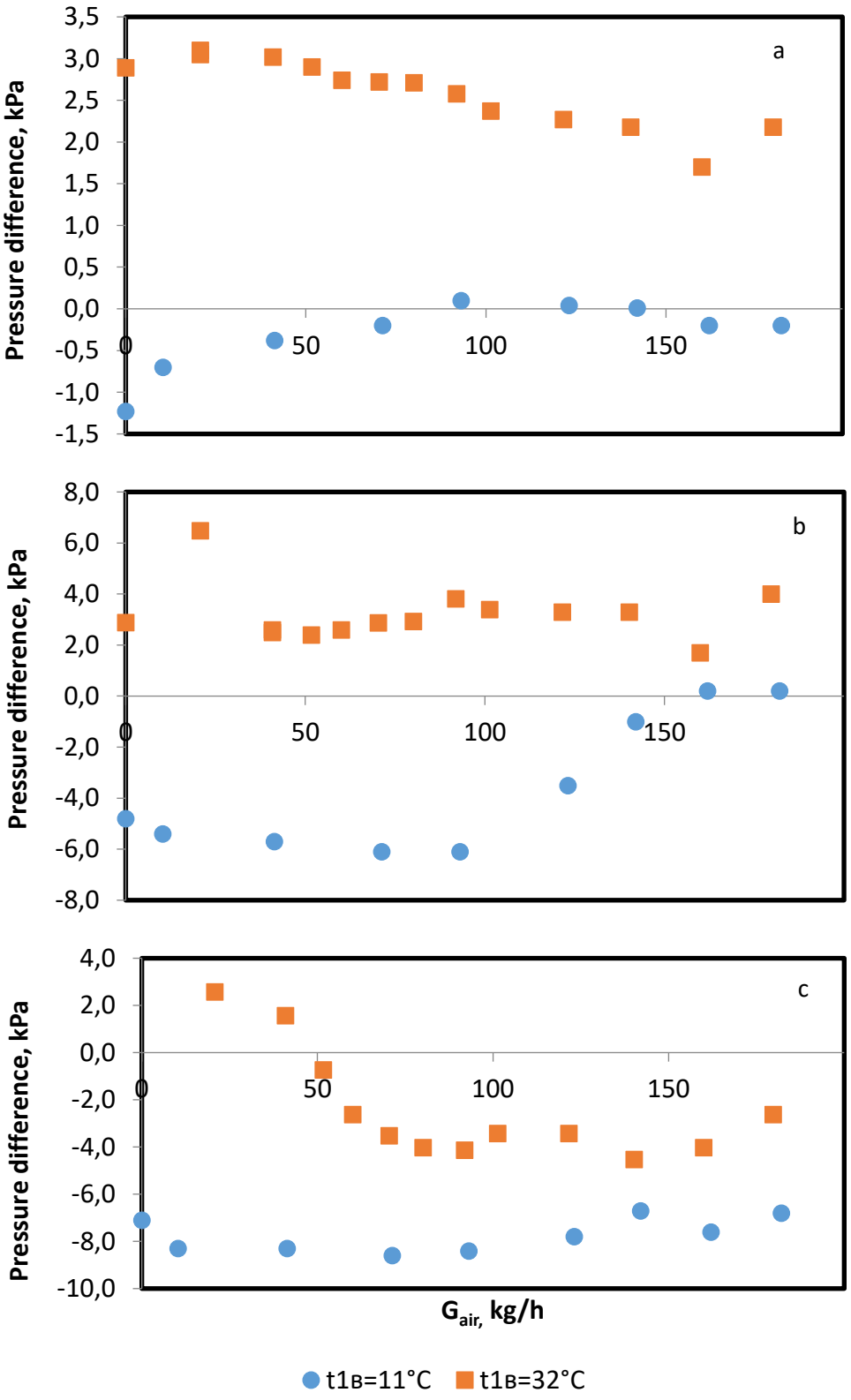

Fig. 4.1 Pressure difference at the inlet and outlet of the intercooler of the EPO-3-80 ($\Delta P_i = P_{i1} - P_{i2}$);
a –cooler I, b = cooler II, c –cooler III.

It should be noted that for almost all modes of ejector functioning, pressure at the entrance to cooler III was lower than at the exit. This is a consequence, according to the author, of full vapor condensation in this cooler.

In Fig. 4.2, the dependence of the relation of SAM pressures at the entrance and the exit of the cooler ($\delta P_i = P_{i1} / Pi_2$) on pressure at the entrance of the cooler is presented (pressure behind the diffuser of the corresponding stage). It is important to note that $\delta P < 1$ means the pressure drop in the cooler – the lower the δP, the bigger the drop. From Fig. 4.2, it is clear that at a low cooling water temperature at the entrance ($t_{1в} = 11°C$), SAM pressure at the entrance to cooler I in many modes is lower than at $t_{1в} = 32°C$. The lower the pressure at the entrance to the cooler, the higher the pressure drop. Increasing the pressure drop in the cooler via a reduction of the pressure at the entrance can occur, according to us, by increasing the velocity in front of the cooler, which is connected with the specific volume increase (reduction of SAM density). In the second cooler, the pressure drop dependence from the pressure in front of the cooler is less. In the third cooler (Fig. 4.2), the pressure drop takes place both at a low water temperature at the entrance and at a high temperature. As pressure in front of cooler III is rather high (more than 92 kPa), the influence of water temperature on the processes in the heat exchanger is insignificant. Everything is defined by the gas-dynamic processes. The distinction in δP_i at different water temperatures at the entrance is as follows: when carrying out tests at $t_{1в} = 11°C$, the barometric pressure was about 103 kPa, and at $t_{1в} = 32°C$ – 100 kPa.

It should also be noted that the observed effect disappears even at $t_{1в} = 11°C$ in some modes. This indirectly demonstrates the absence of a systematic error in the measurements and allows us to consider various trials to explain the recorded effect.

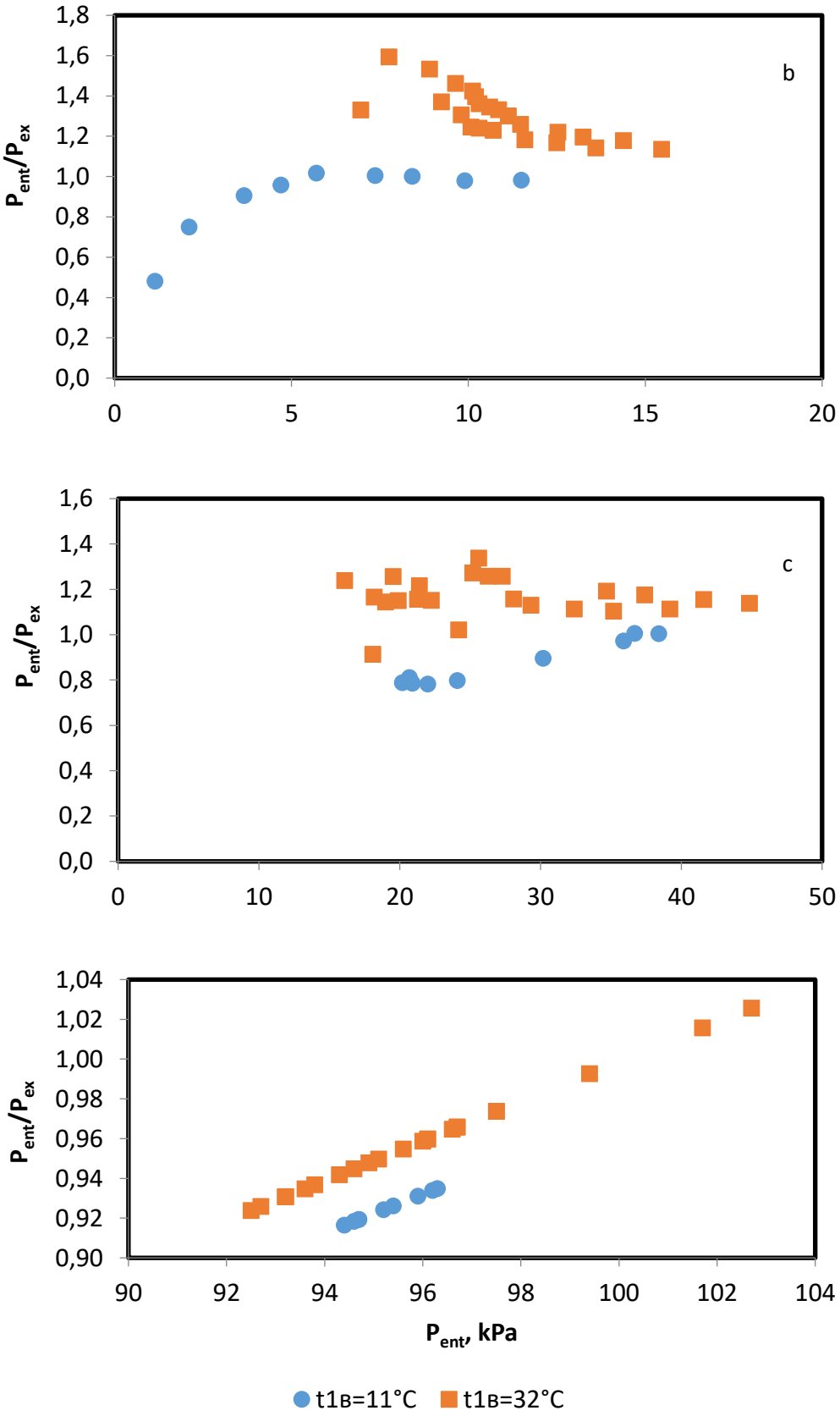

Fig. 4.2 Relation of pressures at the entrance and exit of the intercooler of the EPO-3-80 ejector ($\delta P_i = P_{i1} / P_{i2}$); a –cooler I, b = cooler II, c –cooler III

4.2. Development of the model of steam-air mixture pressure increasing in the intermediate cooler of a multistage ejector

Increases in the pressure in the cooler is connected, according to us, with gas-dynamic effects at the entrance to the cooler or inside the cooler. In this regard, we will consider a number of possible trials to examine pressure increases in gas streams [20, 134-136]:

- condensation drop;
- the cumulative effect of external influences, described by L. A. Vulis as a law of turned impact [137];
- a pressure drop in wet steam.

It is known [136] that condensation drops arise in high-speed (supersonic) streams of steam. Temperature falls in a high-speed stream can lead to overcooling of the steam in relation to saturation temperature and to sudden, nonequilibrium condensation. Such condensation drops lead to a pressure increase in the stream and can be observed in the Laval nozzles [136]. In experiments with the EPO-3-80 ejector, the velocities of stream in front of coolers reached 40 to 200 m/s in various modes. In one of the modes (with vapor pressure after the first-stage diffuser near 1.4 kPa), the velocity reached up to 450 m/s but also remained subsonic in these conditions. Thus, an increase of pressure in the cooler because of a nonequilibrium condensation drop is extremely improbable.

4.2.2. External influences to the stream

The parameters of a gas stream (pressure, velocity, temperature, etc.) can change because of external impacts. The treatment of such influences can be the supply and removal of heat, mass or mechanical energy, a change in the channel geometry, etc. Depending on the value of the flow rate (supersonic or subsonic), the same external influence can cause changes of a stream’s parameters, but opposite value. For an explanation (evaluation) of the gained effect (a pressure drop in the

cooler during the movement of a subsonic stream), we exclude the ratio considering the following external influences: heat removal from superheated steam, mass removal as a result of vapor condensation (on tubes) and changes of the channel section for the gas flow in the heat exchanger. We obtained a ratio following postulates in [20, 134,135].

Here we provide (in a differential form) the equations of mass preservation, gas condition (gas is considered ideal) and Bernoulli:

$$\frac{dG}{G} = \frac{d\rho}{\rho} + \frac{dw}{w} + \frac{dF}{F}; \tag{4.1}$$

$$\frac{dP}{\rho} = R \cdot dT + R \cdot T \cdot \frac{d\rho}{\rho}; \tag{4.2}$$

$$\frac{dP}{\rho} = -w \cdot dw, \tag{4.3}$$

where G – mass flow rate, kg/s; ρ – density, kg/m^3; w – gas velocity, m/s; F – cross section area, m^2; P – gas pressure, Pa; R – gas constant, Dj/(K kg); T – gas temperature, K.

We exclude dw/w и $d\rho/\rho$ from equations (4.1) – (4.3) and replace $(k \cdot \rho \cdot T)$ with a^2, where k – gas isentropic exponent , a – speed of a sound in a gas. After this transformation, we obtain the following:

$$\frac{dP}{\rho} = R \cdot dT + \frac{a^2}{k} \cdot \left(\frac{dG}{G} + \frac{dP}{w^2 \cdot \rho} - \frac{dF}{F} \right). \tag{4.4}$$

Here we provide the energy conservation equation:

$$dQ = dh + w \cdot dw = c_p \cdot dT + w \cdot dw = k/(k-1)\, R \cdot dT + w \cdot dw, \tag{4.5}$$

where h – heat content in gas, Dj/kg; c_p – isobaric heat capacity of gas, Dj/(kg K); it is considered that $c_p = k/(k-1) \cdot R$.

Substituting (4.5) to (4.4), after transformation we obtain:

$$\left(M^2 - 1\right) \cdot \frac{dP}{\rho} = dQ \cdot (k-1) \cdot M^2 + w^2 \cdot \left(\frac{dG}{G} - \frac{dF}{F} \right), \tag{4.6}$$

where M = w/a – Mach number.

Equation (4.6) allows for the analysis of the influence of external factors on pressure in a stream. As the stream entering the heat exchanger is subsonic, value

(M^2–1) < 0 in the left part of formula (4.6). Pressure increases in the heat exchanger ($dP = P_{вых}–P_{вх} > 0$); therefore, the left part of formula (4.6) has a negative value.

The first variable in the right part of equation (4.6) should also be negative, as the SAM loses energy from overheating. The temperature of the SAM upstream from the heat exchanger is higher than the saturation temperature determined by the value of partial steam pressure in the mix. A high temperature of the SAM upstream from the heat exchangers is recorded in measurements of tests of the EP-3-80 ejector. For a number of the modes, the temperature of the mix was defined by formula (2.9), given in [18], and received from the equation of heat balance for flows in a stage's suction chamber and in a section of the diffuser outlet:

$$t_{см} = t_{в} + \frac{h_{р} - h_{пс}}{U \cdot c_{в}}, \qquad (4.7)$$

where $t_{см}$, $t_{в}$ – temperatures of mix, air, °C; $h_{р}$, $h_{пс}$ – heat content of primary steam and steam in the mix, kDj/kg; U – entrainment ratio; $c_{в}$ – air isobaric heat capacity, kDj/(kg K).

The temperature of the mixture, calculated by formula (4.7) at 90°-120°C, exceeded the saturation temperature at the partial pressure of steam in the mixture and corresponded well to the measured values of the ambient temperature behind the first-stage diffuser. In accordance with the law of inverted effect, the cooling of a subsonic flow ("thermal diffuser") leads to a decrease in its velocity and an increase of pressure in the flow [20, 134-136].

It should be noted that, according to formula (4.7), the air-steam mixture at the outlet of the diffusers of multistage steam-driven ejectors is always overheated. This factor further complicates the description of the processes occurring in the cooler, since the evaluation of the effect of overheated steam temperature on the heat transfer coefficient during condensation is not straightforward.

In the research of S. S. Kutateladze [139], it is suggested to calculate the heat transfer coefficient during steam condensation according to the well-known Nusselt

dependence with the corresponding amendments and substitute the value q, kDj/kg in place of the phase transition heat (r) [138].

$$q = r + c_p \Delta T_п, \quad (4.8)$$

where c_p – steam heat capacity, Wt/(m K); $\Delta T_п = T_п – T_н$ –difference of superheated steam temperature ($T_п$) and saturation temperature at the steam pressure ($T_н$), K [138].

$$q = (r + c_p \Delta T_п) \cdot g_п + q_2, \quad (4.9)$$

where $g_п$ – mass condensation rate, kg/(m^2 c); q_2 – heat quantity, supplied to the condensate film from the uncondensed part of the superheated steam due to convective heat exchange, Вт/м^2.

According to (4.8) and (4.9), during the condensation of superheated steam with a temperature 100 ... 200 K higher than the saturation temperature, the heat transfer coefficient is slightly (up to 5%) higher than during the condensation of saturated steam.

In a number of works where the condensation of superheated steam in pipes was studied experimentally, it was shown that the superheating of steam reduces the heat transfer coefficient several times [140]. In research [141], it is noted that the results obtained regarding heat transfer during the condensation of superheated steam inside pipes differ significantly from the data of [138]. The low experimental values of heat transfer coefficients K≈500–2700 Wt/m^2 K (depending on the mode of steam flow in the pipes), as well as the experimentally confirmed fact that if the steam content at the outlet of the pipe is higher than 0, the steam remains overheated.

It should also be noted that the method of designing a heat exchanger for superheated steam in the outlet [142] proposes the allocation of an overheating zone, where the heat transfer coefficient on the steam side is determined only by convection. The calculations carried out by the author in this case show that, with the value of steam overheating ($\Delta T_п$ = 150–200 K), up to 20–30% of the heat exchange surface can enter the overheating zone.

The above considerations do not lead to an exact analytical solution of equation (4.6). However, if we proceed to the differential representation of this

formula, then we can obtain a maximum estimate of the increase (drop) of the pressure in the intercooler.

The removal of heat from the gas stream is determined by the formula:

$$\Delta Q = c_p \cdot (T_{вх} - T_{вых}), \qquad (4.10)$$

where $T_{вх}$, $T_{вых}$ – temperatures of the SAM at the inlet (at the corresponding diffuser outlet) and outlet (in the suction chamber of the following stage or at the ejector exhaust).

The effect of mass transfer ("flow diffuser") is determined by the condensation of steam from the air-steam mixture. According to (4.6), the removal of gas from a subsonic flow slows it down and increases the pressure. To estimate the maximum value of the mass-exchange gradient within the framework of this study, calculations for the heat exchanger with the condensation of pure water vapor were carried out. Fig. 4.3 presents the value of $\Delta G/G$ for different zones in the cooler. From the figure it can be seen that the maximum change in the mass of the gas in the cooler is $\Delta G/G = 0.9$ (when steam condenses from the SAM, the change in the mass of the flow is less).

In the considered cooler design, the cross-section of the SAM inlet to the heat exchanger is larger than the flow area between the tubes in the tube bundle and the cross-sectional area between the case and the segmented partition. To obtain the maximum estimate of pressure increase, the influence of the geometric factor ("geometric diffuser") in equation (4.6) was not taken into account ($\Delta F/F = 0$).

Fig. 4.3. Steam mass change in cooler zones.

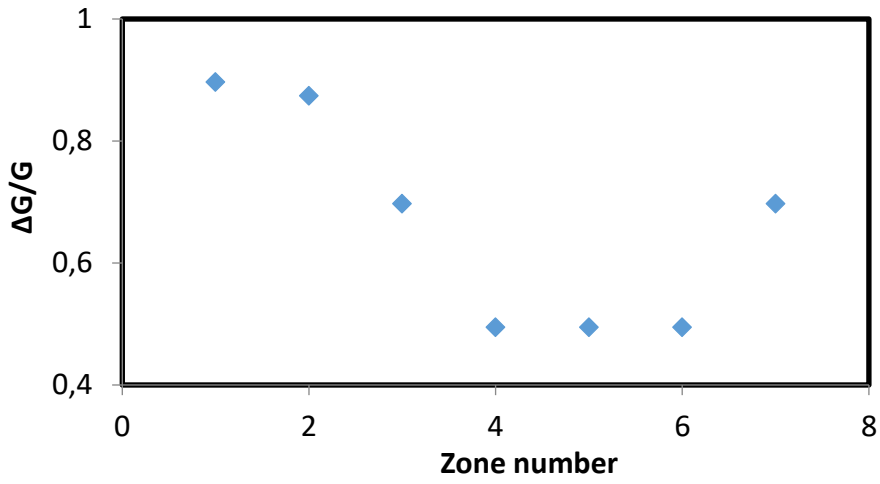

In Fig. 4.4, a comparison of the calculation results for a number of pressure increase modes in coolers using formula (4.6) with the author's experimental data is offered. For the first stage, the calculated data are in satisfactory agreement with the experimental data; for the second and third stages, the values of the calculated data are 3-4 times lower than the experimental ones.

The analysis showed that the observed effect of a pressure increase in the intercoolers of multistage steam jet ejectors is difficult to explain using the effects of cumulative external influences ("heat and flow diffuser") on the gas flow.

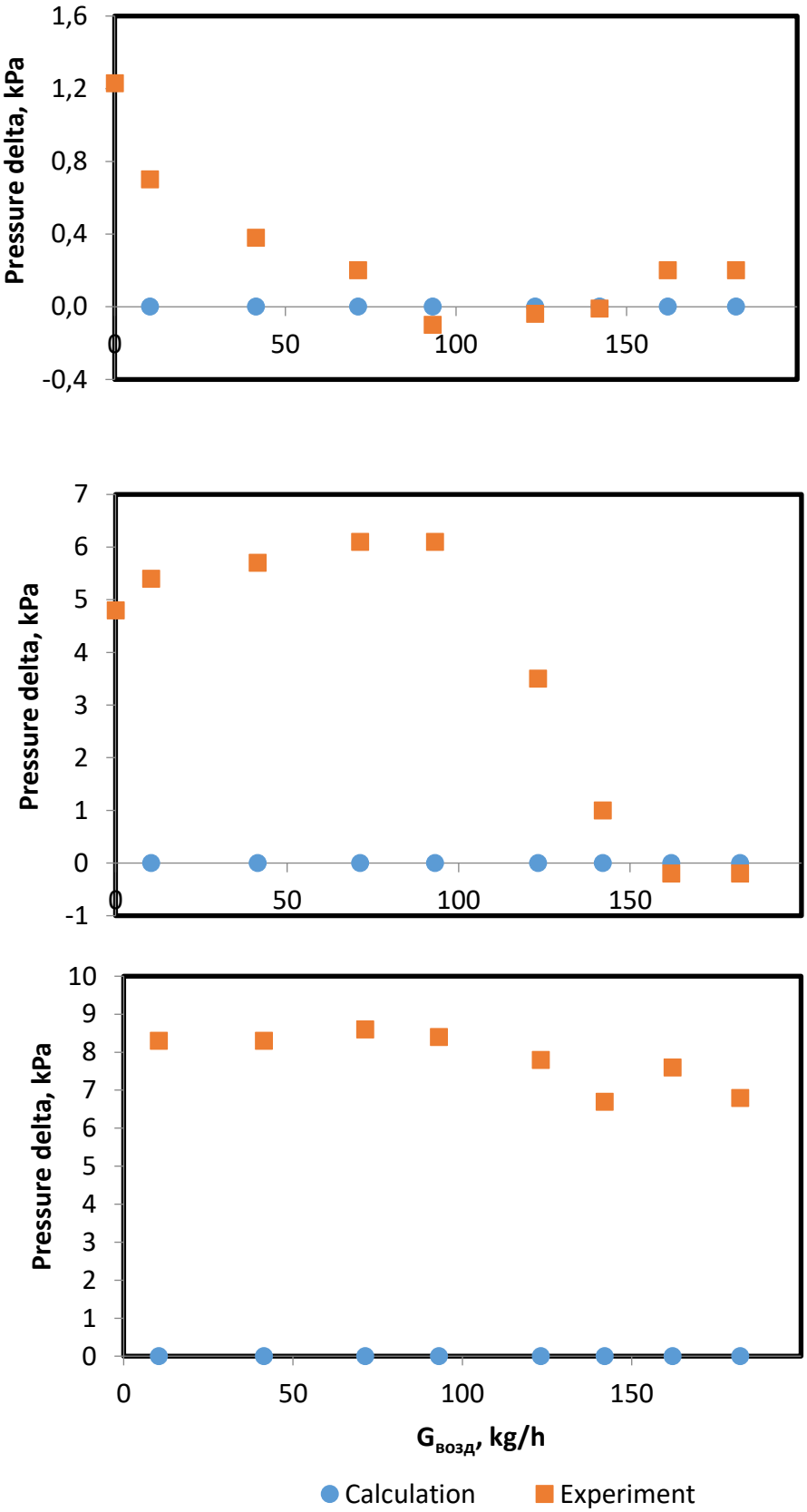

Fig. 4.4. Pressure increase in the intercoolers of multistage steam-driven ejectors. Comparison of experimental data calculated by (4.6) and experimental data: a –stage I, b – stage II, c –stage III

4.2.3. PRESSURE DROPS IN WET STEAM

The next physical process that can be used to explain the pressure increase in an ejector cooler is a pressure drop in a wet steam. The complexity of this approach lies in the fact that, as shown above, the air-steam mixture at the outlet of the diffuser (the entrance to the cooler) is always overheated relative to the vapor pressure in the mixture.

In this study, we assume that the increase in SAM pressure occurs in the form of a pressure drop in a narrow region to the inlet of the heat exchanger. Let us assume that the steam (air-steam mixture), entering the heat exchanger at a velocity of 40–200 m/s, removes the flowing condensate film from the surface of vertical heat exchange tubes; in addition, the steam captures and breaks apart drops and trickles of liquid flowing down from the intermediate partitions. As is shown in [143], the droplet separation from the surface of the tubes in the beam during the co-current or countercurrent movement of the vapor and the condensate film begins at vapor flow rates of 15–20 m/s. With the cross movement of steam and condensate, the breakdown of the film is observed, other things being equal, at a steam speed 1.2 times less than in the case of coaxial motion of the phases. At the entrance to the cooler, a gas-steam mixture (fog) is formed. As is shown in [136], the speed of sound in a two-phase medium drops sharply. The flow at the entrance to the cooler can become supersonic — a pressure drop occurs in the wet vapor. To assess the correctness of the proposed hypothesis, it is necessary to estimate the speed of sound in a wet gas-vapor mixture at the inlet to the heat exchanger. If at the calculated values of the degree of dryness of wet steam at the entrance to the cooler it is shown that the Mach number of the flow is $M > 1.0$, then this means the proposed hypothesis to explain the effect obtained (a pressure drop in the cooler) is correct.

To formulate a physico-mathematical model of the pressure drop process in wet steam at the inlet to the heat exchanger, the author has made a number of assumptions and additions based on the results of his own experiments and [136]:

1. The vapor-air mixture in front of the heat exchanger is overheated relative to the saturation temperature, which is determined by the pressure of the mixture. At the entrance to the heat exchanger, the mixture is cooled, and some of the moisture in the fog evaporates. Accordingly, the mass of steam in front of the heat exchanger increases.

2. At the entrance to the heat exchanger, a saturated gas-steam mixture (fog) is formed.

3. The temperature of the mixture before and after the pressure drop corresponds to the saturation temperature at the pressure of the mixture.

4. The speed of the droplets is close to the velocity of the gas phase (there is no slip).

5. The specific volume of the liquid phase in comparison with the volume of gas is neglected.

6. The Klaperon equation (ideal gas) is applicable to the gas phase.

7. The pressure drop is calculated taking into account the gas-dynamic resistance of the tube bundle. This is determined by the fact that the pressure of the mixture is measured after the cooler: the pressure drop occurs, according to the author, at the entrance to the cooler.

To visualize the proposed hypothesis, an image of the supply of steam-air mixture to the intercooler and part of the heat exchange surface is shown in Fig. 4.5.

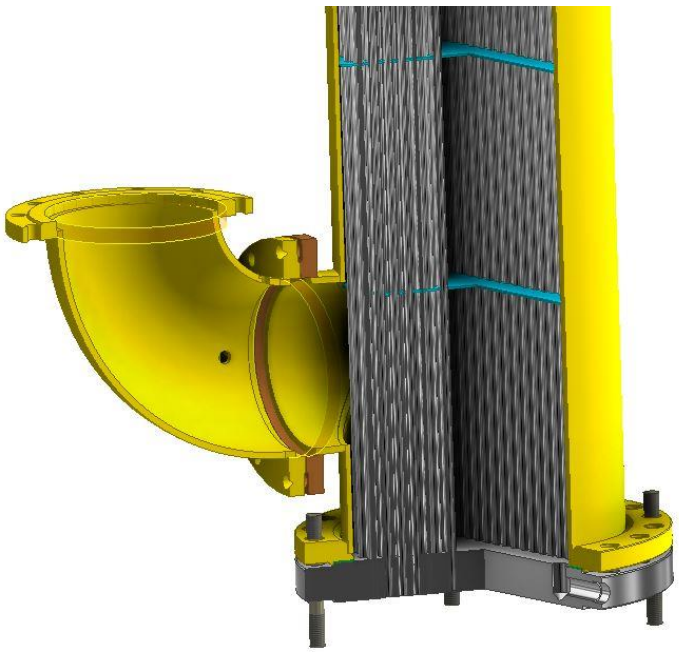

Fig. 4.5. Intercooler inlet for the air-steam mixture

The equations of conservation of mass, momentum and energy, using [136], are written as follows:

$$\frac{w_2}{w_1} = \frac{\beta_{пв2} \cdot T_2 \cdot P_1}{\beta_{пв1} \cdot T_1 \cdot P_2}\ , \qquad (4.11)$$

$$P_2 - P_1 = \frac{\rho_{пв1} \cdot w_1}{\beta_{пв1}} \cdot \left(w_1 - w_2\right)\ , \qquad (4.12)$$

$$r_1 \cdot \beta_{п1} + h_{пк1} \cdot \beta_{пк1} + h_{в1} \cdot \beta_{в1} + w_1^2 / 2 = r_2 \cdot \beta_{п2} + h_{пк2} \cdot \beta_{пк2} + h_{в2} \cdot \beta_{в2} + w_2^2 / 2\ . \qquad (4.13)$$

In equations (4.11) - (4.13), the indices “1, 2” designate the parameters of the medium before and after the drop; “к, в, п” - parameters of condensate (moisture), air and steam; double indices refer to a two-component mixture: “пв” - vapor-air (gas component); “пк” - steam and condensate. Notation for the variables is: w – velocity; T, P – temperature, pressure; ρ – density of the component; r, h – heat of phase transition, heat content; β – weight fraction of the component; $\beta_п = m_п/(m_п + m_к + m_в)$ – fraction of steam; $\beta_{пк} = (m_п + m_п)/(m_п + m_к + m_в)$ – fraction of steam and condensate; $\beta_в = m_в/(m_п + m_к + m_в)$ – air fraction (here, m is the mass of the component).

To derive the continuity equation (4.11), the equation of the state of an ideal gas was used; formula (4.12) was obtained on the conditions that there is no slip (the velocity of the gas and liquid phases in the stream are the same) and the small size of the volume of the liquid phase in comparison with the gas phase.

According to [131], we introduce dimensionless speeds:

$$C_1 = \frac{w_1}{\sqrt{k \cdot R \cdot T_1}}; C_2 = \frac{w_2}{\sqrt{k \cdot R \cdot T_1}}, \quad (4.14)$$

where R is taken for air-steam mixture determined by taking into account the mass content of the components.

Then the system of equations can be represented as:

$$\frac{C_2}{C_1} = \frac{\beta_{пв2} \cdot T_2 \cdot P_1}{\beta_{пв1} \cdot T_1 \cdot P_2}, \quad (4.15)$$

$$\frac{P_2}{P_1} - 1 = \frac{k}{\beta_{пв1}} \cdot C_1 \cdot (C_1 - C_2), \quad (4.16)$$

$$r_1 \cdot \beta_{п1} + h_{пк1} \cdot \beta_{пк1} + h_{в1} \cdot \beta_{в1} + k \cdot R \cdot T_1 \cdot C_1^2 / 2 = r_2 \cdot \beta_{п2} + h_{пк2} \cdot \beta_{пк2} + h_{в2} \cdot \beta_{в2} + k \cdot R \cdot T_1 \cdot C_2^2 / 2 . \quad (4.17).$$

In equations (4.15) - (4.17), the unknown quantities are the mass of moisture before and after the pressure drop, as well as the flow rate after the pressure drop. The mass (consumption) of steam in front of the heat exchanger is defined as the sum of the consumption of primary steam and steam formed from evaporated moisture at the entrance to the heat exchanger.

The system of equations is solved by an iterative method.

According to [143], the speed of sound in a gas-vapor mixture is determined by the formula:

$$\frac{1}{a_{см}^2} = \rho_{см} \cdot \left[\frac{v_в}{\rho_в \cdot a_в^2} + \frac{v_{пк}}{\rho_{пк} \cdot a_{пк}^2} \right], \quad (4.18)$$

where a – speed of sound; ρ – density; v – component volume quota; indicies: см, в, пк – mix, air, vapour-condensate; $\rho_{см} = \rho_в \cdot v_в + \rho_{пк} \cdot v_{пк}$.

The speed of sound in a wet steam was determined according to the schematic from [136] (Fig. 4.6). The degree of dryness of wet steam (x) was determined in the usual way through the weight fraction of steam in the steam-water mixture. In equations (4.15) - (4.17), $x = \beta_{пв}$ at zero air flow.

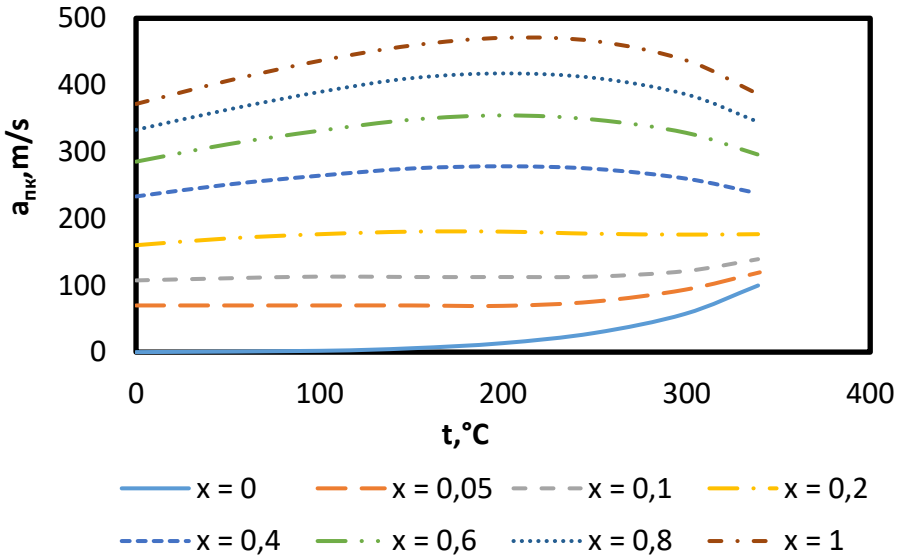

Fig. 4.6. Dependence of the speed of sound in a two-phase medium vapor-condensate ($a_{пк}$) as a function of steam temperature for varying degrees of dryness of the steam-water mixture (x) 131]

The results of calculating the Mach number before and after the pressure drop are shown in Fig. 4.7. It can be seen from the figure that for all three stages of the ejector coolers, the Mach number is M > 1 before the pressure drop, which indicates the correctness of the formulated hypothesis explaining the pressure drop in the coolers.

In accordance with the obtained solution of equations (4.15) - (4.17), the degree of steam dryness in various modes of operation of the ejector in its first stage is x <0.75. For the second and third stages, it is x <0.09. The degree of steam dryness before and after the drop varies slightly. For the formation of wet steam in accordance with equations (4.15) - (4.17), up to 10% of the moisture contained in the tubes in the cooler in the form of condensate is required.

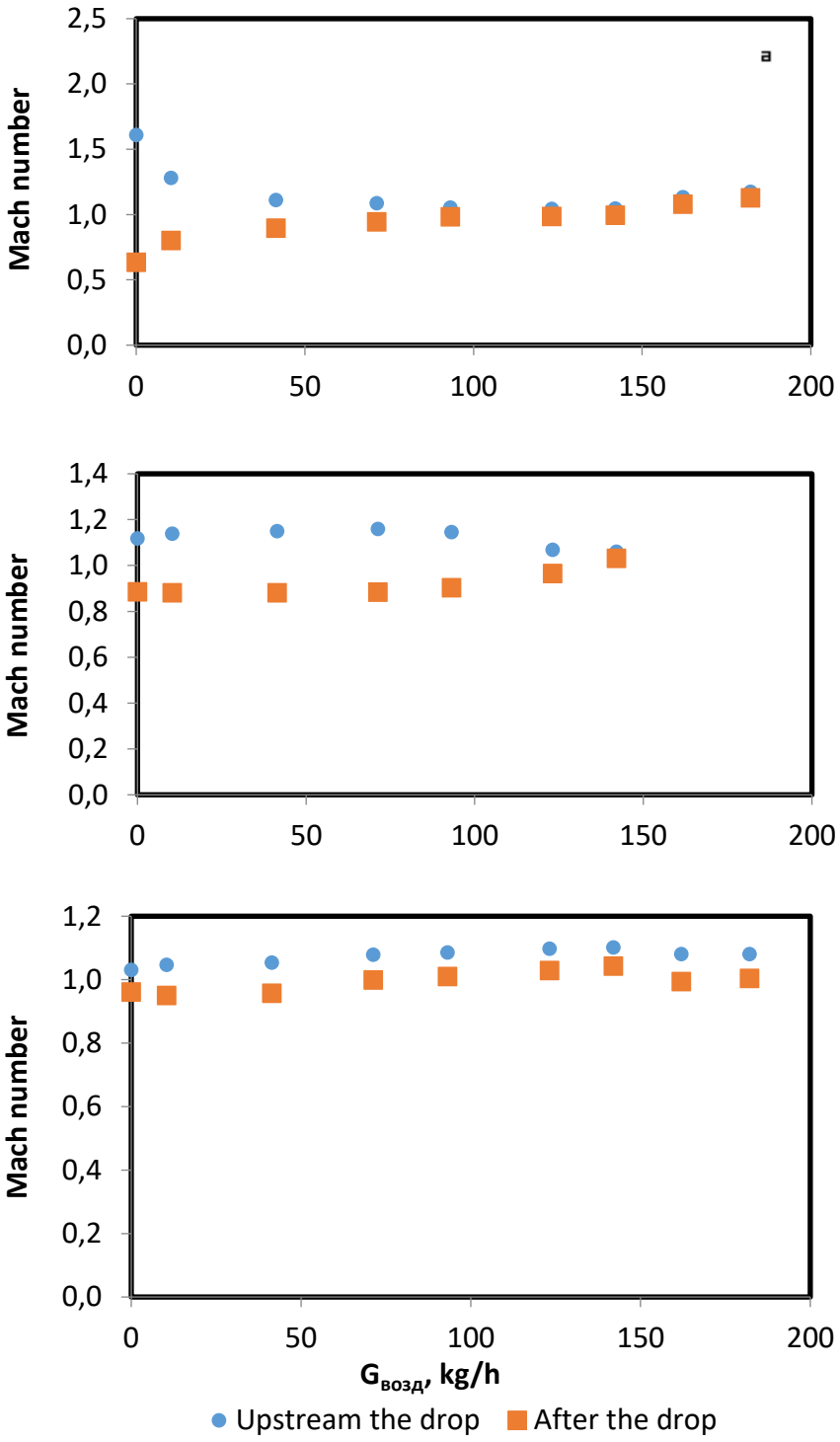

Fig. 4.9. The Mach number before and after the pressure drop: a - stage I of the cooler; b – stage II; c – stage III.

In conclusion, we consider the results of tests of the EPO-3-80 ejector in which the effect of pressure increase was absent. When analyzing the operating parameters of the intercoolers as condensing-type heat exchangers, the calculation

of the value of underheating was performed. The value of underheating is extremely high due to incomplete steam condensation in the intercoolers. The maximum recorded values of underheating for each stage at various temperatures of cooling condensate are presented in Table 4.1.

Таблица 4.1

Stage	when $t_{1в}$ = 11°C	when $t_{1в}$ = 32°C
I	45	20
II	38	42
III	60	60

For the first-stage cooler, as follows from Fig. 4.2(a), the pressure in front of the cooler at a low cooling condensate temperature ($t_{1в}$ = 11°C) is lower than at a high one ($t_{1в}$ = 32°C). Accordingly, the velocity of the vapor-air mixture behind the diffuser at $t_{1в}$ = 32°C reached 50...80 m/s, which is not enough for the manifestation of a pressure drop in a wet mixture. For the second stage of the cooler, in which the values of vapor pressure behind the diffuser were approximately the same in all modes (see Fig. 4.2(b)), there was no pressure drop at high cooling condensate temperatures. In our opinion, this is due to the high temperature of the steam condensate flowing through the tubes. Since the steam enters the cooler is overheated, the high temperature of the condensate flowing from the tubes does not allow for the formation of a uniform saturated steam-water (vapor-gas mixture). The available temperature difference between the temperature of steam and cooling water at $t_{1в}$ = 11°C reaches Δt = 50-60°C, and $t_{1в}$ = 32°C – only Δt = 30-40°C. As a result, the velocity of the air-steam mixture remains subsonic. For the third stage, all conditions are fulfilled: a high SAM rate at the inlet to the cooler and a significant available temperature difference, which leads to the formation of a saturated two-phase mixture and an increase in pressure, both at low and high temperatures of the cooling water at the entrance to the heat exchanger.

4.3. RESULTS

1. In the course of experimental studies on the EPO-3-80 ejector, the gas-dynamic effect of increasing the pressure of the air-steam mixture in the intermediate coolers was recorded. The pressure of the air-steam mixture at the outlet of the coolers exceeds the pressure at the inlet by ΔP = 1.0-8.6 kPa.
2. 3 various hypotheses are considered to explain the obtained effect. A physico-mathematical model is proposed that describes the obtained effect as a pressure drop in a two-phase, two-component mixture formed at the inlet to the heat exchanger. The calculation of velocities and pressure drops in the wet-steam flow was carried out. It was confirmed that the effect obtained can be described by the proposed model.
3. An assessment of underheating in the intermediate coolers of the ejector. The maximum values of underheating on the first stage differ at low and high temperatures of cooling water (45°C and 20°C, respectively); the maximum value of underheating in the second stage is 38–40°C, and in the third stage up to 60°C.
4. The obtained results justify the need to revise and further clarify the method of designing multistage steam ejectors in terms of the influence of gas-dynamic processes in the intermediate coolers on the pressure in the next stage.

Chapter 5.

EVALUATION OF THE TECHNICAL AND ECONOMIC EFFICIENCY OF CONDENSATION UNITS FUNCTIONING WITH A NEW EJECTOR

When evaluating the efficiency of condensing units, it is necessary to take into account the peculiarities of operation of condensing and cogenerating turbines. This chapter presents, as an example, an analysis of the effect of high air suction on the efficiency of various steam turbines. A feasibility study is necessary for turbines of thermal power plants with deviations in the vacuum in the condenser from the standard values that appear during long-term operation. Deviations in vacuum values are caused by excessing of steam turbine's running hours in connection with the elevated air suction in the LPP of turbine units.

5.1. OPERATION OF THE DEVELOPED EJECTOR IN A CONDENSATION TURBINE

An evaluation of the effectiveness of the ejector in a specific condensing unit can be carried out by analyzing the efficiency of the condensing unit as a whole. For example, it is known that for condensation turbines a pressure change in the condenser of 1 kPa causes a change in the total power of the turbine unit of 1% [1, 4, 8]. At the same time, the deepening of the vacuum in the condenser of cogeneration turbines when operating in cogeneration modes (with minimal steam flow rate into the compartment behind the regulating diaphragm) does not entail a significant increase in the power generated.

In Fig. 5.1, retrospective (according to monthly average data) deviations of the standard vacuum value from the actual value in the condenser of the K-200-130 LMZ turbine are presented.

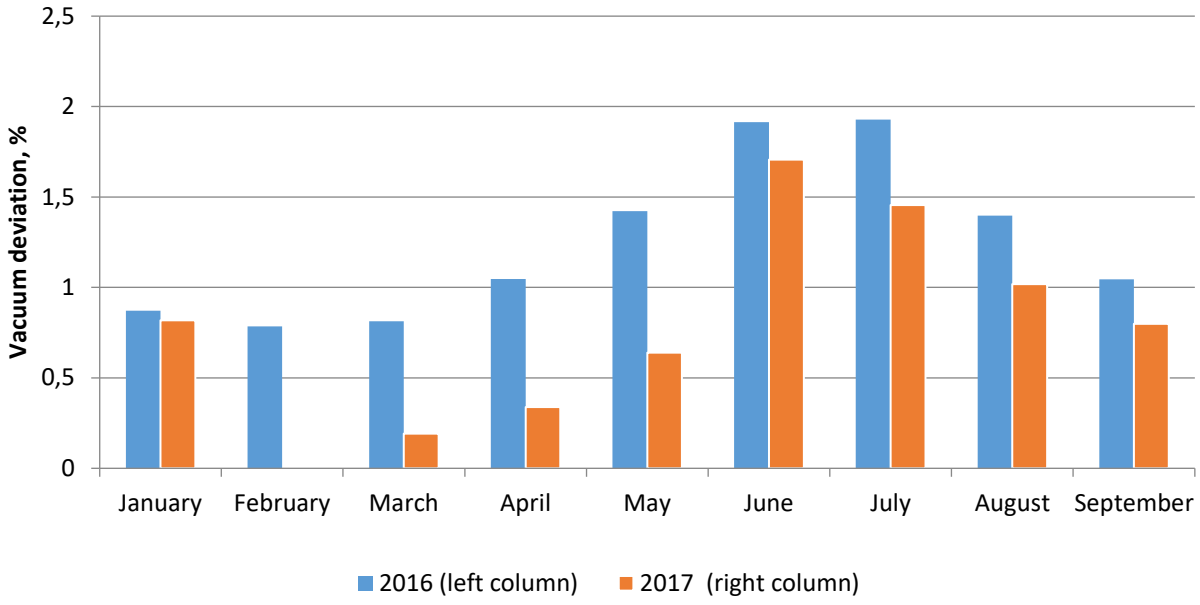

Fig. 5.1. Retrospective deviation of the actual vacuum value in the condenser from the standard values

In Fig. 5.1, the excess of the actual vacuum over the standard one when the turbine was operated in 2016 (i.e. when operating two serial EP-3-700 ejectors) ranged from 0.8 to 1.9%. When the EPO-3-80 ejector was switched on and the standard serial ejectors were disconnected, the vacuum deviation decreased on average by $\Delta V = 0.5\%$. Data for February 2017 is missing, since turbo installation was reserved.

A large scatter of ΔV values is determined by various factors, including steam consumption by the condenser, the amount of air suction in the vacuum system and, especially, the change in circulating (cooling) water temperature at the inlet to the condenser.

The influence of the temperature of the circulating water at the inlet, depending on the season, weather conditions and the regional location of the TPP, must be taken into account when analyzing the joint operation of the condenser and ejector. In Fig. 5.2, the dependence of the vacuum deviation in the capacitor of the K-200-130 LMZ turbine on the value of the water temperature at the inlet to the condenser (t_{1w}) is given.

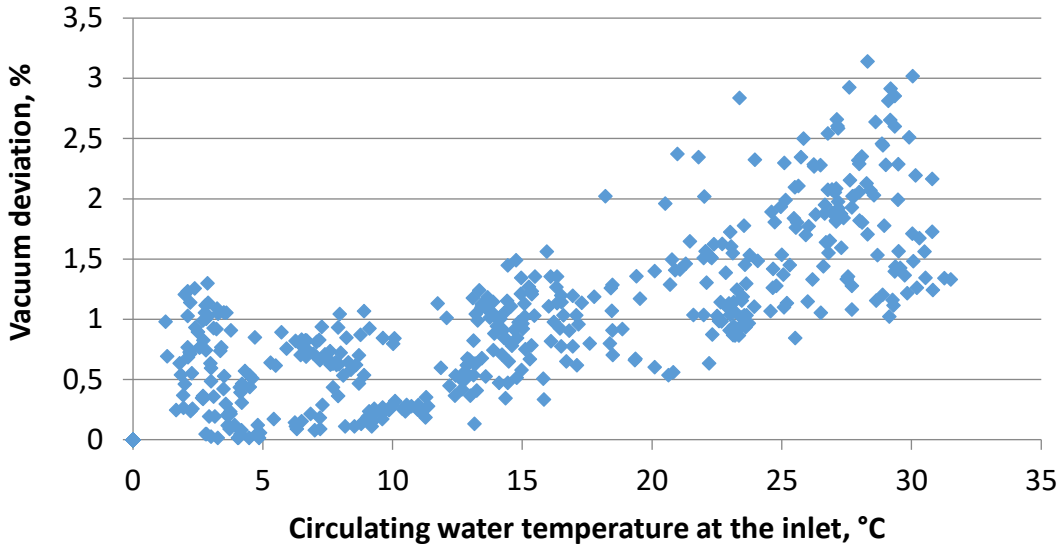

Fig. 5.2. The change in the deviation of the standard vacuum value in the condenser from the actual value depending on the temperature of the circulating water at the inlet to the condenser

It is seen that as t_{1w} increases, the effect of air suction on the vapor pressure in the condenser increases as well. This is explained by the fact that with the increase in water temperature, the heat transfer coefficient on the water side also increases. The vapor side starts to limit heat exchange in the condenser. Therefore, a decrease in the heat transfer coefficient from the steam side due to increased air suction leads to a more significant decrease in the heat transfer coefficient. Consequently, the decrease in vacuum is also more significant, with a high temperature of cooling water entering the condenser rather than with a low water temperature.

According to [145], a pressure change in the condenser of 1 kPa causes a change in the power of the K-200-130 LMZ turbine by 1.9 MW. In Fig. 5.3, the additional power calculated from the monthly average differences of vacuum deviations in 2016 and 2017 is shown. The calculation is provided for the K-200-130 LMZ turbine operating with two serial ejectors, the EP-3-700 in 2016 and the new EPO-3-80 ejector in 2017.

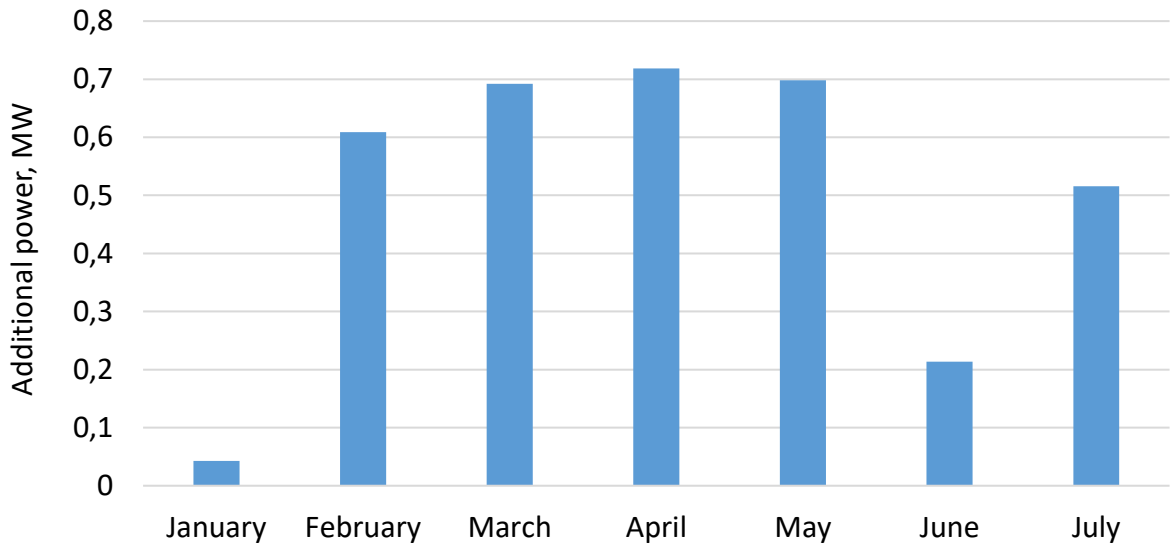

Fig. 5.3. Additional power generation by the turbine through reducing the deviation from the standard vacuum

The value of the additional power generated in the turbine due to the deepening of the vacuum averaged N = 0.87 MW. Taking the specific fuel consumption equal to b = 323 g of fuel equivalent / KW * h and the cost of fuel about 3,000 rubles/ton, the average turbine operating time about 6000 h/year, the resulting economic effect is more than 5 million rubles/year (70,000 euro). The results of the successful implementation of the EPO-3-80 ejector at Surgut GRES-1 are confirmed by the Implementation Act (see Appendix 1).

5.2. FUNCTIONING OF THE GENERAL EJECTORS IN COGENERATING TURBINES

The analysis of the deviation of the vacuum values in the condenser to the efficiency of STU operation is also applicable to cogenerating turbines; however, the parameters of the turbine's operation should be taken into account. When cogenerating turbines operate with minimal steam flow rate to the compartment behind the regulating diaphragm, the deepening of the vacuum in the condenser does not entail a significant increase in the power generated by the turbine [8, 88].

To determine the effect of the deepening of the vacuum in the condenser, the calculations of LPP power for T-250 / 300-240 UTZ turbine were carried out. Currently, 30 turbines of this type are installed and operated in the TPP of large cities (Moscow, St Petersburg, Kiev, Kharkov and Minsk). It is especially necessary to note that a significant part of the time they operate in heating modes with a fully closed diaphragm.

In the framework of this research,[3] only the operation of stages installed in the compartment behind the diaphragm at low heat extraction was considered. The flow part of the compartment for the lower heat extraction section consists of two streams, each of which has 3 stages. Various cogeneration modes of turbine operation were considered in the range of steam flow rate to the LPP from 10 t / h to 80 t / h in total for two flow stages, with a pressure change in the upper regulated heating section from 0.1 MPa to 0.2 MPa with two-stage water heating and with a change in pressure in the lower regulated heating section from 0.08 MPa to 0.15 MPa at one-stage water heating.

The calculations are performed in specialized software. In this case, the full geometry of the flow part was used, including the profiles of the turbine blades, the gaps in the overband and diaphragm seals, etc. The evaluation of ventilation losses was carried out in accordance with [146]. All calculation results are summarized for the two streams.

Additionally, it should be noted that the design studies were carried out taking into account the design state of the LPP (profiles of the blades), which do not take into account its actual condition. Appearing during operation, leaching and other changes in the profiles of the blades, as well as possible increases in steam consumption to LPP with a fully closed regulating diaphragm, may impose an additional error on the results obtained.

[3] Calculations were carried out with the participation of the head of UTZ calculations department, M. Yu. Stepanov.

As an example, a graph of the change in LPP power at a pressure of P_t = 0.2 MPa in a cogenerating mode with two-stage water heating is shown in Fig. 5.4.

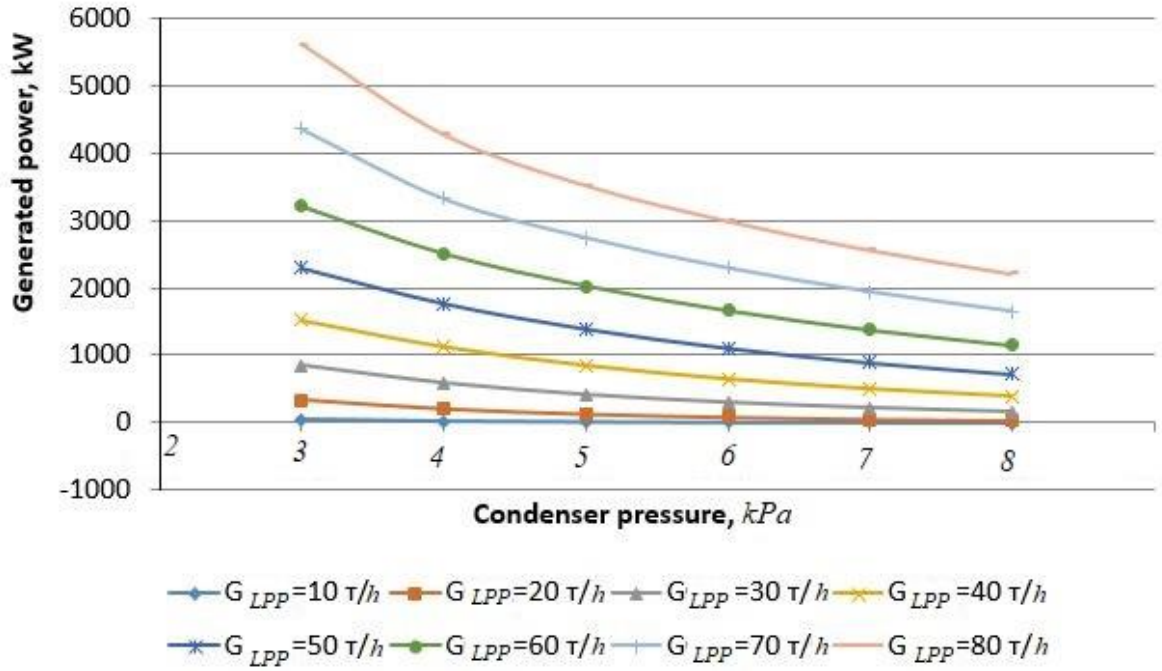

Fig. 5.4. The dependence of the total electric power of the LPP on the pressure in the condenser, the two-stage heating mode at Pt =0.2 MPa.

As can be seen from the graph, with an increase of the pressure in the condenser in the range of P_c = 3-8 kPa, the amount of generated power decreases at all values of steam consumption by the condenser. When steam consumption by the condenser is G_{LPP} = 80 t / h, the generation of electric power increases to 3.5 MW. It should be noted that at increased steam consumption by the condenser, depending on the technical condition of the flow part, the additional power output may increase from vacuum deepening.

For an example of the distribution of electrical power generation in stages, in Fig. 5.5 the change in the power of each stage is shown separately when the steam flow rate to the condenser is G_{LPP} = 80 t / h.

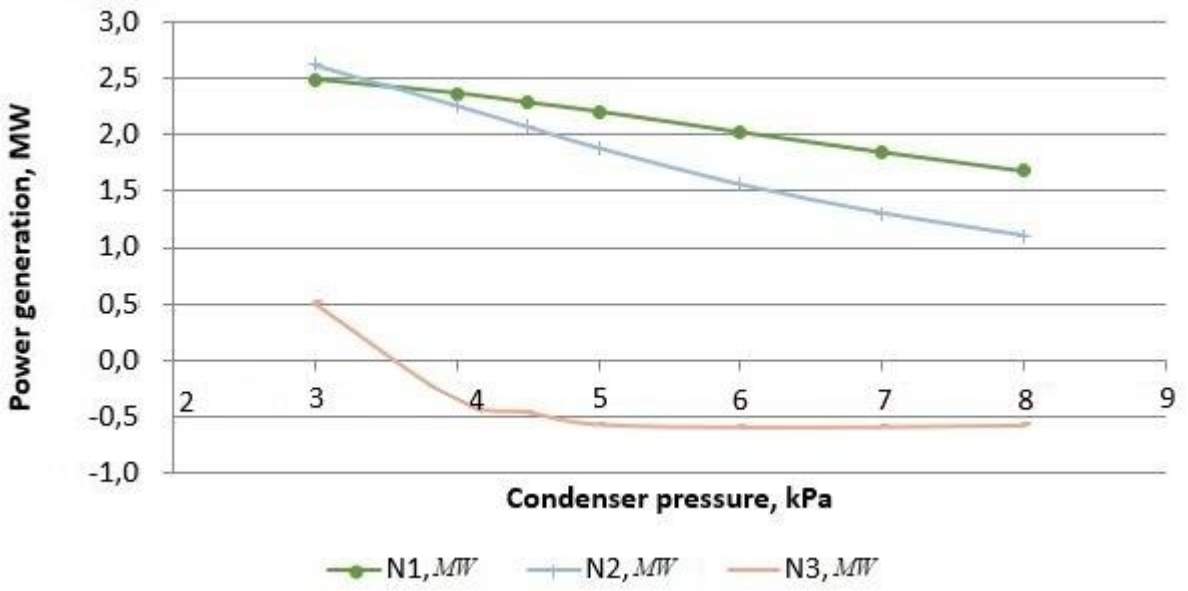

Fig. 5.5. The dependence of the total electric power of the LPP on the pressure in the condenser, the heat and power mode with two-stage heating at P_{he} = 0.2 MPa at G_{LPP} = 80 t / h: N1, N2, N3 - power generated by stages I, II and III, respectively

The decrease in the generated power with increasing pressure from P_c = 3 kPa to P_c = 8 kPa will be about ΔN_1 = 0.8 MW in the first stage, ΔN_2 = 1.5 MW in the second stage and ΔN_3 = 1.0 MW in the last stage of the LPP.

It should be noted that according to the calculation results, in most of the modes studied the first and second stages of the LPP generate electricity, while the last stage has a negative output when the pressure in the condenser is above 3.5 kPa, presumably due to the significant amount of ventilation losses.

In Fig. 5.6., the change in the power in the last stage depending on the pressure in the condenser and the steam consumption throughout the stage is presented.

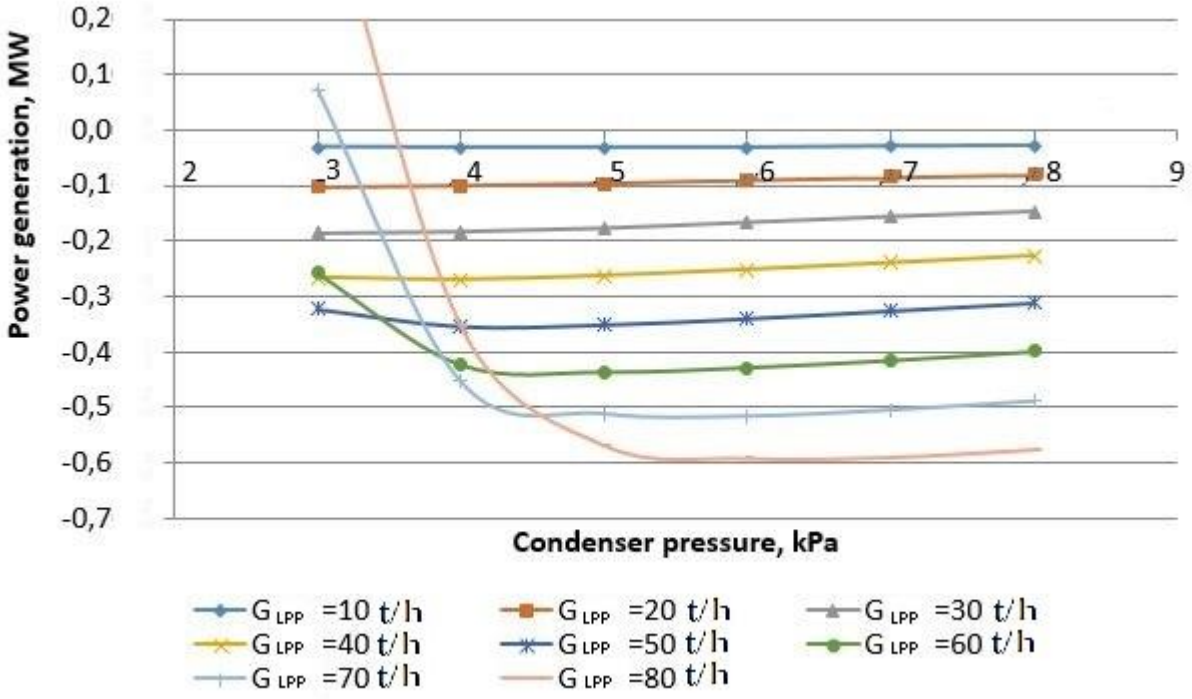

Fig. 5.6. The dependence of the electric power of the third-stage on the pressure in the condenser, the heat-generating mode with two-stage heating at P_{he} = 0.2 MPa

As can be seen from the graph, when steam consumption throughout a stage is no more than G_{LPP} = 50 t / h: the change of pressure in the condenser has little effect on the losses and is no more than ΔN = 40 kW. The increase of steam consumption throughout the stage increases the amount of losses (minus generation of electricity in the stage). When the steam flow rate is G_{LPP} = 80 t / h and the pressure in the condenser is more than 3.5 kP, the loss is about 600 kW.

Based on the experimental data about the decrease of vacuum deviation by ΔV = 0.5% from 4.3 kPa to 3.8 kPa when implementing the developed ejector, Fig. 5.7 presents the change in power output.

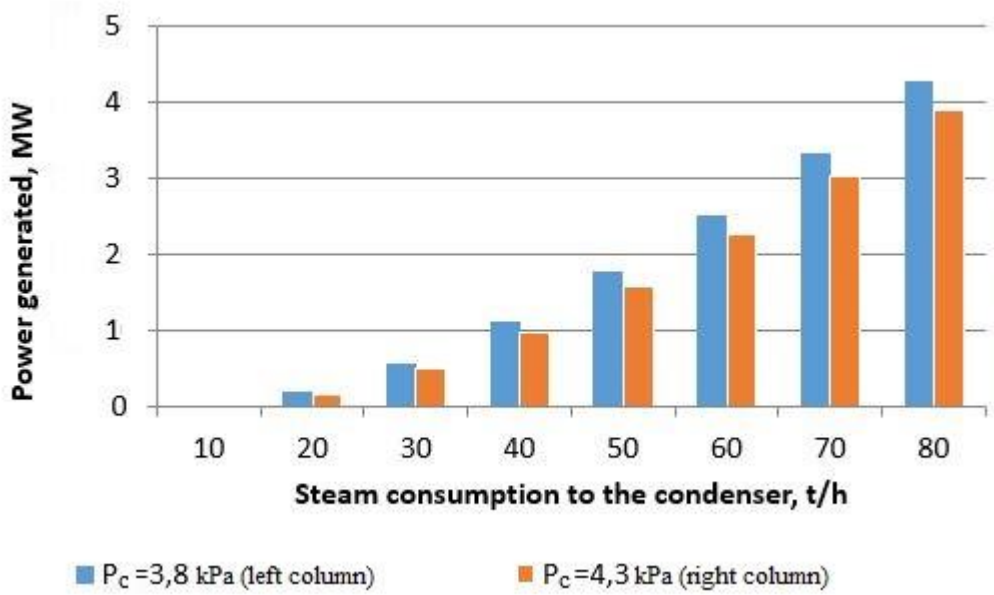

Fig. 5.7. The dependence of the electric power of the LPP on the steam consumption by the condenser.

With an increase in steam consumption to the condenser from 10 t / h to 80 t / h, the value of electric power increases from 0.012 MW to 4.277 MW. At the same time, additional power generation with a deepening of the vacuum by ΔV = 0.5% is from 7 kW to 378 kW, respectively. The maximum additional power generation with steam consumption by the condenser G_{LPP} = 80 t / h and a vacuum deepened by ΔV = 0.5% is equal to ΔN = 378 kW (0.15% of the power of the turbine unit) and corresponds to the resulting economic effect of more than 630,000 rubles/year (9,000 euro). In the calculation, the specific fuel consumption of the T-250/300-240 UTZ turbine is assumed to be b = 270 g / KWh, the cost of fuel is 3,000 rubles / t, and the turbine life per year is 2,100 hours (heat generation mode).

Thus, it can be concluded that in the operation modes of heat-generating turbine installations with a fully closed diaphragm, an increase in the effect of air suction and a corresponding increase in vapor pressure in the condenser have a significant impact on the loss in the last stage of the LPP. Due to the fact that such modes of operation are often found in the operation of turbine installations, it is advisable to modernize the ejectors and install more efficient ones to maintain a deeper vacuum in the condenser of the cogeneration turbine.

5.3. RESULTS

1. The expected economic effect from the installation of the developed high-performance EPO-3-80 ejector on K-200-130 LMZ condensing turbine was 5 million rubles/year (70,000 euro/year). The effect was achieved by generating additional power N = 0.87 MW.
2. It is shown that at high air suction and with an increase in pressure in the condenser of a cogeneration turbine, it is advisable to use a highly efficient ejector even in modes with a fully closed diaphragm. When the pressure in the condenser of the T-250 / 300-240 UTZ turbine is deepened by $\Delta V = 0.5\%$, the value of the additional generated power can be about N = 378 kW, which is 0.15% of the turbine capacity and corresponds to an economic effect of about 630,000 rubles/year (9,000 euro/year).

Chapter 6

RESEARCH AND DEVELOPMENT OF CHILLER TYPE EJECTORS

At present an actual direction of ejectors research is their application in various energy conversion systems, for example, in refrigeration units (chillers) [53,96,147]. Refrigeration cycle plants are widely used in a large number of industrial facilities. The use of ejectors for this type of units permits to increase their efficiency by reducing the maintenance cost (in case of a technological source of primary heat) and reliability due to rejection of centrifugal pumps.

To carry out the ejector research, an experimental test-bench was developed on the basis of the laboratory of Thermodynamics of the University of Florence [98]. The test-bench was developed jointly with Federico Mazzelli, Jafar Mahmoudian and Andrea Rocchetti under the direction of Adriano Milazzo.

6.1. WORKING FLUID

As the first benefit of the ejector chillers implementation is the economic one, then steam would be the obvious choice as a working fluid, being costless, safe for operators and environment and available everywhere. In any industrial environment where steam is produced for other purposes, steam ejectors are unrivalled as simple and relatively effective means for refrigeration [148]. However, synthetic fluids may have some peculiar advantages. The first point is undoubtedly the volumetric cooling capacity. Water, notwithstanding its unrivalled latent heat, has a very low vapour density at low temperature (Table 6.1), while common refrigerants have much higher values. The influence of volumetric cooling capacity on the size of an ejector chiller is not as straightforward as in vapour compression cycles featuring volumetric compressors. However, the values in Table 1 suggest that a steam ejector chiller is likely to be much more bulky for a given cooling capacity.

Table 6.1

Fluid	Latent heat [kJ/kg]	Vapour density [kg/m^3]	Volumetric cooling capacity [kJ/m^3]	Saturation pressure [bar]	
				0°C	100°C
Water	2501	0.00485	12.13	0.00612	1.014
R134a	198.6	14.43	2866	2.929	39.72
R245fa	204.5	3.231	660.7	0.5295	12.65
R1233zd(E)	204.9	2.820	577.7	0.4788	10.50
Fluid properties calculated via NIST REFPROP [4]					

The second point is the operating pressures within the various parts of the chiller. Water has very low saturation pressure at all temperature levels encountered along an ejector cycle. The generator, if operated e.g. at 100°C, is at ambient pressure, but the evaporator typically works below 1 kPa. This requires very accurate sealing of the circuit. On the other hand, R134a has a rather high pressure at typical generator temperatures (Table 6.1), which makes the operation and the energy consumption of the generator feed-pump more troublesome. R245fa is a good compromise, as it goes slightly below ambient pressure at evaporator but remains within a moderate 12.6 bar at 100°C.

The third point is the slope of the upper limit curve on the temperature–entropy diagram. R245fa and R1233zd have an inward slope of the limit curve. This means that the primary nozzle and the whole ejector are free from liquid condensation even if the expansion starts on the limit curve with no superheating. R134a and water, on the other hand, have a “wet expansion” and therefore they need a substantial superheating at generator exit.

The last point that favours synthetic fluids is the absence of icing, which may represent a serious problem for steam ejector chillers and limits their operation to above zero.

On the other hand, F-gas regulations limit the use of fluids with GWP>150 in Europe and other countries have similar limitations. Therefore R245fa (GWP = 950) could prove unusable in most applications. HFOs (Hydro-Fluoro-Olefins) are currently proposed as “drop-in” replacement of HFCs [149]. Among them, R1233zd

has similar thermodynamic properties and hence experimental results gathered with R245fa may be an indication for the performance of an equivalent system using the low-GWP alternative fluid.

Considering all mentioned arguments, we decided to perform our experimental activity firstly with R1233zd and then move to steam. The goals of the researches are both to get ejector performances and parameters ranges for each fluid itself and to compare — to study the influence of noted thermophysical properties of fluids at design features and performances of the ejectors.

6.2. EXPERIMENTAL SET-UP

Jet device

The chiller ejector of CRMC (constant rate of momentum change) design was tested with R245fa as a working fluid in 2006 by Eames et al. [150]. The flow sections of the ejector were calculated by imposing a constant rate of deceleration along the mixer/diffuser. The experimental results showed that, for saturation temperatures of 110°C at generator and 10°C at evaporator, the COP could be as high as 0.47, with a critical condenser temperature of 32.5°C.

The energy conversion coefficient COP, as is known, is the ratio of the thermal power of the evaporator divided by generator power (as long as we neglect the pump power). The generator power may be evaluated as the difference of thermal powers of condenser and evaporator.

$$\mathrm{COP} = \frac{Q_E}{Q_C - Q_E} \tag{6.1}$$

Q_E – evaporator thermal power;

Q_C – condenser thermal power.

Raising generator temperature to 120°C decreased the COP to 0.31, but the critical condenser temperature increased to 37.5°C. Superior performance of CRMC design has been recently confirmed in [151]. It the test-bench a modified version of the CRMC ejector is presented.

Our ejector was designed starting from a scaled-up version of Eames' design, introducing a bell-shaped end on the suction side and a conical outlet on the discharge side. The manufacturing problems due to the small inner diameter and substantial length forced to build the ejector in three pieces, carefully aligned by flanged connections. In this way, a roughness of the internal surface from 4 to 6 microns was obtained.

The tested arrangement is the result of a long refinement work of a big scientific team, as described in publications [97],

98]. General dimensions of the tested ejector configuration are reported in Table 6.2.

Table 6.2

	Nozzle	Diffuser
Throat diameter [mm]	10.2	31.8
Exit diameter [mm]	20.2	108.3
Length [mm]	66.4	950
Material	Aluminium	Aluminium

Nine ports have been drilled perpendicularly to the ejector inner surface in order to measure the local static pressure. The holes are placed at 100 mm intervals, starting at 50 mm from the inlet flange of the ejector, as shown in Fig. 6.1.

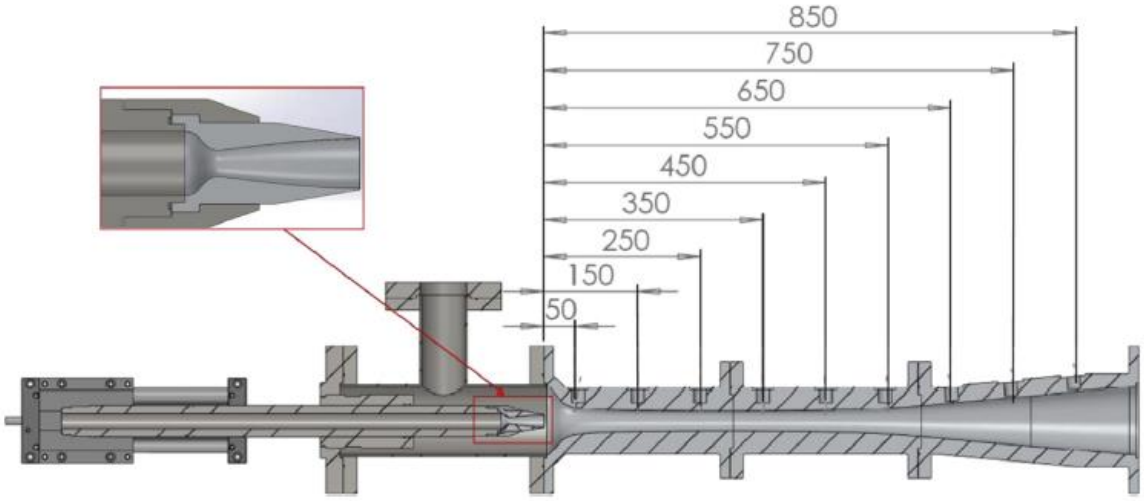

Fig. 6.1. CRMC ejector with static pressure ports and movable primary nozzle

The throat of the diffuser, which can be seen at fig. 6.1, is marked by a black vertical line at the distance of 300 mm from the diffuser inlet.

The ejector is equipped with a movable primary nozzle, in order to optimize the axial position relative to the diffuser. A reference position is having the nozzle exit plane coincident with the inlet plane of the bell-shaped inlet of the suction chamber. At present the mechanism cannot be operated when the system is running, but in principle it could be modified for continuous adjustment during operation. For example, it can be modified in accordance with the design, presented in Chapter 3.

Set-up scheme

The ejector is part of a heat-powered refrigeration system (Fig. 6.2) designed to give 40 kW of refrigeration to a chilled water stream entering at 12 and exiting at 7°C.

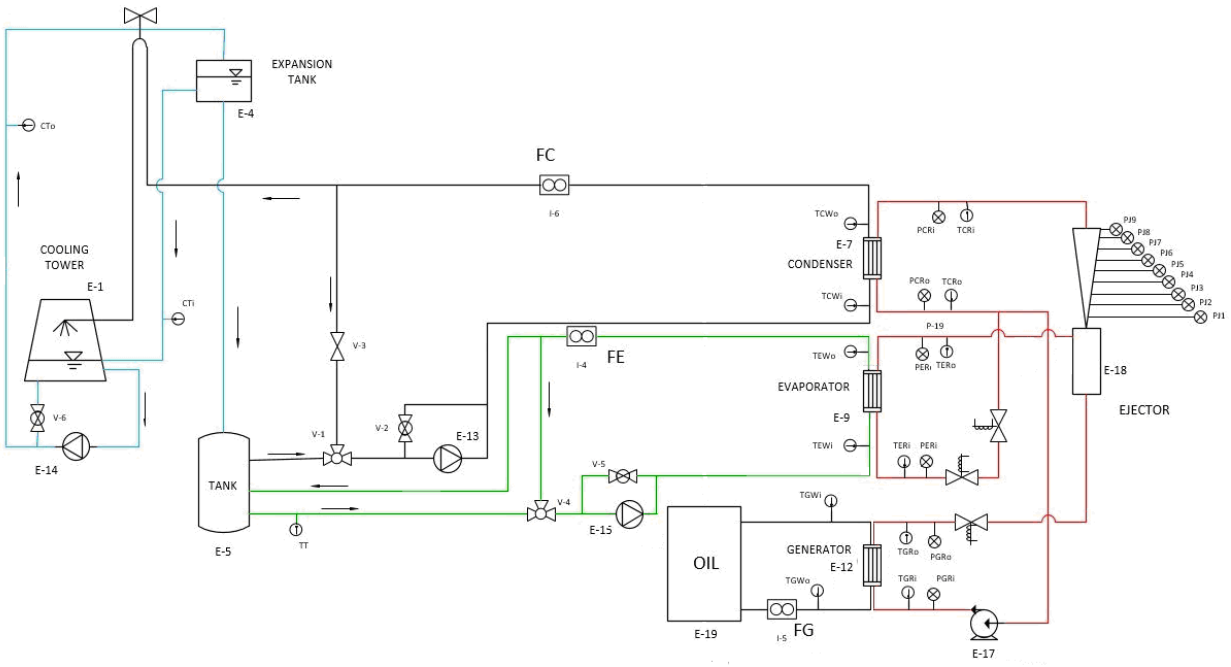

Fig. 6.2. Experimental set-up

In the original set-up the heat source was hot water at 90 — 100°C. Now a thermal oil electric heater is used as heat source, in order to explore a wider temperature range. An evaporative cooling tower discharges the system power into the ambient air outside the laboratory. The cooling tower receives the warm water directly from the condenser and feeds a buffer tank, in order to have a stable water source at near ambient temperature. The tank water is used to give the heat load to the evaporator and to cool the condenser. By-pass branches are used to regulate the temperature at evaporator and condenser inlets.

The prototype is conceived with a "ready to market" structure. Some pictures are presented in fig. 6.3. During components placing, several features had to be taken into account to permit easy connection with external water circuits, allow user access for assembly and disassembly operations and create a compact and movable structure. A vertical arrangement was chosen for heat exchangers. This allowed reduction of space and mitigation of cavitation problems at the pump inlet. As a consequence, the main axis of ejector is vertical as well.

Fig. 6.3. Pictures of the chiller

Measurement scheme

Mass flow meters and temperature sensors are mounted on the condenser and evaporator water circuits, in order to have the instantaneous energy balance of the system. Water mass flow measurements in the external circuit are carried out with Endress+Hauser Promag electromagnetic flow meters. Electric power consumption of the feeding pump is measured by an electronic wattmeter. Temperature and

pressure sensors are mounted in all the significant points along the refrigerant circuit, while 9 pressure probes are mounted along the ejector as mentioned above. The location of the transducers can be seen from the top right photo. Piezoresistive pressure transducers produced by Keller are used to obtain pressure values.

During compressing the temperature of the fluid is increasing (fig. 6.4).

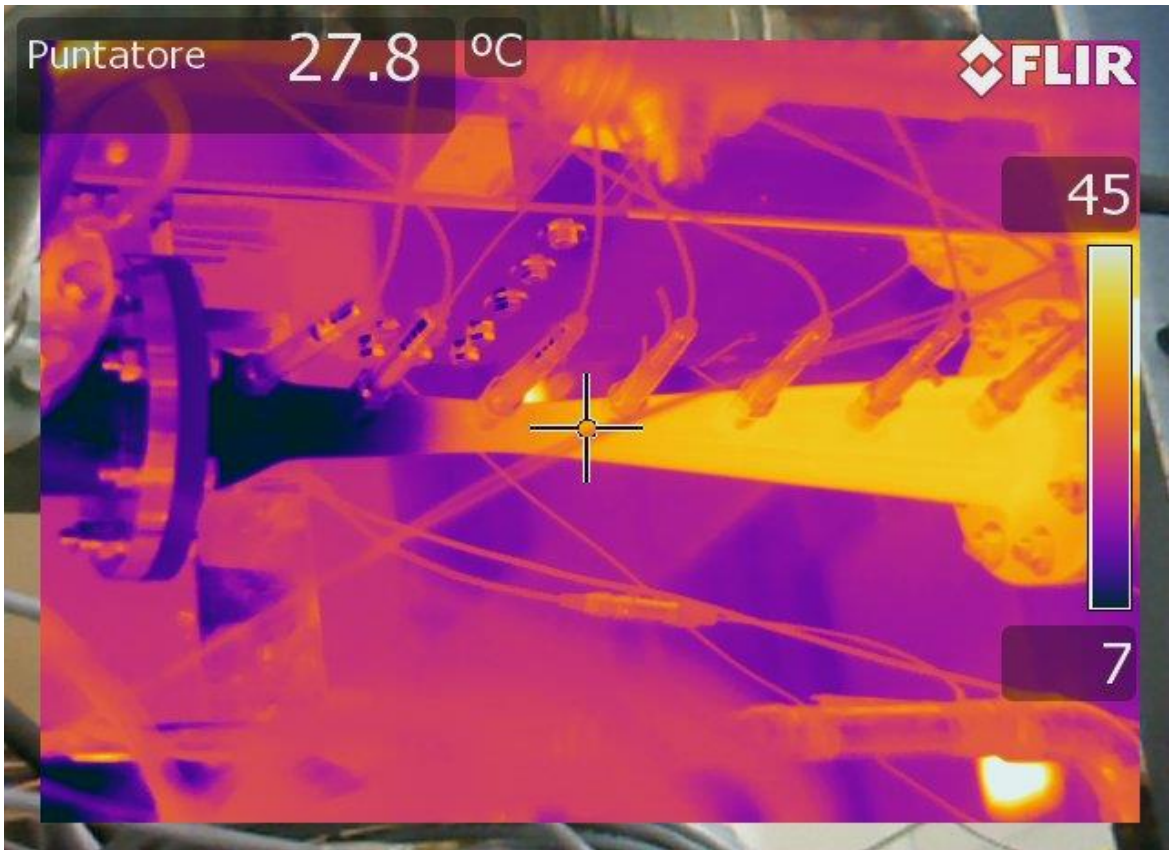

Fig. 6.4. Infrared image of the ejector prototype in operation

Temperature measurement probes are placed at the inlet and outlet connection of each heat exchanger. Resistance values of temperature sensors are read and converted by a National Instruments cFP-RTD-124 module. The specifications of the main sensors are reported in Table 6.3.

Table 6.3

Instrument	Model/type	Position	ADC Module	Total uncertainty
Piezoreistive pressure transducer	PA25HTT 0-30 bar	Diffuser	NI9208	±(0.1% + 0.22% FS)
	PR23R 0.5-5 bar	Evaporator	NI9208	±(0.1% + 0.22% FS)
	PA21Y 0-30 bar	Generator, Condenser	NI9208	±(0.08% + 1.0% FS)
Resistance temperature detector	Pt100	Whole Plant	NI9216, NI9217	±0.25°C
Thermocouple	T	Cooling Tower, Tank	NI9213	±1.0°C
Electromagnetic water flowmeters	Endress Hauser Promog 50P	Condenser	NI9219	±(0.5% + 0.04% FS)
Compact Rotamass mass flowmeter	YOKOGAWA RCCT28	Evaporator	NI9219	±(0.05% + 0.1% FS)
Vortex flowmeter	YOKOGAWA YF105	Generator	NI9219	±(0.8% + 0.1% FS)

All the experimental points have been measured after at least 15 minutes of stable operation and are averaged over 5 minutes. The generator feed pump has a variable frequency control, but has been always operated at 100% rotation speed.

Heat fluxes and refrigerant mass flow rates are measured by equivalence with the thermal fluxes flowing through the external water circuit. Due to this indirect method of measuring the mass fluxes, steady conditions are always sought to assure equality between water and refrigerant thermal fluxes. Nonetheless, the lack of direct mass flow measurement can lead to low accuracy of the experimental data. Hence, an extensive and detailed uncertainty analysis was performed to understand the level of confidence in the measurements.

Set-up operation

Installation operates as follows. The electric heater provides heating of the oil circuit, which in turn transfers heat to the working fluid of the installation in the Generator. The working fluid boils, evaporates, and at the pressure created by a

multistage centrifugal pump, it is supplied to the Ejector as a working fluid. The ejector draws fluid in from the Evaporator in a gaseous state and ensures its compression in the diffuser in ε = 1.5—3 times. Downstream the diffuser, the working fluid of the installation enters the condenser, where it changes its aggregation state to liquid. Further, the flow of the working fluid is bifurcated: part of the flow through the expansion (throttle) valve is drawn in into the evaporator, where it evaporates and enters the suction chamber of the ejector; another part of the flow of the working fluid is directed to a multistage centrifugal pump feeding the generator.

Using the three-way control valve in the auxiliary cycle circuit, the temperatures (and corresponding pressures) in the condenser and evaporator are adjusted. When the temperature (and the corresponding pressure) of the oil is changed by means of an electric heater of the generating cycle, the pressure of the ejector's working flow changes as following.

The table shows the parameters that are changed during the experiment, the allowable ranges of the set values and the values investigated in the current experiment.

Table 6.4

Changed parameter	**Units**	**Design range**	**Change step**	**Investigated range**
Temperature (inlet) – Condenser	°C	20—40	0.5	30—37
Saturation temperature – Evaporator	°C	0—20	2.5	2.5—10 (±0.1)
Pressure - Generator	bar	9—12	0.5	10—11 (±0,2)
Nozzle exit position (NXP)	mm	–50—+50	5	–10 — +10

The experimental studies were carried out with the following parameters adjusted: the nozzle in the axial position, the pressure of the working stream in the generator and the water temperature (saturation pressure) in the condenser. The pressure in the Evaporator is maintaining at 4 different values using a three-flow control valve.

As a result of the experiment, the COP and the entrainment ratio were obtained at various saturation pressures in the condenser.

6.3. EXPERIMENTAL RESULTS

This section presents some results of experimental studies at the developed set up. Ongoing research is the first step towards the development of a similar refrigeration unit, only with steam ejector. In this regard, the data obtained are analyzed in terms of a qualitative assessment of the ejector parameters, and not quantitative.

Figures 6.5—6.6 show the static pressure profiles in the diffuser in various modes at the primary flow pressures P_p = 10 bar and P_p = 11 bar respectively. The difference between the modes lies in the fact that during the transition to each subsequent mode saturation pressure in the condenser (back pressure of the ejector) rises due to an increase in the temperature of the cooling water at the condenser inlet by 0.1—0.3 ° C. Temperatures in °C are presented in the modes legend.

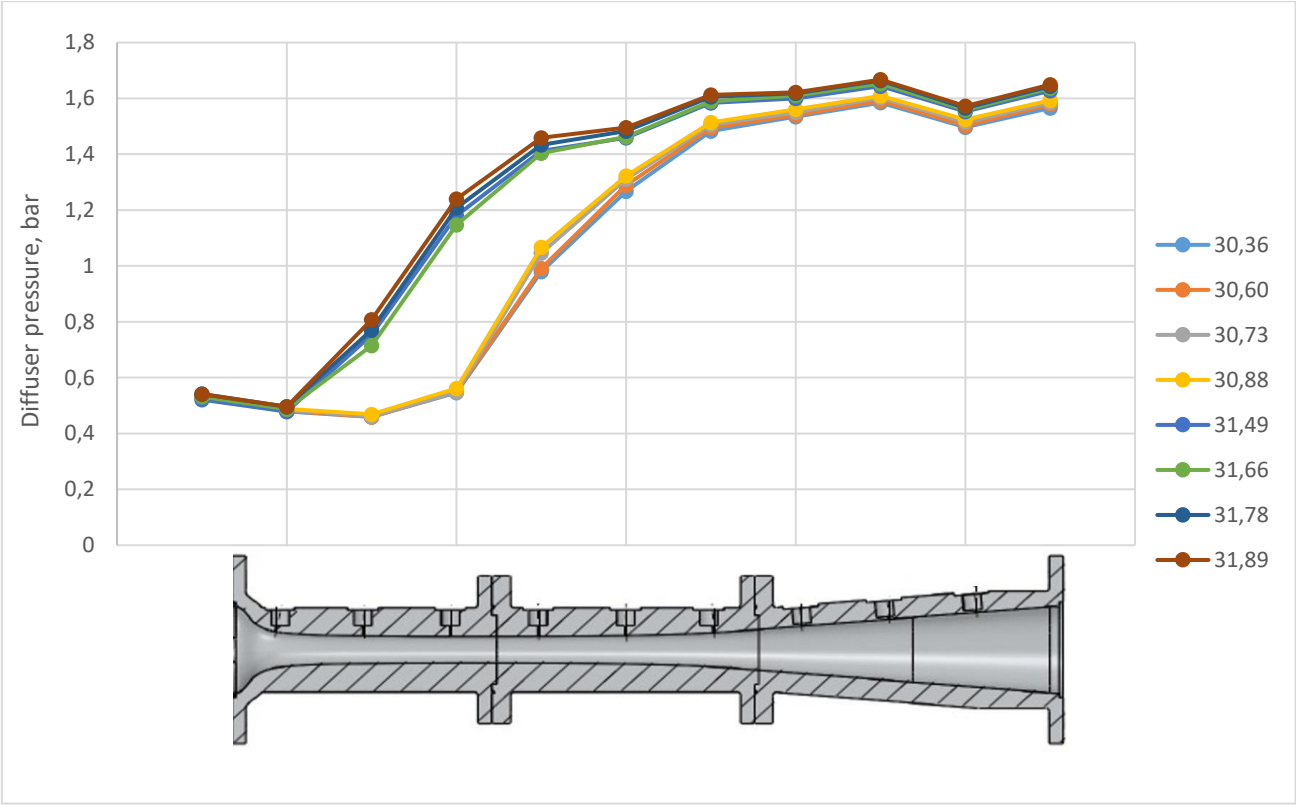

Fig. 6.5. Static pressure distribution along the diffuser length under various conditions at a primary flow pressure of P_p = 10 bar

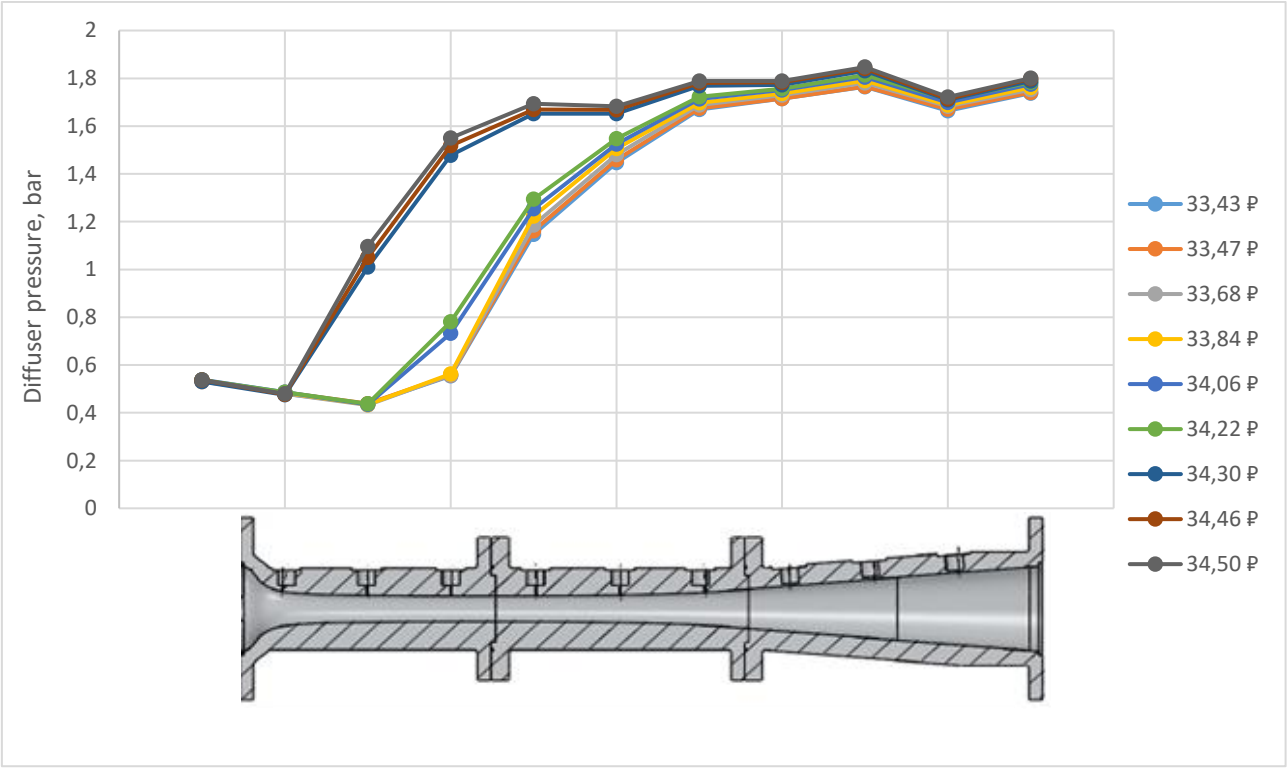

Puc. 6.6. Static pressure distribution along the diffuser length under various conditions at a primary flow pressure of P_p = 11 bar

It can be seen from the graphs that for several initial modes the pressures are almost equal, with a slight pressure decrease in the mixing chamber, after which the flow compression starts next to the diffuser throat and the pressure begins to increase significantly. The pressure in the sharply expanding part of the diffuser remains almost unchanged. Perhaps this indicates that diffuser is too long, which is excessive. With an increase in backpressure, the profile changes abruptly and the modes with increased backpressure differ significantly from the first ones. In this case, the pressure in the diffuser increases sharply, even in the narrowing part. In our opinion, this is due to the transition of the ejector from the on-design to the off-design mode, while the backpressure of the diffuser starts to significantly effect on the ejector characteristics. At the same time, we maintain the flow rate of the injected mixture constant, i.e. the pressure in the diffuser does not increase due to an increase in the flow rate of the injected mixture, but rather because of backpressure.

Based on the tests, the limiting temperatures (and the corresponding back pressures) are determined, above which the pressure profile in the diffuser changes abruptly (Table 6.5).

Table 6.5

Primary flow pressure, bar	Suction pressure, bar, (saturation temperature in the evaporator, °C)	Limiting temperature of the condenser cooling water, °C	Limiting back pressure, bar
10	0,53 (2,5)	30,9	1,59
	0,59 (5)	31,4	1,62
	0,66 (7,5)	31,7	1,64
	0,73 (10)	31,9	1,66
11	0,53 (2,5)	34,2	1,78
	0,59 (5)	34,5	1,80
	0,66 (7,5)	35,2	1,84
	0,73 (10)	35,6	1,87

A comparison of the modes (pressure profiles in the diffuser) with various pressures of the primary flow is shown in Fig. 6.7.

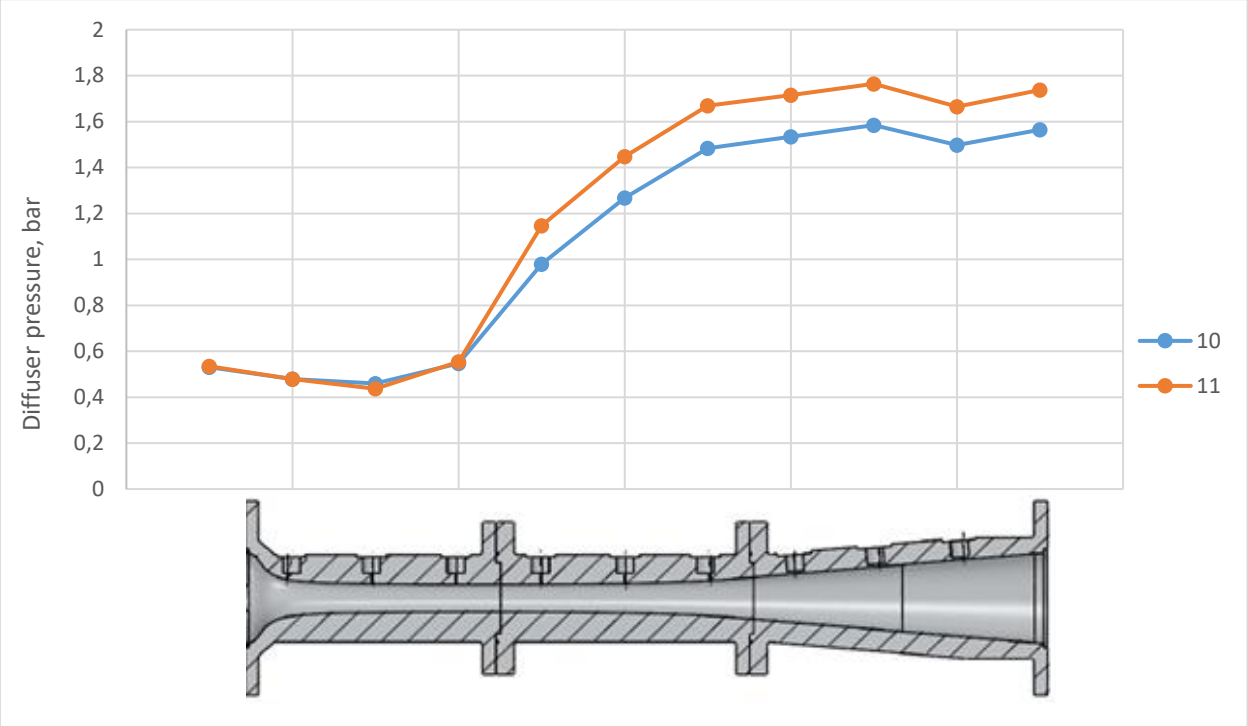

Fig. 6.7. Static pressure distribution along the diffuser length at various primary flow pressures

As an example, the modes with the saturation temperature in the evaporator t_{satE} = 2.5°C are shown. The graph shows, that the pressure in the suction chamber coincides in both modes, which is specially regulated by the experimental process. In this case, the outlet pressure increases by 11%, the compression ratio of the diffuser increases by 16% — with an increase in the primary vapour pressure from 10 to 11 bar.

To analyze the operation mode of the ejector Fig. 6.8 shows the entrainment ratios of the ejector depending on its back pressure, precisely — on the condenser saturation temperatures.

Fig. 6.9 presents the characteristics of the refrigeration cycle (COP), characterizing the cooling ability of the chiller with the ejector employed. Specifications are presented for similar modes.

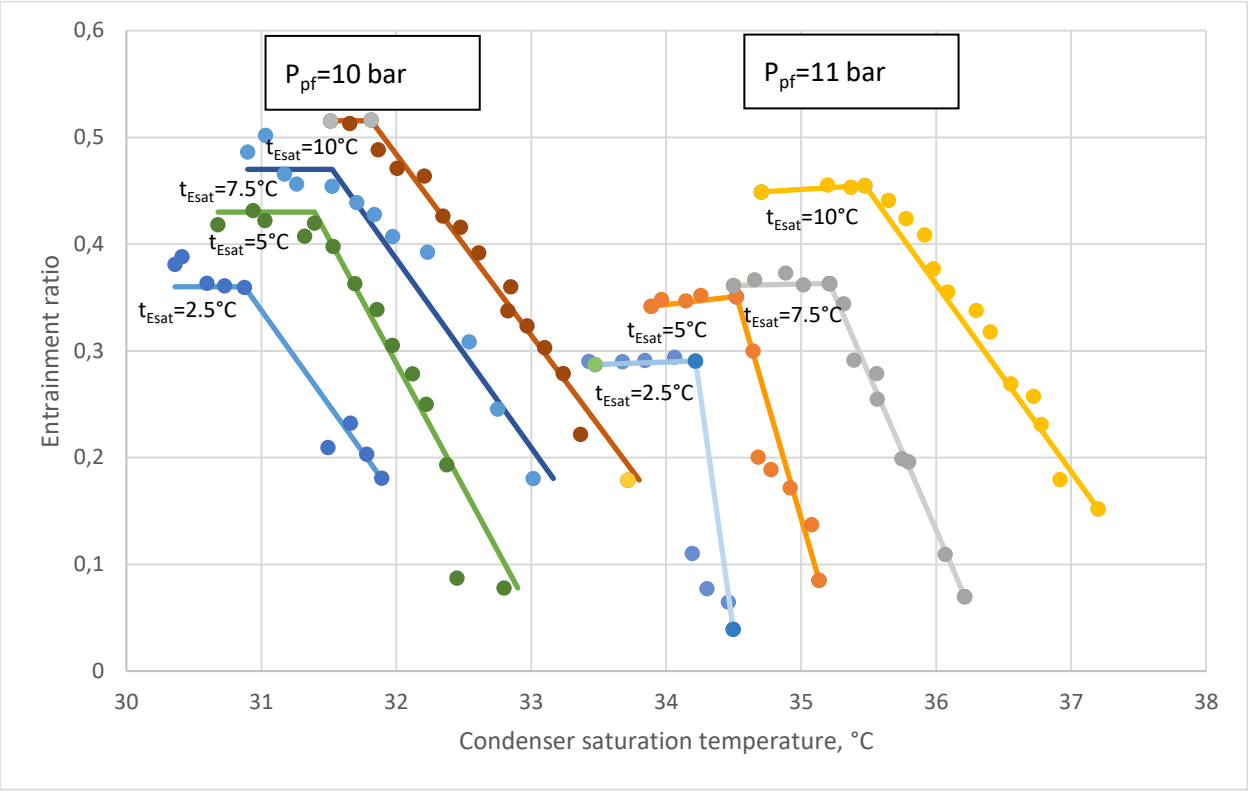

Fig. 6.8. Entrainment ratios at various primary and suction pressures

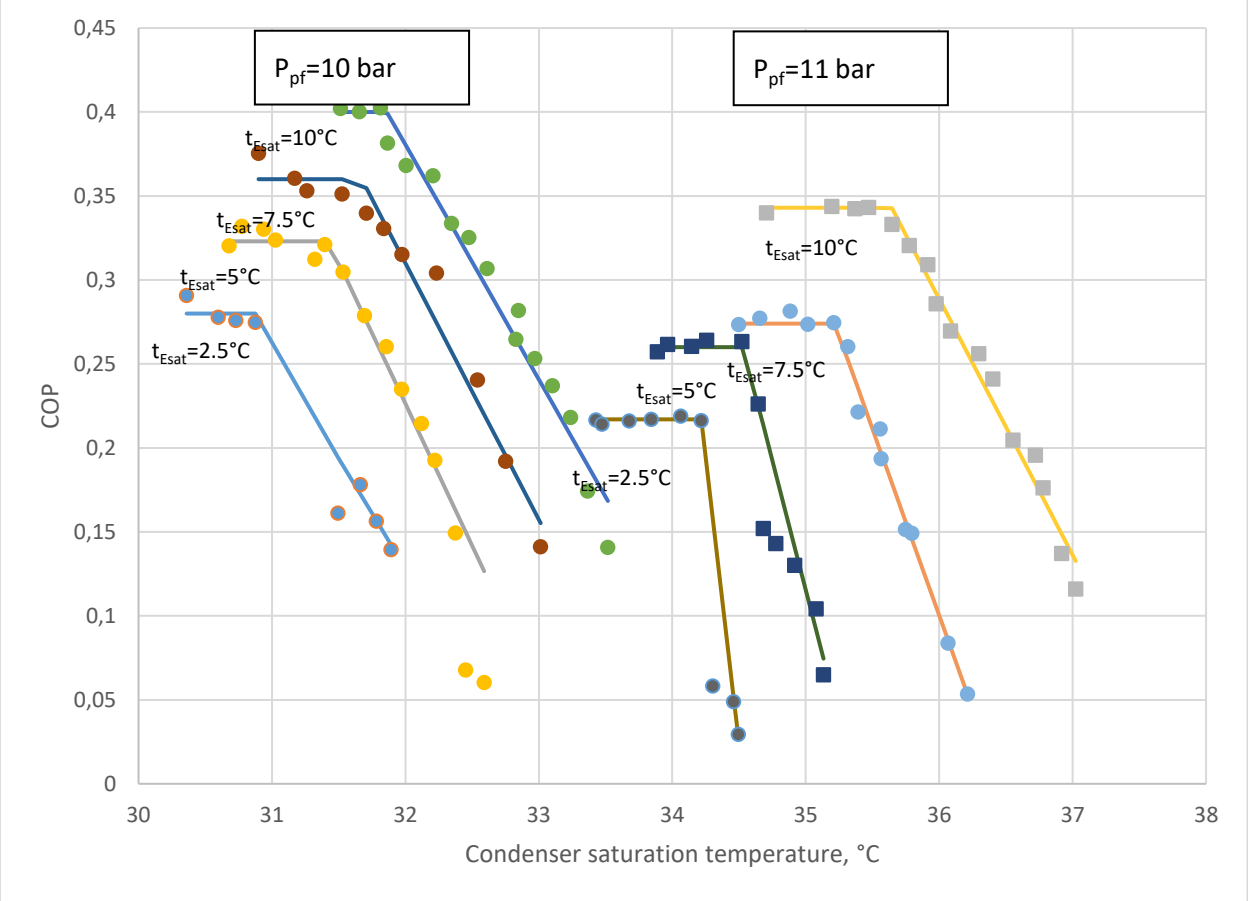

Fig. 6.9. COP at various primary and suction pressures

At the graphs presented, the approximation of the obtained modes was carried out using two linear functions (for each mode). As one can see on the graphs, the characteristics of each mode are completely equidistant to each other. This confirms that the characteristic of the refrigeration cycle is completely dependent on the characteristics of the ejector itself. The same obviously follows from the analysis of its formulas parameters.

The results obtained confirm that the suction pressure rise allows for COP increase, as well as for the maximum back pressure of the ejector, i.e. for condenser saturation temperature, at which the ejector switches to off-design mode. In this case, the compression ratio of the ejector decreases — the entrainment ratio rises and entails an increase in COP.

It can also be concluded that an increase in the pressure of the primary stream by 10% (from 10 to 11 bar) would significantly increase the limiting back pressure of the ejector. At the same time, the cooling capacity of the cycle is reduced due to an increase in the thermal capacity of the condenser — the additional heat given to the primary vapor is transferred to the condenser cooling water. Additional heat is associated both with a higher temperature of the working stream, and with an increased flow rate (due to higher pressure).

Fig. 6.10 shows the characteristic of the ejector — a change in the suction pressure of the ejector from an increase in the flow rate of the injected mixture. Characteristics are given at various pressures, bar.

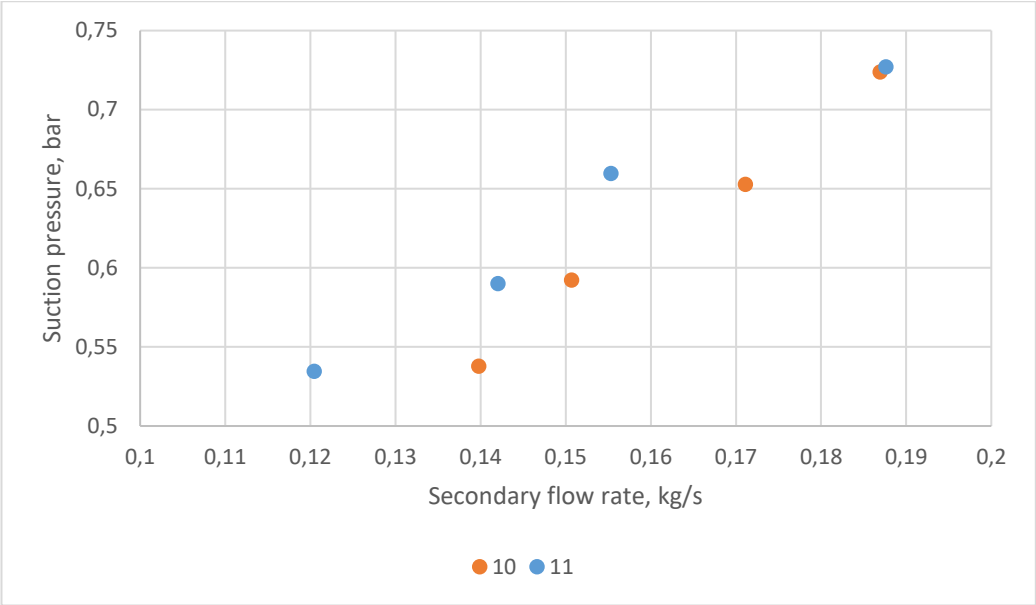

Fig. 6.10. Suction pressure changes against the ejectors capacity

According to the graph, at a lower pressure of the primary flow and the same secondary flow rate, the suction pressure of the ejector is significantly lower — for about 10%. In our opinion, this indicates the inexpediency of a further increase in primary pressure in view of ejector efficiency — the relative reduction in COP reaches 21%. However, the increase in pressure can be justified by the requirements for refrigeration cycle characteristic, i.e. functioning with higher back pressure.

Fig. 6.11 presents the characteristics of the refrigeration unit (COP) obtained at various positions of the nozzle relative to the diffuser. The characteristics are obtained in the modes with fixed pressure of the primary flow (P_{ps} = 11 bar) and suction pressure (P_I = 0.73 bar), i.e. at saturation temperature in the evaporator being –10 °C.

The “down” position corresponds to the retreating of the nozzle from the diffuser, the “up” position, on the contrary, to moving the nozzle inside the diffuser.

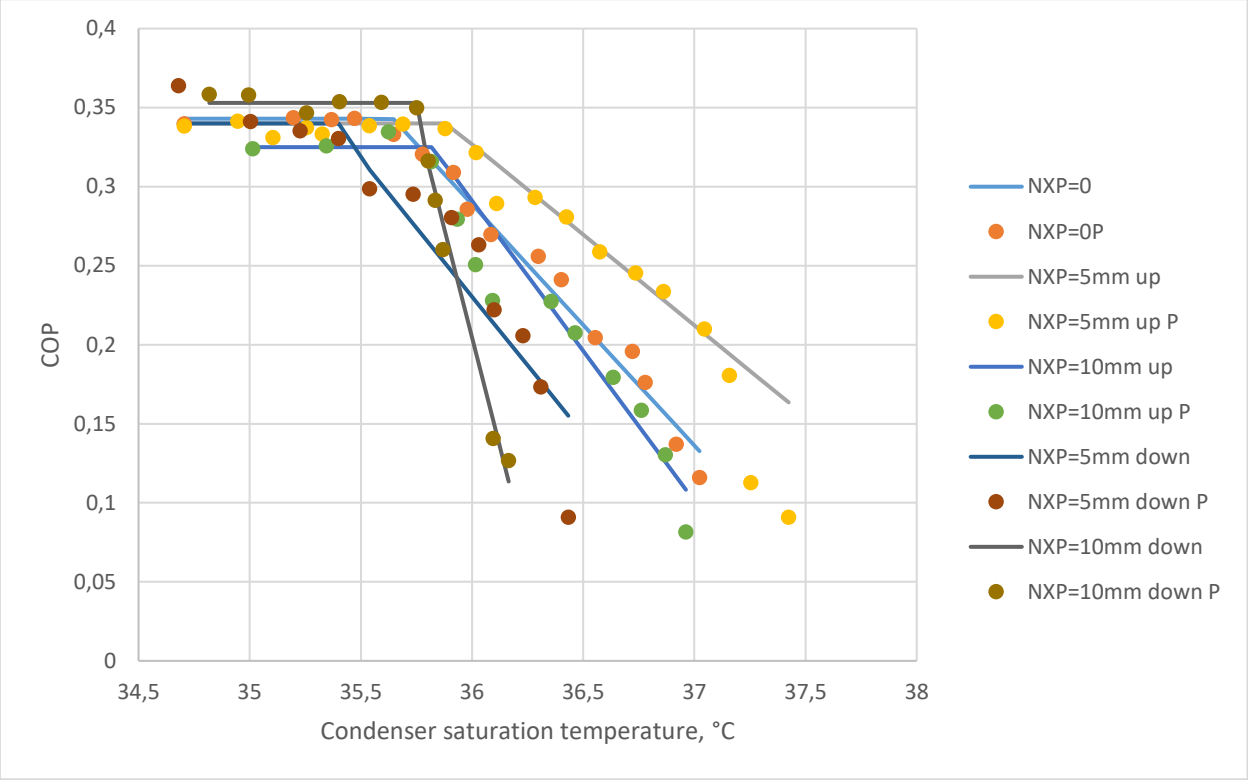

Fig. 6.11. Comparison of the COP values at various nozzle positions

As it follows from the graph, in the studied range of nozzle positions there is no clear dependence between nozzle position and the cycle characteristics. The most effective position for the set conditions can be considered the position of the nozzle "5 mm down", when the highest COP is achieved. The difference in COP of various modes does not exceed 2%.

In this case, it could be interesting to investigate the angle of the off-design mode curve. A significant difference in the inclines of the curves can be related to the different nature of the flow of the secondary jet — in some modes the flow speed is subsonic; in some – it flows sonic, but the section, where it crosses the sonic level moves from the diffuser into the suction chamber.

6.3. STEAM EJECTOR DESIGN

Based on the study of the operating parameters of ejector chillers, an idea is formed about the necessary characteristics of the unit. The following main parameters were taken to develop of a steam ejector for a refrigeration unit (Table 6.6):

Table 6.6

№	Parameter	Designation	Parameter
1	Primary steam pressure, MPa	P_{ps}	0,02
2	Primary steam temperature, °C	T_{ps}	120
3	Injected steam flow rate, kg/h	G_{II}	5
4	Injected steam temperature, °C	t_{II}	12
5	Suction pressure, Pa	P_I	1400
6	Backpressure, Pa	t_{1w}	7000
7	Compression ratio	P_2/P_1	5

In this case, parameter № 3 (Injected steam flow rate) is selected on the basis of the required refrigeration capacity of the unit or, in the case of an experimental test-bench, of sufficient measurement error of refrigeration capacity. In the calculation, as a first approximation, it was decided to keep the existing diffuser in the experimental bench. In this regard, the secondary flow rate is determined based on the choice of the corresponding diffuser geometry — the closest to the existing one. The main geometric dimensions of the nozzle in this case are:

Table 6.7

Parameter	Designation	Unit	Magnitude
Nozzle critical section diameter	d_{cr}	mm	5.2
Nozzle outlet section diameter	d_{ex}	mm	62.2

In the second approximation a complete replacement of the jet device in the installation is planned; to do this a calculation has been made with the same basic parameters, but taking into account an increase in the flow rate of secondary stream from 5 kg/h to 12 kg/h.

The following basic geometrical dimensions of the jet device were obtained:

Table 6.8

Parameter	Desig-nation	Unit	Value
Nozzle critical section diameter	d_{cr}	mm	8,4
Nozzle outlet section diameter	d_{ex}	mm	29,8
Mixing chamber conic part inlet diameter	d_c	mm	73,4
Mixing chamber cylindrical part diameter	d_{cyl}	mm	51,9
Diffuser outlet diameter	d_d	mm	106,0

Nozzle conic part length	L_n	mm	101,6
Distance between the nozzle exit plane and the mixing chamber inlet	l_1	mm	0
Mixing chamber conic part length	L_c	mm	87,6
Mixing chamber cylindrical part length	L_{cyl}	mm	259,6
Diffuser length	L_d	mm	220,1

It is assumed that the developed jet device should be tested by CFD methods at experimental bench in the laboratory of Thermodynamics group of the University of Florence.

6.4. RESULTS

1. Literature review and comparing analysis of various working fluids for a chiller have been provided. Refrigerants and water steam have been observed. Both of them have advantages and disadvantages, connected with its thermodynamic parameters. It was decided to perform the experimental activity firstly with R1233zd and then move to water steam. An experimental bench with an ejector chiller has been designed are produced. The ejector is equipped by static pressure measurements along the diffuser.
2. The limiting counter pressures for the ejector have been found at various primary pressures, suction pressures and nozzle exit positions. It has been showed the abrupt change of the flow shape is performed at this counter pressure. An increase in the pressure of the primary stream by 10% (from 10 to 11 bar) would significantly increase the limiting back pressure of the ejector. At the same time, the cooling capacity of the cycle is reduced.
3. Several nozzle exit positions have been tested in the range of -10 - +10 mm. There is no clear dependence between nozzle position and the cycle characteristics in the studied range. The most effective position for the set conditions can be considered the position of the nozzle “5 mm down”, when the highest COP is achieved. The difference in COP of various modes does not exceed 2%.

4. Basing on the refined design method and gotten experience of tests with ejector chillers, a new jet devices are designed for chillers with water steam.
5. For further improving of steam ejector chiller characteristics, a new scheme with a multistage ejector should be designed. Such design can increase the compression ratio, which means the rise of limiting back pressure or letting a colder medium into the evaporator.

RESULTS AND CONCLUSION

1. In the results of the breakdown analysis of more than 500 steam turbine units, the distribution of turbine breakdowns and their technological subsystems is presented. It has been proved that of all the breakdowns of condensing units that led to turbine shutdown, 23% of the breakdowns were caused by the ejectors. In the examination of more than 100 serial ejectors, the characteristic defects associated with design flaws, operating conditions and ejector repairs have been identified.

2. Based on the generalization of the results of industrial tests of 34 serial multistage steam-driven ejectors in various operating conditions, it was found that the performance of ejectors does not always correspond to the blueprint characteristics. This is due both to the state of the ejectors themselves and to the specific conditions in which the working and blueprint characteristics are obtained.

3. Based on the analysis of test results (a comparison of experimental operating and design characteristics) on the geometric characteristics of 24 standard dimensions of serial multistage ejectors, a number of regularities and relationships between the geometric parameters were established. It was established that for ejectors with a low value of the main geometric parameter F^* in the first stage (25 ... 30), the “effective crosscut”, in which the velocity of the entrained flow reaches the speed of sound, is located in the middle of the mixing chamber (parameter $\mu = 1.35 ... 1,50$). In this case, the compression ratio decreases from the first stage to the last. In ejectors with a high F^* value in the first stage (60 ... 70), the “effective crosscut” is located in the cylindrical part of the mixing chamber or close to it (parameter $\mu = 1.0 ... 1.1$), and the compression ratios increase from the first stage to the last. It is shown that various turbine manufacturers adhere to different approaches in the design of ejectors. For condensation turbines, an approach with a high value of the main geometrical

parameter in the first stage ejector is chosen, while a low value of the main geometrical parameter is used for heat-generating ones.

4. According to the results of the computation modeling of the gas dynamics of a jet ejector apparatus, it was proposed to designate the transition zone from the first segment of shock waves to the second segment a “sound pipe”, where the shock waves in the working flow are extinguished by the entrained flow. The length of the “sound pipe” is associated with the axial position of the nozzle. It was proposed to refine the method of designing the ejector to take the values of the diameter of the working stream jet from the nozzle exit section to the cylindrical part of the mixing chamber; the same static pressure values for the working and entrained flows in the critical “effective crosscut” are also taken.

5. Using the selected method and the results of the research, a refined methodology for the design and calibration calculations of a multistage steam-driven ejector has been developed.

6. Based on the refined methodology for calculating and analyzing the design features and failures of serial ejectors, the new EPO-3-80 ejector for the K-200-130 LMZ turbine with the high air suction G_{air} = 120—130 kg/h in the LPP was installed in a TPP. An extended measurement scheme has been developed, which allows one to determine, among other things, the gas-dynamic resistance of intermediate coolers. The operating characteristic of the ejector is compared with the design characteristics of other ejectors. The new ejector’s high level of capacity is demonstrated.

7. As a result of the research conducted, a gas-dynamic effect of a significant change in the pressure of the steam-air mixture in the ejector’s intercoolers was detected. The pressure of the steam-air mixture at the outlet from the coolers decreases compared with the pressure at the inlet to the cooler by ΔP = 1.0 ... 4.0 kPa or increases by ΔP = 1.0 ... 8.6 kPa. A physico-mathematical model is proposed that describes the effect of pressure increase as

a pressure leap in a two-phase two-component mixture formed at the inlet of the heat exchanger. The results obtained justify the need for further refinement of the method for calculating multistage steam-driven ejectors, i.e. the influence of gas-dynamic processes in the intercooler on the pressure in the next stage.

8. The use of a new ejector allows one to obtain significant technical and economic effects when it is used both in condensation and heat-generating turbines with increased air suction into the vacuum system. The maximum economic effect of the K-200-130 turbine is more than 5 million rubles a year. The maximum calculated effect of the T-250/300-240 UTZ heat-generating turbine operating in the fully closed diaphragm mode will be up to 630,000 rubles for the heating period.

9. As a perspective direction of implementation of the refined method the ejector chillers are considered. Literature review and comparing analysis of various working fluids for a chiller have been provided. It is concluded, that steam could be a very perspective fluid, taking into account that it is cheap and environmental friendly. An experimental bench with an ejector chiller has been designed are produced. The ejector is equipped huge measurement scheme, including static pressures along the diffuser.

10. With R1134zd as a working fluid the experimental bench was tuned-up. The ejector characteristics, gotten at various primary pressures, suction pressures and nozzle exit positions, allow us to formulate the requirements for a steam ejector, which can be used for such a chiller. Basing on the refined design method, a new jet devices are designed for chillers with water steam.

11. The prospects for the further development of the dissertation research topic are as follows:

- A study of gas-dynamic processes in ejector jet devices aimed at improving the parameters of ejector functioning;

- Refining the method for designing multistage steam-driven ejectors in terms of the effect of gas-dynamic processes in intercoolers on the pressure in the subsequent stages;
- Improving the design of multistage ejectors for various types of turbine installations and operating conditions;
- For further improving of steam ejector chiller characteristics, a new scheme with a multistage ejector should be designed.

REFERENCES

1. Shcheglyaev, A.V. Steam turbines: Textbook for higher education institutions. In 2 parts, 6th ed. Processed and complemented by Prof. B.M. Troyanovsky. M.: Energoatomizdat. 1993. 384 pages.
2. Kirillov, I.I., Kirillov A.I. Theory of turbomachines. Examples and task. Leningrad: Mechanical engineering. 1974. 320 pages.
3. Trukhny, A.D. Stationary steam turbines. M: Enernoatomizdat. 1989. 636 pages.
4. Kostiuk, A.G. Steam and gas turbines for power plants [An electronic resource]: textbook for higher education institutions / A.G. Kostiuk, V.V. Frolov, A.E. Bulkin, A.D. Trukhny; under the editorship of A.G. Kostiuk. M.: MEI publishing house. 2016.
5. Troyanovsky, B.M. Steam and gas turbines of nuclear power plants / Manual for institutions of higher education, M: Energoatomizdat. 1985. 256 pages.
6. Kirsanov, I.N. Stationary steam turbines: [Studies. a grant for techn. schools]. - Moscow; Leningrad: Gosenergoizdat. 1956. 200 pages.
7. Kapelovich, B.E. Operation of steam-turbine installations. 2nd ed. M.: Energoatomizdat. 1985. 304 pages.
8. Turbine installations/VA. Rassokhin, L.A. Homenok, V.B. Mikhaylov, etc. Under Yu.S. Vasilyev's editorship. — M.: Mechanical engineering. 2015. 1030 pages.
9. Heat exchangers of technological subsystems: Turbine plants / Aronson K.E., Brezgin V.I., Fords Yu.M., Homenok L.A., etc. / Encyclopedia / Moscow, 2016 – 472 pages.
10. Efimochkin, G.I. Comparison and the choice of the air-deleting devices for condensers of modern steam turbines / G.I. Efimochkin // Power plants. 1976. No. 100. Pages 29—33.

11. Ranga, N. Evacuation Systems for Steam Surface Condensers: Vacuum Pumps or Steam Jet Air Ejectors // Proceedings of the ASME 2016 Power Conference “POWER 2016”. June 26—30, 2016, Charlotte, North Carolina. P. 9.
12. Standards for Steam Surface Condensers. 10th edition. Cleveland, Ohio: Heat Exchange Institute. 2011. P. 101.
13. Standards for Steam Jet Vacuum Systems. 7th edition. Cleveland, Ohio: Heat Exchange Institute. 2012. P. 142.
14. Shempelev, A.G. Development, research and realization of methods of increasing the efficiency of the equipment of technological subsystems of heating steam-turbine installations: thesis for a scientific degree competition doct. of techn. sciences / Yekaterinburg: UGTU-UPI, 2011.
15. Blyudov, V. P. Condensation devices of Blyudov steam turbines / // M.-L.: Gosenergoizdat. 1951. 207 pages.
16. Berman, L.D. Air pumps of condensation installations in steam turbines/L. D. Berman L.D., N.M. Zinger. M.; L.: Gosenergoizdat. 1962. 96 pages.
17. Milman, O.O., Fedorov, VA. Air and condensation installations / ISBN 5-7046-0810-8 / M.: MEI publishing house. 2002. 208 pages.
18. Sokolov, E.Ya. Jet devices / E.Ya. Sokolov, N.M. Zinger//M.: Energoatomizdat. 1989. 352 pages.
19. Robozhev A.V. Method of calculation of multistage steam-ejecting ejectors / A.V. Robozhev//MEI, Manual for Higher Education Institutions. M. 1965 P. 76.
20. Abramovich G.N. Applied gas dynamics / G.N. Abramovich//M.: Science. 1991. 600 pages.
21. Deich M.E. Technical gas dynamics//M.: Energy. 1974. 345 pages.
22. Shklover, G. G. Research and calculation of condensing units of steam turbines / Shklover, O.O. Milman. M.: Energoatomizdat. 1985. 240 pages.
23. Efimochkin, G.I. A method of calculation of an air-and-water ejector with extended mixing / Efimochkin G.I., Korenov B.E. / Heat-and-power engineering, 1976. No. 1. Pages 84-85.

24. Leshchinsky, A.M. Gas ejector (its options) / A.M.Leshchinsky/Ampere-second. No. 459616. Appl. 04.07.1983, publ. 15.04.1985, bulletin No. 14. 2 pages.
25. Putilov, M.I. Calculation of optimum distance from a nozzle to the mixing chamber in jet devices / M.I. Putilov//Heat-and-power engineering. 1967. No. 7. Pages 70-74.
26. Putilov, M.I. On the question of nozzle distance from the mixing chamber in jet devices / M.I. Putilov//Heat-and-power engineering. 1967. No. 12. Pages 64-66.
27. Millionshchikov, M.D. High-speed gas ejectors / Millionshchikov M.D., Ryabinkov G. of M/Saturday. Research on the TsAGI supersonic gas ejectors / BNI. M. 1961. Pages 5-32.
28. Tseitlin, A.B. Steam-ejecting vacuum pumps//A.B.Tseitlin//M.-L.: Energy. 1965. 400 pages.
29. Rayzman, I.A. Liquid ring vacuum pumps and compressors / I.A. Rayzman//KGTU: Kazan. 1995. 258 pages.
30. Belevich, A.I. Development and deployment of methods for designing steam-ejecting installations of condensers of steam turbines / Belevich A.I.//Thesis for the degree of Candidate of Technical Sciences, M.: VTI of F.E. Dzerzhinsky, 1986. 188 pages.
31. Methodical instructions by calculation and design of steam-ejecting ejectors of condensing units of turbines of thermal power plant and the NPP / A.I. Belevich//RD 34.30.105. M.: Ministry of Energy USSR. 1985. 53 pages.
32. Belevich, A.I. Constructions and characteristics of steam-ejecting ejectors of turbines of thermal power plant and NPP / Belevich A.I.//Collection of works VTI. M.: Energoatomizdat. 1985. Pages 42-48.
33. Tsegelsky, V.G. Jet devices. M.: MSTU publishing house of N.E. Bauman. 2017.
34. Alexandrov, V.Yu. Optimum ejectors (theory and calculation). M.: Mechanical engineering. 2012. 136 pages.

35. Alexandrov, V. Yu., Klimovsk, K. K. Comparison of the efficiency of gas ejectors with isobaric and cylindrical mixing chambers / Alexandrov V. Yu., Klimovsk K. K.//Conversion in mechanical engineering No. 2. 2008. Pages 70-74.
36. Experimental and theoretical research on the operation modes of supersonic gas ejectors with cylindrical and conic Mixing / Tsegelsky cameras B. G., Akimov M.V., Safargaliyev T. D.//News of higher educational institutions. Mechanical engineering. 2012. No. 3. Pages 48-58.
37. A pilot study of the influence of length of the conic mixing chamber and the mouth of the diffuser on the characteristics of the supersonic gas ejector / Tsegelsky V.G., Akimov M.V., Safargaliyev T. D.//News of higher educational institutions. Mechanical engineering. 2013. No. 4. Pages 30-44.
38. Keenan, J.H., Neuman, E.P., Lustwerk, F. An investigation of ejector design, analysis and experiment, J. Appl. Mech. 1950. Pages 299-309.
39. Performance prediction of steam ejector using computational fluid dynamics: Part 1. Validation of the CFD results / T. Sriveerakul, S. Aphornratana, K. Chunnanond // International Journal of Thermal Sciences. No. 46. 2007. Pages 812–822
40. Computational fluid dynamics simulation of the supersonic steam ejector. Part 1: Comparative study of different equations of state; Part 2: Optimal design of geometry and the effect of operating conditions on the ejector / H T Zheng, L Cai, Y J Li and Z M Li // Proceedings of the Institution of Mechanical Engineers, Part C: Journal of Mechanical Engineering Science 2012 226: 709 originally published online 5 September 2011 DOI: 10.1177/0954406211415777
41. Performance prediction of a steam ejector using computational fluid dynamics: Part 2. Flow structure of a steam ejector influenced by operating pressures and geometries / T. Sriveerakul, S. Aphornratana, K. Chunnanond // International Journal of Thermal Sciences. No. 46. 2007. Pages 823–833.

42. Modelling and simulation of steam jet ejectors / Narmine H. Alya, Aly Karameldin, M.M. Shamloul // Desalination. No. 123. 1999. Pages 1-8.
43. Investigation and improvement of ejector refrigeration system using computational fluid dynamics technique / K. Pianthong, W. Seehanam, M. Behnia, T. Sriveerakul, S. Aphornratana // Energy Conversion and Management. No. 48. 2007. Pages 2556–2564.
44. Experimental studies of a steam jet refrigeration cycle: Effect of the primary nozzle geometries to system performance / Natthawut Ruangtrakoon, Satha Aphornratana, Thanarath Sriveerakul // Experimental Thermal and Fluid Science. No. 35. 2011. Pages 676–683.
45. Numerical investigation on the mixing process in a steam ejector with different nozzle structures / X. Yang, X. Long, X. Yao // International Journal of Thermal Sciences. No. 56. 2012. Pages 95-106.
46. Experimental and numerical analysis of a variable area ratio steam ejector / Szabolcs Varga, Armando C. Oliveira, Xiaoli Ma, Siddig A. Omer, Wei Zhang, Saffa B. Riffat // International Journal of Refrigeration. 2011. 168e1675.
47. Numerical optimization on the geometrical factors of natural gas ejectors / WeiXiong Chen, DaoTong Chong, JunJie Yan , JiPing Liu // International Journal of Thermal Sciences 50 (2011) 1554-1561
48. Computational fluid dynamic analysis and design optimization of jet pumps / J. Fan, J. Eves, H.M. Thompson, V.V. Toropov, N. Kapur, D. Copley, A. Mincher // Computers & Fluids. No. 46. 2011. Pages 212–217.
49. Configuration dependence and optimization of the entrainment performance for gasegas and gaseliquid ejectors / Cui Li, Yanzhong Li, Lei Wang // Applied Thermal Engineering. No. 48. 2012. Pages 237-248.
50. CFD simulation on the effect of primary nozzle geometries for a steam ejector in refrigeration cycle / Natthawut Ruangtrakoon, Tongchana Thongtip, Satha Aphornratana, Thanarath Sriveerakul // International Journal of Thermal

Sciences. No. 63. 2013. Pages 133-145.

51. Numerical assessment of steam nucleation on thermodynamic performance of steam ejectors / Navid Sharifi, Masoud Boroomand, Majid Sharifi // Applied Thermal Engineering. No. 52. 2013. Pages 449-459.
52. Numerical investigation of geometry parameters for design of high performance ejectors / Yinhai Zhu, Wenjian Cai, Changyun Wen, Yanzhong Li // Applied Thermal Engineering. No. 29. 2009. Pages 898–905.
53. Bartosiewicz, Y., Aidoun, Z., Desevaux, P., Mercadier, Y. Numerical and experimental investigations on supersonic ejectors. Int. J. Heat Fluid Flow. No. 26. 2005. Pages 56-70.
54. Gagan, J., Smierciew, K., Butrymowicz, D., Karwacki, J. Comparative study of turbulence models in application to gas ejectors. International Journal of Thermal Sciences. №78. 2014. Pages 9-15.
55. Sharifi, N., Sharifi, M. Reducing energy consumption of a steam ejector through experimental optimization of the nozzle geometry. Energy. №66. 2014. Pages 860-867.
56. Varga, S., Oliveira, A.C., Diaconu, B. Numerical assessment of steam ejector efficiencies using CFD. International journal of refrigeration. №32. 2009. Pages 1203–1211.
57. Pianthong, K., Seehanam, W., Behnia, M., Sriveerakul, T., Aphornratana, S. Investigation and improvement of ejector refrigeration system using computational fluid dynamics technique. Energy Conversion and Management. №48. 2007. Pages 2556–2564.
58. Yinhai Z., Wenjian C., Changyun W. Simplified ejector model for control and optimization. Energy Conversion and Management. №49. 2008. Pages 1424-1432.
59. Shock train and pseudoshock phenomena in internal gas flows. Matsuo, K., Miyazato, Y., Kim, H.-D., Progr. Aerospaces. №35. 1999. Pages 33–100.
60. Ejector Modeling and Examining of Possibility of Replacing Liquid Vacuum

Pump in Vacuum Production Systems / Sohrabali Ghorbanian and Shahryar Jafari Nejad // International Journal of Chemical Engineering and Applications. Vol. 2, No. 2. April 2011.

61. Estimation of an ejector's main cross sections in a steam-ejector refrigeration system / G.K. Alexis // Applied Thermal Engineering. No 24. 2004. Pages 2657–2663.
62. Numerical study on the performances of steam-jet vacuum pump at different operating conditions / Xiao-Dong Wang*, Jing-Liang Dong // Vacuum. 84. 2010. Pages 1341-1346.
63. Vertical ground coupled steam ejector heat pump; thermal-economic modeling and optimization / Sepehr Sanaye, Behzad Niroomand // International Journal of Refrigeration. No. 34. 2011. Pages 1562 -1576.
64. CO 153-34.20.501-2003. Rules of technical operation of power plants and networks of the Russian Federation. M.: Energoservice, 2004.
65. Ejectors of condensation installations of steam turbines: Manual / Aronson K.E., Ryabchikov A.Yu., Brezgin D.V., Murmansky I.B. – Yekaterinburg: Publishing house of Ural Federal University, 2015 – 131 pages.
66. Gas and steam turbine installations: ejectors of condensation installations: Manual for higher education institutions / Aronson K.E., Ryabchikov A.Yu., Brezgin D.V., Murmansky I.B. M.: Yurayt publishing house, 2017 – 129 pages.
67. Reliability of the equipment of steam-turbine installations: manuals / Fords Yu.M., Aronson K.E., Murmansky B.E., Murmansky I.B., Nirenstein M.A., V.B., Plotnikov P.N., //Yekaterinburg: Publishing house of Ural Federal University, 2017 – 144 pages.
68. Shklover, G. G. Calculation of the steam-ejecting ejector taking into account vapor condensation in the intermediate cooler / Shklover G. G.// Power machine construction. No. 12. 1968. Pages 19 - 21.
69. Berman, L.D. Calculation of superficial heat exchangers for vapor condensation from steam-air mix/L. D. Berman, S.N. Fuchs//Power system. No. 7. 1959.

Pages 74-84.

70. Berman, L.D. Heat exchange at vapor condensation from steam-gas mix/L. D. Berman, S.N. Fuchs//Power system. No. 8. 1958.
71. Leshchinsky, A.M. Increase in efficiency and maneuverability of the condenser and ejector of a thermal power plant / Avtoref installations. to a yew. on the article PhD in Technological Sciences in the form of the scientific report / Moscow, 1989.
72. Stalemate. SU 382909. USSR. Vertical shell-and-tube heat exchanger / V.I. Velikovich, A.M. Leshchinsky and A.G. Sheynkman (SSSR) Appl. 28.03.1973.//BI. No. 23. 1973. 2 pages.
73. Stalemate. SU 283482. USSR. The steam-ejecting ejector with the counterflow refrigerator / V.I. Velikovich, A.M. Leshchinsky and A.G. Sheynkman (SSSR) Appl. 06.10. 70.//BI. No. 31. 1970. 2 pages.
74. Patent for invention No. 183318. Gas-jet ejector / Kogan P.A.// Published 17.06.1966.
75. Patent for invention No. 661150. Gas-jet ejector / Shkret L.Ya., Birch A.I., Lobkov A.N., Gogelgants F.A., Rubtsov I.N.//Published 05.05.1979.
76. Patent for invention No. 987205. Gas-jet ejector / Polushkin B. M., Andryukov N.A., Nazarov V.G., Tsyrlin E.G., V.O. Rubies// Published 17.01.1983.
77. Patent for invention No. 1263916. Ejector / Tymoshenko G.M., Yatsenko A.F., Selivra S.A., Gorbatenko A.V.//Published 15.10.1986.
78. Patent for invention No. 1242651. Ejector / Filimonov V.V.// Published 12.12.1984.
79. Patent for invention No. 1413300. Multistage steam-ejecting ejector / Leshchinsky A.M.// Published 28.04.1986.
80. Patent for invention No. 787736. Ejector / Shakiro G.F.//Published 15.12.1980.
81. Patent for invention No. 937791. Jet device / Gurov E.I., Desyatov A.T., Morkovkin I.M., Narkunskaya Z.N., Redelhi VA.//Published 23.06.1982.
82. Patent for invention No. 953281. Jet device / Gurov E.I., Desyatov A.T.,

Morkovkin I.M., Narkunskaya Z.N., Redelhi VA.//Published 23.08.1982.

83. Patent for invention No. 1038619. Jet device / White hares of Accusative, Grigorenko N.M., Desyatov A.T., Kovalenko V. D., Martynov V.V., Morkovkin I.M., Narkunskaya Z.N., Handros L.G.// Published 04.08.1980.
84. Patent for invention No. 1670188. Jet vacuum pump / Karpov L. S., Ozin M.V., Ozin V.M., Maximov A.E., Biryukova O.V.//Published 28.11.1988.
85. Patent for invention No. 1249206. Ejector / Pryamitsyn E.I., Karaganov L.T., Krishtal V.N., Simkhovich S.L., Baburov V. P., Lithuanian O. P.// Published 27.08.1984.
86. Ramm, V.M. Steam-ejecting vacuum and ejector installations / V.M. Ramm//M.: Goskhimizdat, 1949. 85 pages.
87. Uspensky, V. A. Jet vacuum pumps/VA. Uspensky, Yu.M. Kuznetsov//M.: Mechanical engineering, 1973. 144 pages.
88. Barinberg, G.D. Steam turbines and turbine plants of the Ural turbine plant / G.D. Barinberg, Brodov Yu.M., Goldberg A.A., Ioffe L. S., Kortenko V.V., Sakhnin Yu.A. Ekaterinburg: Aprio, 2007. 460 pages.
89. The K-300-240 HTGZ steam turbine//Under the editorship of Yu.F. Kosyak//M.: Energoizdat, 1982. 272 pages.
90. The K-500-240 HTGZ steam turbine//under the editorship of V.I. Savvin//M.: Energoatomizdat, 1984. 264 pages.
91. Kiryukhin, V.I. Steam turbines of low power of KTZ / V.I. Kiryukhin [etc.]. M.: Energoatomizdat, 1987. 216 pages.
92. Shklover, G. G. Dimensionless characteristics of steam-ejecting KTZ / Shklover G.G, Rosinsky A.Z., Gerasimov A.V.//Heat-and-power engineering. No. 9. 1966. Pages 42-48.
93. A one-dimensional theory of a supersonic gas ejector with an isobaric mixing chamber / Vasilyev Yu.N.//Scientific notes of TsAGI. T. XIV. No. 1. 1983. Pages 26-38.
94. An optimum gas ejector with an isobaric mixing chamber / Vasilyev

Yu.N.//Scientific notes of TsAGI. T. XIV. No. 2. 1983. Pages 77-85.

95. Comparison of extreme theoretical characteristics of supersonic gas ejectors with isobaric and cylindrical mixing chambers / Vasilyev Yu.N.//Scientific notes of TsAGI. T. XIV. No. 5. 1983. Pages 47-57.

96. Eames, I.W. A new prescription for the design of supersonic jet-pumps: the constant rate of momentum change method. Appl. Therm. Eng. No. 22. 2002. Pages 121-131.

97. Mazzelli, F., Milazzo, A. Performance analysis of a supersonic ejector cycle working with R245fa. International Journal of Refrigeration. Volume 49. 2015. Pages 79-92.

98. Milazzo, A., Rocchetti, A., Eames, I.W. Theoretical and experimental activity on ejector refrigeration. Energy Procedia. No. 45. 2014. Pages 1245-1254.

99. Comparison of traditional and CRMC ejector performance used in a steam ejector refrigeration / Borirak Kitrattanaa , Satha Aphornratanaa, Tongchana Thongtipb, Natthawut Ruangtrakoonc / 2017 AEDCEE, 25-26 May 2017, Bangkok, Thailand.

100. Shklover, G. G. Influence of properties and parameters of the entrained gas on the operation of a steam-ejecting ejector / Shklover G. G., Milman O.O., Gerasimov A.V., Capital A.G.//Power system. 1975. No. 12. Pages 55-59.

101. Kaula, R.J.. Condensation installations. Principles and details of the device of modern steam condensation installations / R.J. Kaula, I.V. Robinson//State technical publishing house. 1930.

102. Wiegand, J. Anwendung und Konstruktion von Dampf- und Gasstrahlapparaten / J Wiegand // Vortrag auf dem 93. Dachema - Kolloquium am 16.02.1962 in Frankfurt am Main. Chemie-Ingenieur-Technik. Vol. 34, No. 6. 1962. Pages 448-449.

103. ESDU Ejectors and Jet Pumps Data Item 86030, 1986. ESDU International Ltd, London, UK.
104. Standards for Steam Jet Vacuum Systems. 7th edition. Cleveland, Ohio: Heat Exchange Institute. 2012. P. 142.
105. RD 34.30.302-87. Methodical instructions on tests and operation of steam-ejecting ejectors of condensation installations of turbines of thermal power plant and the NPP: M.: RAO UES of Russia. 1987. 34 pages.
106. Calculation of the steam-ejecting EP-3-25/75 ejector. B-800209 fig. CDB HTZ. 1960. 13 pages.
107. Addy, A.L., Dutton, J.C., Mikkelsen, C.D. Supersonic Ejector-diffuser Theory and Experiments. Report No. UILU-ENG-82-4001. Department of Mechanical and Industrial Engineering, University of Illinois, Orbana-Champaign, Urbana, Illinois, USA. 1981.
108. Brodov, Yu.M. Condensation installations of steam turbines: studies. a grant for higher education institutions / Yu.M. Brodov, R.Z. Savelyev. M.: Energoatomizdat. 1994. 288 pages.
109. Shklover, G. G. A thermolysis of moving steam in screw heat exchangers / Shklover G. G.//Power system. No. 5. 1963.
110. Shklover, G. G. Vacuum vapor condensation in screw KTZ / Shklover G.G., Rodivilin M.D., Titivkin A.V.//Power plant engineering. No. 8. 1963.
111. Kogan, P.A. Definition of the optimum geometrical characteristics of gas-jet devices / Kogan P.A., Namis I.A., Yakushin A.N.//Power system. No. 9. 1967. Pages 69-72.
112. Development and approbation of elements of a system of monitoring the state and diagnostics of the condenser of the steam turbine / Aronson K.E., Brodov Yu.M., Shempelev A. / Power system. No. 7. 2003. Pages 67-69.
113. Berman, L.D. Creation of operational characteristics of steam-ejecting ejectors according to tests on dry air / Power plants. No. 6. 1954.
114. Barbasova, T.A. Creation of design characteristics of a steam-ejecting ejector

for the optimization of work of the condensation-combined heat and power plant / Barbasova T.A., Vakhromeev I.E., Divnich P.N., Schneider D.A.//Messenger of IuUrGU. No. 23. 2007. Pages 63-64.

115. Yelizarov, V.S. Modernization of the EP-3-700-1 ejector of an LMP / Yelizarov V.S., Nikolaev G. V. / Power plant engineering. No. 4. 1976. Pages 41-42.

116. Reconstruction of EP-3-600 ejectors / E.I. Antonov, D.P. Kuznetsov, T.P. Lavrukhina, I.Z. Tsyrkin/Energetik. No. 5. 1962.

117. Nesterov, A.M./ Energetik. No. 7. 1964.

118. Berman, L.D. Guidelines on thermal calculation of superficial condensers of powerful steam turbines of thermal and nuclear power plants / Berman L.D., Zernova E.P.//M.: Soyuztekhenergo.1982. P. 106.

119. Grazzini, G. Entropy parameters for heat exchanger design / G. Grazzini and F. Gori // Int. J. Heat Mass Transfer. Vol. 31, No. 12. 1988. Pages 2547-2554.

120. Efros, E.I., Shempelev, A.G. Development and research of some ways to increase the efficiency of condensation devices of heating turbines at low-steam operating modes//Improvement of the heating technical equipment of thermal power plants and the introduction of systems of service, diagnosis and repair. Materials of the II All-Russian scientific and practical conference. Yekaterinburg, 1998. Pages 166-167.

121. The Standard 8.586.2-2005 (ISO 5167-2:2003) Measurement of an Expense and Amount of Liquids and gases by means of the standard narrowing devices. Moscow: Standartinform, 2006. 43 pages.

122. Reviews of damage of the heating mechanical equipment of power plants with cross communications and thermal networks for 1986-2000. M.: SPO ORGRES. 89 pages.

123. Analysis of the operation of 150-1200 MW power blocks for 1986-2000. M.: SPO ORGRES. 67 pages.

124. Zaydel, A.N. Errors of measurements of physical quantities / A.N. Zaydel. L.:

Science, 1985. 112 pages.

125. Turbulent mixture of gas streams / G.N. Abramovich, S.Yu. Krasheninnikov, A.N. Sekundov, etc.; under the editorship of G.N. Abramovich. Moscow: Science. 1974. 272 pages.

126. Certificate on the state registration of the computer program No. 2016611885 Russian Federation. A program complex for the “Design and Testing Calculation of Steam-Ejecting Ejectors” / Aronson, K.E., Murmansky I.B., Brezgin D.V., Chubarov A.A., Brodov Yu.M.// Applicant and patent holder: Ural Federal University named after the first President of Russia B. N. Yeltsin. – Application No. 20156185492. Date of registration in the Register of the computer programs: 12.02.2015.

127. Repair of steam turbines / Manual / V.N. Rodin, A.G. Sharapov, B.E. Murmansky, Yu.A. Sakhnin, V.V. Lebedev, M.A: Kadnikov, L.A. Zhuchenko; under the general editorship of Yu.M. Brodov of V.N. Rodin//Yekaterinburg: UGTU UPI. 2002. 203 pages.

128. Patent for useful model No. 170935 Russian Federation, MPK F04F5/00. Steam-ejecting three-stage ejector /, Merchants V. K., Ryabchikov A.Yu., Aronson K.E., Murmansky I.B., Zhelonkin N.V., Brezgin D.V.//Applicant and patent holder: Ural Federal University named after the first President of Russia B. N. Yeltsin. – No. 2016119824. Appl. 23.05.2016; publ. 15.05.2017. Bulletin 14. 9 pages.

129. Patent for invention No. 2645635 Russian Federation, MPK F04F5/30. Steam-ejecting three-stage ejector / Merchants V. K., Ryabchikov A.Yu., Aronson K.E., Murmansky I.B., Zhelonkin N.V., Brezgin D.V.,.// Applicant and patent holder: Ural Federal University named after the first President of Russia B. N. Yeltsin. – No. 2016126736. Appl. 04.07.2016; publ. 26.02.2018. Bulletin 6. 4 pages.

130. Idelchik, I.E. Reference book on hydraulic resistance / Under the editorship of M.O. Steinberg//3rd ed., reworked and additional materials. M.: Mechanical

engineering. 1992. 672 pages.

131. Report on tests of the OE-A, B main ejectors of 22.02.2006. PTO of Surgut-1 Power Station. 23 pages.

132. Report on carrying out tests of the ejector installation of the condenser of the turbine of the power unit of Branch of JSC OGK-2-Surgut-1 Power Station. 2014. 31 pages.

133. Aronson, K.E. Efficiency of functioning of intermediate coolers of multistage steam-ejecting ejectors of steam turbines / K.E. Aronson, A.Yu. Ryabchikov, Yu.M. Brodov, N.V. Zhelonkin, I.B. Murmansky//Power system. No. 3. 2017. Pages 15-21.

134. Deich, M.E. Hydraulic gas dynamics: Manual for higher education institutions / M.E. Deich, A.E. Zaryankin//M.: Energoatomizdat. 1981. 384 pages.

135. Samoylovich, G.S. Hydraulic gas dynamics: Textbook for students of higher education institutions / G.S. Samoylovich//M.: Power plant engineering. 1990. 384 pages.

136. Deich, M.E. The gas dynamics of two-phase environments / M.E. Deich, G.A. Filippov//M.: Energy. 1968. 423 pages.

137. Vulis, L.A. Thermodynamics of gas streams/L. A. Vulis//M.: Energy. 1960. 303 pages.

138. Kutateladze, S.S. Bases of the theory of heat exchange / S.S. Kutateladze//M.: The higher school. 1979. 446 pages.

139. Isachenko, V. P. Heat exchange at condensation / V. P. Isachenko//M.: Energy. 1977. 240 pages.

140. Miropolsky, Z.L. Thermolysis at condensation of superheated and saturated steam in pipes / Z.L. Miropolsky, R.I. Shneerova//Heat exchange. Soviet research. 1974. Pages 298-304.

141. Milman, O.O. Features of vapor condensation in pipes and channels / O.O. Milman, V.A. Fedorov, A.V. Kondratyev, A.V. Ptakhin//Power system. No. 4.

2015. Pages 71-80.

142. Leading Technical Materials 108.2.1.23-84. Calculation and design of superficial heaters of high and low pressure/L.: NPO Tskti. 1987. 216 pages.

143. Zhikharev, A. S. Influence of speed on the efficiency of the separation of drops at partial vapor condensation in a pipe bunch/Ampere-second. Zhikharev, Yu.S. Mantrova//News of MSTU of MAMI. Vol. 3, No. 3(21). 2014. Pages 49-153.

144. Simulations of cavitating flows in turbopumps (Conference Paper) / Ahuja, V., Hosangadi, A., Ungewitter, R.J. / 41st Aerospace Sciences Meeting and Exhibit. 2003. Reno, NV; United States.

145. Standard power characteristics of a net turbine unit of a K-200-130 LMP//Editor: N.A. Natanson//Edition of the specialized center of scientific and technical information of ORGRES//Moscow. 1972. 31 pages.

146. Usachyov, I. P. Assessment of ventilating losses in steps of low pressure of cylinders of steam turbines / Usachyov I. P., Neuymin V.M.// Creation of steam and gas turbines. Experience of the Turbomotor plant Energomash. No. 6. 1979. Pages 13-15.

147. GrazzinI, G., Milazzo, A., Paganini, D., 2012. Design of an ejector cycle refrigeration system. Energy Convers. Manag. 54, 38—46.

148. Power, R.B., Steam Jet Ejectors for the Process Industries, Author-Publisher, 1994, www.jetwords.com

149. Fang, Y., Croquer, S., Poncet, S., Aidoun, Z., Bartosiewicz, Y., “Drop-in replacement in a R134 ejector refrigeration cycle by HFO refrigerants”, International Journal of Refrigeration, 2017, doi.org/10.1016/j.ijrefrig.2017.02.028

150. Eames, I.W., Ablwaifa, A.E., Petrenko V., “Results of an experimental study of an advanced jet-pump refrigerator operating with

R245fa", Applied Thermal Engineering, 2007, doi.org/10.1016/j.applthermaleng.2006.12.009

151. Kittratana, B., Aphornratana, S., Thongtip, T., Ruangtrakoon N., "Comparison of traditional and CRMC ejector performance used in a steam ejector refrigeration", Energy Procedia, 2017, doi.org./10.1016/j.egypro.2017.10.229

152.

APPENDIX

Appendix 1

Утверждаю
Заместитель директора - главный инженер
филиала ПАО «ОГК-2» Сургутской ГРЭС-1
_____А.А. Тетюков
«28» 02 2017 г.

Справка

о внедрении результатов научно-исследовательской работы
Мурманского И.Б.

На энергоблоке ст.№ 5 с турбиной К-200-130 Сургутской ГРЭС-1 осенью 2016 г. установлен новый высокоэффективный с увеличенной производительностью эжектор ЭПО-3-80 вместо основного серийного эжектора ЭП-3-700. Основные работы по расчету и проектированию эжектора проведены Мурманским Ильей Борисовичем. Он являлся также исполнителем шеф-монтажных работ, ответственным за проведение испытаний эжектора.

Проведенные испытания эжектора показали, что эжектор обеспечивает отсос из вакуумной системы турбоустановки воздуха до 130 кг/ч и поддерживает нормативные значения давления в конденсаторе.

В настоящее время эжектор успешно функционирует в составе паротурбинной установки, поддерживая уровень вакуума в конденсаторе на нормативных значениях. Небольшой опыт эксплуатации нового эжектора показывает, что его характеристики во всех диапазонах работы эжектора лучше, чем фактические характеристики работающих на филиале эжекторах. Сургутская ГРЭС-1 планирует установку эжекторов данного типа и на других энергоблоках станции.

Начальник ЦНиИ Д.Г. Голиков

Translation

Reference

on the implementing of the researches of I. Murmanskii

At the power unit №5 with a K-200-130 turbine at Surgutskaya GRES-1 in the autamn, 2016, a new high-performance ejector EPO-3-80 with an increased capacity was installed instead of the serial general ejector EP-3-700. The main work on the calculation and design of the ejector was carried out by Murmanskii Ilia Borisovich. He was also the contractor of the installation work, responsible for testing the ejector.

The tests of the ejector showed that it provides the suction of a large amount of air (up to 130 kg / h) from the vacuum system of the turbine unit and at the same time maintains a low pressure in the condenser, which corresponds to the regulatory documents for this type of turbine. Given that when the turbine was operated on a serial ejector, the excess of the actual steam pressure in the condenser relative to the standard values was up to 3%, the annual fuel economy from the use of the new ejector EPO-3-80 reaches 3-5 thousand tons of equivalent fuel.

At present, the ejector successfully operates as part of a steam turbine installation, maintaining the vacuum level in the condenser in standard values with exceptionally high air suction. The operating experience of the new ejector shows that its characteristics are much better than the characteristics of a serial ejector. Surgut GRES-1 plans to install a new ejector on other turbines of the station.

Head of workshop of adjustments and testings
Production and technical Department D. Golikov

НестандартМаш

ЗАО «Нестандартизированное оборудование и оснастка»
г.Екатеринбург, ул.Шефская 3г. Тел\факс: 8(343) 389-08-39(49)
ИНН: 6660019626 КПП: 667001001 ОГРН 1026604964737
р\с: 40702810562240000691 к\с: 30101810000000000795
в ПАО КБ «УБРиР» г. Екатеринбург БИК: 046577795
сайт: n-mash96.ru e-mail: n-mash@mail.ru

Справка

об использовании результатов диссертационной работы Мурманского И.Б.

Предприятие ЗАО «Нестандартмаш» выпускает широкую номенклатуру теплообменного оборудования для паротурбинных установок: подогреватели низкого давления и сетевой воды, маслоохладители и эжекторы. Эжекторы выпускаются с новыми конструкциями струйных аппаратов и промежуточных охладителей по проектам, разработанным лабораторией теплообменных аппаратов кафедры «Турбины и двигатели» Уральского федерального университета имени первого Президента России Б.Н. Ельцина. В 2016 году Нами изготовлен эжектор ЭПО-3-80 для Сургутской ГРЭС-1, в котором реализованы технические решения, представленные в диссертационной работе Мурманского И.Б. «Совершенствование многоступенчатых пароструйных эжекторов конденсационных установок паровых турбин». Данные технические решения использованы в конструкциях струйных аппаратов, промежуточных охладителей и отдельных узлов многоступенчатого эжектора.

Мурманским И.Б. осуществлено как проектирование данного эжектора, так и авторский надзор за его изготовлением на заводе.

Использование результатов диссертационной работы Мурманского И.Б. при производстве эжекторов позволило повысить их качество, расширить номенклатуру выпускаемых аппаратов и исключить рекламации от заказчиков.

Генеральный директор
ЗАО «Нестандартмаш» Е.В. Ткаченко

Translation

Reference

on the use of the results of dissertation of I. Murmanskii

The company CJSC Nestandartmash produces a wide range of heat exchange equipment for steam turbine plants: low pressure heaters and boilers, oil coolers and ejectors. Ejectors are produced with new designs of jet apparatuses and intercoolers according to the designs developed by the laboratory of heat exchangers of the department “Turbines and Engines” of the Ural Federal University named after the first President of Russia B.N. Yeltsin. In 2016, we manufactured an ejector EPO-3-80 for the Surgut state district power station-1, in which the technical solutions presented in the dissertation work of I. Murmanskii were implemented. “Improvement of multi-stage steam-jet ejectors of steam turbine condensing units”. These technical solutions are used in the design of jet apparatus’, intercoolers and individual components of a multi-stage ejector.

I. Murmanskii carried out design of this ejector as well as provided supervision of its manufacture at the plant.

Using the results of the dissertation of I. Murmanskii in the production of ejectors, it was possible to improve their quality, expand the range of manufactured devices and eliminate complaints from customers.

CEO of CJSC Nestandartmash E.V. Tkachenko

ООО«Энерготех-Эжектор»

Юр.адрес: 620026, г.Екатеринбург, ул. Белинского, д. 86офис.607
Почт. адрес: 620026, г.Екатеринбург, ул. Белинского, дом 86, офис 608 ОГРН 1146670013214
ИНН 6670424895 КПП 668501001; р/сч. 40702810816540009820 в ОАО «Сбербанк России»
к/сч. 30101810500000000674 ,БИК 046577674; ОКПО 13711837; ОКАТО 65401373000; ОКВЭД 29.23.1, 29.12.3 ……; Тел.(343)278-60-90. e-mail: etekh-ek@mail.ruhttp://www.energotekh-ek.ru

Справка
об использовании результатов диссертационной работы Мурманского И.Б.

Предприятие ООО «Энерготех-Эжектор» занимается проектированием, разработкой и производством пароструйных эжекторов для нужд энергетических предприятий. Разработаны новые конструкции эжекторов ТЭС, отвечающие современным требованиям к надёжности и эффективности энергетического оборудования. Новые конструкции разработаны совместно с лабораторией теплообменных аппаратов кафедры «Турбины и двигатели» УрФУ. В 2016-2018гг. рассчитаны, спроектированы, изготовлены и поставлены на ТЭС эжектор ЭПО-3-80 и три новых эжектора ЭПО-3-120. Расчёт сопел и диффузоров, разработка и проектирование эжекторов проведено на основе результатов, полученных в диссертационной работе Мурманского И.Б. «Совершенствование многоступенчатых пароструйных эжекторов конденсационных установок паровых турбин». Спроектированные конструкции новых эжекторов имеют высокие показатели эффективности и надежности.

Разработка новой конструкций ЭПО-3-80 и ЭПО-3-120 выполнена при непосредственном участии Мурманского И.Б.

Использование результатов диссертационной работы Мурманского И.Б. при проектировании и производстве эжекторов позволяет существенно повысить эффективность разрабатываемого оборудования.

С уважением,
Управляющий ИП

Сальников Евгений Геннадьевич

Translation

Reference

on the use of the results of dissertation of I. Murmanskii

The LLC “Energotech-Ejector” enterprise is engaged in the design, development and production of steam jet ejectors for the needs of energy enterprises. For a number of ejectors, new designs have been developed that meet modern requirements for the reliability and efficiency of equipment. New designs were developed in conjunction with the laboratory of heat exchangers of the department "Turbines and Engines" of Ural Federal University. In 2017-2018. three ejectors EPO-3-120 were designed, manufactured and delivered to 2 TPPs. The calculation of nozzles and diffusers, the development and design of ejectors is carried out on the basis of the results obtained in the thesis of I. Murmanskii “Improvement of multi-stage steam-jet ejectors of steam turbine condensing units”. Engineered ejector designs have high performance and reliability.

The development of the new design was carried out with the direct participation of I. Murmanskii.

Using the results of the dissertation of I. Murmanskii in the production of ejectors can significantly increase the efficiency of the developed equipment.

CEO E.G. Salnikov

Appendix 2

List of the author's main publications

Articles published in refereed journals listed by VAK.

1. Reliability of steam-driven ejectors of turbine units / Brodov Yu. M., Aronson K. E., Ryabchikov A. Yu., Murmansky B. E., Murmansk I. B., Zhelonkin N. V. // Scientific and technical journal "Reliability and safety of energy." - 2016. - № 2 (33) - p. 60-64; 0.4 p.sh. / 0.1 p.sh

2. K. É. Aronson, Y. M. Brodov, B. E. I. B. Murmansky, N. V. S. I. Khaet // Power Technology and Engineering. – 2017. – 50(5) – С. 546-548; 0,3 п.л./0,1 п.л. (Scopus).

3. Analysis of experimental characteristics of multistage steam-jet electors of steam turbines / K. E. Aronson, A. Y. Ryabchikov, Y. M. Brodov, D. V. Brezgin, N. V. Zhelonkin, I. B. Murmansky // Thermal Engineering. – 2017 – 64(2) – С. 104-110; 0,4 п.л./0,1 п.л. (Scopus).

4. Functioning efficiency of intermediate coolers of multistage steam-jet ejectors of steam turbines / K. E. Aronson, A. Y. Ryabchikov, Y. M. Brodov, N. V. Zhelonkin, I. B. Murmansky // Thermal Engineering. – 2017. – 64(3) – С. 170-175; 0,5 п.л./0,2 п.л. (Scopus).

5. Ejectors of power plants turbine units efficiency and reliability increasing / K. E. Aronson, A. Yu. Ryabchikov, I. B. Murmansky et al. // Journal of Physics Conference. – 2017. – № 891 – UNSP 012249; 0,6 п.л./0,3 п.л.(Scopus, WoS).

6. Investigation of the effect of pressure increasing in condensing heat-exchanger / I. B. Murmansky, K. E. Aronson, Yu. M. Brodov et al. // Journal of Physics Conference Series. – 2017. – № 891 – UNSP 012122; 0,6 п.л./0,2 п.л. (Scopus, WoS).

Other publications:

7. Reliability of steam-driven ejectors of steam turbine units of thermal power plants / Brodov Yu. M., Aronson K. E., Murmansky I. B., Khayet S. I. // Energetic. - 2016. - № 12 - P. 40-41; 0.4 pp / 0.1 pp
8. Steam-driven ejector for steam turbines of the PGU CJSC "UTZ" / Aronson K. E., Ryabchikov A. Yu., Brezgin D. V., Zhelonkin N. V., Murmansky I. B., Chubarov A. A. // Academy of Energy. - 2016. - №1 (69) - p.30-35; 0.4 pp / 0.1 pp

9. Gas dynamics and heat-and-mass transfer in multistage steam-driven pumps with intermediate condensers / Brodov Yu. M., Aronson K. E., Ryabchikov A. Yu., Brezgin D. V., Murmansky I. B., Zhelonkin N. V. // Energy Production and Management in the 21st Century II, vol. 205. – 2016. – C. 105-113; 0,8 п.л./0,3 п.л. (Google scholar).

Patents and programs

10. Certificate of state registration of computer programs №2016611885 Russian Federation. Software complex for computer "Design and calibration calculation of steam-driven ejectors" / Aronson K. E., Murmansky I. B., Brezgin D. V., Ryabchikov A. Yu., Chubarov A. A., Brodov Yu. M .; applicant and patent holder Ural Federal University named after the first President of Russia B. N. Yeltsin. - №20156185492, applied 09/17/2015; registered in the registry of computer programs 02/12/2016.

11. Patent for utility model №170935 Russian Federation, IPC F04F5 / 00. Three-stage steam-driven ejector / Brodov Yu. M., Kuptsov V. K., Ryabchikov A. Yu., Aronson K. E., Murmanskii I. B., Zhelonkin N. V., Brezgin D. V.; applicant and patent holder Ural Federal University named after the first President of Russia B. N. Yeltsin. - №2016119824; applied 05/23/2016; publ. 15.05.2017 Byul. 14. - 9 s.

12. Patent for invention №2645635 Russian Federation, IPC F04F5 / 30. Three-stage steam-driven ejector / Brodov Yu. M., Kuptsov V. K., Ryabchikov A. Yu., Aronson K. E., Murmanskii I. B., Zhelonkin N. V., Brezgin D. V., Khayet S. I. ; applicant and patent holder Ural Federal University named after the first President of Russia B. N. Yeltsin. - № 2016126736; applied 07/04/2016; publ. 02.26.2018 Byul. 6. - 4 s.

Teaching materials

1. A turbine is very simple: a training manual / Brodov Yu.M., Nirenstein MA, Murmansk IB - Yekaterinburg: UrFU, 2012 .-- 191 p. (7.75 pp. / 1.5 pp.).
2. Repair of power equipment of thermal power plants / Ryabchikov A.Yu., Murmanskiy B.E., Murmanskiy I.B. // Multimedia course of lectures. - Yekaterinburg. UrFU, 2013. (500 p. / 200 p.)
3. Oil coolers in the oil supply systems of turbine units: a training manual / K.E. Aronson, A.Yu. Ryabchikov, N.V. Zhelonkin, I.B. Murmansk. - Yekaterinburg: UrFU, 2013 .-- 191 p. (9.7 p.p. / 1.5 p.p.).

4. Ejectors of steam turbine condensation units: studies. manual / Aronson, K .E., Ryabchikov, A. Yu., Brezgin, D. V., Murmanskii, I. B. - Ekaterinburg: Izd. UrFU. - 2015. - 131 p.
5. Reliability of equipment for steam turbine installations: studies. manual / Brodov Yu. M., Aronson K. E., Murmansky B. E., Murmansky I. B., Nirenstein M. A., Novoselov V. B., Plotnikov P. N. ., Ryabchikov A. Yu. - Ekaterinburg: Izd. UrFU. - 2017. - 144 p.
6. Steam-gas-turbine units: ejectors of condensing plants: a textbook for universities / Aronson KE, Ryabchikov A.Yu., Brezgin DV, Murmanskiy IB - M: Yurayt Publishing House, 2017; Yekaterinburg: Publishing House of the Ural University. - 129 p. ISBN 978-5-534-01709-0, ISBN 978-5-7996-1490-4 (5.5 bp / 2 bp).
7. The current situation and trends in the design and operation of condensers of powerful steam turbines of TPPs and NPPs (study guide) / Brodov Yu.M., Aronson K.E., Ryabchikov A.Yu., Nirenshtein M.A., Zhelonkin N.V., Brezgin D.V., Murmanskiy I.B., Gomboragchaa N. / Textbook edited by Dr. Tech. sciences, prof. Yu.M. Brodov. Yekaterinburg, publishing house of the Ural University. 2019.104 p. ISBN 978-5-7996-2536-8

In total there are 50 works published, including: 14 abstracts of reports in international conferences, 15 All-Russian conferences, 2 regional conferences.

Appendix 3

Geometrical characteristics of flow parts of jet devices – nozzles and diffusers

№	Parameter	EP-3-2 (EP-3-2A; EP-3-3) UTZ			EPO-3-135 UTZ			EPO-3-200 UTZ		
1	Stage number	**I**	**II**	**III**	**I**	**II**	**III**	**I**	**II**	**III**
2	Capacity by dry air or air-steam mixture (nominal/maximal), kg/h	85/135			85/135			105/200		
3	Primary steam flow rate, kg/h	850			296	296	258	900		
4	Primary steam pressure, MPa	0,49			0,49			0,49		
5	Primary steam temperature, °C	155			155/330			155/330		
6	Suction pressure of the I stage at nominal/maximal capacity, kPa							4/9	15/25	4/9
7	Volume capacity, m^3/h				4230 at t_I=32°C и G_{air}=45 kg/h					
8	Cooling condensate flow rate, t/h (min/max)				200			125/500		
9	Cooling condensate temperature, °C, nominal/maximal	26/70			25			35/80		
10	Nozzle throat diameter, mm	12	12	10,4	12	12	10,4	2x8,5	12	2x8,5
11	Nozzle exit diameter, mm	55,4	33	18	35	33	18	33	33	33
12	Length of supersonic part of a nozzle, mm	165	80	36	165	80	36	93	80	93
13	Distance between nozzle exit and diffuser inlet, mm	50	-5	4	75	30	29	30	30	30
14	Diameter of diffuser inlet, mm	100	63	80	100	63	42	74	68	74
15	Length of diffuser narrow part, mm	315	190	135	290	165	110	253	195	253
16	Length of diffuser narrow part, mm	67	43	28	67	43	28	47,5	47,5	47,5
17	Length of diffuser cylindrical part, mm	290	225	110	290	225	110	253	261	253
18	Diameter of diffuser outlet, mm	127	87	60	127	87	60	90	90	90
19	Diffuser widen part, mm	1030	730	475	428	318	223	810	760	810
20	Square of heat exchanger surface, m^2				15,3	17,9	17,9	2x8	8	2x8
21	External diameter of pipes / wall thickness, mm	19*1			19,1			—		
22	Pipes material	L68			08H18N10T			Carbon steel (St3, St20)		
23	Average length of pipes, mm				1200	1500	1500	—	—	—
24	Number of pipes, pc.	194			133	133	133	2x7	7	2x7

Continuation A.3

№	Parameter	EP-3-600 LMZ			EP-3-700 LMZ			EP-2-400 LMZ	
1	Stage number	I	II	III	I	II	III	I	II
2	Capacity by dry air or air-steam mixture (nominal/maximal), kg/h	70			70			60	
3	Primary steam flow rate, kg/h	200	200	200	700			400	
4	Primary steam pressure, MPa	1,27			0,49			1,57	
5	Primary steam temperature, °C	400	400	400				400	
6	Suction pressure of the I stage at nominal/maximal capacity, kPa	2,5						1,2/3,3	9,1/30,5
7	Volume capacity, m^3/h	3000						1500	
8	Cooling condensate flow rate, t/h (min/max)	75	46	29				40	20
9	Cooling condensate temperature, °C, nominal/maximal							25-30	
10	Nozzle throat diameter, mm	6,8	6,8	6,8	14	11	10	6	6
11	Nozzle exit diameter, mm	32	21	14	42	22	14	36	23
2	Length of supersonic part of a nozzle, mm	137	51	13	136	51	17	143	81
13	Distance between nozzle exit and diffuser inlet, mm	65	40	20	50	0	0	75	5
14	Diameter of diffuser inlet, mm	135	70	33	98	52	36	70	39
15	Length of diffuser narrow part, mm	256	146	77	391	205	156	180	172
16	Length of diffuser narrow part, mm	92	46	22	65	35	26	50	26
17	Length of diffuser cylindrical part, mm	265	165	140	260	140	130	50	105
18	Diameter of diffuser outlet, mm	135	89	60	115	73	49	58	29
19	Diffuser widen part, mm	400	400	370	284	215	134	315	312
20	Square of heat exchanger surface, m^2	14,3	8,4	5,1	14,3	8,4	5,1	10,9	5,4
21	External diameter of pipes / wall thickness, mm	19x1			19x1			19x1	
22	Pipes material	L68						L68	
23	Average length of pipes, mm	2450	2350	2250	2450	2350	2250	2000	
24	Number of pipes, pc.	98	60	38	98	60	38	90	45

Continuation A.3

№	Parameter	EP-3-25/75 HTZ			EP-3-50/150 HTZ			EPO-3-100/300 HTZ			EPO-3-55/150 HTZ			EPO-3-100/220 HTZ		
1	Stage number	I	II	III	I	II	III	I	II	III	I	II	III	I	II	III
2	Capacity by dry air or air-steam mixture (nominal/maximal), kg/h	25/75			70 at t_1=36°C, 180 at t_1=20°C P_{out}=105 kPa			350 at t_1 = 30°C P_{out}=131 kPa			240 at t_1 = 25°C P_{out}=145 kPa			310 at t_1 = 4°C P_{out}=145 kPa		
3	Primary steam flow rate, kg/h	135	254	407	385	804	945	1452	1047	1247	1225	1390	932	1093	1093	1760
4	Primary steam pressure, MPa				0,51	0,51	0,51	0,51	0,51	0,51	0,51	0,51	0,51	0,816	0,816	0,816
5	Primary steam temperature, °C	400	400	400	160	160	160	160	160	160	160	160	160	170	170	170
6	Suction pressure of the I stage at nominal/maximal capacity, kPa	4,2 dry air; 2,7 at G_{air}=25 kg/h; 5,4 at G_{air}=75 kg/h			1,3 at t_1=30,5°C; 3,5 at t_1=20°C			3,78			3,68			4,18		
7	Volume capacity, m^3/h	2850			5750			11100			9100			5900		
8	Cooling condensate flow rate, t/h (min/max)				222	167	112	149	78	-	500	297	203	337	245	168
9	Cooling condensate temperature, °C, nominal/maximal															
10	Nozzle throat diameter, mm	9	12,4	15,6	13,5	19,5	22	28,5	22,5	24,5	24	25,5	21	16	16	20,3
11	Nozzle exit diameter, mm	42	32	30	67	56	40	112	54	40	105	70	35	76	45	31
12	Length of supersonic part of a nozzle, mm				242	165	82	330	150	117	340	240	70	273	163	43
13	Distance between nozzle exit and diffuser inlet, mm	78	71	-1	160	92	68	116	64	0	130	80	32	154	87	67
14	Diameter of diffuser inlet, mm	113	85,5	54,4	162	110	63	172	112	82	225	120	65	157	92	68
15	Length of diffuser narrow part, mm	330	242	210	340	186	93	325	420	300	262	200	110	113	122	72
16	Length of diffuser narrow part, mm	73	55,2	35	114	84	50	147	85	55	170	96	52	133	75	58
17	Length of diffuser cylindrical part, mm	300	220	140	340	250	150	912	650	360	497	500	220	792	600	422
18	Diameter of diffuser outlet, mm	138	130	104	250	216	125	370	196	161	290	184	111	300	187	138
19	Diffuser widen part, mm	370	425	390	780	660	400	1000	666	636	571	365	304	622	480	428
20	Square of heat exchanger surface, m^2	14	9,63	7,55	40	30	20	30	12,5	-	49,1	35,7	24,5	40	30	20
21	External diameter of pipes / wall thickness, mm	19*1	19*1	19*1	19*1	19*1	19*1	19*1	19*1	19*1	19*1	19*1	19*1	19/1	19/1	19/1
22	Pipes material	L68			L68						MNZhMC-5-1-1					
23	Average length of pipes, mm	1095	1095	1095	3300	3300	3300	3780	3780	-	2900	2900	2900	2900	2900	2900
24	Number of pipes, pc.	224	154	122	202	152	102	113	59	-	283	206	141	283	206	141

Continuation A.3

№	Parameter	EO-8 KTZ		EO-10 KTZ		EO-15 KTZ		EO-17 KTZ		EO-20/1 KTZ		EO-20/2 KTZ		EO-30 KTZ		EO-50 KTZ	
1	Stage number	I	II	I	II	I	II	I	II	I	II	I	II	I	II	I	II
2	Capacity by dry air or air-steam mixture (nominal/maximal), kg/h	10		13		18		22		20/23,5		20/18		30		42	
3	Primary steam flow rate, kg/h	134		61		93		102		80		80		155		155	
4	Primary steam pressure, MPa	0,39		1,6		1,6		1,6		1,6		1,6		1,6		0,59	
5	Primary steam temperature, °C	425		425		425		425		425		425		425		380 (saturated)	
6	Suction pressure of the I stage at nominal/maximal capacity, kPa	4,80		3,50		3,30		4,00		6,4/ 7,1		5,5/5, 0		3,40		3,60	
7	Volume capacity, m^3/h	235		363		536		528		286		337		865		1140	
8	Cooling condensate flow rate, t/h (min/max)	4,1/8,2		4,8		8		12		18,8		9,5		18			
9	Cooling condensate temperature, °C, nominal/maximal																
10	Nozzle throat diameter, mm	6,6	6,6	2,35	2,54	2,9	3,13	3	3,3	2,7	2,9	2,7	2,9	3,9	3,9	8	9,45
11	Nozzle exit diameter, mm	24	13	14,8	8,2	18,8	11	18,6	10,3	11,0	8,2	11,0	8,2	24,0	12,0	28,9	16,9
12	Length of supersonic part of a nozzle, mm	119	47	104	52	110	66	123	77	69	56	69	56	166	77	162	57
13	Distance between nozzle exit and diffuser inlet, mm	10	9	22	6	27	6	36	4	25	4	25	16	-	-	65	25
14	Diameter of diffuser inlet, mm	35,6	21,1	32	17	38	19	39,8	21	35,4	18,5	35	18,5	52	25	60	36
15	Length of diffuser narrow part, mm	157	83	85	65	95	50	100	78	100	60	130	75	205	100	236	142
16	Length of diffuser narrow part, mm	26	13,8	22,3	10,9	27,5	13,45	29,4	14,2	23,2	13,2	23,2	13,2	35	16,7	39,2	23,6
17	Length of diffuser cylindrical part, mm	130	55	85	44	105	55	98	50	98	50	98	50	140	67	157	94
18	Diameter of diffuser outlet, mm	50	28	48	28	48	32	60	34	50	34	52	34	73	42	78	47
19	Diffuser widen part, mm	133	104	128	119	98	123	112	100	100	118	142	118	215	133	277	164
20	Square of heat exchanger surface, m^2	1,14	1,14	1,08	1,08	1,16	1,16	1,18	1,18	0,7	0,7	1,16	1,16	1,4	1,4		
21	External diameter of pipes / wall thickness, mm	19x1		16x1		19x1		19x1		19x1		19x1		19x1		19x1	
22	Pipes material																
23	Average length of pipes, mm	various length		various length		various length		various length		various length		various length		various length		various length	
24	Number of pipes, pc.																

4.1. Results of experimental tests of EPO-3-80 with “dry” air at calculated nozzle position

Air flow rate through the	G_{air}	kg/h	0,0	10,3	30,8	52,4	71,3	93,1	102,7	123,1	142,0	162,0
Condenser pressure	P_c	MPa	0,041									
Primary steam pressure (abs.)	P_{ps}	MPa	0,6	0,6	0,6	0,6	0,6	0,6	0,6	0,6	0,6	0,6
Primary steam temperature	T_{ps}	°C	240	240	240	240	240	240	240	240	240	240
I stage suction pressure	P_{11}	kPa	0,98	1,01	1,11	2,50	3,10	4,60	5,80	8,40	9,80	12,10
I stage back pressure	P_{12}	kPa	7,44	5,05	6,85	8,70	10,20	11,90	13,40	15,30	16,64	18,40
II stage suction pressure	P_{21}	kPa	7,00	6,96	7,86	9,80	11,20	12,65	13,80	15,50	17,20	18,40
II stage back pressure	P_{22}	kPa	29,54	27,83	28,70	30,03	31,20	32,80	33,80	35,30	36,60	37,80
III stage suction pressure	P_{31}	kPa	34,21	34,49	35,90	36,92	38,01	39,10	40,40	41,90	43,20	44,20
III stage back pressure	P_{32}	kPa	96,50	92,20	92,10	92,40	92,90	94,40	94,50	94,90	95,30	95,60
I stage suction temperature	t_{11}	°C	231,7	44,0	41,4	47,2		38,6	38,5	38,2	38,0	37,8
I stage back temperature	t_{12}	°C										
II stage suction temperature	t_{21}	°C	102,4	40,1	28,1	25,5		22,5	24,1	29,6	18,7	16,4
II stage back temperature	t_{22}	°C										
III stage suction temperature	t_{31}	°C	175,5	101,9	55,1	40,8		33,5	43,1	29,3	27,9	25,9
III stage back temperature	t_{32}	°C										
Exhaust temperature	T_{air}	°C	19,3									
Cooling condensate (CC) flow rate (through the intercoolers)	G_{cc}	t/h	182									
CC temperature upstream the ejector	t_{cc1}	°C	10,6	11,6	11,8	11,8		11,8	11,6	11,5	11,6	11,5
CC temperature after the I stage	t_{cc2}	°C	12,4	13,2	13,3	13,4		13,4	13,2	13,0	13,2	13,0
CC temperature after the II stage	t_{cc3}	°C	13,0	13,8	14,0	14,1		14,1	13,9	13,8	13,8	13,9
CC temperature after the III stage	t_{cc4}	°C						15,6	15,4	15,4	15,4	15,4

Continuation A.4.1

Air flow rate through the	G_{air}	kg/h	0,0	10,3	52,4	71,3	93,1	123,1	142,0	162,0
Condenser pressure	P_c	MPa	0,041							
Primary steam pressure (abs.)	P_{ps}	MPa	0,7	0,7	0,7	0,7	0,7	0,7	0,7	0,7
Primary steam temperature	T_{ps}	°C	245	245	245	245	245	245	245	245
I stage suction pressure	P_{11}	kPa	1,10	2,00	1,80	2,40	2,60	4,20	5,50	7,20
I stage back pressure	P_{12}	kPa	4,74	3,02	9,06	9,60	10,40			
II stage suction pressure	P_{21}	kPa	2,80	3,02	4,50	5,20	6,50	8,50	10,10	11,70
II stage back pressure	P_{22}	kPa	20,72	20,20	26,80	27,50	29,20	32,30	33,90	36,95
III stage suction pressure	P_{31}	kPa	25,76	26,06	27,10	28,20	29,80	32,80	34,02	35,90
III stage back pressure	P_{32}	kPa	94,70	93,30	93,00	93,30	93,70	94,30	94,40	94,10
I stage suction temperature	t_{11}	°C	45,3		47,8	46,8				38,4
I stage back temperature	t_{12}	°C			144	140				128
II stage suction temperature	t_{21}	°C	133,4		12,4	12,5				13,3
II stage back temperature	t_{22}	°C			67	67				64
III stage suction temperature	t_{31}	°C	179,1		25,7	26,0				23,2
III stage back temperature	t_{32}	°C			180	181				178
Exhaust temperature	t_{air}	°C								
Cooling condensate (CC) flow rate (through the intercoolers)	G_{cc}	t/h								
CC temperature upstream the ejector	t_{cc1}	°C	11,4		11,7	11,8				12,2
CC temperature after the I stage	t_{cc2}	°C	13,2		13,5	13,7				14,0
CC temperature after the II stage	t_{cc3}	°C	14,3		14,9	14,9				15,2
CC temperature after the III stage	t_{cc4}	°C	15,9		16,1	16,2				16,8

4.2. Results of experimental tests of EPO-3-80 with “dry” air at adjusted nozzle position

Air flow rate through the	G_{air}	кг/ч	0,0	10,3	41,4	71,3	93,1	102,7	123,1
Condenser pressure	P_c	МПа	0,045						
Primary steam pressure (abs.)	P_{ps}	МПа	0,6						
Primary steam temperature	T_{ps}	°C	240	240	240	240	240	240	240
I stage suction pressure	P_{11}	кПа	0,73	0,82	1,80	3,50	6,70	6,70	9,10
I stage back pressure	P_{12}	кПа	3,77	5,15	6,60	9,00	11,90	11,80	13,90
II stage suction pressure	P_{21}	кПа	5,90	7,34	9,00	11,40	14,40	14,50	16,60
II stage back pressure	P_{22}	кПа	26,88	28,50	30,10	31,90	34,20	34,80	36,20
III stage suction pressure	P_{31}	кПа	32,65	34,58	36,70	38,50	40,30	41,20	42,60
III stage back pressure	P_{32}	кПа	94,20	93,90	93,70	94,10	95,40	96,10	96,50
I stage suction temperature	t_{11}	°C	63,7	54,1	45,8	37,5	36,0	36,0	35,9
I stage back temperature	t_{12}	°C	134	143	145	140	138	142	136
II stage suction temperature	t_{21}	°C	146,2	97,5	32,1	24,3	22,7	21,7	21,3
II stage back temperature	t_{22}	°C		175	175	174	168	170	167
III stage suction temperature	t_{31}	°C	189,2	155,1	55,8	40,2	34,4	32,0	31,5
III stage back temperature	t_{32}	°C	198	182	188	193	186	178	185
Cooling condensate (CC) flow rate (through the intercoolers)	G_{cc}	t/h				206			
CC temperature upstream the ejector	t_{cc1}	°C	11,4	11,4	11,6	11,5	11,5	11,5	11,6
CC temperature after the I stage	t_{cc2}	°C	14,7	14,9	14,9	14,9	14,8	15,0	14,9
CC temperature after the II stage	t_{cc3}	°C	16,9	17,3	17,2	17,1	16,5	17,0	17,0
CC temperature after the III stage	t_{cc4}	°C	20,0	20,1	19,9	19,9	20,1	20,3	20,2
I stage drain temperature	t_{d1}	°C	38,0						
II stage drain temperature	t_{d2}	°C	57,0						
III stage drain temperature	t_{d3}	°C	53,0						

Continuation A.4.2

Air flow rate through the	G_{air}	kg/h	0,0	10,3	41,4	71,3	93,1	123,1	142,0	162,0	182,1
Condenser pressure	P_c	MPa	0,047								
Primary steam pressure (abs.)	P_{ps}	MPa	0,7								
Primary steam temperature	t_{ps}	°C	240	240	240	240	240	240	240	240	240
I stage suction pressure	P_{11}	kPa	0,80	0,98	1,35	1,68	1,90	2,18	2,90	4,50	6,00
I stage back pressure	P_{12}	kPa	1,14	2,10	3,66	4,70	5,70	7,36	8,41	9,90	11,50
II stage suction pressure	P_{21}	kPa	2,37	2,80	4,04	4,90	5,60	7,32	8,40	10,10	11,70
II stage back pressure	P_{22}	kPa	20,70	20,20	20,90	22,00	24,10	30,20	35,90	36,70	38,40
III stage suction pressure	P_{31}	kPa	25,50	25,60	26,60	28,10	30,20	33,70		36,50	38,20
III stage back pressure	P_{32}	kPa	95,90	94,70	94,70	94,40	94,60	95,20	96,30	95,40	96,20
I stage suction temperature	t_{11}	°C	36,0	36,4	36,2	34,6	38,4	31,5		33,1	33,9
I stage back temperature	t_{12}	°C	144	146	148	151	154	152	144	146	148
II stage suction temperature	t_{21}	°C	63,2	49,8	29,5	16,5	15,0	14,0		14,0	14,0
II stage back temperature	t_{22}	°C	180	181	181	181	163	75	70	70	73
III stage suction temperature	t_{31}	°C	162,1	67,0	49,9	43,8	35,9	28,9		25,9	24,9
III stage back temperature	t_{32}	°C	200	199	190	193	193	189	182	173	177
Exhaust temperature	t_{air}	°C									
Cooling condensate (CC) flow rate (through the intercoolers)	G_{cc}	t/h									
CC temperature upstream the ejector	t_{cc1}	°C	11,6	11,7	11,8	11,9	11,9	11,9		12,0	12,0
CC temperature after the I stage	t_{cc2}	°C	15,4	15,5	15,7	15,7	15,7	15,8		15,8	16,0
CC temperature after the II stage	t_{cc3}	°C	19,1	19,6	19,6	19,4	19,3	19,1		18,8	18,8
CC temperature after the III stage	t_{cc4}	°C	21,4	21,4	21,4	21,6	21,8	22,0		22,1	22,4

Continuation A.4.2

Air flow rate through the	G_{air}	kg/h	0,0	0,0	20,7	40,9	51,7	60,1	70,4	80,1	91,9	101,3	121,6	140,2	179,7
Condenser pressure	P_c	mmHg	465												
Primary steam pressure (abs.)	P_{ps}	MPa	0,83	0,81	0,83	0,83	0,81	0,81	0,81	0,81	0,81	0,81	0,81	0,81	0,81
Primary steam temperature	t_{ps}	°C	250												
I stage suction pressure	P_{11}	kPa	1,65	0,89	1,06	1,40	1,54	1,62	1,75	1,86	1,97	2,75	3,41	4,18	5,42
I stage back pressure	P_{12}	kPa	9,86	6,96	9,64	10,12	10,20	10,30	10,60	10,85	11,13	11,47	12,53	13,24	14,38
II stage suction pressure	P_{21}	kPa	6,74	5,23	6,59	7,10	7,30	7,56	7,88	8,14	8,55	9,10	10,26	11,06	12,20
II stage back pressure	P_{22}	kPa	25,81	24,20	25,62	18,20	19,00	19,90	21,27	22,25	28,10	29,34	32,40	35,20	39,20
III stage suction pressure	P_{31}	kPa	23,41	23,70	19,14	15,60	16,60	17,30	18,40	19,32	24,28	25,95	29,10	31,90	35,20
III stage back pressure	P_{32}	kPa	101,20	92,70	102,70	101,70	99,40	97,50	96,60	96,10	96,00	96,70	96,70	95,60	95,10
I stage suction temperature	t_{11}	°C		159,8											
I stage back temperature	t_{12}	°C	39,3	36,6			34,9			34,8		34,6			35,1
II stage suction temperature	t_{21}	°C	67,2	67,0			60,2			62,5		67,0			72,6
II stage back temperature	t_{22}	°C		160,4			90,5								
III stage suction temperature	t_{31}	°C		159,1											
Cooling condensate (CC) flow rate (through the intercoolers)	G_{cc}	t/h	168	193			187			203		190			199
CC temperature upstream the ejector	t_{cc1}	°C	38,1	32,8			34,0			34,0		33,5			33,3
CC temperature after the I stage	t_{cc2}	°C	40,0	34,6		5493,0	36,0		7688,1	35,8		35,3		5726,7	35,1
CC temperature after the II stage	t_{cc3}	°C	43,2	37,5			38,3			37,9		37,2			36,8
CC temperature after the III stage	t_{cc4}	°C	44,7	38,7			40,0			39,6		39,4			38,9
I stage drain temperature	t_{d1}	°C	19,0	56											52
II stage drain temperature	t_{d2}	°C	64,0	62											66
III stage drain temperature	t_{d3}	°C	52,0	50											57

Continuation A.4.2

Air flow rate through the	G_{air}	kg/h	0,0	20,7	40,9	60,1	80,1	91,9	101,3	121,6	140,2	160,0	179,7
Condenser pressure	P_c	mmHg	465										
Primary steam pressure (abs.)	P_{ps}	MPa	0,86	0,86	0,86	0,85	0,85	0,85	0,85	0,85	0,85	0,85	0,85
Primary steam temperature	t_{ps}	°C	253	253	253	255	250	250	250	250	250	250	250
I stage suction pressure	P_{11}	kPa	0,93	1,13	1,46	1,70	1,93	2,06	2,70	2,85	3,30	4,40	6,03
I stage back pressure	P_{12}	kPa	7,75	8,90	9,24	9,80	10,07	10,30	10,70	11,60	12,50	13,60	15,46
II stage suction pressure	P_{21}	kPa	4,86	5,80	6,74	7,50	8,08	8,30	8,70	9,80	10,70	11,90	13,60
II stage back pressure	P_{22}	kPa	18,10	16,10	19,55	21,40	25,20	26,30	27,30	34,70	37,40	41,60	44,85
III stage suction pressure	P_{31}	kPa	19,80	13,00	15,55	17,60	19,80	20,90	21,70	29,10	31,80	36,00	39,40
III stage back pressure	P_{32}	kPa	92,50	94,90	94,60	93,80	93,20	93,20	93,20	93,60	94,30	96,10	97,50
I stage suction temperature	t_{11}	°C	147,9			152,9						150,9	149,9
I stage back temperature	t_{12}	°C	35,8			35,8						36,2	36,6
II stage suction temperature	t_{21}	°C	84,4			60,2						65,2	67,3
II stage back temperature	t_{22}	°C	171,2			125,9						88,6	57,1
III stage suction temperature	t_{31}	°C	159,1			168,0						164,0	84,5
Cooling condensate (CC) flow rate (through the intercoolers)	G_{cc}	t/h	440,0			440						455	
CC temperature upstream the ejector	t_{cc1}	°C	32,4			32,1						32,0	32,2
CC temperature after the I stage	t_{cc2}	°C	34,5			34,1						34,1	34,3
CC temperature after the II stage	t_{cc3}	°C	37,7			36,2						36,1	36,2
CC temperature after the III stage	t_{cc4}	°C	38,6			38,1						38,7	38,4
I stage drain temperature	t_{d1}	°C	19,0									50,0	51
II stage drain temperature	t_{d2}	°C	64,0									61,0	60
III stage drain temperature	t_{d3}	°C	52,0									57,0	59